

“In-Situ Sampling and Characterization of Naturally  
Occurring Marine Methane Hydrate Using the  
D/V JOIDES Resolution.”

DOE COOPERATIVE AGREEMENT: DE-FC26-01NT41329

FINAL TECHNICAL REPORT - PHASE 1

Frequency of Report: Final

Reporting Period Start Date: October 1, 2001

Reporting Period End Date: February 28, 2004

Name of Submitting Organization: Joint Oceanographic Institutions

Principal Authors: Dr. Frank R. Rack, and the  
ODP Leg 204 Scientific Party\*

Date Report Issued: April 2004

Frank R. Rack (Joint Oceanographic Institutions; 1201 New York Ave.,  
NW; Suite 400; Washington, DC, 20005; Tel: (202) 232-3900, ext. 1608;

Email: [frack@joiscience.org](mailto:frack@joiscience.org)); and the  
ODP Leg 204 Scientific Party.

## DISCLAIMER

**This report was prepared as an account of work sponsored by an agency of the United States Government. Neither the United States Government nor any agency thereof, nor any of their employees, makes any warranty, express or implied, or assumes any legal liability or responsibility for the accuracy, completeness, or usefulness or any information, apparatus, product, or process disclosed, or represents that its use would not infringe privately owned rights. Reference herein to any specific commercial product, process, or service by trade name, trademark, manufacturer, or otherwise does not necessarily constitute or imply its endorsement, recommendation, or favoring by the United States Government or any agency thereof. The views and opinions of authors expressed herein do not necessarily reflect those of the United States Government or any agency thereof.**

**The international Ocean Drilling Program is managed by Joint Oceanographic Institutions, Inc., under contract with the U.S. National Science Foundation. Funding for the program is provided by the following agencies:**

**Australia/Canada/Chinese Taipei/Korea Consortium for Ocean Drilling  
Deutsche Forschungsgemeinschaft (Federal Republic of Germany)  
Institut National des Sciences de l'Univers-Centre National de la Recherche Scientifique (INSU-CNRS; France)  
Ocean Research Institute of the University of Tokyo (Japan)  
National Science Foundation (United States)  
Natural Environment Research Council (United Kingdom)  
European Science Foundation Consortium for Ocean Drilling (Belgium, Denmark, Finland, Iceland, Ireland, Italy, The Netherlands, Norway, Portugal, Spain, Sweden, and Switzerland)  
Marine High-Technology Bureau of the State Science and Technology Commissions of the People's Republic of China**

**Any opinions, findings, and conclusions or recommendations expressed in this report are those of the author(s) and do not necessarily reflect the views of the National Science Foundation, the participating agencies, Joint Oceanographic Institutions, Inc., Texas A&M University, or Texas A&M Research Foundation.**

## ABSTRACT

The primary accomplishments of the JOI Cooperative Agreement with DOE/NETL were the deployment of specialized tools and measurement systems for use on ODP Leg 204, which studied hydrate deposits on Hydrate Ridge, offshore Oregon. Earlier deployments of these tools on ODP Leg 201 (Peru Margin) were made to prepare the tools and measurement systems for extensive use on ODP Leg 204. Prior to undertaking these field deployments, a baseline survey of the state-of-the-art in pressure coring systems was conducted (**Task 1.1**) and delivered to DOE/NETL shortly after this contract was awarded.

The operational results from the frequent use of the PCS Gas Manifold with the Pressure Core Sampler (PCS) tool on ODP Legs 201 and 204 (**Task 2.0**) are evaluated. The ODP Pressure Core System (PCS) was deployed 17 times during ODP Leg 201 and 39 times during ODP Leg 204. It successfully retrieved cores from a broad range of lithologies and sediment depths along both the Peru margin and on Hydrate Ridge. The PCS gas manifold was used in conjunction with the PCS throughout ODP Legs 201 and 204 to measure the total volume and composition of gases recovered in sediment cores.

The DVTP, DVTP-P, APC-methane, and APC-Temperature tools (ODP memory tools) were used extensively during ODP Legs 201 and 204 aboard the D/V *JOIDES Resolution* (**Task 3.0**). The data obtained from the successful deployments of these tools has been evaluated by the scientists and engineers involved in this testing.

Infrared-thermal imaging systems (IR-TIS) were deployed on ODP Legs 201 and 204. These systems were used to identify methane hydrate intervals in the recovered cores (**Task 4.0**) through systematic measurements followed by discrete sampling and preservation of these samples.

Leg 204 scientists and LDEO logging engineers conducted LWD and VSP experiments during ODP Leg 204 and evaluated the results (**Task 5.0**). Tool modifications were made to create a LWD Resistivity-at-the-Bit with Coring (RAB-C) tool, which resulted from the integration of the ODP motor-driven core barrel (MDCB) inner core tube with the Schlumberger/Anadrill RAB landing sub.

ODP and FUGRO engineers deployed the modified FUGRO Piezoprobe tool for use with the ODP APC/XCB bottom hole assembly (BHA) on ODP Leg 204 (**Task 6.0**). This required changes to the lay out, space out, and completion of crossover subs for the piezoprobe deployment and the establishment of operational protocols for tool use.

Finally, a series of additional holes were cored at the crest of Hydrate Ridge (Site 1249) to accomplish the rapid recovery and preservation of hydrate samples as part of a hydrate geiatric study. This report will present an overview of the results obtained from tool and instrument deployments on ODP Legs 201 and 204 as part of this project.

*In-Situ Sampling and Characterization of Naturally Occurring Marine Methane Hydrate Using the D/V JOIDES Resolution.*

**TABLE OF CONTENTS**

<b>Disclaimer</b>	<b>2</b>
<b>Abstract</b>	<b>3</b>
<b>Table of Contents</b>	<b>4</b>
<b>Introduction</b>	<b>5</b>
<b>Executive Summary</b>	<b>6</b>
<b>Experimental</b>	<b>8</b>
<b>Results and Discussion</b>	<b>41</b>
<b>Conclusion</b>	<b>142</b>
<b>References</b>	<b>146</b>
<b>List of Acronyms and Abbreviations</b>	<b>155</b>
<b>List of ODP Leg 204 Shipboard Scientific Party Members</b>	<b>157</b>
<b>Appendices</b>	<b>162</b>

## INTRODUCTION

The primary accomplishments of the JOI Cooperative Agreement with DOE/NETL were the deployment of specialized tools and measurement systems for use on ODP Leg 204, which studied hydrate deposits on Hydrate Ridge, offshore Oregon. Earlier deployments of these tools on ODP Leg 201 (Peru Margin) were made to prepare the tools and measurement systems for extensive use on ODP Leg 204. Prior to undertaking these field deployments, a baseline survey of the state-of-the-art in pressure coring systems was conducted (**Task 1.1**) and delivered to DOE/NETL shortly after this contract was awarded.

The operational results from the frequent use of the PCS Gas Manifold with the Pressure Core Sampler (PCS) tool on ODP Legs 201 and 204 (**Task 2.0**) are evaluated. The ODP Pressure Core System (PCS) was deployed 17 times during ODP Leg 201 and 39 times during ODP Leg 204. It successfully retrieved cores from a broad range of lithologies and sediment depths along both the Peru margin and on Hydrate Ridge. The PCS gas manifold was used in conjunction with the PCS throughout ODP Legs 201 and 204 to measure the total volume and composition of gases recovered in sediment cores.

The DVTP, DVTP-P, APC-methane, and APC-Temperature tools (ODP memory tools) were used extensively during ODP Legs 201 and 204 aboard the D/V JOIDES *Resolution* (**Task 3.0**). The data obtained from the successful deployments of these tools has been evaluated by the scientists and engineers involved in this testing.

Infrared-thermal imaging systems (IR-TIS) were deployed on ODP Legs 201 and 204. These systems were used to identify methane hydrate intervals in the recovered cores (**Task 4.0**) through systematic measurements followed by discrete sampling and preservation of these samples.

Leg 204 scientists and LDEO logging engineers conducted LWD and VSP experiments during ODP Leg 204 and evaluated the results (**Task 5.0**). Tool modifications were made to create a LWD Resistivity-at-the-Bit with Coring (RAB-C) tool, which resulted from the integration of the ODP motor-driven core barrel (MDCB) inner core tube with the Schlumberger/Anadrill RAB landing sub.

ODP and FUGRO engineers deployed the modified FUGRO Piezoprobe tool for use with the ODP APC/XCB bottom hole assembly (BHA) on ODP Leg 204 (**Task 6.0**). This required changes to the lay out, space out, and completion of crossover subs for the piezoprobe deployment and the establishment of operational protocols for tool use.

A series of additional holes were cored at the crest of Hydrate Ridge (Site 1249) specifically geared toward the rapid recovery and preservation of hydrate samples as part of a hydrate geriatric study partially funded by the Department of Energy (DOE). In conclusion, all project objectives were met within time and budget requirements.

*In-Situ Sampling and Characterization of Naturally Occurring Marine Methane Hydrate Using the D/V JOIDES Resolution.*

## EXECUTIVE SUMMARY

The primary accomplishments of the JOI Cooperative Agreement with DOE/NETL were the deployment of specialized tools and measurement systems for use on ODP Leg 204, which studied hydrate deposits on Hydrate Ridge, offshore Oregon. Earlier deployments of these tools on ODP Leg 201 (Peru Margin) were made to prepare the tools and measurement systems for extensive use on ODP Leg 204.

Prior to undertaking these field deployments, a baseline survey of the state-of-the-art in pressure coring systems was conducted (**Task 1.1**) and delivered to DOE/NETL shortly after this contract was awarded.

The PCS is a downhole tool designed to recover a cylindrical sediment core -- including gas and interstitial water -- at in situ pressure (Pettigrew, 1992). When properly sealed at depth, controlled release of pressure from the PCS through a manifold permits collection of gases that would otherwise escape on the wireline trip. The operational results from the frequent use of the PCS Gas Manifold with the Pressure Core Sampler (PCS) tool on ODP Legs 201 and 204 (**Task 2.0**) are evaluated herein.

The ODP Pressure Core System (PCS) was deployed 17 times during ODP Leg 201 and 39 times during ODP Leg 204. It successfully retrieved cores from a broad range of lithologies and sediment depths along both the Peru margin and on Hydrate Ridge. The PCS gas manifold was used in conjunction with the PCS throughout ODP Legs 201 and 204 to measure the total volume and composition of gases recovered in sediment cores.

The HYACINTH project, a European Union (EU) funded effort to develop tools to characterize methane hydrate and measure physical properties under in-situ conditions, provided additional pressure-coring tools for collaborative testing during ODP Legs 201 and 204. The FUGRO pressure corer (FPC) was deployed 7 times during ODP Legs 201 at sites located offshore Peru in preparation for deployments offshore Oregon on ODP Leg 204. The initial FPC deployments met with limited success in recovering pressurized cores, but much was learned about the operation of the tool with shipboard systems on the D/V JOIDES *Resolution*. Both the FPC and the HYACE Rotary Corer (HRC) were then deployed on the D/V JOIDES *Resolution* during ODP Leg 204 to field-test these coring systems at several sites located offshore Oregon. The field-testing of these tools by JOI/ODP provided a corollary benefit to DOE/NETL at no cost to this project. The testing was negotiated as part of a cooperative agreement between JOI/ODP and the HYACINTH partners.

Two core-logging chambers (ODP-LC) were fabricated for use on ODP Leg 204. These chambers were able to accept standard ODP APC/XCB core sections in their existing core liners and allowed them to be re-pressurized and logged to collect gamma ray attenuation (bulk density) and compressional-wave acoustic velocity measurements. These measurements were made using a vertical multi-sensor (pressure) core logging

*In-Situ Sampling and Characterization of Naturally Occurring Marine Methane Hydrate Using the D/V JOIDES Resolution.*

(MSCL-V) system that was deployed on Leg 204. These chambers allowed physical properties data to be collected on hydrate cores recovered using conventional coring techniques and re-pressurized.

The DVTP, DVTP-P, APC-methane, and APC-Temperature tools (ODP memory tools) were used extensively during ODP Legs 201 and 204 (**Task 3.0**). The data from tool deployments have been evaluated.

An infrared-thermal imaging system (IR-TIS) was deployed for the first time on ODP Leg 201 to identify methane hydrate intervals in the recovered cores. A second system was purchased for ODP Leg 204 and both systems were used throughout the cruise to identify cold anomalies in cores (**Task 4.0**). A track-mounted infrared-thermal imaging system (IR-TIS) was deployed for the first time on ODP Leg 204 to automate the process to routinely identify methane hydrate intervals in the recovered cores through systematic measurements followed by discrete sampling and preservation of these samples.

Leg 204 scientists and LDEO logging engineers conducted LWD and VSP experiments during ODP Leg 204 and evaluated the results (**Task 5.0**). Tool modifications were made to create a LWD Resistivity-at-the-Bit with Coring (RAB-C) tool, which resulted from the integration of the ODP motor-driven core barrel (MDCB) inner core tube with the Schlumberger/Anadrill RAB landing sub.

ODP and FUGRO engineers deployed the modified FUGRO Piezoprobe tool for use with the ODP APC/XCB bottom hole assembly (BHA) on ODP Leg 204 (**Task 6.0**). This required changes to the lay out, space out, and completion of crossover subs for the piezoprobe deployment and the establishment of operational protocols for the deployment and use of this tool on Leg 204.

Finally, a series of additional holes were cored at the crest of Hydrate Ridge (Site 1249) specifically geared toward the rapid recovery and preservation of hydrate samples as part of a hydrate geriatric study partially funded by the Department of Energy (DOE).

This report will present an overview of the results obtained from tool and instrument deployments on ODP Legs 201 and 204 as part of this project. The overall conclusion is that all objectives of this project were successfully achieved, the tools and experimental systems worked well, and much was learned about conducting hydrate coring operations, preserving naturally-occurring hydrates in the field, and making in situ measurements. All of these results have been communicated broadly through talks at professional and technical meetings as well as to DOE/NETL program managers. Additional information and data are available online at the ODP Publications website for Leg 201: <[http://www-odp.tamu.edu/publications/201\\_IR/201TOC.HTM](http://www-odp.tamu.edu/publications/201_IR/201TOC.HTM)> and for Leg 204: <[http://www-odp.tamu.edu/publications/204\\_IR/204TOC.HTM](http://www-odp.tamu.edu/publications/204_IR/204TOC.HTM)>. Additional technical reports and data pertaining to the project tasks are contained in the appendices to this report.

*In-Situ Sampling and Characterization of Naturally Occurring Marine Methane Hydrate Using the D/V JOIDES Resolution.*

## EXPERIMENTAL

### INTRODUCTION

Gas hydrate is an ice-like substance that contains methane or other low molecular weight gases in a lattice of water molecules. Methane hydrates are stable under the temperature and pressure conditions generally found in the Arctic and near the seafloor at water depths greater than 500 m. They are quite common beneath the slope of both active and passive continental margins, where methane originates from the decomposition of organic matter. International interest in this material has increased considerably in the past several years because of increasing recognition that the large volumes of gas stored in these structures represent a significant fraction of the global methane budget and may therefore be a potential energy resource for the future (see review by Kvenvolden and Lorenson, 2001). Several authors have also suggested that sudden, widespread dissociation of subseafloor gas hydrates in response to changing environmental conditions may have had a significant effect on past climate (eg. Revelle, 1983; Nisbet, 1990; Paull et al., 1991; Katz et al., 1999; Dickens, 2001). These effects remain speculative, as the volume of gas stored in the gas hydrate reservoir and its behavior during changing environmental conditions are currently poorly constrained.

In order to evaluate the economic potential of hydrates, their role as a natural hazard, and their impact on climate, we need to know:

- How are hydrates and underlying free gas distributed vertically and horizontally in the sediment?
- What controls their distribution (i.e. the sources of gas, fluid migration, and the physical chemistry of hydrate formation)?
- What are the effects of this distribution on the mechanical properties of the seafloor?
- How can hydrate and gas distribution be mapped regionally using remote sensing geophysical techniques?
- How does hydrate respond to changes in pressure and temperature resulting from tectonic and oceanographic perturbation?
- How can we use the isotopic record as a proxy for past tectonic and climate changes?
- Does the hydrate system harbor a rich biosphere? This question is of broad interest, particularly given the recent recognition that the biosphere extends deeper into the earth and that it has a larger impact on the geologic record than previously thought.

ODP has a critical role to play in addressing the above questions because it provides the only means available to the international academic community of directly sampling gas hydrates and underlying sediments beneath the oceans. Hydrates have been sampled during several ODP cruises. Leg 164 to the Blake Ridge was the first (and, prior to Leg

*In-Situ Sampling and Characterization of Naturally Occurring Marine Methane Hydrate Using the D/V JOIDES Resolution.*

204, the only) Leg focused primarily on understanding the dynamics of hydrate formation. Hydrates were secondary objectives of ODP cruises to the Chile (Leg 141) and Oregon (Leg 146) accretionary complexes, which were focused on understanding the mechanics and hydrology of accretionary wedges. Results from these expeditions have highlighted the need to 1) dedicate a Leg to exploring gas hydrate formation in active accretionary wedges, and 2) develop new tools and techniques to better estimate in situ hydrate and gas concentrations. ODP Leg 204 was dedicated to addressing these needs.

Additional results and data that relate to ODP Legs 201 and 204, as well as specific outcomes from this DOE/NETL project, are available online at the ODP Publications website for Leg 201: <[http://www-odp.tamu.edu/publications/201\\_IR/201TOC.HTM](http://www-odp.tamu.edu/publications/201_IR/201TOC.HTM)> and for Leg 204: <[http://www-odp.tamu.edu/publications/204\\_IR/204TOC.HTM](http://www-odp.tamu.edu/publications/204_IR/204TOC.HTM)>.

Accurate quantification of hydrate and gas concentrations has been elusive so far due to hydrate dissociation and gas loss during core retrieval unless core is retrieved at in situ pressure (Paull and Ussler, 2001). Furthermore, commonly used geochemical proxies for estimating the in situ hydrate concentration of sediments are not adequate because the initial composition of pore waters is not known and can be very variable. Consequently, a major focus of Leg 204, following on the testing conducted during Leg 201, was to acquire samples under pressure using the ODP PCS system and the recently developed HYACE system (<http://www.tu-berlin.de/fb10/MAT/hyace.html>), which includes a laboratory transfer chamber for maintaining pressure while making physical properties measurements (<http://www.geotek.co.uk/hyace.html>).

Drilling results to date also suggest that there are other factors controlling the depth to which gas hydrates are stable in addition to temperature, pressure and methane solubility (e.g. Ruppel, 1997) and that hydrate may persist in a metastable state outside the stability field (Guerrin et al., 1999; Buffett and Zatsepina, 1999). To address these outstanding issues, we had frequent deployments of tools to measure in situ temperature and pressure, especially in zones where logging-while-drilling (LWD) data indicated rapid changes in the physical properties of the sediments.

Because of the recognition that estimation of hydrate and free gas concentrations using geophysical remote sensing techniques is more complicated than previously thought (e.g. MacKay et al., 1994; Holbrook et al., 1996), Leg 204 also conducted an extensive suite of downhole and two-ship seismic experiments.

### ***Geological and Geophysical Setting of Hydrate Ridge***

Hydrate Ridge is a 25 km long and 15 km wide ridge in the Cascadia accretionary complex, formed as the Juan de Fuca plate subducts obliquely beneath North America at a rate of about 4.5 cm/yr. Sediment on the subducting plate contains large volumes of sandy and silty turbidites. At present, most of this sediment is accreted to the continental margin, either by offscraping at the deformation front or by underplating beneath the

*In-Situ Sampling and Characterization of Naturally Occurring Marine Methane Hydrate Using the D/V JOIDES Resolution.*

accretionary complex some 10s of kilometers east of the deformation front (MacKay et al., 1992; MacKay, 1995).

Hydrate Ridge has been the site of many geological and geophysical cruises since cold seeps were first discovered on this part of the margin nearly 20 years ago (Kulm et al., 1986). Hydrate Ridge is characterized by: a northern peak having a minimum water depth of about 600 m, and a southern peak with a water depth of about 800 m. Hydrate Ridge appears to be capped by hydrate, as indicated by a nearly ubiquitous and strong BSR (Trehu et al., 1999).

A regional 2-D multichannel seismic survey was acquired in 1989 as a site survey for ODP Leg 146, which was designed primarily to study dynamics of fluid flow in accretionary complexes. The location where an upward deflection of the BSR is cut by a fault on the northern summit of Hydrate ridge was selected for ODP Site 892 (ODP Leg 146 Scientific Party, 1993). At this site, massive H<sub>2</sub>S-rich hydrates were recovered from 2-19 mbsf (Kastner et al., 1995). No hydrate was recovered from near the BSR, but geochemical pore water and temperature anomalies suggested the presence of disseminated hydrate in the pore space to 68 mbsf (Kastner et al., 1995; Hovland et al., 1995). Vertical seismic profiles (VSP) indicated the presence of free gas for at least 20 m beneath the gas hydrate stability zone (MacKay et al., 1994). Trehu and Flueh (2001) argue, based on seismic velocities and attenuation, that free gas is present for 500-600 m beneath the BSR at Site 892. Methane at Site 892 is primarily of biogenic origin (Kvenvolden, 1995), but higher order hydrocarbons of thermogenic origin are also present (Hovland et al., 1995; Schluter et al., 1998).

Since 1996, there have been several cruises/year, which have generated an extensive database of swath bathymetry, deep-towed sidescan, and seafloor observations and samples collected via submersible and remotely operated vehicle (Suess and Bohrmann, 1997; Torres et al., 1998, 1999; Bohrmann et al., 2000; Linke and Suess, 2001). In addition, a high-resolution 3-D seismic survey was conducted in 2000 as a site survey for Leg 204 (Trehu and Bangs, 2001; Trehu et al., 2002). Those data provide a framework for interpreting the Leg 204 results.

### ***Seafloor Observations of Southern Hydrate Ridge***

Sidescan data, seafloor camera tows, and diving with manned and remotely operated submersibles demonstrated the presence of extensive massive carbonate pavement on the northern summit of Hydrate Ridge (Carson et al., 1994; Clague et al., 2001, Sample and Kopf, 1995; Bohrmann et al., 1998; Greinert et al., 2001). Until recently, massive authigenic carbonate pavement was thought to be absent on the southern summit of Hydrate Ridge. During Alvin dives in 1999, however, a 50 m high carbonate "pinnacle" was discovered 250 m southwest of the summit (Torres et al., 1999). Deep-towed sidescan data indicate that the pinnacle is located in the center of a buried carbonate apron with a diameter of ~250 meters. Authigenic carbonates on the Cascadia margin

*In-Situ Sampling and Characterization of Naturally Occurring Marine Methane Hydrate Using the D/V JOIDES Resolution.*

form from methane oxidation within the sediments and discharge of isotopically light dissolved inorganic carbon at seafloor. The relative absence of carbonate on the southern summit of Hydrate Ridge was interpreted to indicate that this hydrate/gas system is younger than that on the northern summit, providing a spatial proxy for temporal evolution of hydrate-bearing accretionary ridges (Trehu et al., 1999). This interpretation is supported by U-Th dating of recovered carbonates (Teichert et al., 2001), which indicates that the pinnacle is <12,000 years old whereas the carbonate carapace on northern Hydrate Ridge is > 100,000 years old.

One especially interesting feature of southern Hydrate Ridge is the abundance of massive hydrate at the seafloor near its summit. This was first discovered in 1996, when over 50 kg of massive hydrate were recovered in a TV-guided grab sample (Bohrmann et al., 1998). The samples show dense interfingering of gas hydrate with soft sediment. In most cases, pure white hydrate occurs in layers several millimeters to several centimeters thick. Host sediment is often present as small clasts within the pure gas hydrate matrix. On a macroscopic scale, the fabric varies from highly porous (with pores of up to 5 cm in diameter) to massive (Suess et al., 2001). Thin sections show a structure in which gas bubbles have been filled with hydrate. Wet bulk densities of 80 hydrate samples measured on board R/V Sonne range from 0.35 g/cm<sup>3</sup> to 7.5 g/cm<sup>3</sup>. Pore space was estimated from the change in sample volume before and after compression to approximately 160 bar (Bohrmann et al., 2002). The samples show high variability in pore volumes ranging from 10-70 vol.%, and the values are negatively correlated with sample density. From this correlation, the end-member density at zero porosity was estimated to be ~0.81 g/cm<sup>3</sup>. This value is lower than the theoretical density of pure methane hydrate (0.91 g/cm<sup>3</sup>). Field-emission scanning electron microscopy indicates that this is due to submicron porosity of the massive hydrate (Techmer et al. 2001).

The low bulk density of the natural methane hydrates from Hydrate Ridge results in a strong positive buoyancy force, implying that the hydrate remains on the seafloor only because of the shear strength of the host sediment. Unusual seafloor topography observed on southern Hydrate Ridge during ALVIN and ROPOS surveys, which is characterized by mounds and depressions with a wavelength of a few meters, may result from spontaneous breaking off of hydrate from the seafloor. This may be an important mechanism for transporting methane from the seafloor to the atmosphere.

Vigorous streams of methane bubbles have been observed emanating from vents on the seafloor on the northern and southern peaks of Hydrate Ridge (Suess and Bohrmann, 1997; Suess et al., 1999; Torres et al., 1998, 1999) as well as from a similar, but smaller, reflective high in the accretionary complex known as SE Knoll. Because the seafloor at all three sites is well within the hydrate stability zone, the presence of methane bubbles beneath and at the seafloor suggests rapid transport of methane to the seafloor from sediments beneath the hydrate stability zone. Because seawater is undersaturated in methane, the persistence of gas bubbles in the water column suggests that they are protected by a thin coating of hydrate (Suess et al., 2001). Disappearance of the acoustic

*In-Situ Sampling and Characterization of Naturally Occurring Marine Methane Hydrate Using the D/V JOIDES Resolution.*

"bubble" plumes at 450-500 m below the sea surface (near the top of the hydrate stability zone) suggests that the hydrate shell dissociates and that most of the methane in the bubble plumes is dissolved in the ocean rather than reaching the atmosphere.

### ***High-resolution 3-D seismic data***

Two 2-D multichannel seismic profiles acquired in 1989 across southern Hydrate Ridge suggested a complicated subsurface plumbing system related to the presence of hydrate and free gas. Prior to a 3-D high-resolution seismic survey in 2000 (Trehu and Bangs, 2001), the relationship between subsurface reflections and the summit vents was not known because no profiles crossed the summit. The 3-D survey comprised 81 profiles spaced 50 meters apart and covered the southern summit of Hydrate Ridge and the western edge of the adjacent slope basin. Shots from 2 GI guns fired simultaneously were recorded on the Lamont portable 600-m-long, 48-channel towed streamer and on an array of 21 UTIG 4-component ocean bottom seismometers. The locations of the ship and of the streamer were determined via differential GPS and four compasses, respectively, and 3-D fold was monitored during the cruise to identify locations where additional data were needed. Excellent data quality was obtained in spite of strong winds and high seas. The data contain frequencies up to ~250 Hz, providing considerable stratigraphic and structural resolution.

### ***Stratigraphic and structural controls on hydrate development***

The structural and stratigraphic setting of Hydrate Ridge contrasts with that of the adjacent slope basin to the east. Beneath the slope basin, the seismic signature of the hydrate is quite similar to that on the Blake Ridge, with an intermittent BSR and enhancement of stratigraphic reflectivity beneath the BSR (Holbrook et al., 1996). Sedimentation rate in this basin is likely very rapid, based on radiocarbon dating of a core in a neighboring basin just north of Hydrate Ridge (Karlin, 1983), which indicates a sedimentation rate of 120 cm/1000 yr. Sediments in that core are siliceous hemipelagic ooze with calcareous microfossils, and similarity in high frequency energy penetration between the two basins suggests a similar sediment composition. Because of this expected high sedimentation rate and high carbon content in the sediments, we suspect that the source of methane in this setting will be dominantly local, with little or no contribution from subducted sediments. In contrast, fluids migrating upward from underthrust sediments may be a significant source of methane for hydrate beneath Hydrate Ridge (Hyndman and Davis, 1992). Leg 204 tested the hypothesis that the distribution, texture, and chemistry of hydrate and related pore fluids beneath Hydrate Ridge differ from those the slope basin.

### ***Formation of massive hydrate near the seafloor***

The presence of massive hydrate near the seafloor is enigmatic, as most models for hydrate formation in a region of diffuse fluid flow predict a decreasing gradient in

*In-Situ Sampling and Characterization of Naturally Occurring Marine Methane Hydrate Using the D/V JOIDES Resolution.*

hydrate concentration above the BSR (eg. Paull et al., 1994; Rempel and Buffett, 1998; Xu and Ruppel, 1999). Several explanations have been proposed, including formation in the past when the stability boundary was near the seafloor, formation at depth and exposure by erosion (Bohrmann et al., 1998), and transport of methane through the hydrate stability field as free gas isolated from water (Suess et al., 2001). The third explanation is most likely given the observations of vigorous plumes of bubbles at the seafloor and in the water column where the massive hydrates are observed. One objective of Leg 204 was to obtain insight into the mechanisms whereby the gas is isolated from water, thus delaying hydrate formation as it passes through the stability field. In addition, drilling through these massive hydrate deposits provided new constraints on their extent, texture, structural setting, and the chemistry of interstitial waters.

### ***Calibration of geophysical estimates of hydrate and gas volumes***

Better calibration of regional estimates of hydrate and free gas volumes based on geophysical mapping and modeling techniques is of critical importance towards estimating the global abundance of hydrate and evaluating their role in climate change and potential for economic exploitation. Recent experience during Legs 146 and 164 has underlined the complexity of this issue. During Leg 204, we drilled through hydrates in a variety of settings with different seismic characteristics and measured the physical properties of the hydrate stability and underlying free gas zones with temperature and pressure probes and through downhole logging and a series of nested seismic experiments, thus providing data to calibrate various techniques for remote sensing of hydrate distribution and concentration.

### ***Hydrates and slope stability***

The possible relationship between hydrates and slope failure is presently poorly understood. On the one hand, hydrates may stabilize slopes by cementing sediment grains. On the other hand, if hydrates impede fluid flow, they may weaken the underlying sediment by trapping fluids and free gas. There may be a feedback between these two processes such that the presence of hydrate initially delays slumping, leading to less frequent but larger episodes. Several investigators have noted the possible correlation of hydrates and slope instability (e.g. Booth et al., 1994; Trehu et al., 1995; Paull et al., 1996) and have discussed how such slope instability might release massive amounts of methane into the ocean (Paull et al., 1996; Nisbet and Piper, 1998). One objective of Leg 204 was to determine the mechanical and hydrological properties of hydrate-bearing sediment to better constrain models of slope instability.

### ***Impact on the geochemical and geological record***

Geochemical consequences of hydrate formation and destabilization include: modification of the isotopic composition of the water in pore fluids; changes in the

*In-Situ Sampling and Characterization of Naturally Occurring Marine Methane Hydrate Using the D/V JOIDES Resolution.*

isotopic composition of the dissolved carbonate species, which is incorporated into carbonate phases; and sequestering of the in situ generated  $H_2S$  into the hydrate structure. Isotopic composition of carbonate cements recovered by drilling during Leg 146 were used by Sample and Kopf (1995) to infer the history of fluid flow in this margin as well as the depth of the source of the carbon reservoirs. Bohrmann et al. (1998) have suggested that the stability of the massive gas hydrate deposits on the southern summit of Hydrate Ridge has changed with time, and that carbonate phases associated with the hydrates can be used to document the changes. Benthic foraminifers might also record this decrease in  $\delta^{13}C$ , and thus the isotopic signal might reveal episodes of  $CH_4$  venting in the past (Wefer and al., 1994; Dickens et al., 1995, 1997; Kennett et al., 1996). One objective of Leg 204 was to determine the isotopic composition of the pore fluids and carbonates associated with hydrate to provide the framework needed to unravel the history of hydrate formation and destabilization recorded in benthic foraminifera and authigenic carbonate phases elsewhere.

### ***Biological communities associated with hydrate and underlying free gas zones***

Micro-organisms playing an important role in both methane formation and oxidation and are therefore a critical component of the hydrate system. Identification of these organisms and determination of their abundances, spatial variability and rates of activities is just beginning. Important questions addressed during Leg 204 included: What impact do these organisms have on the volume of methane produced and oxidized beneath Hydrate Ridge? At what depths are they concentrated? What effect do they have on sediment diagenesis and the development of magnetic minerals? Does the hydrate-related biosphere differ between Hydrate Ridge and the adjacent slope basin? How do microorganisms affect sediment and porewater chemistry and texture, and vice-versa?

### ***Biological communities associated with hydrate and geochemical implications***

Communities of tube worms, bacterial mats, clams and other fauna are associated with seafloor hydrates and methane vents on Hydrate Ridge and elsewhere (e.g. Kulm et al., 1986; MacDonald et al., 1989; Suess et al., 1999, 2001; Sassen et al., 2001). Micro-organisms are at the base of the food chain in these communities. Recent work suggests the complex complementary relationships between sulfate reducing, methanogenic, and methanotrophic micro-organisms in hydrate-bearing sediments (e.g. Parkes et al., 2000; Boetius et al., 2000). These micro-organisms must be playing an important role in methane formation and oxidation and are therefore a critical component of the hydrate system. Identification of these organisms and determination of their abundances, spatial variability and rates of activities is just beginning.

Particularly interesting are recently discovered organisms that play a critical role in anaerobic methane oxidation (AMO), which is the process forming the carbonates that remain in the geologic record of the history of past fluid flow and hydrate formation

*In-Situ Sampling and Characterization of Naturally Occurring Marine Methane Hydrate Using the D/V JOIDES Resolution.*

and dissociation (eg. Sample and Kopf, 1995; Bohrmann et al., 1998; Greinert et al., 2001). Very high rates of AMO have been measured in sediment overlying massive gas hydrates on southern Hydrate Ridge (Boetius et al., 2000), and attributed to structured aggregates consisting of a central cluster of methanotropic archaea coated by sulfate reducing bacteria. That microbes oxidize methane by utilizing sulfate in the absence of oxygen was long suspected by geochemists, based on interstitial sulfate and methane gradients. Borowski et al. (1996) showed that steep sulfate gradients and shallow depths to the sulfate-methane interface are a consequence of the increased influence of AMO, and Boetius et al. (2000) were the first to observe the microorganisms that presumably catalyze anaerobic methane oxidation. These bacterial aggregates appear to be abundant in sediments of Hydrate Ridge and mediate AMO when enough sulfate is available.

Analysis of sulfide minerals provides a possible opportunity to reconstruct past biological activity because most of the reduced sulfide produced during bacterial sulfate reduction in non-hydrate-bearing sediments is ultimately sequestered in various iron phases, which usually involve multiple steps terminating in the formation of sedimentary pyrite. In the Cascadia margin, the sequestering of sulfide into the clathrate structure (e.g. Kastner et al., 1995, Bohrmann et al., 1998) essentially removes it from further reaction with ferrous iron complexation. There is a wealth of information on the significance of iron-sulfide interactions within marine sediments (e.g. Berner, 1970, and many others). The burial of this mineral phase contributes significantly to the oxygen level of the atmosphere, the sulfate concentration in seawater, and the pH of the oceans over geologic time scales (e.g. Garrels and Perry, 1974; Holland, 1978; Boudreau and Canfield, 1993). Another significant effect of H<sub>2</sub>S sequestering by hydrates is the development of anomalous intervals of high greigite content at the intervals in which gas hydrates were recovered or were inferred to exist (Housen and Musgrave, 1996). Based on the rock magnetic properties at Site 889, Housen and Musgrave (1996) identified the presence of a "fossil gas hydrate zone" which extended downwards to 295 mbsf during the last glaciation.

## **METHODS AND PROCEDURES**

### ***Leg 201 – Infrared Thermal Imaging***

Infrared thermal imaging was introduced on Leg 201 for technique development, prior to its critical use and deployment during Leg 204. IR imaging was shown to successfully identify thermal anomalies in sediment cores, attributed to the location of gas hydrate (cold anomalies) and voids (warm anomalies). The primary benefits of using IR (rather than running a hand down the length of the core) include more precise identification of thermal anomalies and the estimation of hydrate volume in processed images. It is also quicker, simpler, and more compact than a system of thermistors.

Small-scale hydrate nodules and disseminated gas hydrate were the primary form of hydrate identified, suggesting the camera can detect small quantities. Another proposed use for the camera is for the lithologic characterization of ambient-temperature cores

*In-Situ Sampling and Characterization of Naturally Occurring Marine Methane Hydrate Using the D/V JOIDES Resolution.*

because of slight variations in their thermal emission properties attributable to sediment composition or water content. Data were collected during Leg 201 to examine this possibility.

### ***Leg 201 – Infrared (IR) Thermal Image Processing***

In order to develop downcore temperature profiles from the infrared thermal image data, the following process was established through experimentation over the course of ODP Leg 201:

- (1) ThermaCam “Researcher” software was embedded as an object into an Excel spreadsheet. The sequence file containing each image from the core scan was selected and opened in “Researcher”.
- (2) An analysis box was hand selected in the first image of the sequence file. The analysis box was placed to avoid areas of significant reflection or other interference.
- (3) The sequence file was played from beginning to end to ensure appropriate box placement. The sequence file was reset to the beginning.
- (4) In Excel, a macro was written to run the sequence file and extract the maximum, minimum, and average temperature from the analysis box in each image, as well as the time at which each image was taken.
- (5) The curated depth was assigned as the depth of the first image.
- (6) The recovered interval of core was divided into the total number of images in the sequence file. This interval was sequentially added to the top depth, providing a depth for each image (or temperature distribution).

Following this process, the data files were plotted individually as downcore temperature profiles and combined to provide downhole temperature profiles. Where core recovery was in excess of 100%, the overlapping depth interval was removed from the upper core by hand. Similar techniques were employed on ODP Leg 204.

## **LEG 204 – METHODS AND PROCEDURES**

### ***Site Planning Based on Three-Dimensional Seismic Data***

The three-dimensional (3-D) seismic reflection data, collected before the cruise, imaged a 4 km<sup>o</sup> – 11 km volume recorded to 3 s two-way traveltime (Tréhu and Bangs, 2001). The survey used a differential GPS navigation system provided by RACAL Geodetic. Four base stations (Vancouver, British Columbia, Canada; Washington state; northern

*In-Situ Sampling and Characterization of Naturally Occurring Marine Methane Hydrate Using the D/V JOIDES Resolution.*

California; and San Diego, California) provided differential corrections at 1 Hz. Fixes were smoothed with a 15-s running average filter to eliminate ship's motion and determine shot locations in real time. The single 600-m streamer was navigated with compass readings at 150-m intervals along the streamer. Streamer configuration was constructed from compass data for each shot. Tests of navigation accuracy conducted in port show that the ship's position fell within a 2-m radius 95% of the time. During the experiment, the streamer was located by reconstructing the streamer position from the compass readings. Locations are better in the direction parallel to the streamer than perpendicular to it, but both are probably within 5 m of uncertainty.

Horizontal and vertical resolution of the 3-D seismic images is dependent on the frequency content of the data, which becomes lower and more bandwidth limited with depth of penetration. The Hydrate Ridge 3-D seismic data have an approximate bandwidth of 25–200 Hz and a dominant frequency of 125 Hz at the seafloor. The vertical resolution of these data is therefore 3 m based on resolving distinctions of one-quarter of the dominant frequency's wavelength. The common midpoint spacing of 10 m in the in-line and 25 m in the cross-line direction effectively integrates the seismic acoustic impedance data over an estimated first Fresnel zone radius of ~75 m at the seafloor.

First-order depth conversions of the seismic reflection data were calculated using velocities obtained from ocean-bottom seismometer data acquired with the 3-D data (Arsenault et al., 2001). These were further refined during the cruise using major seismic horizons correlated to the core and logging data and through velocities obtained from the wireline and core data.

### ***Navigation***

During Leg 204, surface navigation consisted of dynamic positioning at the surface relative to an acoustic beacon placed on the seafloor at each drill site. A Global Positioning System (GPS) was used after the selective availability signal was removed, thereby providing the accuracy of P-code GPS. There is no navigation information for the bottom of the drill string; therefore, its exact position relative to the ship's position is unknown. We assume that the hole's position is directly below the rig floor. During previous drilling, deviation of the hole from the ship's position was determined from cores recovered at shallow depths by the advanced piston corer (APC). Little significant deviation from the vertical was noted.

### ***Drilling Operations***

Three standard coring systems were used during Leg 204: the APC, the extended core barrel (XCB), and the rotary core barrel (RCB). These standard coring systems and their characteristics are summarized in Graber et al. (2002) [For further information about tools, see: <<http://www-odp.tamu.edu/publications/tnotes/tn31/INDEX.HTM>>] and in

*In-Situ Sampling and Characterization of Naturally Occurring Marine Methane Hydrate Using the D/V JOIDES Resolution.*

the “Explanatory Notes” chapters of the ODP Initial Reports volumes; e.g., Leg 201 methods, see: <[http://www-odp.tamu.edu/publications/201\\_IR/201TOC.HTM](http://www-odp.tamu.edu/publications/201_IR/201TOC.HTM)> ; Leg 204 methods, see: <[http://www-odp.tamu.edu/publications/204\\_IR/204TOC.HTM](http://www-odp.tamu.edu/publications/204_IR/204TOC.HTM)>. Most cored intervals were ~9.6-m long, which is the length of a standard core barrel. In other cases, the drill string was “washed ahead” without recovering sediments in order to advance the drill bit to a target depth where core recovery needed to be resumed. In addition to these conventional coring tools several pressure-coring systems were used. In situ temperature and pressure were measured at ~10 depths in each hole. Logs of geophysical and geochemical parameters were obtained during logging-while-drilling (LWD) and using wireline tools.

Drilled intervals are referred to in meters below rig floor (mbrf), which are measured from the kelly bushing on the rig floor to the bottom of the drill pipe, and meters below seafloor (mbsf), which are calculated. When sediments of substantial thickness cover the seafloor, the mbrf depth of the seafloor is determined with a mudline core, assuming 100% recovery for the cored interval in the first core. Water depth is calculated by subtracting the distance from the rig floor to sea level from the mudline measurement in mbrf. This water depth usually differs from precision depth recorder measurements by a few to several meters. The mbsf depths of core tops are determined by subtracting the seafloor depth (mbrf) from the core top depth (mbrf). The resulting core top data in mbsf are the ultimate reference for any further depth calculation procedures.

### ***Drilling Deformation***

When cores are split, many show signs of significant sediment disturbance, including the concave-downward appearance of originally horizontal bedding, haphazard mixing of lumps of different lithologies (mainly at the tops of cores), fluidization, and flow-in. Core deformation may also occur during retrieval because of changes in pressure and temperature as the core is raised and during cutting and core handling on deck. These changes were particularly important during Leg 204 because temperature and pressure variations induce exsolution of gas from interstitial waters (IWs) and dissociation of gas hydrate, which also releases large amounts of gas. This type of disturbance and can, therefore, serve as proxies for the presence of gas hydrates in situ.

### ***Curatorial Procedures and Sample Depth Calculations***

Numbering of sites, holes, cores, and samples follows the standard Ocean Drilling Program (ODP) procedure. A full curatorial identifier for a sample consists of the leg, site, hole, core number, core type, section number, and interval in centimeters measured from the top of the core section. For example, a sample identification of 204-1244A-1H-1, 10–12 cm, represents a sample removed from the interval between 10 and 12 cm in Section 1 of Core 1 (“H” designates that this core was taken with the APC system) of Hole 1244A during Leg 204. Cored intervals are also referred to in “curatorial” mbsf. The mbsf of a sample is calculated by adding the depth of the sample below the section

*In-Situ Sampling and Characterization of Naturally Occurring Marine Methane Hydrate Using the D/V JOIDES Resolution.*

top and the lengths of all higher sections in the core to the core top datum measured with the drill string.

A sediment core from less than a few hundred mbsf may, in some cases, expand upon recovery (typically 10% in the upper 300 mbsf), and its length may not necessarily match the drilled interval. In addition, a coring gap is typically present between cores. Thus, a discrepancy may exist between the drilling mbsf and the curatorial mbsf. For instance, the curatorial mbsf of a sample taken from the bottom of a core may be larger than that of a sample from the top of the subsequent core, where the latter corresponds to the drilled core top datum. If a core has incomplete recovery, all cored material is assumed to originate from the top of the drilled interval as a continuous section for curation purposes. The true depth interval within the cored interval is not known. This should be considered as a sampling uncertainty in age-depth analysis and correlation of core facies with downhole log signals.

### ***Core Handling and Analysis***

Cores were generally handled according to the ODP standard core-handling procedures as described in previous Initial Reports volumes and the Shipboard Scientist's Handbook, with modifications required to quickly identify intervals containing gas hydrates and to maintain approximately sterile conditions for microbiological sampling. Precautions were also taken to identify and safely deal with hydrogen sulfide.

To identify gas hydrates, cores were scanned with both handheld and track-mounted infrared (IR) cameras. Intervals with significant thermal anomalies were marked with magic marker, and whole-round cores were removed and stored in liquid nitrogen or pressure vessels. Some suspected gas hydrate-bearing intervals were cut and immediately dropped into liquid nitrogen-filled dewars on the catwalk. Others were rapidly frozen. Others were placed in pressure chambers. Others were allowed to dissociate for various shipboard IR calibration experiments or geochemical analyses.

Certain cores were identified ahead of time as being candidates for microbiological sampling and tagged with tracers. When these cores were brought on board, appropriate sections for microbiological study were identified by the microbiologist on shift and taken immediately to the microbiology laboratory, which was located in a refrigerated van aft of the drilling floor. Gas samples for routine shipboard safety and pollution-prevention samples were collected on the catwalk. Whole rounds (10 to 20 m long) were taken for interstitial water (IW) analysis. The cores were then compressed with a plunger to remove large voids and cut into nominally 1.5-m sections. The remaining cut sections were transferred to the core laboratory for further processing.

Whole-round core sections not used for microbiological sampling were run through the multisensor track (MST), and thermal conductivity measurements were performed. The cores were then split into working and archive halves (from bottom to top). Investigators

*In-Situ Sampling and Characterization of Naturally Occurring Marine Methane Hydrate Using the D/V JOIDES Resolution.*

should be aware that older material may have been transported upward on the split face of each section.

Visual core descriptions (VCDs) were prepared of the archive halves augmented by smear slides and thin sections. The archive halves were photographed with both black-and-white and color film. In addition, close-up photographs were taken of particular features for illustrations in site chapters, as requested by individual scientists. All sections of core not removed for microbiological sampling were additionally imaged using a digital imaging track system equipped with a line-scan camera. A few cores of special interest were measured for color reflectance and high-resolution magnetic susceptibility (MS) using the archive multisensor track (AMST), but this was not standard procedure for most cores because of time limitations. No paleomagnetic studies were done on board because of limited personnel. Moreover, shipboard biostratigraphy indicates that most cores were too young for magnetostratigraphy to have provided significant temporal resolution.

The working half was sampled both for shipboard analysis, such as physical properties, carbonate, and bulk X-ray diffraction (XRD) mineralogy and for shore-based studies. Both halves of the core were then put into labeled plastic tubes, sealed, and placed in cold storage space aboard the ship. At the end of the leg, the cores were transferred from the ship into refrigerated containers and shipped to the ODP Gulf Coast Core Repository in College Station, Texas.

### ***Infrared Thermal Imaging***

IR thermal imaging of the surface of the core liner was fully implemented during Leg 204. The initial development of the technique was accomplished during Leg 201, where IR imaging was shown to successfully identify thermal anomalies associated with gas hydrate and voids.

Thermal anomalies in marine sediment cores on short length scales (less than a few meters) could result from (1) adiabatic gas expansion, (2) gas exsolution from pore water, or (3) gas hydrate dissociation. All of these processes cool cores (Ussler et al., unpubl. data). However, discrete, strong cold anomalies in Leg 204 cores were shown to be directly associated, spatially, with gas hydrate. These negative temperature anomalies, in general, were caused by gas hydrate dissociation in the core line after the core arrived on deck. Variations in heat capacity also impact core temperatures, but generally differences in thermal conductivity or density are relatively small and do not result in large enough heat capacity differences to cause discrete, negative thermal anomalies.

IR imaging on Leg 204 also confirms earlier thermistor measurements that show variations in thermal structure along entire cores, which are typically warmer at the bottom and cooler at the top (Ussler et al., unpubl. data). Gas expansion and gas exsolution may account for the observed gradient along cores. If so, the thermal structure

*In-Situ Sampling and Characterization of Naturally Occurring Marine Methane Hydrate Using the D/V JOIDES Resolution.*

developed principally during ascent of the core through the upper part of the water column. Alternatively, the thermal structure along entire cores may reflect differences in frictional heating during coring, creating warmer temperatures near the core barrel shoe (APC) or bit (XCB) and cooler temperatures near the core top. Analysis of data from the advanced piston corer methane (APCM) tool from Leg 204 is expected to help determine the origin of temperature gradients typically observed along each core. Regardless of the origin of the overall thermal structure of cores, the discrete, negative thermal anomalies associated with gas hydrate are superimposed on the broader gradient, providing a robust proxy for the location and abundance of gas hydrate in cores. Gas shows up as warm anomalies because of the low heat capacity of gas voids compared to sediment and in spite of the cooling effect of gas expansion.

The primary benefits of using IR cameras (rather than running a hand down the length of the core) include the following: (1) more precise identification of thermal anomalies, (2) the estimation of hydrate volume in processed images, and (3) determinations of shapes of gas hydrate. The IR camera is also quicker and simpler to use and has a much higher spatial resolution than an array of thermistors. Hydrate veins or lenses, hydrate nodules, and disseminated gas hydrate were all identified. The resolution of thermal anomalies observed indicates that the camera can detect small volumes of gas hydrate if they are adjacent to the core liner. Determining precise, quantitative volumetric estimates of gas hydrate in cores was an objective during Leg 204, but realizing this objective will require further analysis of collected data.

IR images were used to do the following:

1. Rapid identification of gas hydrate in cores from temperature anomalies on the surface of the core liner for immediate sampling of gas hydrate;
2. Preliminary assessment of the abundance of gas hydrate in cores based on the volume of core that shows thermal anomalies of varying  $\Delta T$ s;
3. Quantification of the relative proportions of different gas hydrate textures;
4. Estimation of the cross-sectional temperature gradient in cores prior to sampling for microbiology;
5. Assessment of the thermal structure of entire cores and the differences in thermal structure between APC and XCB cores.

### ***IR Imaging Methodology***

Two ThermaCam SC 2000 cameras (FLIR Systems) and an AVIO Neo Thermo model TVS-610 (Nippon Avionics Co., Ltd.) were used to map temperature variations along core. The FLIR Systems cameras provide temperature-calibrated images over a temperature range from  $-40^{\circ}$  to  $\geq 1500^{\circ}\text{C}$ . For shipboard measurements, the cameras were set to record a more limited range of temperatures from  $-40^{\circ}$  to  $\geq 120^{\circ}\text{C}$  (Range 1). To perform the critical task of rapid identification of gas hydrate within the core on the catwalk, one of the FLIR Systems IR cameras was mounted on a track above the catwalk and driven automatically by a stepper motor controlled by a LabView software program.

*In-Situ Sampling and Characterization of Naturally Occurring Marine Methane Hydrate Using the D/V JOIDES Resolution.*

The camera was mounted in such a way that a 20-cm field of view along the core was obtained with the camera lens located 55 cm from the top of the surface of the core liner. To minimize the effect of external IR radiation reflecting off the core-liner surface, the camera was enclosed within a cardboard sheath covered on the outside with aluminized Mylar and lined on the inside with black felt (Fig. F10). After operations at Site 1244 were complete, the catwalk was also shaded with cardboard and the camera enclosure was extended to minimize ambient IR reflections from the core liner.

Images and data for each core were acquired immediately after the core liner was wiped dry. The mounted camera was moved down the core in 20-cm increments, starting 10 cm from the core top. Each image was saved with a unique identifier (header file) that included information about the position of the center of the image. Initially, all images were automatically saved over the shipboard computer network. Network slowdowns early in the cruise necessitated modification of the system to save images for a single core directly on the computer controlling the camera. Images were then manually transferred over the network to a laptop computer dedicated to processing of the IR images.

Camera span and level parameters were automatically adjusted to optimize visual contrast on the computer screen for the expected downcore temperature variation. A physical properties scientist or technician observed the scan results visually, either by following the camera-mounted monitor or by looking at the monitor connected to the computer controlling the scan. As soon as each scan was completed, scientists typically examined the scan results on the laptop computer running ThermaCam Researcher software in the core laboratory. The locations of thermal anomalies were marked on the core and wholeround samples (e.g., hydrate and microbiology samples) were collected as defined by the core-sampling plan for the hole. After catwalk sampling, the cores were cut into 1.5-m sections and many cores were re-imaged to provide an image sequence matching the length of the curated core sections.

The track-mounted IR imaging camera was supplemented on most cores by discrete imaging using a second FLIR Systems camera or an AVIO Neo Thermo camera in a handheld mode. In this mode, one of the physical-properties scientist walked along the catwalk with the IR camera pointed perpendicular to the core liner, usually just after the track scan was completed. This approach provided immediate confirmation of temperature anomalies from a viewpoint rotated 90° from the orientation of the track scan. If anomalies were detected, they were marked on the core, stored on the camera's memory card, and logged on a log sheet; later, the files were transferred to the ship's computer network for storage, analysis, and archiving. Temperature anomalies detected with the handheld camera were compared with the track scans, and decisions were made to guide the sampling of any gas hydrate present. In some instances, subtle thermal anomalies or observations of gas escaping from holes drilled into the core liner triggered the decision to perform an additional track scan. Results from successive scans could then

be directly compared; typical results show the spatial expansion of cold zones over time periods of only a few minutes.

### ***Thermal Image Processing***

To develop downcore profiles of temperature anomalies, the following procedures were established, building on the experience from Leg 201:

1. ThermaCam Researcher software was embedded as an object into a Microsoft Excel spreadsheet. The folder containing sequential images from the core scan was selected and opened in Researcher.
2. An analysis box was used to extract temperature data from the central part of the core image.
3. In Microsoft Excel, a macro was written to extract the pixel-by-pixel temperature values as ASCII data.
4. These ASCII data were then transferred to a UNIX workstation to extract the pixel-by-pixel temperature values from the analysis box imbedded in each image as well as the depth of the center of each image. Depths were then calculated and assigned to each pixel in successive images from a given core.

Following this process, the data files were combined to provide profiles of downhole temperature anomalies. Where core recovery was >100%, the overlapping depth interval was manually edited and the data were deleted from the resulting profile.

### ***Extraction of Thermal Anomaly Data***

Downcore thermal profiles and IR images were used to extract individual negative thermal anomalies (cold zones on the core liner). Parameters obtained were (1) core and section (if available); (2) depth interval on uncut liner (top and bottom); (3)  $\Delta T$  (peak anomaly temperature–background temperature); and (4) gas hydrate texture or shape description and other comments on anomaly shape. A unique identifier was assigned to each IR anomaly for reference in text and figures. Results were tabulated for each site. Thermal anomalies were identified from the downcore temperature profiles derived from the images as described in the previous section. An analysis of thermal data on board showed that  $\Delta T$  values indicative of hydrate were insensitive to ambient catwalk temperature and illumination conditions. The  $\Delta T$  values provide an approximate measure of hydrate abundance, albeit influenced by the proximity of hydrate to the core liner. Gas hydrate undergoing dissociation and directly in contact with the core liner produces a larger  $\Delta T$  than hydrate insulated from the liner by sediment.

It is important to note that depth measurements were recorded on uncut core liners before sectioning and removal of gas voids. Hence, depth assignments do not precisely match the curated depths of core sections; typically depth differences are <1 m. Hydrate samples are included on IR anomaly tables and provide specific data on curated and uncut core-liner depth discrepancies.

*In-Situ Sampling and Characterization of Naturally Occurring Marine Methane Hydrate Using the D/V JOIDES Resolution.*

### *Comparison of Thermal Anomaly Data with Sw*

Extracted thermal anomalies were plotted as a function of depth and, for many sites, compared with pore water saturation (Sw) derived from resistivity logs using Archie's Relation. The visual comparison of the two data sets provided a useful means of assessing the overall similarity of the two methods in detecting differences in gas hydrate abundance as a function of depth. Calculation of Sw is ordinarily used to estimate volume fraction of pore space occupied by pore water in a homogeneous media as opposed to a more resistive fluid such as gas or liquid hydrocarbons. In the GHSZ, it is assumed that the resistive material is gas hydrate, which may be present in veins that are very heterogeneous. This heterogeneity may cause large errors when calculating Sw in hydrate-bearing sediment and hence should be used with caution. Sw estimates from Hydrate Ridge typically range from 1.0 to 0.5 (usually 1.0 to 0.85), but in some cases (Site 1249) values as low as ~0.1 were obtained. These values are interpreted as:

$$1 - Sw = \text{volume fraction of hydrate};$$

including all hydrate regardless of size of hydrate features (not just porescale hydrate). IR anomalies and Sw were plotted back-to-back with depth on the ordinate,  $\Delta T$  increasing to the left, and Sw increasing to the right on the abscissa. The position of the Sw plot extending to the right from the abscissa provides a visual depiction of the estimated hydrate concentration for direct comparison with the IR thermal anomalies. Values  $>1$  (physically impossible) are truncated in this and other plots of Sw in this volume.

### *Definition of Terms for Hydrate Shapes*

A variety of gas hydrate shapes were observed during the leg, providing significant new insight into how those shapes and textures are distributed in marine sediments. Use of terms for describing hydrate shapes evolved during the leg as sites were drilled. Defining terms used is particularly important for hydrate studies because of the ephemeral nature of gas hydrates. Gas hydrates must be either described within minutes after sampling and prior to dissociation or they must be preserved in pressure vessels or liquid nitrogen where, for the most part, they are not available for further description shipboard. However, IR thermal imaging provided permanent information on hydrate shapes to a resolution of ~0.5 cm. These IR images together with visual observations and photographs of gas hydrate form the basis for the terms described below to define terms defining macroscopic (scales approximately  $\geq 0.5$  cm) geometries of gas hydrates:

- Layer: tabular gas hydrate feature that transects the core conformable to bedding. Its apparent thickness is, typically, on the order of a few centimeters. Layers thicker than ~10 cm are generally considered massive hydrate (interval 204-1250C-11H-3, 94–95 cm).

*In-Situ Sampling and Characterization of Naturally Occurring Marine Methane Hydrate Using the D/V JOIDES Resolution.*

- **Lens:** a hydrate layer or other feature with tapering margins. Many hydrate layers may be lenses on a scale larger than the core diameter.
- **Vein:** tabular gas hydrate feature that transects the core at an angle to bedding. Its apparent thickness is, typically, on the order of a few centimeters. Veins thicker than ~10 cm are generally considered massive hydrate (interval 204-1244C-8H-1, 47–52 cm).
- **Veinlet:** thin, tabular hydrates ~1 mm thick or less, commonly present adjacent to veins or layers and oriented in mutually orthogonal directions. Veinlets are visible by eye or with the aid of a hand lens but were commonly the smallest macroscopic hydrate features observed during Leg 204.
- **Nodular:** spherical to oblate features typically 1–5 cm in diameter. Two-dimensional circular shapes in IR images on core liners are usually described as nodular, recognizing that 3-D shapes may actually be blades or rods. Shipboard examination of liquid nitrogen–preserved cores clearly shows that some nodular IR features are, in fact, nearly spherical in shape, whereas others are rod or blade shaped with long dimensions significantly greater than the core diameter (interval 204-1244C-10H-2, 70–103 cm).
- **Disseminated:** hydrate grains less than ~3 mm distributed throughout the sediment matrix. This includes grain size ranging from ~3 mm to pore scale and produces IR anomalies that have diffuse boundaries. IR data typically cannot distinguish between disseminated hydrate and a single hydrate nodule in the center of the core. Any distributed form of hydrate with a small dimension <3 mm may be described as disseminated (interval 204-1249C-2H-1, 108–140 cm).
- **Massive:** the presence of hydrate in core greater than ~10 cm in thickness and with less than ~ 25% intercalated sediment (Section 204-1249C-1H-CC).

### ***Downhole Tools and Pressure Coring on Leg 204***

During Leg 204, a suite of downhole tools was employed to measure in situ temperature and pore pressure, to retrieve cores under pressure, and to estimate the in situ concentration of methane and other natural gases. Temperature, pressure, and gas composition and concentration are the critical factors for determining the extent of the GHSZ and whether gas hydrate can form in that zone. In addition, temperature affects rates of sediment diagenesis and microbial activity. Pore pressure is important because fluid flow occurs if the pressure gradient differs from hydrostatic, thus transporting natural gas into the GHSZ, providing nutrients for microbes, and modifying the temperature and pressure field.

*In-Situ Sampling and Characterization of Naturally Occurring Marine Methane Hydrate Using the D/V JOIDES Resolution.*

In situ sediment thermal measurements were made during Leg 204 using the APC temperature (APCT) tool and the Davis-Villinger Temperature Probe (DVTP) (Davis et al., 1997). Temperatures and pressures were measured using a DVTP modified to include a pressure port and sensor (Davis-Villinger Temperature-Pressure Probe [DVTTP]) that was previously used during Legs 190 and 201. Pressure was also measured during a trial run of the Fugro-McClelland piezoprobe, which operates on similar principles as the DVTTP.

Retrieval of cores at in situ pressure was a high priority during Leg 204. Natural gas in deep sediment may be present in three phases. If the concentration (molality) of gas in pore water is less than the solubility, the gas is dissolved. If the concentration of gas is greater than its solubility, gas is present as a free phase (bubbles) below the GHSZ and as solid hydrate within the GHSZ. Knowledge of the gas concentration in deep sediment is critical for understanding the dynamics of hydrate formation and the effect hydrates have on the physical properties of the sediment. However, reliable data on gas concentration are difficult to obtain. Because gas solubility decreases as pressure decreases and temperature increases, cores recovered from great depth often release a large volume of gas during recovery (Wallace et al., 2000; Paull and Ussler, 2001). The only way to determine true in situ concentrations of natural gas in the seafloor is to retrieve cores in an autoclave that maintains in situ conditions. The original ODP pressure core sampler (PCS) has proven to be an essential tool that is very effective for estimating in situ gas concentrations (Dickens et al., 1997, 2000b) and was used extensively during Leg 204. However, it is less effective for studies of physical properties of gas hydrate-bearing sediments at in situ conditions.

The HYACINTH (deployment of Hydrate Autoclave Coring Equipment [HYACE] tools in new tests on hydrates) program, funded by the European Union (EU), is developing the next generation of pressure corers. Both HYACE coring systems were used during Leg 204. The Fugro Pressure Corer (FPC) is designed for sediments that are normally cored with the APC and XCB, and the HYACE Rotary Corer (HRC) is designed to drill more lithified sediments and rocks normally cored with the XCB and RCB. These pressure cores are contained in an inner plastic liner that can be transferred (under full pressure) from the autoclave into other pressure chambers. When transferred into a logging chamber, the pressurized cores can be logged using the V-MSCL. This was used to make measurements on cores collected by the HYACE coring tools and on standard ODP cores re-pressurized to in situ pressures. By measuring VP, P-wave attenuation, and GRA density at in situ pressures and by pressure cycling, we anticipated being able to distinguish between hydrate and free gas while also measuring some in situ properties that would help to constrain models of hydrate and free gas distribution.

### ***Advanced Piston Corer Temperature (APCT) Tool***

The APCT tool fits directly into the cutting shoe on the APC and can, therefore, be used to measure sediment temperatures during regular piston coring. The tool consists of

*In-Situ Sampling and Characterization of Naturally Occurring Marine Methane Hydrate Using the D/V JOIDES Resolution.*

electronic components, including battery packs, a data logger, and a platinum resistance–temperature device calibrated over a temperature range of 0°–30°C. Descriptions of the tool and of the principles behind analysis of the data it acquires can be found in Pribnow et al. (2000) and Graber et al. (2002) and the references therein. The thermal time constant of the cutting shoe assembly where the APCT tool is inserted is ~2–3 min. The only modification to normal APC procedures required to obtain temperature measurements is to hold the corer in place for ~10 min after cutting the core. During this time, the APCT tool logs temperature data on a microprocessor contained within the instrument as it approaches equilibrium with the in situ temperature of the sediments. Following deployment, the data are downloaded for processing. The tool can be preprogrammed to record temperatures at a range of sampling rates. Sampling rates of 10 s were used during Leg 204. A typical APCT measurement consists of a mudline temperature record lasting 10 min for the first deployment at each borehole and 2 min on subsequent runs. This is followed by a pulse of frictional heating when the piston is fired, a period of thermal decay that is monitored for 10 min or more, and a frictional pulse upon removal of the corer.

A second source of uncertainty in these data is possible temporal change of the bottom-water temperature resulting from tides, seasons, and longer-term climate change. Evidence for short-term changes in this region is seen in data from a near-bottom current meter that was deployed for 6 months at a water depth of 800 m in the saddle between the northern and southern summits of Hydrate Ridge (R. Collier, pers. comm., 2000). These data show peak-to-peak tidal variations of up to 0.3°C, a superimposed variation with a timescale of 2 months and peak-to-peak amplitude of 0.04°C, and an apparent seasonal variation of 0.3°C. These multiple sources of bottom-water temperature variation, which occur on a timescale that will not be felt at seafloor depths greater than a few meters lead to significant temporal variability in the mudline temperature. Because of these observations, it may, in general, be inappropriate to include the mudline temperature when determining the subsurface temperature gradient from downhole temperature data. Mudline temperatures, however, are reported in the data tables because they can provide a useful data point for postcruise studies.

### ***Davis-Villinger Temperature Probe***

The temperature measurement aspects of the DVTP are described in detail by Davis et al. (1997) and summarized by Pribnow et al. (2000) and Graber et al. (2002). The probe is conical and has two thermistors; the first is located 1 cm from the tip of the probe and the other 12 cm above the tip. A third thermistor, referred to as the internal thermistor, is in the electronics package. Thermistor sensitivity is 1 mK in an operating range of –5° to 20°C, and the total operating range is –5° to 100°C.

The thermistors were calibrated at the factory and on the laboratory bench before installation in the probe. In addition to the thermistors, the probe contains an accelerometer sensitive to 0.98 m/s<sup>2</sup>. Both peak, and mean acceleration are recorded by

*In-Situ Sampling and Characterization of Naturally Occurring Marine Methane Hydrate Using the D/V JOIDES Resolution.*

the data logger. The accelerometer data are used to track disturbances to the instrument package during the equilibration interval. In a DVTP deployment, mudline temperatures (within the drill pipe) are measured for 10 min during the first run within each hole and for 2 min during subsequent runs, before descent into the hole for a 10-min equilibration time series at the measurement depth in the subseafloor. The time constants for the sensors are ~1 min for the probe-tip thermistor and ~2 min for the thermistor 12 cm from the tip. Only data from the probe tip thermistor were used for estimation of in situ temperatures.

### ***In Situ Temperature Data Reduction***

The transient thermal-decay curves for sediment thermal probes are a function of the geometry of the probes and the thermal properties of the probe and sediments (Bullard, 1954; Horai and von Herzen, 1985). Data analysis requires fitting the measurements to predicted temperature decay curves calculated based on tool geometry and the thermal properties of the sediment. Pribnow et al. (2000) discuss data analysis procedures and uncertainties. For the APCT tool, the software program TFIT, developed by K. Becker and J. Craig, was used. The DVTP and DVTPP data can be analyzed using the software program CONEFIT, developed by Davis et al. (1997). However, during Leg 204, DVTP and DVTPP data were generally noisy and CONEFIT did not yield stable solutions. In some cases, we assumed that the temperature had reached equilibrium. In other cases, no estimate of in situ temperatures was attempted on board.

Mudline temperature is determined from the time the tool is held near the seafloor prior to penetration of the APC. Initial APC penetration is marked by a temperature pulse, which results from friction. A second pulse is observed when the tool is extracted from the sediment. The best fitting time of penetration and in situ temperature are calculated from data delimited by three points that are picked by the shipboard analyst. The thermal conductivity of the sediment must also be specified. Thermal conductivities measured from the core interval closest to the APCT measurement were used. The estimated uncertainty of the derived in situ temperature for good-quality measurements is 0.1°C (Pribnow et al., 2000), although the uncertainty may be considerably larger for poor-quality measurements. Because of problems with instrument calibration that became evident during the leg, temperature gradients may be better resolved than absolute values of temperature, provided the same tool was used to make all measurements at a given site.

### ***Davis-Villinger Temperature-Pressure Probe***

Simultaneous measurement of formation temperature and pressure was achieved using a modified DVTP. The probe has a tip that incorporates both a single thermistor in an oil-filled needle and ports to allow hydraulic transmission of formation fluid pressures to a precision Paroscientific pressure gauge inside. A standard data logger was modified to accept the pressure signal instead of the second thermistor signal in the normal DVTP

*In-Situ Sampling and Characterization of Naturally Occurring Marine Methane Hydrate Using the D/V JOIDES Resolution.*

described above. Thermistor sensitivity of the modified tool is reduced to 0.02 K in an operating range of  $-5^{\circ}$  to  $20^{\circ}\text{C}$ . A typical deployment of the tool consists of lowering the tool by wireline to the mudline where there is a 10-min pause to collect data. Subsequently, the tool is lowered to the base of the hole and latched in at the bottom of the drill string, with the end of the tool extending 1.1 m below the drill bit. The extended probe is pushed into the sediment below the bottom of the hole and pressure is recorded for  $\sim 40$  min. If smooth pressure decay curves are recorded after penetration, then theoretical extrapolations to in situ pore pressures are possible.

Temperature data from the DVTPP were treated as discussed for the DVTP. For both the DVTPP and the piezoprobe (discussed below), the pressure response is qualitatively similar to, but slower, than the thermal response. The decay time is a function of the sediment permeability and the magnitude of the initial pulse, which is a function of the taper angle and diameter of the tool (Whittle et al., 2001; Heeseman, 2002).

### ***Fugro-McClelland Piezoprobe***

In April 2001, a proposal was submitted to the U.S. Department of Energy to modify and implement the use of the Fugro-McClelland piezoprobe tool on the *JOIDES Resolution* during ODP Leg 204. The piezoprobe has been tested and proven (e.g., Ostermeier et al., 2000; Whittle et al., 2001) on numerous geotechnical cruises that measured pressure and temperature, but it had not been adapted for ODP until Leg 204. To adapt it on the *JOIDES Resolution* for testing and use with the APC/XCB bottom-hole assembly (BHA) required modifications prior to the leg. The modifications made by Fugro-McClelland and ODP were designed to (1) adapt the piezoprobe for a Schlumberger wireline, (2) increase the landing ring size, (3) implement a stabilizer sleeve to prevent bending, (4) shorten the bit to minimize risk of bending, and (5) extend pawls for the four-cone APC bit used on the *JOIDES Resolution*.

The piezoprobe works within the borehole and measures pressure through a transducer at its tip, which is similar to the pop-up pore pressure instrument (PUPPI) (see Schultheiss and McPhail, 1986). The probe is lowered through the drill pipe, measures hydrostatic pressure, and is pushed into the sediment  $\sim 1$  m beyond the base of the borehole, where pressure is again measured. The resultant pressure vs. time curves for multiple experiments provide estimates of in situ pressure as a function of depth. The pressure decay can be used to evaluate the permeability and coefficient of consolidation (e.g., Elsworth et al., 1998; Schnaid et al., 1997), two parameters that are necessary to describe fluid flow and deformation within the shallow subsurface. The narrow taper of the piezoprobe allows a pressure decay to be measured in low-permeability sediments within an hour, a time frame that is reasonable for use on the *JOIDES Resolution*. The piezoprobe also records temperature data during each measurement. Similar to the APCT tool and the DVTP tool, the temperature decay can be used to estimate in situ temperature. During Leg 204, the piezoprobe was deployed twice, with the second run being successful.

*In-Situ Sampling and Characterization of Naturally Occurring Marine Methane Hydrate Using the D/V JOIDES Resolution.*

## Comparison between the Piezoprobe and the Davis-Villinger Temperature-Pressure Probe

The DVTTP and the piezoprobe both provide the ability to make estimates of in situ temperature and pressure in low-permeability strata at a relatively quick rate (i.e., multiple measurements per hole and dozens of measurements per cruise). The basic operational procedure for each is similar to that for the temperature tools: (1) insert probe at the base of the borehole, (2) monitor pressure disturbance from probe insertion, and (3) record pressure decay and extrapolate out to infinite time for estimate of in situ pressure. The decay time is a function of the sediment permeability and the size of the initial pulse. The magnitude of the pressure pulse is a function of the taper angle and diameter of the tool (Whittle et al., 2001). The piezoprobe has a narrower diameter (6.4 mm) and smaller taper angle ( $<2^\circ$ ) than the DVTTP (diameter = 8 mm and taper =  $2.5^\circ$ ) and therefore produces a smaller pressure disturbance.

Whittle et al. (2001) have demonstrated that it is beneficial to monitor the pressure decay long enough so that a significant proportion of the pulse has dissipated before recovery of the tool; with the piezoprobe, this takes  $\sim 2$  hr in low-permeability strata (Whittle et al., 2001), longer than is generally allowed for the DVTTP during ODP legs.

### ***ODP Pressure Core Sampler (PCS)***

The PCS is a downhole tool designed to recover a 1-m-long sediment core with a diameter of 4.32 cm at in situ pressure up to a maximum of 10,000 psi (Pettigrew, 1992; Graber et al., 2002). It consists of an inner core barrel and a detachable sample chamber. When its valves seal properly, controlled release of pressure from the PCS through a manifold permits collection of gases that would otherwise escape on the wireline trip. The PCS currently provides the only proven means to determine in situ gas abundance in deep-sea sediments where gas concentrations at depth exceed saturation at atmospheric pressure and room temperature (Dickens et al., 1997). The analysis of recorded data (e.g., time series of pressure and the volume of released gas) may also help to determine if gas hydrate is present in the cored interval (Dickens et al., 2000b).

After retrieval, the PCS is placed into an ice bath to keep the inside temperature at  $\sim 0^\circ\text{C}$ . A manifold is connected to the PCS to decrease pressure by releasing gas under manual control. Only a small volume of gas ( $\sim 100$ – $150$  mL) should be collected during the first gas release. This is because it has been empirically determined that the first gas sample thus obtained is contaminated by air. Additional gas releases should lead to immediate pressure drops. Ideally, the pressure in the PCS should then increase with time as gas exsolves from pore water or from decomposing gas hydrate. Gas should be released when pressure does not increase significantly over a 10- to 15-min time interval, and the process should be repeated. Sometimes gas may be released before the pressure has built up because of constraints with operational logistics.

*In-Situ Sampling and Characterization of Naturally Occurring Marine Methane Hydrate Using the D/V JOIDES Resolution.*

At the end of the experiment, ice should be removed from around the PCS and the PCS should be warmed up to release all gas remaining in the core. Splits of gases are collected into a 1-L bubbling chamber that consists of an inverted graduated cylinder placed in a plexiglass tube filled with a saturated NaCl solution. After measuring the volume of collected gas, gas aliquots are sampled from a valve at the top of the cylinder using a syringe.

Prior to Leg 204, the PCS was successfully used to study in situ gases during ODP Leg 164 on the gas hydrate-bearing Blake Ridge (Paull, Matsumoto, Wallace, et al., 1996; Dickens et al., 1997) and during Leg 201 at sites along the gas-rich Peru margin (Dickens et al., 2003). One of the objectives of PCS use during Leg 201 was to test the coring capabilities in a variety of lithologic conditions. Several modifications to the PCS were made prior to Leg 201 (Dickens et al., 2003), including the addition of an optional cutting shoe for rotary coring and the construction of a new gas manifold. The PCS was deployed 17 times during Leg 201. Dickens et al. (2003) concluded that (1) the tool performed better during Leg 201 than on Leg 164, (2) the PCS can operate successfully in a variety of submarine environments, and (3) cores collected at shallow sediment depth can be degassed to generate gas concentration profiles.

Two significant modifications were made between Legs 201 and 204 in order to better address the scientific objectives of Leg 204. First, a methane tool was installed inside the PCS to measure temperature, pressure, and conductivity during the PCS recovery (see below). Second, pressure transducers that permit continuous monitoring of pressure, both on the manifold and inside the PCS were installed. Pressure is recorded on a personal computer every 5 s and is presented as a graph during the experiment. An ASCII file of the data is preserved at the end of the experiment. These modifications should permit better monitoring of pressure and temperature inside the PCS after the core is retrieved from the subsurface.

### ***Methane Tools***

The Advanced Piston Corer Methane (APCM) tool and the Pressure Coring System Methane (PCSM) tool continuously record the temperature, pressure, and electrical conductivity changes in the core headspace from the time the core is cut through its ascent to the rig floor. The APCM sensors are mounted in a special piston head on the standard ODP APC piston, and the data acquisition electronics are embedded within the piston. The PCSM is a slimmed-down version of the APCM, which is mounted on the top of the PCS manifold mandrel.

Both tools operate passively and require little shipboard attention. Variations in the relative amounts of gas stored in different types of sediment can be determined by establishing families of ascent curves composed of data from successive cores. Models indicate that these data will also provide information on whether gas hydrate was present

*In-Situ Sampling and Characterization of Naturally Occurring Marine Methane Hydrate Using the D/V JOIDES Resolution.*

in the sediment before core retrieval. The two methane tools are being developed through a collaborative activity involving the ODP engineering staff and Monterey Bay Aquarium Research Institute (MBARI). They are derivatives of MBARI's Temperature-Pressure-Conductivity (TPC) tool.

Both tools are very similar in construction, the only difference being that the APCM replaces the piston-rod snubber in the APC coring system and therefore has a seal package on its exterior. The tools consist of an instrumented sensor head with the electronics and battery pack housed in a sealed case. The three sensors (temperature, pressure, and conductivity) and a data port are packaged in the face of the 23/8-in-diameter sensor head. The temperature sensor is a  $\pm 0.05^{\circ}\text{C}$  accuracy thermistor installed in a 3/16-in-diameter  $\times$  1/-in-long probe. The pressure sensor is a 0- to 10,000-psi "Downhole Series" transducer with a  $\pm 0.15\%$  full-scale accuracy that is especially designed for temperature stability. The electrical conductivity sensor is a three-pin bulkhead connector with an inconel body and gold-plated 0.040-in-diameter Kovar pins. The data port is a three-pin keyed bulkhead connector for RS-232 communication. The electronics consists of two boards, an analog to digital (A/D) board and a commercial microcontroller board. The microcontroller board plugs directly into the A/D board, and the A/D board is mounted on an aluminum backbone. The microcontroller includes a Motorola 68338 processor, a DOS-like operating system, and 48 MB of flash memory. The A/D board is an ODP/MBARI-designed board with one A/D device for the pressure transducer and one for the thermistor and conductivity sensors. The battery pack consists of an assembly of two double-C lithium/thionyl chloride batteries in series and an integral hard-mounted nine-pin connector. The 1-in-diameter 9-in-long battery pack provides 7.3 V, with a 100-mA rating. The APCM is installed on the APC piston after the APC piston-rod snubber and piston-head body is removed from the lower piston rod. The connection at the lower piston rod consists of a threaded connection with a transverse spring pin running through the thread relief. The spring pin prevents the connection from unscrewing as a result of vibration. After the spring pin is punched out, the piston-rod snubber is removed and replaced with the APCM. This swap-out operation takes <3 min. The PCSM replaces the accumulator on the PCS and threads onto the top of the PCS manifold mandrel.

The APCM and PCSM tools were successfully deployed 107 times during Leg 204, but all data analysis was deferred until postcruise.

### ***HYACINTH Coring Equipment***

Although the PCS was successful during Leg 164, there were a number of aspects worthy of improvement as described by Dickens et al. (2000a). A proposal submitted to the EU resulted in HYACE, which was a 3-yr project aimed at developing new wireline pressure coring tools that would address a wide range of scientific problems. The HYACE project resulted in the development of two new pressure-coring tools.

*In-Situ Sampling and Characterization of Naturally Occurring Marine Methane Hydrate Using the D/V JOIDES Resolution.*

These tools underwent only limited testing on land and at sea during ODP Legs 194 and 201 (Leg 201 was after the end of the HYACE project and at the beginning of the HYACINTH project). The current HYACINTH project is a continuation of the HYACE project and is also funded by the EU. It is designed to bring these new coring tools into operational use and to develop new techniques of subsampling and analyzing cores under pressure. Leg 204 provided the opportunity for further testing and use of these new coring tools. Other important objectives of Leg 204 were to test and use the HYACINTH family of pressure chambers and the core-transfer mechanisms and to measure the physical properties of cores at in situ pressures.

The design and operation of the HYACE tools differs in two significant respects from that of the existing PCS. First, the HYACE tools penetrate the seabed using downhole driving-mechanisms powered by fluid circulation rather than by top-driven rotation with the drill string. This allows the drill string to hang stationary in the hole while core is being cut, which should improve core quality and recovery. Second, the HYACE tools recover lined cores, which enables them to be transferred under pressure into a family of chambers, allowing cores to be preserved and studied under pressure.

Two different coring tools have been developed in order to accommodate a wide range of lithologies, a “percussion” corer and a “rotary” corer. Both tools have been designed for use with the same ODP BHA as the PCS (i.e., the APC/XCB BHA). The FPC is designed for recovering unlithified sediment ranging from clay to sand and gravel. When used in a gas hydrate-bearing environment, it is considered to be most applicable where any hydrate present has not significantly cemented the sedimentary particles. The core barrel is driven into the sediment by a hammer mechanism that is driven by fluid circulation. In soft sediments, the core barrel strokes out quickly so that in these lithologies the FPC essentially behaves like a push core.

The HRC is designed to cut a rotary core in more lithified sediment formations and incorporates a downhole mud motor. A dry auger-type of bit, extending beyond the reach of the circulating seawater, is used to cut the core, providing as contamination-free a core as is possible with rotary coring. It is designed, primarily, to recover cores in well-lithified sediments and rocks that can be obtained with the XCB and RCB. The phase II PCS development proposed by Pettigrew (1992) is similar to the approach used in the HRC. However, this was not pursued by ODP because of insufficient funds.

Both the FPC and the HRC use specially designed but different flapper valves to seal the tool’s pressure chamber (autoclave), where the core is contained on recovery. This enables larger cores to be cut than with the PCS, which uses a ball valve as the sealing mechanism. The FPC cuts a 58-mm-diameter core, and the HRC cuts a 50-mm-diameter core. Like the PCS, both cores are ~1 m in length. Pressures up to 250 kbar (3625 psi) can be maintained in the present design.

*In-Situ Sampling and Characterization of Naturally Occurring Marine Methane Hydrate Using the D/V JOIDES Resolution.*

After initial testing on land, the FPC and HRC underwent their first sea trials on the *JOIDES Resolution* at the start of ODP Leg 194. The FPC had limited success in recovering a core under pressure, whereas the HRC encountered significant problems because of its failure to latch properly in the BHA (Rack, 2001). A core was finally cut but was not retrieved under pressure. The FPC had further trials during Leg 201, but hole conditions are thought to have been unfavorable, which prevented the recovery of a pressure core. Valuable lessons were learned during both of these engineering trials of the FPC and the HRC (Rack, 2001), and a number of significant modifications were made to the tools and to the handling procedures prior to the start of Leg 204.

### ***Tool Operations***

Both the HRC and the FPC were prepared and assembled on tool trestles located on the port side of the piperacker. Stands of drill pipe normally used from the port side were moved to the starboard side to prevent disruption to the tool preparations as much as possible. The only time the piperacker could not be used was when we added pipe stands during drilling, tripping pipe, and wireline logging. This was particularly helpful in ensuring that the operations went as efficiently as practically possible. The space afforded by using the piperacker was particularly important in view of the fact that the three PCS tools and logging tools were being assembled above the core tech shop.

For deployment, both tools followed similar operational procedures on the rig floor. They were initially transferred from the piperacker working area, where they had been prepared on trestles, into the vertical position. To do this, a tugger line from the derrick was attached to the upper end of the tool while the base of the tool was lowered onto the piperacker skate using the port side racker crane. The tool was then hauled into a vertical position using the tugger line and lowered into the rig floor shuck as the strongbacks were removed. A tugger line supported the heavier strongbacks on the HRC. The tool was deployed in the open drill string and the Drill String Acceleration (DSA) tool was fitted above. When the drill string was closed, the tools were lowered on the wireline while pumping and rotating.

On retrieval from the pipe, both the FPC and the HRC followed a reverse procedure back to the trestles on the piperacker, including replacing the strongbacks. During an early deployment, a problem was encountered whereby the HRC was split into the three main subassemblies as it was removed from the drill string in the vertical position. Although this alleviated the need to reattach the strongbacks when placing the tool subassemblies back to the horizontal position, it took significantly longer and, hence, was subsequently avoided. After disassembly on the trestles, the autoclave was carried to the platform outside the downhole tools laboratory for examination and connection to the pressure transfer system.

### ***Logging Cores at In Situ Pressure***

The other components that make up the HYACINTH system used during Leg 204 are the transfer system, the shear mechanism, and the pressure chambers that are used to store and log the cores under pressure. The HYACE transfer mechanism, which consists of a manipulator chamber and a shear mechanism, is used to extract the core under pressure from either the HRC or FPC autoclave and then transfer it into a storage chamber or logging chamber. The shear mechanism cuts the core at the top, removing the “technical part” of the core (piston assembly, etc.) from the core liner containing the sample prior to inserting it into the other chambers. The manipulator can be used to subsequently transfer the core between the logging and storage chambers if and when required.

The specially adapted Geotek V-MSCL was used to measure gamma density and P-wave parameters while the cores were under pressure in the HYACINTH logging chambers. It was also used to log regular APC cores that had been re-pressurized in specially designed logging chambers. The cores were logged vertically to help control the process of degassing during pressure cycling and final pressure release.

As with the PCS, gases exsolved from solution or released by dissociation of gas hydrate were collected into a 1-L bubbling chamber to determine the in situ abundance of gas in the cores. An analysis of the data recorded during the degassing process should help to determine the relative amounts of free gas and gas hydrate present in the cored interval.

Pressurized core logging is unlike normal core logging with the ODP MST or a standard Geotek Multi Sensor Core Logger (MSCL) in that there are two core liners to consider: (1) the thin plastic core liner (the inner liner) and (2) the thicker glass-reinforced plastic (GRP) pressure tube (the outer liner). To calibrate for measurements of VP and gamma density, similar techniques are used to those developed for the MST and MSCL, which use distilled water and aluminum as standards. In this mode of operation, the inner liner is assumed to have a constant diameter because it cannot be directly measured under pressure. The outer GRP liner was accurately calibrated to account for small variations in diameter and wall thickness along its length. The manufacturing technique necessitates that a change in the internal diameter of ~1 mm occurs along the 1.5 m length. To ensure consistency, the outer liner was always oriented to ensure that the small circumferential variations were effectively negated.

To calibrate VP, the variations in the total P-wave traveltimes along the length of the GRP tube were measured when both the inner liner and the GRP were filled with water of known velocity. All data are subsequently corrected as a function of position in the GRP tube. Changes in traveltimes as a function of pressure were also measured (up to 200 bar). The measured variation in VP with pressure is close to the theoretical variation for water. We therefore conclude that the traveltimes in the liner material are essentially constant with changing pressure. In practice, however, P-wave data for sediment cores were much

*In-Situ Sampling and Characterization of Naturally Occurring Marine Methane Hydrate Using the D/V JOIDES Resolution.*

harder to interpret than initially thought because of the interference of ultrasonic signals that propagate around the cylindrical GRP liner.

To calibrate the gamma density system, we used the same type of “standard section” as is used with the MST. During this step, graduated aluminum and water standards are placed in the GRP tube and logged at 2-mm intervals along the core.

Consideration is given to the variation in GRP tube diameter by logging the complete tube filled with water and filled with air. We confirmed that there are no pressure effects on the measurements by repeating the experiment at pressures up to 200 bar.

### ***Logging While Drilling***

During Leg 204, four Anadrill LWD and measurement-while-drilling (MWD) tools were deployed at eight of the nine sites cored and drilled on southern Hydrate Ridge. These tools were provided by Schlumberger- Anadrill services under contract with the Lamont-Doherty Earth Observatory Borehole Research Group (LDEO-BRG). LWD surveys were successfully conducted during seven previous ODP legs: Leg 156 (Shipley, Ogawa, Blum, et al., 1995), Leg 170 (Kimura, Silver, Blum, et al., 1997), Leg 171A (Moore, Klaus, et al., 1998), Leg 174A (Austin, Christie-Blick, Malone, et al., 1998), Leg 188 (O’Brien, Cooper, Richter, et al., 2001), Leg 193 (Binns, Barriga, Miller, et al., 2002), and Leg 196 (Mikada, Becker, Moore, Klaus, et al., 2002).

LWD and MWD tools measure different parameters. LWD tools measure in situ formation properties with instruments that are located in the drill collars immediately above the drill bit. MWD tools are also located in the drill collars and measure downhole drilling parameters (e.g., weight on bit, torque, etc.). The difference between LWD and MWD tools is that LWD data are recorded into downhole computer memory and retrieved when the tools reach the surface, whereas MWD data are transmitted through the drilling fluid within the drill pipe by means of a modulated pressure wave, or “mud pulsing,” and monitored in real time (see below). MWD tools enable both LWD and MWD data to be transmitted uphole when the tools are used in conjunction. The term LWD is often used more generically to cover both LWD- and MWD-type measurements.

The LWD and MWD tools used during Leg 204 include the resistivity at-the-bit (RAB) tool, the power pulse MWD tool, the Nuclear Magnetic Resonance (NMR-MRP) tool, and the Vision Neutron Density (VND) tool. This was the first time the NMR-MRP tool was used during an ODP leg.

LWD measurements are made shortly after the hole is drilled and before the adverse effects of continued drilling or coring operations. Fluid invasion into the borehole wall is also reduced relative to wireline logging because of the shorter elapsed time between drilling and taking measurements.

*In-Situ Sampling and Characterization of Naturally Occurring Marine Methane Hydrate Using the D/V JOIDES Resolution.*

The LWD equipment is battery powered and uses erasable/programmable read-only memory chips to store logging data until they are downloaded. The LWD tools take measurements at evenly spaced time intervals and are synchronized with a system on the drilling rig that monitors time and drilling depth. After drilling, the LWD tools are retrieved and the data downloaded from each tool through an RS232 serial link to a laptop computer. Synchronization of the uphole and downhole clocks allows merging of the time-depth data (from the surface system) and the downhole time-measurement data (from the tools) into depth-measurement data files. The resulting depth-measurement data are transferred to the processing systems in the downhole measurements laboratory (DHML) on board the *JOIDES Resolution* for reduction and interpretation.

### ***Depth Tracking Systems***

Unlike wireline tools, which record data vs. depth, LWD tools record data vs. time. The Anadrill Integrated Drilling and Logging (IDEAL) system records the time and the depth of the drill string below the rig floor. LWD operations aboard the *JOIDES Resolution* require accurate and precise depth tracking and the ability to independently measure and evaluate the movement of the following:

1. Position of the traveling block in the derrick,
2. Heave of the vessel by the action of waves/swells and tides, and
3. Action of the motion compensator.

### ***Motion Compensator and Draw-works Encoders***

The length of the drill string (combined lengths of the BHA and the drill pipe) and the position of the top drive in the derrick is used to determine the exact depth of the drill bit and rate of penetration. The system configuration is further described below:

1. Drilling line is spooled on the draw-works. From the draw-works, the drilling line extends to the crown blocks, which are located at the very top of the derrick, and then down to the traveling block. The drilling line is passed several times, usually six or eight times, between the traveling blocks and the crown blocks and then fastened to a fixed point called the dead-man anchor.
1. From the driller's console, the driller controls the operation of the drawworks, which, via the pulley system described above, controls the position of the traveling block in the derrick.
2. On the *JOIDES Resolution*, the heave motion compensator is suspended from the traveling block. The top drive is then attached to the motion compensator. The motion compensator uses pistons that are pressure charged, and thus are able to provide a buffer against the waves and swell. As the vessel rises, the pressure on the pistons increases and they extend to keep the bit on bottom, whereas when the

vessel drops, the pistons retract and diffuse any extra weight from being stacked on the bit.

3. The drill string is connected to the top drive; therefore, movement of the top drive needs to be measured to provide the drill string depth.

To measure the movement of the traveling blocks a draw-works encoder (DWE) is mounted on the shaft of the draw-works. One revolution of the draw-works will pay out a certain amount of drilling line and, in turn, move the traveling blocks a certain distance. Calibration of the movement of the traveling block to the revolutions of the draw-works is required.

### ***Hookload Sensor***

A hookload sensor is used to measure the weight of the load on the drill string and can be used to detect whether the drill string is disconnected from the traveling block and held fast at the rig floor (“in-slips”) or not. When drilling ahead, the string is “out-of-slips.” When the drillstring is in-slips, motion from the blocks or motion compensator will not have any effect on the depth of the bit (i.e., it will remain stationary) and the DWE information does not augment the recorded bit depth. When the drill string is out-of-slips, the DWE information augments the recorded bit depth. The difference in hookload weight between in-slips and out-of-slips is very distinguishable. The heave of the ship will still continue to affect the bit depth whether the drill string is in-slips or out-of-slips.

### ***Heave Motion Sensors***

On the *JOIDES Resolution*, the ability to measure the vessel’s heave is addressed in two ways. The rig instrumentation system used by the driller measures and records the heave of the ship and the motion of the cylinder of the active compensator, among many other parameters, at the rig floor. The motion compensator cylinder either extends or retracts to compensate for ship heave that is detected by fixed accelerometers. Both the heave value and cylinder position measurement are transmitted to the Anadrill recording system via the Wellsite Information Transfer System (WITS) line. Software filtering may be used to smooth the time-depth file by applying a weighted average to the time-depth data based on the observed amplitude and period of ship heave. The depth-filtering technique has significantly improved the quality of RAB image logs from previous ODP holes.

### ***Resistivity-at-the-Bit Tools***

RAB tools provide resistivity measurements of the formation and electrical images of the borehole wall, similar to the Formation Micro- Scanner but with complete coverage of the borehole walls and lower vertical and horizontal resolution. In addition, the RAB tool contains a scintillation counter that provides a total gamma ray measurement. Because a

*In-Situ Sampling and Characterization of Naturally Occurring Marine Methane Hydrate Using the D/V JOIDES Resolution.*

caliper log is not available without other LWD measurements, the influence of the shape of the borehole on the log responses cannot be directly estimated.

The RAB tools are connected directly above the drill bit, and they use the lower portion of the tool and the bit as a measuring electrode. This allows the tool to provide a bit resistivity measurement with a vertical resolution just a few inches longer than the length of the bit. A 1-in (2.5 cm) electrode is located 3 ft (91 cm) from the bottom of the tool and provides a focused lateral resistivity measurement (RRING) with a vertical resolution of 2 in (5 cm). The characteristics of RRING are independent of where the RAB tool is placed in the BHA, and its depth of investigation is ~7 in (18 cm). In addition, button electrodes provide shallow-, medium- and deep-focused resistivity measurements as well as azimuthally oriented images. These images can then reveal information about formation structure and lithologic contacts. The button electrodes are ~1 in (2.5 cm) in diameter and reside on a clamp-on sleeve. The buttons are longitudinally spaced along the RAB tool to render staggered depths of investigation of ~1, 3, and 5 in (2.5, 7.6, and 12.7 cm). The tool's orientation system uses the Earth's magnetic field as a reference to determine the tool position with respect to the borehole as the drill string rotates, thus allowing both azimuthal resistivity and gamma ray measurements. Furthermore, these measurements are acquired with an ~6° resolution as the RAB tool rotates.

Two RAB tool-collar configurations that were designed for use during Leg 204 give slightly different resistivity responses depending on the size of the measuring button sleeve and the hole's diameter. The RAB tool used in series in the 63/-in LWD/MWD BHA is called the GeoVision Resistivity (GVR), the most recent upgrade of the tool (Fig. F19). The diameter of its measuring button sleeve is 23.3 cm (91/8 in), and the diameter of the three-cone rotary bit used during Leg 204 is 25 cm (97/8 in). This results in a 1.7-cm gap, or "standoff," between the resistivity buttons and the formation. The standoff causes the formation resistivity to be underestimated slightly, depending on the ratio between the formation and borehole fluid resistivity. For a resistivity ratio of <100, as expected for all Leg 204 sites, a resistivity correction factor of up to 4% may be applied to each of the GVR measurements. Because of its limited depth of penetration into the formation (see below), the correction factor for the shallow button resistivity is greatest.

A RAB-8 tool collar configuration for use with a larger 8-in-diameter BHA was specially designed for ODP. The U.S. Department of Energy provided partial funding support for the modified RAB-8 tool deployment during Leg 204. The design is intended to be run in conjunction with a modified motor-driven core barrel core-liner system, thus allowing for RAB measurements to be made while coring. ODP Leg 204 represents the first ever attempt to core and record LWD data simultaneously. The RAB-8 tool is deployed alone in the BHA, and the standard 25 cm (97/8 in) diameter rotary bit is used. The diameter of the measuring button sleeve for the RAB-8 tool is 24.1 cm (91/2 in); thus, the standoff is half that for the RAB-6 and the resistivity correction factors are negligible for all of the RAB-8 measurements, including the shallow button resistivity.

### ***Resistivity-at-the-Bit Programming***

All logging data are collected at a minimum vertical density of 15 cm whenever possible; hence, a balance must be determined between the rate of penetration (ROP) and the sampling rate. This relationship depends on the recording rate, the number of data channels to record, and the memory capacity (46 MB) of the LWD tool. During Leg 204, we used a data acquisition sampling rate of 5 s for high-resolution GVR images.

The RAB-8 tool was programmed with a sampling rate of 10 s for data acquisition. The maximum ROP allowed to produce one sample per 6-in interval is given by the equation:

$$\text{ROP (in meters per hour)} = 548/\text{sample rate}$$

This relationship gives 110 m/hr maximum ROP for the GVR and 55 m/hr for the RAB-8 tool. For Leg 204, the target ROP was 25–50 m/hr, roughly 25%–50% of the maximum allowable for the GVR and RAB-8 tools. These reduced rates improve the vertical resolution of the resistivity images to 5–10 cm per rotation. Under this configuration, the GVR tool has enough memory to record up to 80 hr of data and the RAB-8 tool can record as long as 30 hr. This would be sufficient, under normal operating conditions, to complete the scheduled LWD operations at the Leg 204 drill sites.

### **SUMMARY**

This project involved very complex operational planning and the enhancement or development of complicated downhole sampling and measurement tools, as well as well-thought out approaches to laboratory procedures and measurements, some requiring the deployment of specialized equipment never before used in scientific ocean drilling. The following section provides more detailed information about the testing and deployment of a range of tools and systems during ODP Legs 201 and 204 with discussions about some of the important results. Further detailed information, including methods and procedures used throughout each of these two expeditions, can be obtained online, for Leg 201 at <[http://www-odp.tamu.edu/publications/201\\_IR/201TOC.HTM](http://www-odp.tamu.edu/publications/201_IR/201TOC.HTM)> and for Leg 204 at <[http://www-odp.tamu.edu/publications/204\\_IR/204TOC.HTM](http://www-odp.tamu.edu/publications/204_IR/204TOC.HTM)>.

## RESULTS AND DISCUSSION

### Introduction

The primary objectives of the JOI proposal to DOE/NETL, which resulted in Cooperative Agreement #DE-FC26-01NT41329, were to sample and characterize methane hydrates using the systems and capabilities of the D/V *JOIDES Resolution* during ODP Leg 204, to enable scientists the opportunity to establish the mass and distribution of naturally occurring gas and gas hydrate at all relevant spatial and temporal scales, and to contribute to the DOE methane hydrate research and development effort. The goal of the work was to provide expanded measurement capabilities on the *JOIDES Resolution* for a dedicated hydrate cruise to Hydrate Ridge off Oregon (ODP Leg 204) so that hydrate deposits in this region are well characterized. This goal was accomplished along with many other aspects of this project, which have contributed to ongoing hydrate studies and joint industry project preparation to characterize hydrate deposits in the Gulf of Mexico.

The projects identified in the JOI proposal were all focused on providing enhanced capabilities for existing tools and developing new approaches to the study of naturally-occurring marine methane hydrate. This was accomplished by the development and testing of tools and measurement systems on ODP Leg 201 (Peru Margin) in preparation for their extensive use on ODP Leg 204 (Hydrate Ridge, offshore Oregon). The following sections describe the results of the deployments of these tools and measurement systems and discuss the significance of these accomplishments.

### ODP Leg 201 – Pressure Coring

#### ODP Pressure Core Sampler (PCS)

The PCS was deployed at six locations drilled during ODP Leg 201. Sites 1225 and 1226 are located in the eastern Equatorial Pacific in 3771 and 3308 meters of water depth, respectively. Sites 1227, 1228 and 1229 are located along the Peruvian Margin in 439, 274, and 151 meters of water depth, respectively. Site 1230 is located on the lower slope of the Peru Trench in 5086 meters of water depth. All six of these locations had been drilled previously on either ODP Legs 112 or 138 (Suess, E., von Huene, R., et al., 1988; Pias et al., 1993).

Sediments at the six locations vary considerably (Suess, E., von Huene, R., et al., 1988; Pias et al., 1993). The sequences at Sites 1225 and 1226 consist mostly of stiff, fine-grained nannofossil ooze. By contrast, the sediment records at Sites 1227, 1228 and 1229 are composed of alternating diatomaceous and siliciclastic packages with occasional hardgrounds and coarse-grained units. The sequence at Site 1230 consists mostly of clay and diatom ooze.

*In-Situ Sampling and Characterization of Naturally Occurring Marine Methane Hydrate Using the D/V JOIDES Resolution.*

The PCS was deployed 17 times on Leg 201, a total surpassed previously only by operations on Leg 164. The first seven runs, at Sites 1225 to 1229, were primarily undertaken to test whether the modified tool and cutting shoes would operate in rotary mode across a range of lithologies. The ten runs at Site 1230 were specifically targeted to construct an “in situ” gas concentration profile from shallow depths near the seafloor to deeper depths below intervals with gas hydrate.

Observations made from conventional cores on Leg 201 and the previous legs suggest that significant gas loss on the wireline trip may have occurred at one site and possibly at two additional sites. Visible gas escape structures appeared in cores below 30 m at Site 685/1230. Structures potentially representing gas release also were documented between 58 and 62 mbsf at Site 681/1229. High headspace methane concentrations (>1000 L/L), which may signify gas concentrations approaching or exceeding saturation at depth, occurred at these two sites as well as at ODP Site 684/1227. Gas hydrate also exists in sediment at Site 685/1230 (Kvenvolden and Kastner, 1990).

### *Post-retrieval Processing*

The PCS cores were degassed in rock polishing room at the top of the laboratory stack. Other than the pre-cruise cutting shoe modifications, the most significant change between Leg 164 and Leg 201 PCS operations was the location of gas venting. The PCS has connected inner and outer chambers with a sampling port to each. The inner chamber contains the sediment core (and excess borehole water in the case of a short core) of approximately 1465 mL, while the outer chamber contains borehole water of approximately 2700 mL. For many of the PCS cores on Leg 164, gas was released from the port to the inner chamber. With this configuration, however, unconsolidated sediment often extruded into the port and manifold at high pressure, clogging the system and preventing gas release. To rectify this problem, gas was released through the port of the outer chamber on PCS cores retrieved toward the end of Leg 164 (Dickens et al., 2000b). This configuration was used for all PCS cores on Leg 201.

Measurements of PCS data were kept simple on Leg 201. Time was recorded to the nearest half minute with a clock. Discrete pressures were obtained in psi using a pressure transducer inside of the PCS. When possible, these pressures were then corrected to account for the expected 14 psi reading at atmospheric pressure. Incremental gas volumes were recorded to the nearest 5 mL. The length of the sediment core was determined to the nearest 1 cm. Unlike on Leg 164, most of the extruded cores were in sufficiently good condition to accurately measure length. A thermometer showed that the temperature inside of the laboratory stayed at  $21 \pm 2^\circ \text{C}$ .

### *Sites 1225 and 1226 (Eastern Equatorial Pacific)*

Two runs of the PCS were made at Site 1225. Core 201-1225A-29P recovered 1.00 meters of sediment under pressure using the Christensen auger shoe, and an additional

### *In-Situ Sampling and Characterization of Naturally Occurring Marine Methane Hydrate Using the D/V JOIDES Resolution.*

0.41 meters of sediment in the extended shoe. However, the recovery pressure was not determined because the port for the internal pressure transducer leaked. After ~30 minutes and possible release of some internal pressure, a gauge inserted into a side port indicated ~1200 psi. Approximately 70 mL of gas escaped through the manifold when the PCS was opened to atmospheric pressure. Core 201-1225C-32P recovered 1.00 meters of sediment using the RBI auger shoe. A gauge inserted ~30 min after recovery and several minutes after placement on ice showed 4800 psi. Over the following hour, the pressure of this core dropped to 4010 psi. No gas volume was determined when the PCS was opened to atmospheric pressure.

The PCS was also deployed twice at Site 1226, although targeted intervals were significantly deeper and harder than at Site 1225. Core 201-1226B-42P reached the rig floor at 6208 psig (6222 psi) with 1.00 meters of sediment using the Christensen auger shoe with cutting edges broken off in the hole. After placing this core on ice, the pressure decreased logarithmically to 4907 psi over 150 minutes. Approximately 60 mL of gas were released upon opening the tool to atmospheric pressure. Using the RBI Auger with PDC cutters, Core 201-1226E-21P recovered 1.00 m of sediment, but at atmospheric pressure. A post mortem autopsy revealed that a chert layer was present at the level of the ball valve and prevented the tool from sealing at depth. There was no damage to the cutting shoe or tool.

Numerous gas release experiments on Leg 164 demonstrated that all PCS cores consistently release 60 to 120 mL of air at high pressure (Paull, Matsumoto, Wallace, et al., 1996; Dickens et al., 2000). Experiments at Sites 1225 and 1226, which have very little methane according to headspace analyses, confirm this finding. Presumably, the air becomes trapped inside of the tool during deployment. Although PCS cores at these sites are scientifically uninteresting, they clearly show that the tool can collect full 1.00 meter-long cores at pressure in sediment other than fine-grained clay of the Blake Ridge.

#### *Sites 1227, 1228 and 1229 (Peru Shelf)*

One run of the PCS was made at Site 1227. However, Core 201-1227A-15P failed to recover a sediment core. Gas was not released from this core.

A single PCS run was also made at Site 1228. Core 201-1228A-23P recovered only 0.07 meter of sediment. A gauge inserted into the side port of the PCS gave a reading of 35 psi before placing the tool on ice. Approximately 60 mL of gas were released when the core was opened to atmospheric pressure. This gas was air as expected.

The PCS was deployed once at Site 1229 in an interval near where gas escape structures were described on Leg 112 (Suess et al., 1988). Core 1229-10P recovered a 0.86 meters of sediment at 78 mbsf. However, the release of gas from this core was not straightforward. First, the pressure transducer apparently failed so a gauge was inserted into the side port. This gauge read 420 psi, a pressure slightly higher than expected assuming

hydrostatic loading at this location. A second transducer was then connected to the side port but pressures oscillated between 19 and 100 psi over time even when the tool was closed on ice. After about an hour, the tool was opened and 2880 mL of gas were incrementally released through the manifold. Essentially all of this “gas” was composed of air. We assume the air was introduced during drilling; however, we do not understand where and how such a large amount of air entered the tool, or whether it relates to the anomalous pressure readings.

#### *PCS Deployments at Site 1230 (Peru Trench)*

Pressures measured on the rig floor for the 10 PCS deployments at Site 1230 ranged between 280 and 8086 psi, or 4 to 105% of hydrostatic pressure. The range in observed pressures, including values higher than hydrostatic, is similar to that obtained at sites on the Blake Ridge (Paull, Matsumoto, Wallace et al., 1996). However, these PCS pressures should not be used to accurately assess downcore variations in pressure. All PCS deployments trap a small volume of headspace air, as noted previously. Consequently, pressures inside of the PCS change as this headspace volume warms and cools between the subsurface and the first measurement on the rig floor (Dickens et al., 2000b).

The length of core recovered by the PCS at Site 1230 varied from 0.18 meters to 1.00 meters, with six of the deployments retrieving the maximum length. This overall core recovery is much better than at Sites 994, 995 and 997 where many PCS runs retrieved cores less than 0.50 meters (Paull, Matsumoto, Wallace, et al., 1996). Core-1230A-25P was extruded as a series of incoherent sediment masses that totaled 0.18 meters, a length that probably represents a maximum. All sediment cores recovered by the PCS are lithologically similar to surrounding cores recovered by APC or XCB at adjacent depths.

Total gas volumes released from the PCS ranged from 200 to 6330 mL. These volumes are primarily mixtures of He, air ( $N_2$  and  $O_2$ ),  $CH_4$  and  $CO_2$ , although not all incremental volumes were analyzed. In general, He and air dominate the first 150 mL of gas because He was used to purge the small manifold volume (~30 mL) prior to gas release, and a small volume of air is trapped in the tool during deployment. With the exception of Core-1230B-4P, the total amount of air does not exceed 110 mL. Methane comprises most of the remaining gas after release of air, although  $CO_2$  increasing constitutes a minor component at low pressure. These results are the same as found on Leg 164.

#### *Gas Release Experiments*

Gas escapes the PCS in a predictable manner. After recording an initial pressure on the rig floor (generally greater than 6000 psig at Site 1230), the pressure rises until the core is surrounded with ice and cooled. Pressure then decreases almost exponentially to reach a baseline value in about 100 minutes. Upon first opening the PCS to the manifold, a small volume of gas escapes and pressure plummets to less than 500 psig. With each successive opening of the PCS, an incremental loss of gas and drop in pressure occurs. The change

#### *In-Situ Sampling and Characterization of Naturally Occurring Marine Methane Hydrate Using the D/V JOIDES Resolution.*

in volume and pressure during these openings decrease with time until warmed, when an additional volume of gas exits the tool. These time-pressure-volume relationships are entirely consistent with gas release experiments at Sites 995 and 997 on the Blake Ridge (Paull, Matsumoto, Wallace, et al., 1996; Dickens et al., 2000a,b).

## **LEG 201 - DOWNHOLE TOOLS**

### **Site 1225 – Downhole Tool Deployments**

At Site 1225, five types of downhole tools were employed consisting of the (Adara) APC-temperature shoe, the DVTP, the DVTP-P, the APC methane tool, and the Fugro Pressure Corer (FPC). The results of these deployments are described below.

#### *In Situ Temperature Measurements*

Six reliable determinations of downhole temperatures were made at depths between 0 and 303 mbsf in Hole 1225A using the APC-temperature tool (APC-T) and the DVTP. *In situ* temperatures were estimated by extrapolation of the station data using thermal conductivities measured on adjacent cores to correct for the frictional heating on penetration. The 95% confidence intervals from the temperature fits are all less than 0.03° C. The estimated *in situ* temperatures from both the APC-T and DVTP define a gradient of 0.0174° C/m in the 300 mbsf of the sediment column.

#### *Davis-Villinger Temperature Probe with Pressure (DVTP-P)*

The Davis-Villinger Temperature Probe with Pressure (DVTP-P) was deployed unsuccessfully twice in Hole 1225A at depths of 205.3 and 303.7 mbsf. The recorded data indicated that during both runs the non-indurated, fine-grained, formation sediments clogged the filter. During the second run, there was a pressure drop to roughly atmospheric level during penetration. This failure was attributed to a leak in the line connecting the pressure transducer to the probe tip.

#### *Other Tools*

The APC Methane tool (APC-M) under development is designed to continuously record temperature, pressure, and conductivity at the face of the ODP APC piston assembly during core ascent. The APC-M provides a continuous record of sediment gas temperatures, internal pressure, and timing of gas headspace formation during core recovery. The APC methane tool was deployed in Hole 1225A continuously from Core 1225A-5H through Core 1225A-14H. The recovered data from this run showed that the tool and data logger initially functioned correctly. Part way through the run during Core 1225A-10H, the data logger stopped recording. Upon recovery, the failure was attributed to a loose battery connection. The data from the APC-M will be analyzed post cruise.

*In-Situ Sampling and Characterization of Naturally Occurring Marine Methane Hydrate Using the D/V JOIDES Resolution.*

## Site 1226 – Downhole Tool Deployments

At Site 1226, three different downhole tools were employed: the APC-temperature shoe, the DVTP, and the DVTP-P. The results of these deployments are described below.

### *In Situ Temperature Measurements*

Fourteen reliable determinations of downhole temperature were made at depths between 0 and 400 mbsf at Site 1226 using the (Adara) APC-temperature tool and the DVTP. In situ temperatures were estimated by extrapolation of the station data using thermal conductivities measured on adjacent cores to correct for the frictional heating on penetration. With the exception of the measurement from 310 mbsf, all of the temperature fits had 95% confidence intervals less than 0.01° C.

The estimated in situ temperatures from both the APC-T and the DVTP define a gradient of 0.0572° C m<sup>-1</sup> in the upper 400 meters of the sediment column.

### *Davis-Villinger Temperature Probe with Pressure (DVTP-P)*

The DVTP-P was deployed twice at Site 1226. During the first run in Hole 1226B at 241.9 mbsf, there was an initial pressure increase of 0.2 MPa during penetration followed by a drop of 12 MPa. Within two minutes pressures abruptly rose again to roughly hydrostatic levels. An average pressure signal equivalent to in situ hydrostatic pressure with ~0.1–0.2 Mpa of noise was recorded during the remainder of the 30-minute deployment. The abrupt drop in pressure was attributed to a leak near the probe tip. The results of the second deployment in Hole 1226E at 326 mbsf show that the pressure leak was successfully repaired. The pressure record rose as expected on penetration and then dropped to hydrostatic over the next minute. The pressure then remained constant at hydrostatic with 0.1–0.2 MPa noise for the remainder of the 20 minute deployment interval. These data indicate that the seal of the formation around the probe tip was probably not very good and that the tool should be pushed in with greater force in the future.

## Site 1227 – Downhole Tool Deployments

At Site 1227, the three downhole tools deployed were the APC-temperature shoe, the DVTP, and the DVTP-P. The results of the temperature and pressure measurements at Site 1227 are described in the two sections below.

### *In situ Temperature Measurements*

Determinations of temperature were made at Site 1227 using the APC-temperature tool and the DVTP. Both of these downhole temperature records were either of poor quality or deviated from the values expected from the ODP Leg 112 Site 684 data (Suess et al.,

*In-Situ Sampling and Characterization of Naturally Occurring Marine Methane Hydrate Using the D/V JOIDES Resolution.*

1988). Data were collected from two DVTP deployments at 81.6 and 110.1 mbsf. Both records show considerable small-scale oscillations and double peaks when the tool is first pushed into the sediments. The record from 81.6 mbsf (after Core 201-1227A- 9H) lasts for only five minutes before the temperature jumps up and again decays for the remainder of the 10 minute deployment. The record for the lower thermistor from 110.1 mbsf (after Core 201-1227A-12H) is too noisy to be used.

In situ temperatures were estimated by extrapolation of the station data using thermal conductivities measured on adjacent cores to correct for the frictional heating on. Generally, the data from the lower thermistor are used to extrapolate the in situ temperature. The poor lower thermistor data quality for the deployment at 110.1 mbsf (after Core 201-1227A-9H) necessitated using the upper thermistor record instead.

The combined in situ temperatures of Sites 1227 and 684 (ODP Leg 112) define a gradient of  $0.0492^{\circ} \text{C m}^{-1}$  in the upper 110 meters of the sediment column.

Comparing lithology from locations that produced good and bad temperature decay profiles showed some differences that may be used to optimize future DVTP deployments. The better DVTP deployment at 81.6 mbsf occurred between cores comprised of clay and nannofossil-bearing diatom ooze (Cores 201-1227A- 9H and -10H). These fine-grained sediments are similar to those from Site 1225 and 1226 where the acquired temperature data were excellent. In contrast, the second deployment location at 100.1 mbsf occurred between cores of pyrite and diatom-rich silty clays with sand-sized particles (Cores 201-1227A- 12H and -13H). These sediments were significantly more coarse-grained than those cored from above and below the better deployment. Accumulation of gravel in the base of the hole does not appear to have differed between the two deployments. Both locations had about 40 centimeters of gravel at the top of the subsequent core.

Another aspect of Site 1227 that may be important is the shallow 423 meters water depth compared to over 3000 meters water depth at Sites 1225 and 1226. The increased noise in the data may be due to the greater influence of heave or currents on the tool in shallow water. It appears that for deployments in shallow water the best strategy may be to choose fine-grained intervals for the deployments.

#### *Davis-Villinger Temperature Probe with Pressure (DVTP-P)*

The DVTP-P was deployed once at Site 1227 at a depth of 132 mbsf (after Core 201-1227A- 14H). The record shows a relatively noise free signal with the expected sharp pressure increase when the tool was pushed into the sediments. Within two minutes the pressure drops to the value initially recorded at the base of the hole. A pressure signal equivalent to in situ hydrostatic pressure with relatively little noise was recorded during the remainder of the 30-minute deployment. The rapid return to hydrostatic pressure suggests that the sealing of the formation around the tool was poor. The abrupt drop in

#### *In-Situ Sampling and Characterization of Naturally Occurring Marine Methane Hydrate Using the D/V JOIDES Resolution.*

pressure for one data value after 40 seconds appears to be a less severe version of the problem experienced at Site 1226 and is attributed to a leak near the probe tip.

### **Site 1228 – Downhole Tool Deployments**

At Site 1228, the downhole tools employed were the APC-temperature shoe, DVTP, DVTP-P, APC-M, and the Fugro Pressure Corer. The results of the temperature and pressure measurements at Site 1228 are described in the sections below.

#### *In Situ Temperature Measurements*

Two reasonably good downhole temperature determinations were made in Hole 1228A using the DVTP. An APC-temperature shoe deployment before Core 201-1228A-1 yielded a value for the bottom water temperature of 13.7° C. There were two successful DVTP deployments at 80.9 and 194.6 mbsf. Two other deployments at 42 mbsf and 137.9 mbsf resulted in unsatisfactory records.

*In situ* temperatures were estimated by extrapolation of the station data using thermal conductivities measured on adjacent cores to correct for the frictional heating on penetration. For both of the successful Site 1228 deployments, the data from the lower thermistor were used to extrapolate the *in situ* temperature. Because we obtained only two good downhole temperature estimates at Site 1228, the results from ODP Leg 112, Site 680 (Suess, et al., 1988) were included in the thermal gradient estimate.

The combined downhole temperatures of Sites 1228 and 680 define a gradient of 0.0336° C m<sup>-1</sup> in the upper 196 mbsf of the sediment column.

Comparing lithology and depth from locations that produced good and bad temperature data showed some differences that may be used to optimize future DVTP deployments. The two successful deployments were located at 80.9 mbsf and 194.9 mbsf. The sediments surrounding the first location were comprised of diatom-rich silty clay and recoveries averaged 70% (Cores 201-1228A-9H and 10H). The second location, near the base of the hole, was overlain by clay-bearing quartz feldspar sand and recovery was 41% (Core 201-1228A-22H). Two failed deployments were located at 42.9 mbsf and 137.9 mbsf. The first interval was comprised of silt, ash, and diatom ooze and the recoveries for the surrounding cores (Cores 201-1228A-5H and 6H) were 80% and 98%. However, for sediments cored in Hole 201-1228B over this same interval, recovery dropped to 60% (Core 201-1228B-5H). The worst deployment was at 137.9 mbsf in sandy clay where no sediments recovered in the subsequent core (Core 201-1228A-17H). Site 1228 was located in shallow water at a depth of 261 meters. These observations indicate that in shallow water sites where recoveries can be poor, deployments may be more successful deeper in the hole and in intervals with higher recoveries.

*In-Situ Sampling and Characterization of Naturally Occurring Marine Methane Hydrate Using the D/V JOIDES Resolution.*

### *Davis-Villinger Temperature Probe with Pressure (DVTP-P)*

The DVTP-P was deployed once at Site 1228 at a depth of 196.9 mbsf (after Core 201-1228A-22H). There was a sharp pressure increase when the tool was pushed into the sediments. The pressure drops within three minutes to about 4.74 MPa, which equals the predicted hydrostatic value for the hole depth and measured salinity gradient. For remainder of the 30-minute deployment, the pressure oscillates at 4.76 +/- 0.02 MPa. The amplitude of the oscillation corresponds to ~4 meters of head making it larger than the ~1-meter heave of the ship. However, periodic displacement of the drillpipe in the borehole, could amplify the oscillations caused by heave.

### *Other Tools*

The APC-Methane tool was successfully run continuously from Cores 201-1228A-9H to 14H. The tool appeared to function correctly and the data will be analyzed post cruise.

The Fugro Pressure Corer (FPC) was tested three times at Site 1228 at 7.3 mbsf, 54.3 mbsf, and 109.4 mbsf (Cores 201-1228E-2M, 1228B-7M, and 1228A-13M respectively). Due to a number of mechanical problems, the FPC failed to retrieve pressurized cores on any of the deployments. The one attempted use of the PCs (201-1228A-23P) resulted in only 7-centimeters of recovery from the 2 meter-long cored interval.

## **Site 1229 – Downhole Tool Deployments**

At Site 1229, the downhole tools employed were the Adara temperature shoe, DVTP, DVTP-P, APC-M, and the Fugro Pressure Corer. The results of the temperature and pressure measurements at Site 1229 are described in the sections below.

### *In situ Temperature Measurements*

One good downhole temperature determination was made in Hole 1229A using the DVTP. An APC-temperature shoe deployment before Core 201-1229A-1H yielded a value for the bottom water temperature of 14.9° C. A successful DVTP deployment was made at 164.9 mbsf. Four other deployments at 33.4 mbsf, 64.8 mbsf, 77.8 mbsf, and 107.9 mbsf resulted in records that could not be used.

Because we obtained only one good downhole temperature value at Site 1229, the results from ODP Leg 112, Site 681 (Suess, et al., 1988) were included in the thermal gradient estimate. Due to a variety of problems documented by the Leg 112 Shipboard Scientific Party (1988), each of the estimates for Site 681 is denoted as either an upper or lower bound on the true formation temperature. These constraints were used to define a line that passed through the single value for Site 1229 and honored the Site 681 estimates. The combined downhole temperatures yield a linear gradient of 0.0355° C m<sup>-1</sup> in the upper 187 meters of the sediment column.

### *In-Situ Sampling and Characterization of Naturally Occurring Marine Methane Hydrate Using the D/V JOIDES Resolution.*

The failure rate for DVTP measurements attributed to formation conditions increased at Site 1229 to a high of 80% compared to 50% at Sites 1227 and 1228 and 0% at Sites 1225 and 1226. The one successful measurement at Site 1229 was the deepest deployment attempted at 164.9 mbsf. It was located in lithologic Unit II, which is comprised of alternating sand and silt, and the subsequent core had the lowest recovery compared to the other four deployments (43%). The four unsuccessful deployments were located at shallower depths in silt, clay, or diatom ooze. These results indicate that deployments of the DVTP in shallow water (<200 meters) may be less likely to succeed at depths below 150 mbsf.

#### *Davis-Villinger Temperature Probe with Pressure (DVTP-P)*

The DVTP-P was deployed once at Site 1229 at a depth of 79.4 mbsf (after Core 201-1229A-9H). The lithology for this depth was comprised of diatom-rich ooze with an average porosity of 75%. The expected sharp pressure increase occurred when the tool entered the formation, followed by a sharp drop within one minute to about 2.42 MPa, which equals the predicted hydrostatic value for the hole depth and measured salinity gradient. For the remainder of the 30-minute deployment, the pressure oscillates at 2.42 +/- 0.02 MPa. The amplitude of the oscillation corresponds to ~4 meters of head, which was comparable to the oscillations at Site 1228. An investigation into the cause of the oscillations is needed.

#### *Other Tools*

The APC Methane tool was run continuously from Cores 201-1229A-1H to 1229A-10H. The tool appeared to function correctly and the data will be analyzed postcruise.

The Fugro Pressure Corer (FPC) was tested twice at Site 1229 at 24.4 mbsf and 174.4 mbsf (Cores 201-1229B-4M and -1229A-20M respectively). Due to a number of mechanical problems, the FPC failed to retrieve pressurized cores on either deployment. The single deployment of the PCS (201-1229D-10P) successfully recovered 0.86 meters of sediment from the 2 meter-long cored interval.

### **Site 1230 – Downhole Tool Deployments**

At Site 1230, the downhole tools employed were the APC-temperature shoe, DVTP, and the DVTP-P. The results of the temperature and pressure measurements at Site 1230 are described in the sections below.

#### *In situ Temperature Measurements*

Three downhole temperature determinations were made at Site 1230 using two DVTP deployments in Hole 1230A and one in Hole 1230B. Two APC-temperature shoe

*In-Situ Sampling and Characterization of Naturally Occurring Marine Methane Hydrate Using the D/V JOIDES Resolution.*

deployments at the seafloor yielded values for the bottom water temperature of 1.74–1.75° C. Data were collected from successful DVTP deployments at 33.3 mbsf, 100 mbsf, and 254.6 mbsf. Three other deployments at 73.5 mbsf, 79.9 mbsf, and 148.3 mbsf resulted in records that could not be used.

The combined downhole temperatures yield a linear gradient of 0.034° C m<sup>-1</sup> in the upper 255 meters of the sediment column.

The failure rate for DVTP measurements attributed to formation conditions at Site 1230 was 50%, compared to 80% at Site 1229, 50% at Sites 1227 and 1228, and 0% at Sites 1225 and 1226. To evaluate the causes of the failures, the conditions of the formation at each location were evaluated by noting the recovery, lithology, and disturbance of the subsequent core. The differences in outcome do not appear to be related to either lithology or core recovery. Instead, the degree of disturbance in the subsequent core may be significant. Although the cause of core disturbance on recovery is not known, areas of multiple fractures, voids, and crumbly fabric were common in the interval with high methane concentrations and gas hydrates. Moreover, the three failed deployments were located at 70–80 mbsf and 148–150 mbsf where the pore water lithium concentrations indicate the highest hydrate concentrations. On the basis of these observations, the best strategy for obtaining high quality temperature data in hydrate-bearing formations may be to identify depths of highest hydrate concentrations in the first hole and avoid these depths by deploying the tool in subsequent holes.

#### *Davis-Villinger Temperature Probe with Pressure (DVTP-P)*

The DVTP-P was deployed twice at Site 1230 with one successful run at a depth of 102.5 mbsf (after Core 201-1230A-14H). The results of this deployment indicate overpressure in the formation relative to the base of the hole. This deployment did not get a pressure spike at the start because the tool was pushed in extremely slowly over several minutes. The slow deployment strategy was suggested to increase the penetration depth of the tool without exceeding acceptable pressure on bit in the relatively stiff formation. The success of this strategy is evident from the 0.14 MPa difference between formation pressure and the hydrostatic pressure measured in the base of the hole for 5 minutes at the end of the deployment. For a reasonable formation permeability of  $\sim 10^{-16}$  m<sup>2</sup>, the measured overpressure is adequate to produce flow at a rate of  $\sim 5$  mm/yr.

## **LEG 201 – GAS HYDRATE STUDIES**

### **Site 1230**

#### *Initial Core Inspection and Hydrate Sampling*

Solid pieces of gas hydrate were recovered from two discrete intervals at Site 1230. Evidence of gas hydrate was identified in several additional cores below 80 mbsf. All

*In-Situ Sampling and Characterization of Naturally Occurring Marine Methane Hydrate Using the D/V JOIDES Resolution.*

cores from Site 1230 were inspected immediately after retrieval for indications of gas hydrate using visual identification and thermal scanning with an infrared camera. Signals of interest included the presence of white nodules, fizzing materials, or unusually cold spots. As soon as the core liner had been placed on the catwalk, the IR camera was run along the core to identify unusually cold core liner temperatures. Intervals recognized by the camera operator as potential gas hydrate zones were immediately cut out of the core and split. The split core surfaces were inspected for hydrate nodules or areas that were fizzing, which might indicate the occurrence of disseminated gas hydrate in the sediment.

Small pieces of massive gas hydrate were recovered from sediments of lithologic Subunit IB at ~80 mbsf (Hole 1230B) and the top of Subunit ID at ~148 mbsf (Hole 1230A). A 5 cm<sup>3</sup> hydrate piece from Core 201-1230B-12H was scraped with a spatula to remove surrounding sediment and placed into a syringe to collect gas and water for geochemical analyses. The remaining scraped sediment was then collected for microbiological analyses. Most other hydrate pieces were too small to be sampled in this manner. One fizzing and anomalously cold 15-centimeter-long whole-round section (Sample 201-1230A-19H-1, 135–150 cm) was also squeezed for interstitial water. Three other sections probably contained disseminated gas hydrate based on observed fizzing and temperatures as low as  $-3.2^{\circ}\text{C}$ , but discrete hydrate pieces were not recovered.

#### *IR Camera*

Infrared (IR) thermal imaging was used to compare non-hydrate bearing and hydrate-bearing cores from Site 1230. Core 1230A-6H did not contain hydrate, and has a homogeneous temperature distribution downcore. In contrast, Core 1230A-19H exhibits wide temperature changes between hydrate-bearing sediment, which is cold compared to surrounding sediment, and voids, which are warm compared to surrounding sediment. The occurrence of gas hydrate in this core was confirmed at the core top (148.3 mbsf). Several other cores exhibited negative temperature excursions of about  $-5^{\circ}\text{C}$  and also may have contained hydrate layers. The shallowest temperature anomaly occurred at ~71 mbsf in Core 1230A-10H. These results from Site 1230 illustrate the potential benefit of infrared thermal imaging for identifying gas hydrate in sediment cores immediately after retrieval.

#### *Lithology and Gas Hydrate Occurrence*

Sediments surrounding the interval of the upper hydrate sample consist of dark gray to olive clay-bearing diatom silt and diatom-rich nannofossil silt (Cores 1230B-11H and 12H; 73.5 mbsf to 90.5 mbsf). Diatom contents range between 20% and 40%. High angle normal faults with offsets of several centimeters occur in Sections 1230B-11H-4, 11H-5, and 12H-6. The sediments are characterized by pervasive cleavage with both low-angle and horizontal attitude. The recovered hydrate samples from Core 1230B-12H consisted of several vertical to sub-vertical wavy veins of white gas hydrate, up to 3 mm thick, separated by dark gray sediment.

#### *In-Situ Sampling and Characterization of Naturally Occurring Marine Methane Hydrate Using the D/V JOIDES Resolution.*

Sediments surrounding the lower hydrate consist of dark gray to black quartz-bearing clay-rich diatom ooze (Cores 1230A-18H and 19H; 138.8 mbsf to 156.8 mbsf). Diatom contents vary between 40% and 75%. The sediments have a stiff and highly fractured appearance and recovery was generally low throughout the subunit, possibly due to a combination of fracturing and high gas concentrations, which may have caused part of the sediment to blow out of the core barrel during retrieval. Horizontal to low-angle foliation is common in most cores of Subunit ID. In addition, Section 1230A-19H-2 was characterized by two high-angle (~30%) cleavage directions, which were measured by shipboard scientists. The co-occurrence of steeply dipping gas hydrate veins, pervasive cleavage, and the presence of high-angle normal faults at least in the upper part of the hydrate-bearing interval suggests a possible close relationship between locations of gas hydrate precipitation and tectonic features at Site 1230.

### *Core Disturbance*

Extensive core disturbance was noted in most of the cores below Core 1230A-3H. The following types of disturbance (ranging from a few cm to tens of cm in vertical extent) were described from this interval and compared with other evidence for gas hydrate:

1. Voids marked by clear separation of sediment and bounded on either side by disturbances of either type 2 or 3 below. In this category we specifically did not include voids where the separation was bounded by planar surfaces without other disturbance, because these can (and were observed to) form on the catwalk when the core liners were drilled to relieve pressure for safety reasons.
2. Crumbling of the sediment. Zones where the sediments are wholly or partially disaggregated adjacent to undisturbed sediment. For this category, we did not consider any core disturbance that was located at the top of a core.
3. Zones of splitting perpendicular to the core axis (i.e., parallel to bedding) where cracks are commonly more closely spaced than elsewhere in the core. In many cases there is a gradation from very closely spaced cracks near the center of the zone, to more widely spaced cracks.

While disturbance alone does not indicate hydrate occurrence, it suggests depth intervals where very high concentrations of methane could potentially support hydrate formation.

## **LEG 204 – OPERATIONAL SUMMARIES**

### **ODP Site 1244**

Site 1244 (proposed site HR1a) is located in 890 meters of water on the eastern flank of Hydrate Ridge ~3 km NE of the southern summit. The 3-D seismic data available from a

*In-Situ Sampling and Characterization of Naturally Occurring Marine Methane Hydrate Using the D/V JOIDES Resolution.*

Leg 204 Site Survey show that the Bottom-Simulating Reflection (BSR), a reflection that cuts across stratigraphic horizons and is generally thought to indicate the presence of free gas at the base of the gas hydrate stability zone (GHSZ), is at a depth of ~125 mbsf at this site. The temperature and pressure at the seafloor at this site are well within the GHSZ, indicating that gas hydrates can exist within the entire stratigraphic section above the BSR if hydrate-forming gases are available in concentrations that exceed their in situ solubility. The 3-D seismic data also indicate that the top of a zone of incoherent seismic reflections that forms the core of Hydrate Ridge is located at a depth of ~300 mbsf at Site 1244. This facies has been interpreted to comprise fractured accretionary complex material. Dipping, faulted, and strongly reflective strata interpreted to be an uplifted and deformed slope basin overlie this facies. An unconformity at ~40 mbsf at this site is correlated with an unconformity observed at 130 mbsf at Site 1251.

The primary drilling objectives at this site were to: (1) determine the distribution and concentrations of gas hydrate within the gas hydrate stability zone; (2) determine the nature of a pair of strong reflections (referred to as B and B') that underlies much of the eastern flank of Hydrate Ridge; (3) determine the composition, structure and fluid regime within the seismically incoherent unit underlying the stratified sediments; and (4) sample the subsurface biosphere associated with these features.

### *Operations*

Six holes were cored at Site 1244. Holes 1244A–1244D were drilled consecutively on 13–17 July; we returned to this site on 19 August to core Holes 1244E and 1244F. During both periods of time, wind speed was 4–21 kt (gusting to 25 kt), seas were 2–5 ft, swell was 6–10 ft, and the prevailing sea-surface current was from the north at ~0.5 kt.

The APCT tool was deployed ten times. In addition there were four DVTTP, two Fugro-McClelland piezoprobe, eight Ocean Drilling Program (ODP) PCS, and one Fugro Pressure Corer (FPC) runs at this site. No Hydrate Autoclave Coring Equipment (HYACE) Rotary Corer (HRC) cores were taken at this site.

Hole 1244A was abandoned when the first core overshot and did not record a mudline. Hole 1244B was spudded at 1325 hr on 13 July. The hole was cored using the advanced piston corer (APC), and one APCT measurement was taken at 35.1 mbsf in this hole. After collecting six APC cores (Cores 204-1244B-1H through 6H), the Fugro piezoprobe was deployed for its first test on the *JOIDES Resolution*. During this deployment, the connection between the top of the tool, the electric logging line failed and the tool was left sitting on the landing ring in the BHA. We therefore had to pull out of the hole with the logging line and the drill string.

Hole 1244C was cored from the seafloor using the APC. The second Fugro piezoprobe test was conducted after Core 204-1244C-6H was taken at a depth of 53.0 mbsf. This was an excellent run with excellent data. A good decay curve was achieved after the tool sat

### *In-Situ Sampling and Characterization of Naturally Occurring Marine Methane Hydrate Using the D/V JOIDES Resolution.*

for ~30 min in the formation. The drill string did not become stuck. There were three runs of the APCT tool in this hole, and the PCS was deployed three times. The cores were gassy (with methane), but no H<sub>2</sub>S was detected. We continued to conduct continuous XCB coring operations in Hole 1244C until we reached the total depth (TD) in Hole 1244C at 333.5 mbsf and concluded coring because of hole instability. Examination of Core 204-1244C-39X (331.5 mbsf) and the initial chemical data from this depth suggested we had reached the deepest target (i.e., the accretionary complex). We had thus fulfilled the JOIDES Pollution Prevention and Safety Panel (PPSP) requirement that we core the primary facies that we expected to encounter during logging while drilling (LWD) prior to proceeding with LWD at all sites. Acquiring LWD data at all of our sites at the beginning of the leg enabled us to use these data in concert with the previously collected 3-D seismic data to anticipate the nature of horizons prior to drilling and better plan the use of special tools for the rest of the leg.

Hole 1244D was spudded at 1505 hr on 16 July with the Anadrill LWD tools, to begin the LWD program of Leg 204. The LWD tools (63/4-in collars) include the resistivity at the bit (RAB)-6 with 91/8-in button sleeve, measurement while drilling (MWD) (Powerpulse), Nuclear Magnetic Resonance porosity (NMR-MRP) tool, and Vision Neutron Density (VND) tool. Drilling proceeded at ~25 m/hr to TD (380 mbsf) without difficulty, and real-time data were transmitted to the surface at a rate of 6 Hz. Some extraneous pump noise affected the data transmission for 2–5 min after each pipe addition but caused minimal real-time data loss. Above TD, the tools were pulled out of the hole without rotating to ~355 mbsf to evaluate the effect of drilling motion on the NMR log. LWD tools and data were retrieved at the rig floor at ~1730 hr on 17 July. Total bit run was ~38 hr.

Hole 1244E was spudded at 0614 hr on 19 August and APC cored to 135.8 mbsf as a dedicated hole for microbiological studies and retrieval of cores under pressure. The PCS was deployed four times at this site. Core 204-1244E-3P (18.2–19.2 mbsf) was retrieved under pressure, but it had little or no core recovery. The other three PCS cores were successfully recovered from above the BSR, which at this site lies at ~124 mbsf.

A deployment of the HYACINTH FPC tool in Hole 1244E resulted in the recovery of Core 204-1244E-8Y (FPC 9) at 50.70 mbsf. This core was recovered under full pressure and was successfully transferred from the autoclave into transfer and logging chambers. Other special tools at this site include six APCT measurements and two deployments of the DVTPP. Whirl-Paks and perfluorocarbon tracer (PFT) used for microbiology were obtained with Cores 204-1244E-4H, 5H, 7H, 9H, 10H, 12H, 13H, 14H, 16H, 17H, 18H, and 19H. Coring to refusal of the APC tool was followed with two wireline logging runs using the triple combination (triple combo) and Formation MicroScanner (FMS)-sonic tool and vertical, constant offset, and one to two stations of walkway vertical seismic profile.

## ODP Site 1245

Site 1245 (proposed site HR3a) is located in 870 meters of water on the western flank of Hydrate Ridge ~3 km NW of the southern summit. The 3-D seismic data available from a Leg 204 Site Survey show that the Bottom-Simulating Reflector (BSR), a reflector that cuts across stratigraphic horizons and is generally thought to indicate the presence of free gas at the base of the gas hydrate stability zone (GHSZ), is at a depth of ~134 mbsf at this site. As at all sites during Leg 204, the temperature and pressure at the seafloor at this site are well within the GHSZ, indicating that gas hydrates can exist within the entire stratigraphic section above the BSR if hydrate-forming gases are available in concentrations that exceed their in situ solubility. A faint reflection that underlies the BSR and is approximately parallel to it has tentatively been interpreted to be a second BSR that may indicate the base of the stability zone of hydrates that include higher hydrocarbons. This site also samples a strong regional seismic reflection, referred to below as Horizon A. Horizon A can be mapped from the northern boundary of the seismic survey, where it clearly follows stratigraphic boundaries, to the summit, where it appears as a “bright spot” beneath the BSR. On its down-dip edge, it appears to lap onto the boundary between coherent folded strata and the seismically incoherent facies interpreted to represent highly deformed sediments of the accretionary complex. It has been interpreted to be a “conduit” that transports fluids from the accretionary complex to the summit. Several unconformities, referred to as Horizons Y and Z, overlie Horizon A and appear to represent discontinuities in sediment accumulation in a slope basin that was formed during growth of an underlying accretionary anticline.

A primary objective at Site 1245 was to determine the distribution, composition and concentration of gas hydrate in the sediments on the western flank of Hydrate Ridge and contrast these parameters with those on the eastern flank of the ridge and in the adjacent slope basin, where the sub-BSR fluid migration pathways inferred from seismic data are distinctly different. Another important objective was to sample sediments and fluids from Horizon A to determine whether this horizon is indeed a conduit supplying methane to form gas hydrate and carbonate on the seafloor at the summit. A third objective was to sample the sedimentary section of the western flank of Hydrate Ridge below the BSR to provide constraints for interpreting variations in BSR strength across the western flank. Site 1245 is also a reference site for a north-south trending transect that extends from Site 1245 to the summit and includes Sites 1247, 1248, 1249 and 1250.

### *Operations*

Five holes were drilled at this site, under good weather conditions. Wind speed was 5–24 kt, gusting to 29 kt; seas were 4–9 ft; swell was 6–15 ft; and the prevailing sea-surface current was from the north at ~0.5–0.9 kt. Hole 1245A was drilled to a depth of 380 mbsf without coring on 18 July 2002 to obtain the initial LWD data for this site. We returned to this site from 6 to 13 August to core Holes 1245B–1245E.

*In-Situ Sampling and Characterization of Naturally Occurring Marine Methane Hydrate Using the D/V JOIDES Resolution.*

The APC temperature (APCT) tool was run ten times and the Davis-Villinger Temperature Tool (DVTP) was run three times at this site. The pressure core sampler (PCS) was run six times, and five deployments were recovered core under pressure. Four deployments of HYACINTH were made at Site 1245, two each with the Hydrate Autoclave Coring Equipment (HYACE) Rotary Corer (HRC) and Fugro Pressure Corer (FPC). Technical and operational difficulties prevented these cores from being recovered under full pressure for further analysis. No in situ pressure measurements were made at this site.

Hole 1245A was drilled to obtain the initial LWD data for this site. Drilling proceeded at ~25 m/hr to total depth (TD) at 380 mbsf without difficulty, and real-time data were transmitted to the surface at a rate of 6 Hz. Given calm heave conditions, the real-time data record was changed to increase the depth resolution of formation evaluation logs with less emphasis on high-resolution weight-on-bit and torque measurements. Mud pump noise affected the data transmission to a lesser extent than at Site 1244. No sliding tests were conducted for the Nuclear Magnetic Resonance (NMR-MRP) tool. Total bit run was ~28 hr.

Hole 1245B was cored to 473.7 mbsf using the APC and XCB. Special tool deployments included five APCT tool and three DVTTP, three PCS from which two PCS cores were successfully recovered under pressure, and one HRC. The HYACINTH FPC (Core 204-1245B-18Y) recovered core; however, the flapper on the corer failed to close. Whirl-Paks and PFT were used for microbiology Cores 204-1245B-23X, 24X, 26X, 31X, 38X, 43X, and 49X. Hole 1245B was terminated at a total depth of 473.6 mbsf.

Hole 1245C was cored to 198.7 mbsf using the APC and XCB. Special tool deployments included five APCT, three PCS, and three Drill String Acceleration (DSA) tool runs. Whirl-Paks and PFT were used for microbiology Cores 204-1245C-1H, 2H, 4H, 5H, 7H, 9H, 12H, 15X, 17X, 20X, 22X–26H, and 28X.

Hole 1245D was cored to 24.0 mbsf using the APC. These three cores were recovered for microbiological and chemical whole-round sampling. Whirl-Paks and PFT were used in all cores. No special tools were deployed in this hole.

Hole 1245E was drilled without coring with the RCB/center bit to 473.7 mbsf, followed with RCB coring to 540.3 mbsf. Hole conditions deteriorated and we were unable to clean up the hole below that point; therefore, we began to pull out for the pre-logging wiper trip. At this point, the pipe became stuck and was not freed even after releasing the bit. After ~15 hr, preparations were made to sever the pipe; however, the pipe was successfully released and the hole was not abandoned. Logging in the upper 300 mbsf with the triple combination (triple combo) and Formation MicroScanner (FMS)-sonic wireline tool strings were successful.

The first helicopter rendezvous at this site occurred at 1308 hr on 13 August. Arriving passengers included Herbert Leyton, Schlumberger vertical seismic profile (VSP) engineer, and Roy Davis, Ocean Drilling Program (ODP)/Texas A&M University (TAMU) photographer. Departing passengers included Bill Gwilliam, from the Department of Energy (DOE)/National Energy Technology Laboratory (NETL), Floris Tuynder, HYACINTH Fugro FPC engineer, and Dean Ferrell, ODP/TAMU senior electronic designer. A second trip of the helicopter brought Ben Bloys along with initial batch of VSP surface equipment. The remaining three-component VSP tools arrived on a third helicopter trip on 14 August. However, the plans for conventional, offset, and walk-away seismic lines were abandoned when the downhole seismometer would not clamp in Hole 1245E and the hole continued to collapse.

### **Site 1246**

Site 1246 (proposed site HR1b) is located in 848 meters of water near the crest of Hydrate Ridge ~3 km N of the southern summit. The 3-D seismic data available from a Leg 204 Site Survey show that the Bottom-Simulating Reflector (BSR), a reflector that cuts across stratigraphic horizons and is generally thought to indicate the presence of free gas at the base of the gas hydrate stability zone (GHSZ), is at a depth of ~114 mbsf at this site. This site also samples a pair of bright, regional seismic reflectors, referred to below as horizons B and B', at depths of ~60 and 100 mbsf, respectively. The temperature and pressure at the seafloor at this site are well within the GHSZ, indicating that gas hydrates can exist within the entire stratigraphic section above the BSR if hydrate-forming gases are available in concentrations that exceed their in situ solubility.

The primary objective at Site 1246 was to sample horizons B and B' when they are within the gas hydrate stability zone (GHSZ). By comparing this site to Site 1244, where horizons B and B' are below the GHSZ, we hope to constrain lithologic and hydrologic explanations for the strong reflectivity of these seismic horizons and obtain insights into the processes that transport fluids into and through the GHSZ. A better understanding of the relationships among seismic reflectivity, sediment lithology and physical properties is needed to develop effective strategies to predict hydrate occurrence from seismic and other remote sensing data

### *Operations*

Two holes were drilled at Site 1246, under good weather conditions. Wind speed was 5–25 kt, gusting to 28 kt; seas were 4–9 ft; swell was 6–12 ft; and the prevailing sea-surface current was from the north at ~0.5 kt. Hole 1245A was drilled for LWD on 19 July 2002, and we returned on 11 August, near the middle of Leg 204, to core Hole 1246B. The APC temperature (APCT) tool was run five times, and no other special tools were deployed at this site.

*In-Situ Sampling and Characterization of Naturally Occurring Marine Methane Hydrate Using the D/V JOIDES Resolution.*

The first helicopter rendezvous took place at Site 1246 on Friday 19 July 2002. The helicopter arrived at 1247 hr and was away again with passengers at 1307 hr. Pressure core sampler (PCS) scientist Jerry Dickens and Fugro piezoprobe engineers Terry Langsdorf and Ko-min Tjok disembarked from the JOIDES Resolution, while sedimentologist Xin Su and HYACINTH engineer Thjunjoto came aboard. Hole 1246A was spudded at 0300 hr on Friday 19 July, and we conducted LWD/measurement while drilling (MWD) from the seafloor at a drilling rate of 25–30 m/hr, to a depth of 180 mbsf without difficulty. Real-time data were transmitted to the surface to evaluate formation properties. Two stands were pulled up from total depth (TD) without rotating (sliding test) to evaluate the drilling effects on the Nuclear Magnetic Resonance (NMR-MRP) tool. Tools were pulled to the rig floor at 1900 hr, and the data from both Holes 1245A and 1246A were downloaded. Total bit run was ~20 hr.

Hole 1246B was cored to 136.7 mbsf using the APC. Five measurements of in situ temperature were made using the APCT tool. No in situ pressure measurements were made, nor were any PCS cores taken at this site. There were no deployments of HYACINTH pressure cores.

### **ODP Site 1247**

Site 1247 (proposed site HR4c) is located in ~845 meters of water on the western flank of Hydrate Ridge ~800 m NW of the southern summit and approximately half way between Site 1245 and the summit. The 3-D seismic data indicate that the seismic stratigraphic setting is similar to that of Site 1245 (see Site 1245 summary). The Bottom-Simulating Reflector (BSR) is at a depth of ~121-124 mbsf at this site. Horizon A is brighter and shallower (~160 mbsf) at Site 1247 than at Site 1245; Horizon Y is also shallower (~60 mbsf) at this site.

A faint, negative-polarity reflection approximately 40 m below the BSR is observed in this region. While the possibility that this event is a source artifact has not been definitively ruled out, an abrupt decrease in the amplitude of Horizon A as it crosses this reflection and approaches the BSR from below suggests that it may be a “second BSR” resulting from the presence of more stable hydrate structures that contain higher order hydrocarbons, as has been suggested for similar features observed elsewhere.

The primary objective at Site 1247 was to sample sediments and fluids from Horizon A approximately half way between Site 1245 and the summit (Site 1249) in order to determine up-dip variations in the physical and chemical characteristics of this horizon and thus understand the role it plays in fluid migration and formation of hydrate on the seafloor at the summit. A second related objective was to investigate the origin of the second “BSR.” Although they are only 75 m apart, the two Holes drilled at this site sample parts of Horizon A with distinctly different seismic characteristics.

### *Operations*

Two holes were drilled at Site 1247 under good weather conditions. Wind speed was 4–19 kt, gusting to 23 kt; seas were 4–7 ft; swell was 6–7 ft; and the prevailing sea-surface current was from the north at ~0.5 kt.

Hole 1247A was drilled without coring to obtain the initial LWD data for this site. We initiated continuous LWD/measurement-while-drilling (MWD) drilling and advanced at a rate of penetration (ROP) of 25–30 m/hr, to a total depth (TD) of 270.0 mbsf. LWD operations began at 2030 on 20 August, with tool initialization at the rig floor. LWD tools included the Resistivity at the Bit (RAB)-6 tool, with 91/8-in button sleeve, MWD, the Nuclear Magnetic Resonance (NMR-MRP) tool, and Vision Neutron Density (VND) tool. Heave conditions increased, and the real-time data record was changed to increase the time resolution of weight-on-bit and torque measurements for heave analysis. LWD tools were pulled to ~60 m above the seafloor for the dynamic positioning move to Site 1248. Total bit run was ~21 hr.

We returned to this site on 22–24 August to core Hole 1247B. Hole 1247B was offset from Hole 1247A by ~87 m to the west. This hole was cored to 220 mbsf using the APC and XCB. Six in situ temperature runs were made at this site using the APCT tool, including a dedicated mudline run; two DVTP runs were also made. No in situ pressure measurements were made at this site.

The PCS was deployed three times at Site 1247. Two of these deployments recovered core under pressure; however, the ball valve did not fully close during the other deployment.

Hole 1247B was logged using the triple combination (triple combo) and Formation MicroScanner (FMS)-sonic tool strings. After wireline logging, a vertical and an offset vertical seismic profile (VSP) covering the interval of 104–214 mbsf was acquired by alternately shooting from the *JOIDES Resolution* and the *Ewing*, which held station ~700 m away. Plans to conduct walk-away VSPs were abandoned when the Schlumberger Vertical Seismic Imager (VSI) would no longer clamp in the hole.

### **ODP Site 1248**

Site 1248 (proposed Site HR6) was drilled in 832 m a water depth of ~300 m northwest of the southern Hydrate Ridge summit. This site is located in the middle of a small (~150 m-in-diameter) high-reflectivity spot on the seafloor imaged by a deep-tow sidescan sonar survey. The small spot is located 300 m north of a larger circular high reflectivity patch around the Pinnacle, a well known active carbonate chemoherm. These are the only two locations on southern Hydrate Ridge where high backscatter reflectivity is observed and are interpreted as seafloor manifestations of fluid venting. TV-sled surveys revealed some evidence for the occurrence of scattered authigenic carbonate fragments within the

*In-Situ Sampling and Characterization of Naturally Occurring Marine Methane Hydrate Using the D/V JOIDES Resolution.*

small high-reflectivity patch, which might be responsible for the higher backscatter signal observed in the sidescan sonar data. The 3-D seismic data show attenuation of the underlying stratigraphic reflectivity, similar to what is observed beneath the Pinnacle. Both areas of high backscatter overlie the intersection of seismic Horizon A, a coarse-grained, ash-rich layer that seems to be a fluid migration pathway, and the Bottom-Simulating Reflector (BSR), which indicates the base of the methane hydrate stability zone as confirmed by multiple proxies for hydrate occurrence (see Site 1245 Summary).

The principal objective at Site 1248 was to investigate whether the sediments below the high-reflectivity seafloor spot contain evidence of active fluid advection within the stratigraphic sequence of Southern Hydrate Ridge and if these fluids are supplied by Horizon A. Furthermore, this site could be a test site to determine whether this inferred incipient venting area may develop into a massive Pinnacle-like carbonate mound on the seafloor.

### *Operations*

Three holes were drilled at Site 1248, under good weather conditions. Wind speed was 8–24 kt, gusting to 28 kt; seas were 4–9 ft; swell was 6–10 ft and the prevailing sea-surface current was from the north at ~0.5 kt.

Hole 1248A was drilled without coring to obtain the initial LWD data for this site to a total depth (TD) of 194.0 mbsf. LWD operations began at 2130 on 20 July by spudding Hole 1248A at 832 m water depth. Drilling proceeded at reduced rates of penetration (ROP) of 15 m/hr and 15 spm circulation to moderate formation washout at shallow depths below seafloor. No real-time measurement-while-drilling (MWD) or nuclear magnetic resonance (NMR) data were recorded over this interval, as the pump rate was insufficient to activate the turbines in these tools. The penetration rate was increased to ~25 m/hr at a bit depth of 30 mbsf to TD (190 mbsf), and real-time MWD and NMR data were recorded. The LWD tools were pulled to ~60 m above the seafloor at 0700 on 21 July. Total bit run took ~15 hr.

Hole 1248B was spudded at 0300 hr on 1 August. Three cores were collected with the APC, after which the hole was abandoned at 17 mbsf. Coring disturbance resulting from near-seafloor massive gas hydrates and a shattered liner during retrieval of Core 204-1248B-3H caused poor core recovery (44%). There was one APCT tool deployment in Hole 1248B. There were no other special tools deployed at this hole.

Hole 1248C was spudded with the XCB in an attempt to increase core recovery. Cores were drilled to 48 mbsf. Recovery was poor (23%) in Cores 204-128C-1X to 5X, and then it increased in Cores 204-1248C- 6H through 17X to 90% of the penetration. Cores 204-128C-6H to 16H were collected with the APC; these were followed by one XCB core to 149 mbsf. Five in situ temperature runs were made at this hole: two APCT tool, two DVTPP, and one DVTP runs.

*In-Situ Sampling and Characterization of Naturally Occurring Marine Methane Hydrate Using the D/V JOIDES Resolution.*

## ODP Site 1249

Site 1249 (proposed Site HR4b) was drilled in 778 m of water on the summit of southern Hydrate Ridge. This area is characterized by active gas venting and gas hydrate formation at the seafloor. Vigorous streams of bubbles emanate from the seafloor at the summit and have been observed during submersible and ROV dives and are consistently observed with high-frequency echo sounders as plumes in the water column. Outcrops of massive hydrate are also visible on the seafloor. These observations are interpreted to indicate that methane bubbles rising through the sediment column are sometimes trapped to form hydrate near the seafloor and sometimes escape into the water column. In the subsurface, a distinctive pattern of chaotic, strong reflectivity is seen in seismic data to extend to ~30 mbsf beneath the region where the seafloor is anomalously reflective in side-scan data. This pattern has been interpreted to result from lenses of massive hydrate intercalated with sediment. The BSR at this site is estimated based on seismic data to be at 115 mbsf, but coring was only permitted to 90 mbsf at this summit site because of the possibility of trapped gas beneath the BSR.

The primary objective at Site 1249 was to determine the distribution and concentration of hydrate with depth at the summit and obtain constraints on how methane bubbles can coexist with hydrate and porewater within the hydrate stability field.

### *Operations*

Twelve holes were drilled at this site, under good weather conditions. Wind speed was 0-8 kt, gusting to 12 kt; seas were 0-4 ft; swell was 4-7 ft; and the prevailing sea surface current was from the north at ~0.5 kt. LWD data were collected from Hole 1249A on 21 July 2002. We returned to this site on 24-26 July for LWD operations in Hole 1249B using the new RAB-8 coring system and to core Hole 1249C to 89.5 mbsf with the APC. We returned to this site again on 4-6 August to core Holes 1249D-1249F. Near the end of the leg, we occupied this site one last time on 27-29 August to core Holes 1249G-1249L with the APC/XCB for a shore-based hydrate geiatrics study. During this last visit, wind speed had increased to 14-19 kt, gusting to 23 kt; seas were 6-7 ft; and swell was 8-10 ft.

All pressure coring systems available were used at Site 1249. The ODP pressure core sampler (PCS) was deployed a total of six times, and the Fugro Pressure Corer (FPC) and HYACINTH Hydrate Autoclave Coring Equipment (HYACE) Rotary Corer (HRC) were each deployed three times at this site. Eleven in situ temperature runs were made at this site: nine using the APC temperature (APCT) tool and two using the Davis-Villinger Temperature-Pressure Probe (DVTTP). Pressure data were measured using the DVTTP.

The *Mauna Loa*, an ocean-going tugboat, came alongside on 25 July and was secured on the starboard side at 0605 hr to transfer freight and personnel to the *JOIDES Resolution*. Personnel included HYACINTH FPC engineers Floris Tuynder and Roeland Baas, logging scientist Gilles Guérin, Dallas Morning News journalist Alexandra Witze,

*In-Situ Sampling and Characterization of Naturally Occurring Marine Methane Hydrate Using the D/V JOIDES Resolution.*

paleontologist Mahito Watanabe, and HRC engineer Felix Weise. A linear X-ray scanner (LXS) from Lawrence Berkley National Laboratory (Freifeld et al., in press, 2002) was installed in the core laboratory, and training of personnel was conducted. In addition, the TAMU logistics coordinator, an LXS scientist (Barry Freifeld), and an LXS student technician/programmer came on board for the day. Off-going personnel included logging scientists Nathan Bangs and David Goldberg, LWD engineers Stefan Mrozewski and Khaled Moudjeber, and geophysicist Martin Vanneste. LWD tools were loaded, and the *Mauna Loa* departed for Coos Bay, Oregon, at 1715 hr.

On 6 August, a helicopter arrived on deck at 1227 hr with passengers Bill Gwilliam from Department of Energy (DOE)/National Energy Technology Laboratory (NETL), Dean Ferrell, electrical technician from the Ocean Drilling Program (ODP)/Texas A&M University (TAMU), and Transocean 3rd engineer Yorn Verschoor. The helicopter departed at 1243 hr carrying passengers Alexandra Witze, a journalist from the Dallas Morning News, and John Beck, ODP/TAMU photographer.

The final rendezvous of the leg took place on 27 August, when the *Mauna Loa* tied up along port side at 0650 hr. We loaded crates for packing the off-going Vertical Seismic Imager (VSI)/Schlumberger equipment, DOE pressure vessels/sample dewars, liquid nitrogen cryofreezers, and equipment for the German film crew (CONTEXT-TV). Schlumberger downhole tools/pallets and off-going samples were off-loaded. Passengers joining the *JOIDES Resolution* included Jan Hartmann and Stephan Braun from German CONTEXT-TV and Randy Showstack, Eos journalist.

The *Mauna Loa* released at 0900 hr to transfer personnel and equipment to and from the Ewing. The *Mauna Loa* returned alongside the *JOIDES Resolution* at 1100 hr and off-loaded the remaining Schlumberger VSI surface equipment. Passengers departing the *JOIDES Resolution* included Alexei Milkov, sedimentologist, and Herbert Leyton, Schlumberger VSP engineer. The *Mauna Loa* departed at 1130 hr.

Hole 1249A was spudded at 0900 hr on 21 July to conduct LWD measurements using the same tools as were used at the other sites during this leg. Drilling proceeded at reduced rates of penetration (ROPs) of 15 m/hr and 15 strokes per minute (spm) circulation to moderate formation washout at shallow depths below seafloor. No real-time measurement-while-drilling (MWD) or nuclear magnetic resonance (NMR) data were recorded over this interval. The ROP was increased to 25 m/hr from a bit depth of 30 mbsf to a total depth (TD) of 90 mbsf, and real-time MWD and NMR data were recorded. The LWD tools were pulled to ~60 m above the seafloor at 1600 hr on 21 July. Total bit run took ~7 hr.

Hole 1249B was drilled using the new LWD RAB-8 and coring system, which permits simultaneous acquisition of core and logging data. LWD operations began with initialization of the RAB-8 at 1315 hr on 24 July. Although exercised fully in Houston, Texas, the inner mandrel in the RAB-8 BHA was too high to make up with the 65/8-in

*In-Situ Sampling and Characterization of Naturally Occurring Marine Methane Hydrate Using the D/V JOIDES Resolution.*

pin above. The inner diameter of the pin was ground down, and the motor-driven core barrel (MDCB) was tested until it passed through. Hole 1249B was finally spudded at 2000 hr. Drilling proceeded ahead to 30 mbsf, and coring operations began with sequential 4.5- and 9-m cores recovered through hydrate-bearing clays to a TD of 74.9 mbsf. Bit rotation varied from 15 to 45 rpm, increasing with depth, and the average ROP using this system was ~8 m/hr. The RAB-8 was recovered at the rig floor at 1200 hr on 25 July, and the data recorded in computer memory were downloaded. Total testing time was ~22 hr.

The recorded RAB data from Hole 1249B are of good quality over the drilled interval and correlate well with the log curves in Hole 1249A. The eight rotary cores recovered from Hole 1249B had an average of 32.9% recovery. These test cores were normally processed and archived and will be correlated to the RAB logs over the same depth interval. RAB-8 images and logs are of high quality but require additional depth correction to account for the coring process. With harder formations and faster rotary coring, both core recovery and log data quality are expected to improve using the RAB-8 coring system.

This successful test marks the first ever logging-while-coring experiment, a new technology that allows for precise core-log depth calibration and core orientation within a single borehole and without a pipe trip. It represents an outstanding example of a successful cooperative effort between Lamont-Doherty Earth Observatory (LDEO) and TAMU to develop and validate the logging-while-coring concept.

Holes 1249C-1249F recovered a 90-m sediment sequence with the APC. Core recoveries were <30% in the uppermost 20 mbsf and increased to 70% deeper in the holes. All pressure coring devices were used to sample this sediment sequence in an effort to capture massive hydrate samples under pressure and to compare the capabilities of each of these tools in sampling gas hydrates. The PCS was deployed six times in these holes, but only three cores were recovered under pressure. Two deployments of the FPC at 8 mbsf did not recover core at in situ pressures. A deployment of the HRC at 8 mbsf in Hole 1249F resulted in successful recovery of core under full pressure, which was rapidly cooled in the ice bath to maintain stability, successfully sheared, and transferred into the HYACINTH logging chamber. It was subsequently logged repeatedly in the Geotek Vertical Multi Sensor Core Logger (V-MSCL) while being degassed over the following 2 days.

Temperature measurements were collected during six runs of the APCT tool (one in Hole 1249C and five in Hole 1249F) and two runs of the DVTPP (one in each of Holes 1249C and 1249F). Whirl-Paks and perfluorocarbon tracer (PFT) were used for microbiology cores in Holes 1249D-1249F and the Drill String Acceleration (DSA) tool was run in Holes 1249C (once) and 1249F (twice).

*In-Situ Sampling and Characterization of Naturally Occurring Marine Methane Hydrate Using the D/V JOIDES Resolution.*

Holes 1249G–1249L were APC/XCB cored for a special shore-based geiatrics experiment in which several means of preserving gas hydrates for future study will be compared. Of the 40 steel pressure vessels that were taken on board, 34 were repressurized with core samples. The total quantity of core preserved in pressure vessels is ~50 m of sediment. The pressure being maintained in each of these vessels is nominally 550-600 psi at 4°-6°C. The remaining ~35 m of core recovered was placed into labeled cloth bags and is preserved in liquid nitrogen cryofreezers. Both the pressure vessels and the cryofreezers were stored in a refrigerated container van aft of the drill floor on the core tech shop roof. We conducted systematic periodic monitoring of the ambient air inside the container van by taking samples and running them through the shipboard gas chromatograph. We also monitored the gas pressures in each of the pressure vessels, the levels of the liquid nitrogen in the cryofreezers, and the temperature in the containers.

Two pressure vessels originally filled and repressurized with sediment containing significant quantities of hydrogen sulfide were taken out of service because of the risk of steel metal fatigue as a result of contact with hydrogen sulfide. In addition, two pressure vessels failed to maintain pressure because of leaks in valve or gauge connections; some of the hardware from these vessels was used to replace faulty gauges on other pressure vessels. Two additional pressure vessels were not used because of the termination of coring. These are available for future studies and for use as “standards” to make gamma ray attenuation (GRA) density measurements.

The Transocean drillers, core technicians, and rig crew did a superb job of handing the cores recovered on deck and transferring them to the ODP Marine Laboratory Technicians and ODP Shipboard Curator for processing on the catwalk. All the personnel involved were extremely fast, efficient, and professional in their handling of these hydrated cores in a way to maximize core preservation and ensure core quality. The safe handling of the pressure vessels, their repressurization, and the resulting preservation of the cores contained inside was successfully carried out in a short space of time immediately following the arrival of a large amount of equipment transported to the *JOIDES Resolution* by supply boat.

In addition to the APC/XCB cores for the geiatrics study, there were three deployments of pressure coring devices in these holes. The HRC deployment at 13.5 mbsf in Hole 1249G successfully recovered a 75-cm core with massive hydrate layers at full pressure and transferred this material into a HYACINTH storage chamber. It was subsequently frozen in Helium under pressure and successfully transferred into liquid nitrogen for preservation. It is probably the most pristine sample of natural gas hydrate ever recovered and preserved.

The FPC was also deployed at 13.5 mbsf in Hole 1249G and recovered 75 cm of core at full pressure. A good GRA density log was obtained from the core in the storage chamber showing massive hydrate layers. This core was designated as a “reference core” and

*In-Situ Sampling and Characterization of Naturally Occurring Marine Methane Hydrate Using the D/V JOIDES Resolution.*

companion to the APC and XCB cores that were taken and repressurized under methane. It was kept in the refrigerator ready for transportation to Texas A&M University for further study.

The HRC was deployed again, deeper in the sediments in Hole 1249L (37.5 mbsf), in an attempt to recover pristine material under pressure from a region where the hydrate is more disseminated. Some pressure was lost during disassembly, but it was rapidly repressurized to in situ pressures before being transferred to the logging chamber.

Temperature measurements were collected with one APCT tool run in each of Holes 1249G, 1249I, and 1249L.

### **ODP Site 1250**

Site 1250 (proposed Site HR4a) was drilled in 792 m water depth ~100 m west of the southern summit of Hydrate Ridge and ~100 m east of the carbonate chemoherm known as the Pinnacle. On southern Hydrate Ridge, the Pinnacle is the only carbonate mound, whereas at northern Hydrate Ridge several major chemoherms are known. The Pinnacle has near-vertical flanks rising about 40 m above the seafloor and a diameter of ~150 m. The carbon source for formation of the Pinnacle is known to be methane from the very low delta  $^{13}\text{C}$  values. Based on  $^{230}\text{Th}/^{234}\text{U}$  dating, the Pinnacle seems to have precipitated during the last 12 ka. The Pinnacle is located in the middle of a high-reflectivity patch mapped by a deep-tow sidescan sonar survey, which might be created by scattered carbonates close to the seafloor and/or the shallow occurrence of gas hydrates. Site 1250 lies close to the eastern rim of the high-reflectivity patch. The pre-cruise 3-D seismic reflection survey data show that the high amplitude reflector known as Horizon A meets the BSR just below the Pinnacle.

The primary objective at Site 1250 was to sample the sediments, fluids, gases and gas hydrates under the high backscatter reflectivity seafloor. The sediments at Site 1250 were expected to be strongly affected by the upward fluid migration that has resulted in the formation of the Pinnacle chemoherm. In this context understanding the role of Horizon A as a conduit for fluid flow and its interaction with the BSR was of special interest.

### *Operations*

Six holes were drilled at Site 1250, under good weather conditions. Wind speed was 0–11 kt, gusting to 16 kt; seas were 0–4 ft; swell was 4–8 ft and the prevailing sea-surface current was from the north at ~0.5 kt. Holes 1245A and 1250B were drilled without coring on 21–22 July 2002 to obtain the initial LWD data for this site. We returned to this site on 2–4 August to core Holes 1250B through 1250E and again on 24–27 August to core Hole 1250F.

*In-Situ Sampling and Characterization of Naturally Occurring Marine Methane Hydrate Using the D/V JOIDES Resolution.*

Hole 1250A was spudded at 1830 hr on 21 July to obtain the initial LWD data for this site. Drilling proceeded at reduced rates of penetration (ROPs) of 15 m/hr and 15 strokes per minute (spm) circulation to moderate formation washout below seafloor. No real-time measurement-while-drilling (MWD) or nuclear magnetic resonance (NMR) data were recorded over this interval. The penetration rate was increased to 25 m/hr at a bit depth of 30 mbsf to a total depth (TD) of 210 mbsf, and real-time MWD and NMR data were acquired. The LWD tools were pulled to the rig floor at 1415 hr on 22 July for a total bit run of ~21 hr, at which time we noted that recording of the RAB tool had failed because of depleted batteries; the LWD operation was repeated in Hole 1250B.

Hole 1250B was spudded at 1400 hr on 23 July, after waiting for the Sonne to finish instrument deployment at this site. Drilling proceeded at a moderate ROP of 25 m/hr and 15 spm circulation to 20 mbsf. No real-time MWD or NMR data were recorded over this interval. The ROP was increased to 50 m/hr and maintained to a TD of 180 mbsf. The pipe was pulled up from the bottom of the hole (BOH) to ~160 mbsf without rotating to evaluate the effect of drilling motion on the NMR log. The tools were recovered at the rig floor at 0600 hr on 23 July.

Holes 1250C and 1250D were APC/XCB cored down to 148 and 147 mbsf, respectively, with average core recoveries of 82% of the total penetration. Because of the high levels of higher hydrocarbons encountered near Horizon A at Site 1248, we decided to terminate drilling in Holes 1250C and 1250C at depths shallower than 150 mbsf. Further penetration was delayed until a better understanding of potential hazards associated with drilling through this horizon were evaluated by drilling further down dip.

Special tools were used for temperature measurements in Hole 1250C, including five APCT tool and two DVTPP runs. Temperature measurements in Hole 1250D included four APCT tool and two DVTPP runs.

The PCS was deployed two times in Hole 1250C and three times in Hole 1250D. Two deployments of HYACINTH tools were made, one with the FPC in Hole 1249C and one with the HRC in Hole 1249D. One good core was recovered with the FPC, but full retraction into the autoclave was prevented as a result of inadvertent line tension during the coring operation. The HRC, on the other hand, recovered a short core at full in situ pressure, which was then transferred under full pressure and logged in the Vertical Multi Sensor Core Logger (V-MSCL) before being depressurized. Unfortunately, the Drill String Acceleration (DSA) tool was still plagued by technical difficulties and failed to provide any useful downhole data.

Hole 1250E, which comprises two cores with 92% core recovery, was drilled to 16 mbsf for special biogeochemistry sampling. No special tools were run in this hole, but Whirl-Paks and perfluorocarbon tracer (PFT) were used for each of these cores.

*In-Situ Sampling and Characterization of Naturally Occurring Marine Methane Hydrate Using the D/V JOIDES Resolution.*

Hole 1250F was APC/XCB cored from 100 to 182 mbsf on 24–27 August to extend the depth of sampling after coring Horizon A at Sites 1245 and 1247. The PCS was deployed three times in Hole 1250F. There were no deployments of the HYACINTH tools, nor were temperature measurements conducted in this hole.

Wireline logging was performed in Hole 1250F using separate runs of the triple combination (triple combo) (Temperature/Acceleration/Pressure [TAP] tool/Dual Induction Tool [DIT]/Hostile Environment Litho-Density Tool [HLDT]/Accelerator Porosity Sonde [APS]/Hostile Environment Gamma Ray Sonde [HNGS]/Inline Checkshot Tool [QSST]) and the Formation MicroScanner (FMS)-sonic (FMS/Dipole Sonic Imager [DSI]/Scintillation Gamma Ray Tool [SGT]) tool strings down to 180 mbsf. Vertical and offset vertical seismic profiles (VSPs) were acquired with the *JOIDES Resolution* and the *Ewing* (located at an offset of ~700 m) alternating shots. This was followed by walk-away VSPs shot by the *Ewing* to downhole seismometers clamped at 91, 138, and 172 mbsf.

### **ODP Site 1251**

Site 1251 (proposed Site HR2alt) was drilled in 1216 m water depth, ~5.5 km east of the southern summit of Hydrate Ridge. The site is located in a slope basin where well-stratified sediments were deposited at a rapid rate. Seismic data record a history of deposition, tilting, folding and depositional hiatuses in the basin that is probably related to the evolution of Hydrate Ridge. A strong BSR suggests that the base of the gas hydrate stability zone (GHSZ) is at ~196 mbsf at this site.

The principal objectives at Site 1251 were to: (1) determine the source of water and gases forming gas hydrates in a setting that is characterized by rapid deposition of hemipelagic sediments and mass-wasting deposits, in contrast to the uplifted sediments of the accretionary complex; (2) determine the distribution of gas hydrates in relation to the typical lithological parameters for the basin; (3) test general models for hydrate formation in regions of rapid sediment accumulation that were developed in the Blake Ridge area from results of ODP Leg 164; (4) provide age constraints on the geological history recorded by seismic stratigraphy.

### *Operations*

Eight holes were drilled at Site 1251, under good weather conditions. Wind speed was 0–11 kt, gusting to 21 kt; seas were 3–7 ft; swell was 5–10 ft; and the prevailing sea-surface current was from the north at ~0.5 kt. Hole 1251A was drilled without coring on 22–23 July 2002 to obtain the initial LWD data for this site, which was followed by coring Holes 1251B–1251G on 26 July–1 August. As planned before the leg, during this period the *Sonne* and *Atlantis* conducted their scheduled research programs at the Hydrate Ridge summit. The *Ewing* was scheduled to arrive on location on 12 August to assist with

*In-Situ Sampling and Characterization of Naturally Occurring Marine Methane Hydrate Using the D/V JOIDES Resolution.*

the seismic profiling experiments. We returned to Site 1251 on 16 August to drill Hole 1251H for wireline logging and seismic profiling.

Hole 1251A was spudded at Site 1245 on 22 July to obtain the initial LWD data for this site. Drilling proceeded at a moderate rate of penetration (ROP) of 25 m/hr and 15 strokes per minute (spm) circulation to mitigate formation washout below seafloor. No real-time measurement-while-drilling (MWD) or nuclear magnetic resonance (NMR) data were recorded over this interval. The ROP was increased to 50 m/hr at a bit depth of 30 mbsf and maintained to a total depth (TD) of 380 mbsf. As a result, the vertical resolution of the Resistivity-at-the-Bit (RAB) tool images is ~10 cm and the NMR spectral data may have lower quality. The LWD string included the RAB tool, MWD, Nuclear Magnetic Resonance (NMR-MRP) tool, and Vision Neutron Density (VND) tool. The LWD operations involved changing the Azimuthal Density Neutron (ADN) tool and replacing the RAB battery prior to running pipe to the seafloor. LWD tools were pulled to the rig floor at 0900 hr on 23 July for a total bit run of 18 hr.

Hole 1251B was APC cored to 194.6 mbsf, with an average core recovery of 80.6%. At this depth, lithified sediments significantly reduced the penetration of the bit, prompting a change to XCB coring, which proceeded to 445.1 mbsf, with an average recovery of 85.5%. Hole 1251B was terminated ahead of the proposed depth of 620 mbsf, as it appeared that the primary scientific objectives had been achieved and hole stability was deteriorating.

In addition to the XCB coring, all three types of pressure coring tools (PCS, FPC, and HRC) were used in this hole. Three PCS cores were retrieved under pressure from Hole 1251B, two above the BSR depth (which at Site 1251 is at ~200 mbsf), and one below the BSR. One FPC and one HRC were also retrieved from this hole. Whirl-Paks and perfluorocarbon tracer (PFT) were used in 13 of these cores, and the Drill String Accelerator (DSA) tool was run twice in this hole. Other special tools in Hole 1251B included four APCT tool and two DVTPP runs.

Hole 1251C was spudded at 0330 hr on 30 July with the APC. When the APC failed to advance, we attempted to recover an XCB core across the same interval, which recovered 5.45 m. The hole was terminated at 17.6 mbsf.

Hole 1251D was spudded at 0715 hr on 30 July, using the XCB to collect the first three cores to 26.9 mbsf, with a recovery of 40%–90%. These cores were followed by APC to refusal at 173.4 mbsf and subsequent XCB coring to 226.5 mbsf. Whirl-Paks and PFT were used on microbiology Cores 204-1251D-22X, 25X, and 26X.

A series of special tools were deployed in Hole 1251D. Temperature measurements were obtained with one run of the APCT tool and two runs of the DVTPP. Four PCS cores were retrieved to complete the depth profile at this site, and deployments of each of the FPC and HRC were conducted as engineering tests for these pressure tools.

*In-Situ Sampling and Characterization of Naturally Occurring Marine Methane Hydrate Using the D/V JOIDES Resolution.*

Holes 1251E through 1251F were each cored by APC to 9.5 mbsf for high-density sampling. Whirl-Paks and PFT were used only in Hole 1251E. No special tools were used in these holes.

Hole 1251G was washed to 2.5 mbsf before one APC core was taken for special sampling of turbidite layers. The hole was then washed down to 20 mbsf, where an additional PCS was deployed. Hole 1251H was drilled to a depth of 445 mbsf as a dedicated hole for wireline logging using separate runs of the triple combination (triple combo) tool string (Temperature/Acceleration/Pressure [TAP] tool/Dual Induction Tool [DIT]/Hostile Environment Litho-Density Tool [HLDT]/Accelerator Porosity Sonde [APS]/Hostile Environment Gamma Ray Sonde [HNGS]/Inline Checkshot Tool [QSST]) and the Formation Micro-Scanner (FMS)-sonic (FMS/Dipole Sonic Imager [DSI]/Scintillation Gamma Ray Tool [SGT]) tool strings. Vertical and offset vertical seismic profiles were attempted with the *JOIDES Resolution* and the *Ewing* (located at an offset of ~700 m) alternating shots.

### **ODP Site 1252**

Site 1252 (proposed Site HR5a) was drilled in 1039 m water depth, ~4.5 km east of the southern summit of Hydrate Ridge. The site is located on the western flank of a secondary anticline that is located east of the crest of Hydrate Ridge. The sediments in the core of the anticline appear to be continuous with the "accretionary complex" sediments sampled near the base of Site 1244, ~1.5 km to the west. Although there is an anomalously bright BSR at a depth of ~170 mbsf within the core of the anticline, the BSR disappears abruptly at an apparent stratigraphic boundary within the accretionary complex sequence and does not extend beneath Site 1252. Sediments onlapping the anticline from the west can be correlated with sediments sampled at Site 1251. Horizontal slices through this anticline reveal that it has a small aspect ratio and high symmetry, suggesting that is perhaps better described as a diapir rather than an anticline. It is at the southern end of an alignment of circular structures that resemble huge pockmarks in high resolution bathymetric and seismic data.

The principal objectives at Site 1252 were to: (1) sample the sediments in the core of the anticline to determine whether they are compositionally and biostratigraphically similar to those at the base of Site 1244; (2) determine the structure of these sediments in order to constrain the mode of growth of the anticline/diapir; (3) determine whether hydrates are present near a very strong BSR but at a site where no BSR is present; and (4) provide age constraints on the geological history recorded by seismic stratigraphy.

### *Operations*

Site 1252 was cored under good weather conditions. Wind speed was 13–11 kt, gusting to 22 kt; seas were 5–6 ft; swell was 7 ft; and the prevailing sea-surface current was from the north at ~0.5 kt. Site 1252 is the only site for which no LWD data were obtained.

Hole 1252A was spudded at 0325 hr on 31 August 2002 and cored with the advanced piston corer (APC) to refusal at 125 mbsf, with excellent recovery. We continued with extended core barrel (XCB) coring to a total depth (TD) of 259.8 mbsf, where the primary scientific objectives were achieved. The only special downhole tool used at this site was the APC temperature (APCT) tool, which was used to measure in situ temperature in seven runs. After coring, wireline logging data were acquired including one run with the triple combination (triple combo) tool string and one run with the Formation MicroScanner (FMS)-sonic tool string. This alternate site was the last site drilled during Leg 204.

The rig was secured to get under way at 2100 hr on 1 September. All thrusters and hydrophones were retrieved and secured. The ship prepared to get under way and departed for Victoria at 2400 hr. We picked up the pilot at 0800 hr on 2 September and docked at Berth “B” north at 0900 hr, thus concluding Leg 204.

## **LEG 204 – INFRARED THERMAL IMAGING OF CORES**

### **Site 1244**

IR imaging of cores drilled at Site 1244 provided on-catwalk identification of hydrate zones in each core. Dissociation of hydrate is an endothermic reaction that produces decreased temperature in intervals of the core containing hydrate. The butyrate core liners are opaque in the IR range detected by the camera used (8–12  $\mu\text{m}$ ). However, the cooled zones associated with hydrates are transmitted through the core liner by thermal conduction, creating an image of the core temperature on the surface of the core liner, which is then detected by the IR-imaging camera.

Each thermal image covered ~20 cm of core. The spatial resolution of the thermal images is lower than a direct image of the core itself but, nonetheless, provides previously unavailable information on the overall shape and character of hydrate occurrences. This information was used to facilitate hydrate sampling and preservation starting at Core 204-1244C-8H.

The shapes of thermal anomalies in the images were compared to the actual hydrate samples observed and photographed after they were taken from the core liners. The thermal images provide a distinction between nodular, vein-filling, and layered hydrate, if hydrate abundance is relatively low, as is the case at this site. In addition, disseminated hydrate is detectable on the IR images as thermal anomalies with a delta-T of ~1°C or

*In-Situ Sampling and Characterization of Naturally Occurring Marine Methane Hydrate Using the D/V JOIDES Resolution.*

less. Successive thermal images were used to produce a downcore thermal log for each core recovered at Site 1244. The logs show the overall thermal structure of each core and include both positive thermal anomalies associated with voids and the tendency of cores to be warmer at the bottom than at the top. This tendency becomes stronger with depth and is especially true for XCB cores. The warmer base of each core may result from the shorter time since exposure to the frictional heating of the bit as well as local frictional heating associated with removal of the cutting shoe and core catcher from the bottom of the core barrel. In addition, the warmer temperatures at the base of the core could reflect thermal transfer associated with gas expansion. The extreme positive thermal anomalies are artifacts associated with the partial absence of core in the last image of the core sequence. Also, note that the XCB-cored interval is cooler than the APC-cored interval at this site, which is presumably caused by the poorer quality of the XCB core and greater contact with cool drilling fluid during core recovery.

An examination of the negative thermal anomalies in Holes 1244C and 1244E shows that the larger anomalies are present between 47 and 85 mbsf, indicating that this is the zone containing the greatest abundance of hydrate at this site. The LWD resistivity log for Hole 1244D was interpreted using Archie's Relation to predict the abundance of hydrate. Recognizing that Hole 1244D is 15 m away from Hole 1244C, the comparison between the Hole 1244D resistivity log and the thermal anomalies associated with the observed hydrate is considered reasonable. The poorest matches in depth among these data are from ~15 to 40 mbsf, from ~100 to 115 mbsf, and below ~125 mbsf. Lack of agreement between the two methods is likely to reflect a combination of disseminated hydrate not detected by IR imaging, uncertainty of hydrate resistivity logs, heterogeneity in hydrate occurrence between Holes 1244A and 1244D, and the response of the resistivity log to the presence of gas below the BSR. The absence of negative thermal anomalies below 126 mbsf is consistent with a BSR depth of 125 mbsf derived from seismic data. PCS and XCB drilling were conducted between 141 mbsf and the bottom of the hole (BOH). At present, it is not known if the use of the XCB reduces the sensitivity of the IR image, but it seems likely given the greater temperature reduction in XCB cores in Figure F27. PCS cores do not permit collection of IR data.

### **Site 1245**

IR imaging of cores drilled at Site 1245 provided on-catwalk identification of hydrate zones in each core. This information was used to facilitate hydrate sampling and preservation for all cores. The IR thermal anomalies for Holes 1245B and 1245C were cataloged, and an interpretation of the overall hydrate texture for each anomaly was made. The majority of the hydrates detectable by IR imaging for Hole 1245B (75%) are present as apparently disseminated layers. Nodular textures account for the remainder of hydrate occurrences (25%). For Hole 1245C, 66% of the IR images indicate disseminated hydrate; nodular and veined hydrate each account for 17%. The preponderance of both disseminated and stratigraphically conformable layers of hydrate in Holes 1245B and

1245C suggests that differences in permeability and porosity related to bedding may control the presence of hydrate at Site 1245.

Cores from both holes show strong cold anomalies between ~5 and 120 mbsf. Hole 1245B also has a single cold anomaly at 129 mbsf corresponding to the BSR depth (134 mbsf). Anomalies in Holes 1245B and 1245C are similar, with a sharp onset at 49.9–51.5 mbsf and cessation of anomalies at 119.5 to 121.3 mbsf, except for the single anomaly near the BSR in Hole 1245B. Although individual anomalies cannot be correlated between the holes, the depths at which clusters are observed are consistent, suggesting that hydrate occurrence is stratigraphically controlled.

The IR thermal anomalies associated with hydrate are also consistent with pore water saturation ( $S_w$ ) estimated from LWD data except near the BSR, where LWD logging indicates greater presence of hydrate than observed using IR imaging. This difference may be explained by the possible inability of IR imaging to detect low concentrations of hydrate disseminated over a relatively large zone and by heterogeneity in the actual concentrations of hydrate between the two holes.

#### **Site 1246**

IR imaging of the cores drilled in Hole 1246B provided identification of hydrate zones in each core on the catwalk. This information was used to facilitate hydrate sampling and preservation for all cores. The IR thermal anomalies are cataloged in Table T9, including an interpretation of the overall hydrate texture for each anomaly. The majority of the hydrate detectable by IR imaging at this site (76%) is present as disseminated layers. Veins, parallel to or crosscutting bedding, account for 16% of IR-detected hydrate. In contrast to Hole 1248B, nodular textures account for only 8% of hydrate detected by IR.

Successive thermal images were used to produce a downcore thermal log for each core recovered in Hole 1246B. The logs show the overall thermal structure of each core. Strong cold anomalies are present from 66 to 109 mbsf, which correspond to the locations of hydrate samples. The temperature anomalies created by the hydrate were extracted by examination of the downcore temperature data and by direct examination of IR images. Subtle cold anomalies are first present at 16 mbsf, and distinct anomalies start at ~33 mbsf. The magnitude of  $\Delta T$  increases toward the BSR, and minor cold anomalies extend below the BSR by ~3 m. Below 117 mbsf, temperature anomalies are probably a result of causes other than hydrates (e.g., contact with cold drilling fluid during extended core barrel coring or gas expansion or exsolution). The IR thermal anomalies that are attributed to hydrates are consistent with pore water saturation ( $S_w$ ) from LWD, except from 15 to 45 and 106 to 118 mbsf, where the current interpretation of LWD logging results shows no hydrate, whereas IR results suggest the presence of relatively small amounts of hydrate. The extent of cold thermal anomalies to a depth of 117 mbsf, which is 3 m below the BSR depth of 114 mbsf is probably within the combined uncertainty of the estimated BSR depth and the curated core depth.

*In-Situ Sampling and Characterization of Naturally Occurring Marine Methane Hydrate Using the D/V JOIDES Resolution.*

The preponderance of both disseminated and stratigraphically conformable veins of hydrate in Hole 1246B suggests that differences in permeability and porosity related to bedding may control the presence of hydrate at Site 1246. The presence of concentrated hydrate is often associated with intensive gas expansion cracks and voids. These voids and cracks have a much higher IR temperature than the surrounding hydrate-bearing sediment. Thus, the overall cold-spot anomaly is often broken up into small intervals interrupted by the relatively higher temperature voids. By removing the voids and artificially compressing the hydrate-bearing intervals, gas hydrate in Section 204-1246B-8H-4 would yield a cold-spot thermal anomaly with a total length of 55 cm.

### Site 1247

IR imaging provided rapid identification of hydrate on the catwalk. The track-mounted IR camera was used twice, both prior to and after sectioning the core liner. The second scan could then be directly correlated to the visual core descriptions and especially to the presence of the mousse-like texture that is indicative of the presence of hydrate.

Data from the first IR scan were used to generate a downhole temperature profile at Hole 1247B. The temperatures in the upper 20 mbsf are  $\sim 2^{\circ}$ – $3^{\circ}$ C colder than those in the deeper part of the hole, but no discrete temperature anomalies were detected over this depth. There was no indication of mousse-like texture within the first three cores, and the LWD resistivity data, converted to pore water saturation ( $S_w$ ) using Archie's Relation, did not predict the presence of any hydrate in the upper 20 mbsf either. The low temperatures observed may, therefore, be the result of a shorter core-handling time on the rig floor before the IR scan and/or seawater contact.

Significant  $\Delta T$  anomalies start to occur at a depth of 45 mbsf. The anomalies cluster in two intervals, from 45 to 65 mbsf and from 80 to 120 mbsf. The BSR depth at Site 1247 is between 121 and 124 mbsf, which matches well with the last thermal anomaly at 118 mbsf. There is an apparent mismatch between the  $S_w$  data and the specific depths of  $\Delta T$  anomalies, suggesting lateral heterogeneity in the presence of hydrate at this site. Note that the distance between Hole 1247A, where LWD data were obtained, and Hole 1247B, where cores were collected, is 87 m. Overall,  $1 - S_w$  is relatively small with values below 0.2, indicating only small concentrations of hydrate present in the sediments, which is consistent with relatively small  $\Delta T$ s from the IR imaging.

Hydrate samples were taken at 93 and 113 mbsf at Site 1247 after their identification by IR imaging. The temperature anomaly associated with interval 204-1247B-14H-5, 39–62 cm, was  $-2.8^{\circ}$ C. However, close inspection of the sample after it had been preserved in liquid nitrogen did not show any visible hydrate crystals. Instead, the sediment texture suggested that disseminated gas hydrate had been present in this sample but was largely dissociated prior to storage in liquid nitrogen. Alternatively, the thermal anomaly could result from gas expansion or gas exsolution. Pore water chlorinities are consistent with

the presence of a few volume percent of hydrate at this depth, favoring the hypothesis that hydrate was present at 93–113 mbsf in Hole 1247B.

### Site 1248

IR imaging of cores recovered at Site 1248 provided on-catwalk identification of hydrate zones in each core. This information was used to facilitate hydrate sampling and preservation as applied to all cores from this site. Most of the hydrate detectable by IR imaging at this site (50%) is present as disseminated layers. However, an unusually high percentage of hydrate appears as nodular textures in the IR images (26%). Veins or layers account for 25% of IR-detected hydrate. No thick zones of concentrated hydrate were detected. Poor recovery in the upper 48 mbsf of Holes 1248B and 1248C prevented direct observation of high concentrations of hydrate as estimated from LWD data. However, the core that was recovered in the upper 48 mbsf exhibited extensive cold anomalies even in partially filled core liners, a result typical of disrupted or dissociated hydrate and consistent with poor recovery in a zone of abundant hydrate.

Typical hydrate thermal anomalies were described along with their textures; nodular texture is relatively abundant in Hole 1248B. The IR thermal anomalies from this site were cataloged, and a qualitative interpretation of the hydrate texture was described for each anomaly. For example, two IR scans of an anomaly taken ~19 min apart show a  $\Delta T$  of 5.5°C in the first scan and ~1°C in the second scan. The second scan has also developed a warm spot at the center of the anomaly that is interpreted to be a void developing where hydrate previously existed. The archive half of the split core clearly shows a small area of mousse-like texture, ~2.5 cm in diameter, associated with the hydrate. The hydrate did not fully penetrate the core, and the disrupted zone (or IR anomaly) is consistent with a variety of shapes, including spherical, cylindrical, or blade-shaped.

Circular-shaped anomalies in Hole 1248C suggest a spherical shape for these nodules; if they were commonly blade shaped, a larger number of oblate shapes would have been observed. A spherical nodule of hydrate 2 cm in diameter in the center of a core would probably exhibit the IR signature of disseminated hydrate because low-temperature hydrate would not be in direct contact with the core liner. Thus, thermal anomalies classified as “disseminated” may represent a range of hydrate textures, from a single nodule in the center of a core to distributed particles of millimeter-size hydrate grains to dispersed pore-filling hydrates present on the sub-millimeter to micrometer scale. Such anomalies are not veins or layers large enough to transect the core or nodules larger than a few centimeters because these features would show up as well-defined large  $\Delta T$  anomalies.

Successive thermal images were used to produce a downcore thermal log for each core recovered at Site 1248. The logs show the overall thermal structure of each core. The dominant features identified in the thermal logs are cold anomalies for the limited amount

of core recovered in the upper 16 and 48 m in Holes 1248B and 1248C, respectively, and relatively abundant discrete cold anomalies from 48 to 124 mbsf in Hole 1248C. Cold anomalies are observed below the BSR for ~5 m. Minor cold anomalies below 124 mbsf are only present at the top of individual cores and are explained by the impact of drilling fluid in the deeper parts of the hole or perhaps by gas expansion or exsolution. This phenomenon is well documented by the IR temperature data and is most common for XCB cores, although some cold core tops were also observed with APC coring.

The presence of gas hydrate 5 m below the BSR may be within the combined uncertainty of the BSR depth and core depth. However, if we take the available depths at face value, the lower two IR anomalies fall below the GHSZ, as inferred from seismic (BSR depth estimated at 119 mbsf) and LWD data (estimate based on Archie saturation at 118 mbsf). They fall within the stability zone of hydrates of higher molecular weight hydrocarbons and within the methane/seawater/hydrate stability zone predicted by in situ temperature measurement (129 mbsf). Considering that there may be a 4-m mismatch between the cored hole and the LWD hole, it is premature to conclude that these two IR anomalies were present below the methane hydrate stability zone, but it is possible.

### Site 1249

IR thermal imaging of all cores was done in Holes 1249B and 1249F, but only the top two cores of Hole 1249C were imaged to speed up the sampling of gas hydrates on the catwalk. IR imaging of cores recovered at Site 1249 enabled the on-catwalk identification of hydrate zones in each core. This information was used to facilitate hydrate sampling and preservation for most cores. The IR thermal anomalies were each identified, along with an interpretation of the overall hydrate texture for each anomaly. Half of the hydrate detectable by IR imaging of Hole 1249F is present as nodular or massive textures (43% nodular and 8% massive).

Apparently, disseminated hydrate accounts for 28% of the presence and vein structures for 21%. Core recovery is poor in Holes 1249B and 1249C above 40 mbsf. Core liners partially filled with hydrate fragments result in a nodular appearance even if the original material is massive or highly concentrated hydrate. For this reason, nodular and massive hydrate presence in the upper part of Hole 1249C is considered to be a single category. Textures differ systematically from the upper to the lower parts of the holes cored at this site, with massive and nodular textures dominating the upper part of Hole 1249F and all of Hole 1249C. Below ~47 mbsf in Hole 1249F, disseminated zones and veins or lenses become the dominant textures of hydrate.

In Hole 1249F, below 47 mbsf, five veins (23% of hydrate below 47 mbsf) appear to crosscut bedding, indicating that a significant amount of hydrate has been emplaced in fractures or faults. From this observation, we infer that stratigraphic control may be of less importance at Site 1249 than at other sites (e.g., Site 1245). Successive thermal images were used to produce downcore thermal profiles for each core recovered in Holes

1249B, 1249C, and 1249F. Extensive cold anomalies are present in Holes 1249B and 1249F above 40–50 mbsf. The temperature anomalies created by hydrate have been extracted from the downcore temperature data and from direct examination of IR images for Hole 1249F.

Temperature anomalies were plotted as a function of depth for Hole 1249F against pore water saturation ( $S_w$ ) calculated from LWD. Results are consistent and show the decrease in IR anomalies at depths mirrored by the change in  $S_w$ . Poor recovery in the upper part of Hole 1249F makes precise assignment of IR anomaly depths impossible. Depth assignment of IR anomalies are in their appropriate stratigraphic sequence, and actual depths are certainly within 9.5 m (length of cored interval) of their estimated in situ depth.

#### *Special Hydrate Dissociation Experiment – Site 1249*

At this site, we conducted a second hydrate dissociation experiment similar to that performed on a core section from Site 1248. Section 204-1249F-9H-3 was used for this experiment, and it contained two different types of gas hydrate. Disseminated hydrate was inferred from IR thermal imaging throughout intervals 204-1249F-9H-3, 0–40 cm, and 95–130 cm. Within interval 204-1249F-9H-3, 80–95 cm, hydrate was present in a vein-type structure. The experiment was conducted over a period of ~3 hr. During this time, the section was scanned six times with the X-ray line scanner and was measured five times with the MST (Non Contact Resistivity system, GRA, and MS). After the experiment was finished, the section was split open lengthwise and discrete samples were taken every 10 cm. The section was finally imaged and analyzed to examine structural controls on gas hydrate occurrence. The temperature increased from an initial average value of 10° to 21°C, which is the average ambient room temperature, over the duration of the experiment.

The electrical conductivity showed a significant change in the upper 40 cm during the 3-hr experiment. GRA and MS did not change during that time. The change in conductivity is 10 times greater than can be accounted for by the temperature increase. The increase in conductivity over the upper 40 cm is similar to that found in an experiment at Site 1248. It can most easily be accounted for by the dissociation of hydrate, in the shape of veins or veinlets rather than as multiple small nodules (disseminated hydrate). Vein structure of electrically insulating hydrate would provide significant resistance to current flow despite its relatively small volume, something that would not be expected from small nodules.

An IR anomaly in interval 204-1249F-9H-3, 80–95 cm, indicates a vein or layer of hydrate, confirmed by X-ray images and a digital photograph taken from the split archive half after the experiment was finished. The images show a fracture dipping across the liner at an angle of ~45°. The fracture appears as a sharp boundary in the X-ray image, taken just after the core was recovered on deck. The digital core photograph shows a mousse-like texture of the sediments, typical for sediments that contained gas hydrates.

#### *In-Situ Sampling and Characterization of Naturally Occurring Marine Methane Hydrate Using the D/V JOIDES Resolution.*

Onshore analyses will be conducted to model the change in resistivity associated with various hydrate concentrations and the thermal anomaly.

#### *Summary – Site 1249*

Physical properties were acquired at Site 1249 from three different holes, which were combined to provide downhole profiles. The measurements were strongly affected by poor core recovery and gas expansion effects. Data interpretation and correlation to lithostratigraphic units is, therefore, limited. In general, the MAD samples provide the highest quality data and correlate well with the LWD data. IR thermal imaging provided the best method to detect the presence of hydrates in the core liners. A complete downhole temperature profile was acquired only in Hole 1249F.

#### **Site 1250**

In all holes cored at this site, a downhole profile of IR temperature was acquired and was used for on-catwalk hydrate detection. Twenty samples, which were thought to be hydrate, were taken on the catwalk; however, the IR images show a much higher number of cold-spot anomalies, which we interpret to indicate additional instances of the presence of hydrate.

IR imaging of cores recovered at Site 1250 enabled the on-catwalk identification of hydrate zones in each core. This information was used to facilitate hydrate sampling and preservation for all cores. The IR thermal anomalies were examined, and an interpretation of the overall hydrate texture for each anomaly was determined. A large fraction (60%) of the anomalies in both Holes 1250C and 1250D are apparently created by disseminated hydrate. Vein-filled features account for 25%–28%, and nodular features account for 12%–14% of the hydrate associated with the IR anomalies. No trends with depth were identified for these three types of anomalies. The abundance of disseminated hydrate and veins or lenses parallel to bedding suggests that stratigraphy exerts a significant control on the occurrence of gas hydrate at this site.

Successive thermal images were used to produce downcore thermal profiles for each core recovered in Holes 1250C and 1250D. Extensive cold anomalies are present between 14 and 109 mbsf in Hole 1250C and between 6 and 113 mbsf in Hole 1250D, which is consistent with a BSR depth of 112 mbsf. The temperature anomalies created by hydrate have been extracted from the downcore temperature data and from direct examination of IR images. Comparison of anomalies from Holes 1250C and 1250D indicates significant differences between the two holes (separated by 40 m, 20 m north and south of Hole 1250A, respectively). Overall downcore trends are similar, but Hole 1250D has more anomalies than Hole 1250C (57 vs. 40 anomalies). Most of the anomalies present in Hole 1250D are small  $\Delta T$ s, but there is no obvious bias in the detection of anomalies. Larger  $\Delta T$ s are present in Hole 1250C. The opposite would be expected if, for some reason,

thermal anomalies were detected less effectively in Hole 1250C. Core recovery was poor in the upper part of both holes, which limited detection of shallow hydrate, if present.

Comparison of pore water saturation ( $S_w$ ) calculated from LWD with thermal anomalies shows a generally good correlation between the two methods of hydrate detection. However,  $S_w$  estimates suggest increasing hydrate concentration approaching the BSR (112 mbsf). IR anomalies show peak hydrate presence at ~45–80 mbsf. Comparison with wireline logging results in Hole 1250F may help to determine if this discrepancy represents heterogeneity in the presence of hydrate on a scale of 25 m horizontally or if the combined uncertainty in IR anomalies and resistivity logging data are responsible for hole-to-hole differences.

IR imaging provided the best method for on-catwalk detection of hydrate. At Site 1250, 20 hydrate samples were collected; however, there is considerable mismatch between the  $S_w$  calculated from the LWD resistivity data and the temperature anomalies in the IR images.

### **Site 1251**

IR imaging of cores drilled at Site 1251 provided identification on the catwalk of hydrate zones in each core. This information was used to facilitate hydrate sampling and preservation for all cores from this site. Thermal images suggest that most of the hydrate observed at this site is present as disseminated layers or zones, except for a major hydrate zone with interlayered sediment in Hole 1251D from 190 to 202 mbsf (near the BSR).

Successive thermal images were used to produce a downcore thermal profile for Holes 1251B and 1251D. The profiles show the overall thermal structure of each core. The dominant features of the profiles are similar to those described for Site 1244, except for the zone of high hydrate abundance noted above. The downcore temperature profiles also include artifacts such as large positive anomalies caused by sun illumination and overall temperature trends that are caused by daily ambient temperature changes on the catwalk. Calibration data, to eliminate the atmospheric and ambient temperature effects, have been collected and will be applied during later data analysis. The artifacts are spatially limited or they create systematic differences in background temperatures that did not impact the identification of hydrates on the catwalk. The detailed analysis of hydrate thermal anomalies for estimating the concentration of hydrate in the subsurface was not affected.

The temperature anomalies created by hydrate have been extracted from the downcore temperature data and from direct examination of IR images. Results demonstrate the overall low abundance of hydrate at this site, which is broadly consistent with pore water saturation ( $S_w$ ) from the LWD data. Comparisons of the thermal anomalies from Holes 1251B and 1251D (24.3 m apart) show that hydrate zones match in general, but specific zones do not correlate between the holes. Comparison of  $S_w$  (Hole 1251A) with thermal anomalies shows a lack of exact depth correlation. Possible reasons for the lack of

detailed correlation include (1) hydrate zones that are not stratigraphically controlled, (2) stratigraphically controlled zones that are laterally discontinuous, or (3) uncertainty in core depth due to poor core recovery. Note that the ~12-m-thick hydrate zone near the BSR in Hole 1251D was not detected in Hole 1251B, where there was nearly zero recovery at the equivalent depth. We suspect but cannot be certain that a thick zone was actually present in Hole 1251B and was not recovered. Sw from LWD resistivity data (Hole 1251A) does show hydrate present over the depth intervals 187–197 and 202–205 mbsf but not with a response consistent with the thermal response in Hole 1251D. There is clearly significant hydrate near the BSR in Holes 1251A and 1251D and possibly in Hole 1251B, but it is likely that there is also significant lateral heterogeneity in hydrate concentration on a scale of ~25 m. This is important because the presence of a 10-m-thick zone of hydrate near the BSR is a significant contribution to the total volume of gas hydrate estimated for slope basins.

The absence of negative thermal anomalies below ~205 mbsf in Hole 1251D is consistent with the BSR depth and measured in situ thermal profile at this site. Minor cold anomalies are present at 213.8 and 350.1 mbsf in Hole 1251B (Anomalies 204-1251B-IR42 and IR43). Both of these anomalies are present at the top of XCB cores, which are commonly slightly cooler than other parts of the core. Likely explanations include a larger than normal quantity of relatively cold drilling fluid entering the top of the core barrel during retrieval or gas expansion during retrieval. Recorded drilling parameters did not change significantly before, during, and after retrieval of these cores. Cooling from gas expansion, similar to that observed at Blake Ridge (Paull, Matsumoto, Wallace, et al., 1996), is perhaps less likely given the relatively low permeability of these sediments and the location of the anomalies at the core tops. In the case of the deep cold anomalies at Blake Ridge, some cores were actually retrieved frozen, apparently as a result of gas expansion in situ. Examples of gas-expansion cooling of the core liner have been observed in IR images (Core 204-1244A-7H), but neither of the anomalies noted here has features suggesting an obvious connection to gas expansion.

The IR data also show the thermal difference between XCB- and APC-cored intervals at this site, similar to that observed at Site 1244. There are at least four possible explanations for the temperature difference: (1) circulation of drilling fluid near the bit face during XCB coring; (2) greater tolerance and size variability between the core liner and the diameter of XCB core, resulting in greater movement of drilling fluid along the core during core recovery; (3) greater frictional heating during collection of APC cores; and (4) greater gas expansion or gas exsolution in XCB cores. At present, we cannot determine which of these four explanations is most important. For future hydrate drilling, it will be important to develop a better understanding of the relative thermal impacts of APC and XCB drilling. In some instances, the XCB is more effective for retrieving and preserving hydrate. For example, there was greater hydrate recovery just above the BSR in Hole 1251D (where the XCB was used) compared to Hole 1251B (where the ACP was used on the same interval). However, the circulation of drilling fluid in the case of XCB

coring almost certainly produces a significant physical disruption of hydrate that needs to be considered in selecting the coring method for these types of sediments.

The thick thermal anomaly (hydrate zone) near the BSR in Hole 1251D provided an opportunity for relating chlorinity of IW to the presence of hydrate, by taking closely-spaced IW samples to correlate the association of a thermal anomaly with a negative chlorinity anomaly. These results demonstrate the importance of selecting some IW samples within a meter or less of gas hydrate to increase the probability of detecting chlorinity anomalies.

Thermal imaging using the track-mounted IR camera on the catwalk provided the best method of detecting zones of gas hydrate in the cores at this site, especially when the hydrate occurred in disseminated form. Relatively low concentrations of hydrate were observed at Site 1251, except near the BSR, where IR anomalies and chlorinity indicate a zone of high hydrate concentration. The lateral extent of this zone is uncertain and important, as its presence or absence results in a relatively large difference in the total amount of hydrate estimated in the slope basin. Discrete samples of hydrate were not found in Hole 1251B, although several zones with cold anomalies were identified. The temperature anomalies observed in Hole 1251B were relatively small compared to the main anomaly encountered at Hole 1251D just above the BSR depth. These small thermal anomalies are interpreted to be indicative of disseminated hydrate.

### **Site 1252**

IR imaging was carried out on all cores recovered prior to and after sectioning and curating. This site has very good core recovery and allowed detailed imaging of the entire sediment column. Only two samples thought to contain gas hydrate were recovered at Site 1252.

IR imaging was used to identify the location of hydrate in cores on the catwalk. The track-mounted IR camera was used twice, both prior to and after sectioning the core liner. The second scan could be directly correlated postcruise to the VCDs, particularly the presence of mousse-like texture that is indicative of the location of hydrate. Data from the first IR scan were used to generate a downhole temperature profile at Hole 1252A. The temperatures in the upper 130 mbsf show an overall linear trend of increasing temperature with depth common to many APC cored holes. The gradient is much less than in situ temperature gradients and apparently reflects a combination of increasing in situ temperature, cooling of the cores during retrieval, and gas expansions or exsolution.

Definite negative  $\Delta T$  anomalies first appear at a depth of 43 mbsf and continue to a depth of 133 mbsf. A single cold anomaly is present at 183 mbsf. Given that this anomaly is present by itself and near a core top, it was probably caused either by drilling fluid incursion during core retrieval or gas expansion/gas exsolution. The depth of the base of GHSZ at Site 1252 is estimated to be at ~170 mbsf, derived by projecting a prominent

BSR westward a few hundred meters to the hole location. The lowest definite thermal anomalies are present at 133 mbsf, indicating that negative  $\Delta T$ s are present within the stability zone for gas hydrate. The lack of thermal anomalies between 133 and 170 mbsf suggests that while pressure-temperature conditions are appropriate for gas hydrate stability in this zone, the chemical composition is not (e.g., lack of methane or water to create sufficient hydrate to cause a thermal anomaly in core samples).

The downcore temperature pattern for Cores 204-1252A-13H and 14H suggests a significant lithologic or gas content change at the bottom of Core 13H and top of Core 14H (118.9 mbsf). At that point, the downcore temperature becomes more irregular as a result of an increase in the number of voids greater than  $\sim 2$  cm in width. At this depth, the accretionary complex sediments were first encountered, overlain by glauconite sand layers. Core 204-1252A-13H exploded on the catwalk just after IR scanning was completed. Both cores contain small amounts of hydrate based on anomaly frequency, thickness, and  $\Delta T$  magnitude. The difference between the exploding core (Core 204-1252A-13H) and the highly fractured core (Core 14H) is probably a reflection of their respective mechanical properties. Core 204-1252A-14H coincides with the presence of indurated carbonate nodules and layers that may be more brittle than other parts of the core (e.g., Core 13H). Further analysis of the wireline logs and acoustic logs is expected to provide additional insight into the gas content and mechanical properties of this part of the hole.

Site 1252 has very low hydrate abundance overall based on IR imaging and the low abundance of mousse-like texture as defined from VCDs. Several cold-spot anomalies were observed but make up a relatively small volume of the core and never exceed a  $\Delta T$  of  $-3^\circ\text{C}$ .

## **LEG 204 – GAS HYDRATE SAMPLE ANALYSIS**

### **Site 1244**

Several pieces of gas hydrate and gas hydrate–cemented sediments were physically recovered from Sections 204-1244C-8H-1 and 10H-2 and 204-1244E-7H-6 and 12H-1. Evidence from electrical logs and dissolved chloride profiles indicates that gas hydrates are definitely present in the subsurface at depths below  $\sim 40$  mbsf and are possibly present at depths below  $\sim 32$  mbsf. Gas hydrate–bearing intervals exist down to the base of the GHSZ, which is at  $\sim 127$  mbsf at Site 1244. The composition of gas given off by decomposed hydrate pieces shows enrichment in ethane relative to the void gas samples analyzed at comparable depth intervals. The gas hydrate pieces from Hole 1244C were analyzed after storage at  $-80^\circ\text{C}$  for 3 or 4 days, but the gas hydrate pieces from Hole 1244E were analyzed immediately. The general trend of the C1/C2 ratio of the void gas (Fig. F22) is offset in the direction of ethane depletion over the general interval where gas hydrate is present. A similar trend was observed in void gas samples from gas hydrate–bearing sediments at Blake Ridge during ODP Leg 164. Whether or not these

*In-Situ Sampling and Characterization of Naturally Occurring Marine Methane Hydrate Using the D/V JOIDES Resolution.*

shifts in the C1/C2 ratio are valid indicators of the presence of gas hydrate will be evaluated in cores from other sites during Leg 204.

In addition to the gas samples obtained from the decomposition of gas hydrate pieces recovered in the core, the gas composition of samples taken during controlled degassing of the PCS was also analyzed. The gas from PCS experiments was enriched in air but generally had the same C1/C2 composition as the void gas samples from adjacent cores.

### **Site 1245**

Gas hydrate pieces and gas hydrate-bearing sediments were recovered from cores on the catwalk and analyzed. Four gas samples from decomposed pieces of gas hydrate were analyzed from Samples 204-1245B-6H-5, 103 cm; 9H-CC; 204-1245C-7H-5, 40 cm; and 13H-4 56–74 cm. The concentration of methane varies from 227,000 to 945,000 ppmv (22.7%–94.5% by volume) as a result of air contamination during sampling. The C1/C2 ratios of the gas from the dissociated gas hydrate from Samples 204-1245B-9H-CC and 204-1245C-13H-4, 56–76 cm, show enrichment of ethane in the gas hydrate relative to the adjacent void gas samples. However, ethane was not enriched in gas from Sample 204-1245B-6H-5, 103 cm, and was below detection levels in the gas hydrate sample from Sample 204-1245C-7H-5, 40 cm.

Five deployments of the pressure core sampler (PCS) successfully retrieved full (1 m long) cores from depths of 17.0–291.2 mbsf. The composition of gas samples obtained during controlled PCS degassing experiments were determined. One PCS sample from Core 204-1245C-16P provided a pressure curve and gas content that confirms the subsurface presence of methane hydrate. Based on the volume-averaged composition, the C1/C2 ratios for gas in the PCS cores fall within the trend defined by vacutainer (VAC) void gas samples, except for the sample recovered from 17.0 mbsf.

### **Site 1246**

A single gas hydrate sample from Section 204-1246C-12H-4 (at 105 mbsf) was analyzed for hydrocarbon composition. The gas from the analyzed sample was ~92% methane, with 5% air contamination. Interestingly, the gas from this hydrate sample contained 8.3 ppmv of propane, a component that should be excluded from Structure I hydrate, along with 17.1 ppmv of ethane. It is not known if this trace of propane was actually present in the gas hydrate or if it was present in some of the sediment associated with the gas hydrate. The C1/C2 ratio of the gas from the gas hydrate is about the same as in void gas samples from this depth at Site 1246.

### **Site 1247**

Gas hydrate pieces and gas hydrate-bearing sediments were recovered at Site 1247 in cores sampled on the catwalk. Two samples were analyzed to determine the gas

composition associated with the dissociation of a gas hydrate (piece recovered from Section 204-1247B-12H-4). The gas from this gas hydrate sample shows enrichment of ethane and depletion of propane relative to what is believed to be the composition of dissolved gas in the core. The composition of the gas derived from the dissociated gas hydrate is consistent with a Structure I methane hydrate. On the C1/C2 plot, the hydrate-bound gas falls on the trend of void gas samples also believed to be derived from gas hydrates and is enriched in ethane compared to “baseline” C1/C2 ratios of dissolved gas.

Two deployments of the PCS successfully retrieved full (1 m long) cores from depths of 23.1 and 123.8 mbsf. Core 204-1247B-16P (123.8 mbsf) shows sufficient gas content to confirm the subsurface presence of methane hydrate. Based on the volume averaged composition, the C1/C2 ratio of this sample is similar to the C1/C2 ratio in void gases from adjacent depths.

### **Site 1248**

Gas hydrate veins, nodules, and gas hydrate–cemented sediments were recovered from cores on the catwalk. At Site 1248, 11 samples of gas hydrates were decomposed and the gas hydrate–bound gases were analyzed. Most gases are relatively pure methane, with minimal air contamination. Two samples from the shallowest cores contain relatively high concentration of H<sub>2</sub>S (25 and 11,812 ppmv). However, these samples also contained a significant amount of surrounding sediment, which may have caused the presence of H<sub>2</sub>S. Similarly, propane and butanes measured in most gas hydrate samples are probably present in associated sediments.

Two clean (minimal contamination from sediment) pieces of gas hydrate were decomposed for geochemical analysis. One sample contains only methane and ethane, suggesting that gas was derived from Structure I gas hydrate. The other sample contains high concentrations of propane (C<sub>3</sub> > C<sub>2</sub>) and butanes, suggesting the possibility of Structure II gas hydrate. Although thermogenic Structure II gas hydrates are common in petroleum basins such as the Gulf of Mexico (Sassen et al., 2001) and the Caspian Sea (Ginsburg and Soloviev, 1998), only Structure I methane hydrates were found at Hydrate Ridge prior to ODP Leg 204 (Gutt et al., 1999). The C1/C2 ratios for gas hydrate–bound gas show the same trend as void gases. However, most gas hydrate samples are slightly enriched in ethane relative to void gases from adjacent depths.

### **Site 1249**

Gas hydrates and gas hydrate–bearing sediments were recovered from cores on the catwalk. A total of 16 hydrate samples were decomposed in syringes, and the gas hydrate–bound gases were analyzed. The concentration of methane varies from 169,544 to 983,641 ppmv as a result of air contamination during sampling. Four samples of gas hydrate–bound gas contain only methane and ethane, consistent with that gas being derived from Structure I gas hydrate. However, the other samples contain considerable

amounts of propane and butanes, suggesting the possibility of Structure II gas hydrate. The C1/C2 ratio also reflects the enrichment of ethane in the gas hydrate-bound gas. Dissociated gas hydrate samples with relatively high C1/C2 ratios may reflect the influence of gas from surrounding sediments.

Three deployments of the PCS successfully retrieved full (1 m) cores from depths of 14.0–71.9 mbsf (Cores 204-1249C-6P and 204-1249F-4P and 14P). The composition of gas samples obtained during controlled PCS degassing experiments were each analyzed. All three PCS samples show pressure curves and gas contents that confirm the subsurface occurrence of methane hydrate. Based on the volume-averaged composition, the C1/C2 ratios for gas from the PCS cores fall on the VAC/void gas trend.

### **Site 1250**

At Site 1250, samples from near the seafloor (1.4–6.5 mbsf) and from depths of 81.5, 86.7, and 100.2 mbsf were analyzed for the composition of gas from dissociated hydrate. The gas from the analyzed samples ranged from 55% to 98% methane, with the balance being mainly air contamination. Some of the shallowest gas hydrate samples gave off minor H<sub>2</sub>S (400–1600 ppmv), and all samples analyzed produced CO<sub>2</sub> (240–5300 ppmv). Gas from several samples contained traces of propane and, in one case, some isobutane. Sample 204-1250D-10H-3, 53–84 cm, produced more propane than ethane. The presence of gas components other than methane and ethane has important implications for hydrate structure. No procedures were used on the ship to evaluate hydrate structure. Many of the samples contained intermixed sediment, and it is not known if trace components could have come from dissolved gas in the sediment rather than from the hydrate itself. The C1/C2 ratios of gas hydrate samples are in the same range as void gas samples from the same depths at Site 1250, although two of the three deeper samples appear somewhat depleted in ethane.

Five deployments of the PCS successfully retrieved cores from depths of 35–120 mbsf (Cores 204-1250C-9P; 204-1250D-5P, 13P, and 18P; and 204-1250F-4P). The composition of gas samples obtained during controlled PCS degassing experiments was analyzed. Based on the volume-averaged composition, the C1/C2 ratios of gas from the PCS cores fall on the VAC/void gas trend.

### **Site 1251**

No gas hydrate pieces or gas hydrate-bearing sediments were physically recovered from cores on the catwalk although several CI- and IR anomalies were observed. Eight deployments of the PCS successfully retrieved full (1 m) cores from depths of 20–291 mbsf. Two of these (Cores 204-1251D-6P and 204-1251B-12P) contained sufficient gas to confirm a subsurface presence of methane hydrate. The compositions of gas samples obtained during controlled PCS degassing experiments were determined. The C1/C2 ratios for gas from all but one of the PCS cores (based on volume-averaged composition)

fall on the vacutainer/void gas trend, confirming that gases exsolved in the core liner are a valid representation of subsurface hydrocarbon composition. Gas from PCS Core 204-1251D-10P at 76.4 mbsf is almost totally lacking in ethane and appears to be from sediment that is undersaturated with respect to methane hydrate. Gas from this sample may reflect ethane depletion in the pore water, which is a possible consequence of the ethane enrichment (theoretically) occurring in the gas hydrates.

### **Site 1252**

No hydrate samples were analyzed at Site 1252.

## **LEG 204 – DOWNHOLE TOOLS**

### **Site 1244**

#### *Downhole Temperature Measurements*

Ten measurements of in situ temperature, including one mudline temperature taken prior to coring, were made with the APCT tool at this site in Holes 1244B, 1244C, and 1244E. APCT 12 was used in Holes 1244B and 1244C, and APCT 11 was used in Hole 1244E. Four additional temperature measurements were made with the DVTPP, generally at depths greater than those suitable for the APCT tool. Measurements were taken at ~30-m intervals and span the depth range of 35.1–149.4 mbsf.

All downhole temperature-tool deployments resulted in temperature histories that showed clear penetration and extraction pulses and smooth temperature decay. APCT data were modeled using the software program TFIT using measured thermal conductivities. Uncertainty in the extrapolated value of in situ temperature results from the subjective analyst picks is  $<0.02^{\circ}\text{C}$  for these high-quality records. Uncertainty resulting from possible errors in measured values of thermal conductivity is also estimated to be  $\sim 0.02^{\circ}\text{C}$ .

DVTPP temperatures were picked from the measured temperature recorded late in the time series. For these relatively long deployments, the temperature appears to have approached equilibrium, so no further extrapolation of the DVTPP temperature data was done at this site. Uncertainties in the in situ temperature estimated from DVTPP data are estimated to be  $\sim 0.1^{\circ}\text{C}$  because the DVTPP data are noisier than the APCT data. Because mudline temperatures recorded by the DVTPP tip #3 were consistently higher than those recorded by APCT 12, an empirically determined shift of  $-1.40^{\circ}\text{C}$  was applied to the DVTPP data measured with tip #3 before plotting the data to determine the subsurface temperature gradient. APCT and DVTPP temperature estimates made at depths of 62.5 and 63.5 mbsf, respectively, yield temperatures that differ by only  $0.074^{\circ}\text{C}$ , verifying this empirical calibration.

*In-Situ Sampling and Characterization of Naturally Occurring Marine Methane Hydrate Using the D/V JOIDES Resolution.*

### *In Situ Pressure Measurements*

The DVTPP pore pressure measurement at 62.5 mbsf in Hole 1244C yielded a rapid decay to a pressure that is within ~20 psi of the predicted hydrostatic pressure. In contrast, the signal from the DVTPP pressure measurement in Hole 1244C decayed gradually, suggesting that the pressure probe was inserted into an intact formation at 150.2 mbsf and measured a true formation pore pressure. Pressure had clearly not reached equilibrium after 35 min in the formation, requiring additional modeling to extrapolate from the data to derive an estimate of in situ pressure. All of the DVTPP runs yield temperature data that are consistent with in situ temperatures measured by the APCT tool but only one of the runs appears to yield an accurate in situ pressure measurement. This suggests that the pressure measurements are more sensitive to minor cracking of the formation around the probe than the temperature measurements.

The Fugro piezoprobe was modified and tested on ODP Leg 204 as part of Task 6.0 of the DOE/NETL Cooperative Agreement with JOI. The first run of the piezoprobe in Hole 1244B was unsuccessful. A second deployment of the piezoprobe in Hole 1244C produced a well-defined pressure-dissipation curve. The results were used with the data collected from postcruise geotechnical testing of sediment from this site to evaluate the in situ state of stress and permeability of the formation and the piezoprobe data was compared with data from the DVTPP as part of a study described in Appendix A.

## **Site 1245**

### *Downhole Temperature Measurements*

Twelve measurements of in situ temperature were made at this site: ten with the APCT tool and three with the DVTP. A detailed sequence of four measurements was made in Hole 1245C at approximately the depth of Horizon A, although there is some uncertainty about hole-to-hole depth correlation. Measurements span the depth range of 38–350 mbsf. APCT data were modeled using the software program TFIT using measured thermal conductivities. No in situ temperatures were derived from DVTP data because the time series suggest that the probe did not penetrate the seafloor properly. The temperature at the BSR, indicated by the downhole measurements, is 0.5°C colder than predicted. Possible explanations for this mismatch will be discussed elsewhere.

### *In Situ Pressure Measurements*

No in situ pressure measurements were made at Site 1245.

**Site 1246***Downhole Temperature Measurements*

Five measurements of in situ temperature were made in Hole 1246B using the APCT tool. Data were modeled using the software program TFIT, using measured thermal conductivities. Uncertainty in the extrapolated value of in situ temperature is  $<0.02^{\circ}\text{C}$  for these high quality records. Uncertainty because of possible errors in measured values of thermal conductivity is also estimated to be  $\sim 0.02^{\circ}\text{C}$ .

The resulting temperature estimates show considerable scatter. Based on a decrease of  $\sim 2.2\%$  in the apparent bottom-water temperature recorded after the measurement on Core 204-1246B-5H, we suspect that APCT 12, which was used for all of these measurements, suddenly recalibrated itself during the second measurement. This observation led us to calibrate all of the APCT tools in an ice bath. Tools were placed in a trash-can full of ice for at least 35 min. A “corrected” temperature gradient for Site 1246 was calculated by assuming that APCT 12 required no correction for the first measurement and a correction of  $+2.5^{\circ}\text{C}$  for the rest of the measurements. This assumption leads to a temperature gradient that is consistent with other sites. APCT 12 was taken out of service, and APCT 11 was used for the rest of the leg. Comparison of data from APCTs 12 and 11 at Site 1244 suggests that APCT 12 was well calibrated prior to this unprecedented spontaneous recalibration.

*In Situ Pressure Measurements*

No in situ pressure measurements were made at Site 1246.

**Site 1247***Downhole Temperature Measurements*

Six in situ temperature runs were made at this site using the APCT tool, including a dedicated mudline run; two DVTP runs were also made. APCT data were modeled using the software TFIT using measured thermal conductivities. Uncertainty in the extrapolated value of in situ temperature resulting from a subjective analyst is  $<0.02^{\circ}\text{C}$  for these high-quality records. Uncertainty resulting from possible errors in measured values of thermal conductivity is estimated to also be  $\sim 0.02^{\circ}\text{C}$ . Both of the DVTP runs yielded apparent temperatures that are not consistent with the APCT data, and the time series suggest that the probe did not penetrate the sediment properly. These data were not used for the determination of the in situ thermal gradient.

The six APCT measurements define a straight line very well, and there is no significant difference in the slope and seafloor intercept if the mudline measurement is excluded. The temperature gradient of  $\sim 0.053^{\circ}\text{C}/\text{m}$  results in a predicted depth to the base of the

*In-Situ Sampling and Characterization of Naturally Occurring Marine Methane Hydrate Using the D/V JOIDES Resolution.*

GHSZ of 151–152 mbsf, considerably deeper than the BSR depth of 129–134 mbsf determined from acoustic logging data and VSP measurements. If we add 0.513°C to each measurement, as suggested by the calibration for APCT 11 in an ice-water bath, the predicted depth to the base of the methane stability zone is 142 mbsf, accounting for half of the apparent mismatch. This is equivalent to the temperature at the BSR being ~0.6°–1.2°C colder than predicted by the methane/seawater stability curve.

#### *In Situ Pressure Measurements*

No in situ pressure measurements were made at Site 1247.

### **Site 1248**

#### *Downhole Temperature Measurements*

Six in situ temperature runs were made at this site: three APCT tool, two DVTPP, and one DVTP runs. APCT data were modeled using the software program TFIT using measured thermal conductivities. The DVTP data were modeled using the software program CONEFIT. Temperatures for the DVTPP runs were measured directly from the data because the longer time taken for this measurement results in temperatures that appear to have reached equilibrium. Neither DVTPP time series from this site shows the frictional pulse that is expected when the temperature probe is extracted, suggesting poor coupling to the sediment, and the deeper measurement shows an anomalous increase in temperature with time after the initial temperature decay. The shallowest APCT tool measurement shows an anomalous extraction pulse.

Excluding the deeper DVTPP measurement and the APCT tool measurement, the data suggest a temperature gradient of ~0.056°C/m and a depth to the base of the GHSZ of 130 mbsf. The apparent mismatch of ~20 m between the observed BSR depth of ~115 mbsf and the depth calculated from the temperature data, assuming a pure methane/seawater system, is similar to that observed at other sites.

#### *In Situ Pressure Measurements*

No in situ pressure measurements were made at Site 1248.

### **Site 1249**

#### *Downhole Temperature Measurements*

Ten in situ temperature runs were made at this site: eight using the APCT tool and two using the DVTPP. APCT data were modeled using the software program TFIT on the basis of measured thermal conductivities. Temperatures were measured directly from the DVTPP data because the tool was deployed long enough to approach equilibrium. The

*In-Situ Sampling and Characterization of Naturally Occurring Marine Methane Hydrate Using the D/V JOIDES Resolution.*

thermal gradient of  $0.054^{\circ}\text{C}/\text{m}$  derived from these data is similar to the thermal gradients at other sites and is not sensitive to whether the mudline temperature is included. The scatter in the data, however, is greater than that at most other sites, especially in the depth range of 20–40 mbsf, where other observations indicate the presence of high concentrations of gas hydrate. This scatter may have several sources, including different calibration for APCT 11 and 12, the effect of gas hydrate on in situ thermal conductivity, and possible dissociation of gas hydrate in situ in response to probe insertion.

Although there is considerable uncertainty about the in situ temperature gradient at this site, it is clear that the temperature gradient is not significantly higher and may even be lower than those at other sites drilled during Leg 204. This implies that upward advection of warm fluid from greater depths must be relatively slow (probably  $<1\text{ cm}/\text{yr}$ ) (Tréhu et al., 2003) and represents an additional constraint on models for the dynamics of hydrate formation at this summit. The low in situ thermal conductivities derived for some of the temperature measurements are consistent with other data, indicating large concentrations of gas hydrate in the subsurface at Site 1249.

#### *In Situ Pressure Measurements*

Pressure data was measured by the DVTTP and analyzed postcruise (see Appendix A).

### **Site 1250**

#### *Downhole Temperature Measurements*

Thirteen in situ temperature runs were made at this site: nine APCT tool and four DVTTP runs. APCT data were modeled using the software program TFIT using measured thermal conductivities. Temperatures for the DVTTP runs were measured directly from the data because the longer time taken for this measurement results in temperatures that appear to have reached equilibrium. Only the deepest of the DVTTP time series shows the frictional pulse that is expected when the temperature probe is extracted. The two shallower DVTTP measurements yield temperature estimates that are slightly higher than, but generally consistent with, the APCT measurements. The DVTTP at 138.5 mbsf did not yield a reliable measurement.

At this site, no dedicated mudline temperature measurement was taken. Mudline temperatures taken for  $\sim 5$  min prior to recovery are very variable and range from  $4.36^{\circ}$  to  $5.51^{\circ}\text{C}$ . The average is given in the table, but we did not include this data point in the determination of temperature gradient. The APCT data alone yield a temperature gradient of  $0.053^{\circ}\text{C}/\text{m}$ . If the DVTTP data are included, the apparent temperature gradient increases to  $0.058^{\circ}\text{C}/\text{m}$ . The apparent mismatch between the observed BSR depth of  $\sim 112$  mbsf and the depth of 128–137 mbsf calculated from the temperature data, assuming a pure methane/seawater system, implies a temperature anomaly of  $0.5^{\circ}$ – $1.0^{\circ}\text{C}$  at the BSR, similar to that observed at several other sites. Although additional analysis of

#### *In-Situ Sampling and Characterization of Naturally Occurring Marine Methane Hydrate Using the D/V JOIDES Resolution.*

the data is needed to resolve questions about instrument calibration, we can conclude that the rate of vertical advection of aqueous fluid must be slow.

### *In Situ Pressure Measurements*

Three in situ pressure measurements were made at this site using the DVTTP. They do not show the expected decay in pressure with time. Analysis was conducted postcruise (see Appendix A).

## **Site 1251**

### *In Situ Temperature Measurements*

Nine measurements of in situ temperatures were made at this site: five with the APCT tool and four with the DVTTP. Four of the APCT tool runs resulted in temperature histories that showed clear penetration and extraction pulses and smooth temperature decay. A fifth APCT tool run turned on prematurely and ran out of memory prior to recovery but recorded long enough to provide a good temperature measurement (Core 204-1251D-20H). APCT data were modeled using the software program TFIT and measured thermal conductivities. Uncertainty in the extrapolated value of in situ temperature is  $<0.02^{\circ}\text{C}$  for these high-quality records. Uncertainty resulting from uncertainty in values of thermal conductivity is  $\sim 0.02^{\circ}\text{C}$ . Additional uncertainty results from uncertainty in instrument calibration.

The DVTTP temperature data do not show the “textbook” response observed during the first deployment. Moreover, the run at 155.6 mbsf was noisy and showed an unrealistic value of  $6.0^{\circ}\text{C}$  for the mudline temperature (measured at the end of the run), probably reflecting a calibration error for DVTTP tool #3. The DVTTP measurement at 198.6 mbsf yielded an anomalously low temperature value compared to the other data. The other two DVTTP deployments yielded temperatures consistent with the APCT data, suggesting that good-quality temperature measurements can be taken in spite of poor-quality pressure records. Moreover, the data suggest that there is no significant change in temperature gradient at the BSR, although this is not well constrained.

Least-square linear fit temperature gradients were calculated for different subsets of the data, excluding the two outliers. The solution is not sensitive to the inclusion or exclusion of the DVTTP data or to the mudline temperature estimate. This temperature gradient predicts that the BSR should be at 202 mbsf, which is not significantly different from the BSR depth of 193 mbsf indicated by seismic data, given uncertainties in the velocity used to obtain the estimate of BSR depth.

### *In Situ Pressure Measurements*

Four in situ pressure measurements were attempted using the DVTTP. The signals from these measurements do not follow the expected decay patterns, suggesting problems with insertion of the probe. Interpretation of these measurements has been the object of postcruise research (see Appendix A).

## **Site 1252**

### *Downhole Temperature Measurements*

One mudline measurement plus six runs within the sediments to determine in situ temperatures were made in Hole 1252A using the APCT tool. Data were modeled using the software program TFIT, using measured thermal conductivities. Uncertainty in the extrapolated value of in situ temperature is  $<0.02^{\circ}\text{C}$  for these high-quality records. Uncertainty resulting from possible errors in measured values of thermal conductivity is also estimated to be  $\sim 0.02^{\circ}\text{C}$ . Additional uncertainty results from uncertainty in instrument calibration. The slope and the seafloor intercept are relatively insensitive to whether or not the mudline temperature is included; both equations predict BSR depths to be within 5 m of the projected depth of the BSR at a depth of  $\sim 170$  meters below seafloor, which is well within the uncertainty.

### *In Situ Pressure Measurements*

No in situ pressure measurements were made at Site 1252.

## **LEG 204 – PRESSURE CORING SYSTEMS**

### **ODP Site 1244**

#### *Pressure Core Sampler (PCS)*

The PCS was successfully deployed seven times at Site 1244. The main objectives of the deployments were (1) to construct a detailed profile of concentration and composition of natural gases in the upper part of the section and (2) to identify the presence/absence and concentration of gas hydrate within the GHSZ.

Specific depth intervals were targeted for deployment of the PCS. Five cores (Core 204-1244F-4P [23.1–24.1 mbsf]; 204-1244E-6P [39.2–40.2 mbsf], 11P [71.6–72.6 mbsf], and 15P [102–103.1 mbsf]; and 204-1244C-14P [119.5–120.5 mbsf]) were recovered from above the BSR at  $\sim 124$  mbsf. The other two cores (Cores 204-1244C-16P [130.5–131.5 mbsf] and 18P [141.5–142.5 mbsf]) were recovered from below the BSR. The PCS cores were degassed for periods of 450–2999 min after recovery on board. No pressure was recorded during degassing of Cores 204-1244C-14P, 16P, and 18P because of the lack of

*In-Situ Sampling and Characterization of Naturally Occurring Marine Methane Hydrate Using the D/V JOIDES Resolution.*

equipment. Pressure transducers were not properly calibrated during degassing of Cores 204-1244E-6P and 15P and 204-1244F-4P, and the pressure record is not reported. Pressure was recorded during degassing of Core 204-1244E-11P. Gas was collected in a series of sample increments (splits), and most were analyzed for molecular composition. In addition, gas splits were sub-sampled for onshore analyses. After degassing, the PCSs were disassembled. The lengths of the cores were measured, and samples were taken for analysis of physical properties.

Gas was collected in 2.5- to 580-mL increments. The measured incremental and cumulative volumes were plotted vs. time. The cumulative volume of released gas varied from 595 mL (Core 204-1244E-4P) to 4530 mL (Core 11P). The volume of the last gas splits varied from 0 mL (Core 204-1244E-15P) to 120 mL (Core 204-1244C-14P). These observations suggest that, in some cases, not all gas was collected.

Gases released from the PCS are mixtures of air (N<sub>2</sub> and O<sub>2</sub>), CH<sub>4</sub>, CO<sub>2</sub>, and C<sub>2</sub>+ hydrocarbon gases. The abundance of air components in the PCS gas samples (1.4%–33.33% of gas mixtures) suggests that air was not always properly displaced from the PCS by seawater during deployments. Methane is the dominant natural gas present in collected gas splits. The molecular composition of gases from the PCS is similar to the composition of gas voids at adjacent depths. Sediments in cores recovered by the PCS have lithologies that are similar to sediments recovered by APC and XCB at adjacent depths. Porosity values measured in APC and XCB cores taken near the PCS were used to estimate the methane concentration in situ.

The concentration of methane in situ was estimated based on data from the degassing experiments (i.e., total volume of methane) and core examination (i.e., length of recovered core and the porosity of sediments). The calculation yields equivalent concentrations varying from 23.7 to 221.2 mM. These concentrations have been compared with the theoretical methane-solubility curve extrapolated from values that were calculated for higher pressures (depths) (Handa, 1990; Duan et al., 1992). Preliminary analysis suggests that gas hydrates have been present in relatively low concentrations in Cores 204-1244E-11P (~2% pore volume) and 15P (~0.5% pore volume). Interestingly, no evidence of the presence of gas hydrate was found in the pressure record during degassing of Core 204-1244E-11P. The presence of gas hydrate in these two cores correlates well with the observed distribution of gas hydrate at Site 1244.

The concentration of methane in cores taken ~4 m above the BSR (Core 204-1244C-14P), ~7 m below the BSR (Core 16P), and ~18 m below the BSR (Core 18P) is estimated to be below saturation. The measurements suggest that there is neither gas hydrate nor free gas in the intervals sampled near the BSR.

Based on PCS measurements, gas hydrate appears to be more abundant in the middle part of the GHSZ. This observation is consistent with visual observations on the catwalk, CI<sup>-</sup> anomalies, and well-logging data. However, the gas hydrate concentration in sediments

appears to be lower than that estimated by other methods. Additional comparison of measured methane concentrations with theoretical methane solubility above and below the BSR will be performed on shore to better estimate if methane was present in situ in solution, in free phase, or as gas hydrate.

#### *Pressure Coring at Site 1244 - HYACINTH Pressure Coring and Logging*

The only HYACINTH pressure core taken at Site 1244 was Core 204-1244E-8Y (FPC 9) at 50.70 mbsf. This core was recovered under full pressure well above the BSR (located at 124 mbsf) and in the GHSZ. Hydrate samples had been collected in the previous APC core (Core 204-1244E-7H) at 49.94 mbsf and were collected from the APC core beneath Core 8Y (FPC 9; Core 9H) at 58.08 mbsf. It was therefore anticipated that this short pressure core might contain some hydrate. No HRC cores were taken at Site 1244.

#### *Fugro Pressure Corer Operations*

A single FPC deployment was made at Site 1244 (Core 204-1244D-2Y; FPC 9). After a number of adjustments based on experience from previous deployments, the outstanding problem was effective and reliable sealing of the lower autoclave valve. For this deployment further minor adjustments were made to the valve and plans were made to adjust the speed profile of the drill string when withdrawing the tool from the bottom.

After assembly and making up in the drill string, the tool was lowered while rotating at 20 revolutions per minute (rpm) and pumping at 160 gallons per minute (gpm), with the APC on (maximum heave = ~1 m). As the tool approached the BHA, the bit was picked up 2 m above TD and rotating was stopped. The tool was landed slowly while some flow was taking place. The pump pressure was increased to 200 psi, and 5 m slack was given on the sand-line. Following this procedure, the bit was lowered to the bottom and the weight was set at ~10 kips. The pump pressure was increased to ~700 psi while the operator held his fingertips to the drill string. This sophisticated sensor system detected the pins shearing and a small amount of hammering. After hammering, the pump pressure was increased to 800 psi to ensure that the end of stroke had been reached. To withdraw the core from the formation, the drill string was lifted ~1 m at a moderate speed (290 m/hr) and then lifted for 3 m at a slower rate (100 m/hr). The tool was then lifted through the drill string on the sand line (slowly at first at a rate of 6 m/min).

Once the tool was laid on the piperacker, a visual observation indicated full closure of the lower valve. The autoclave was removed and placed in the ice trough while the data logger was analyzed. This showed that the valve had closed at the seabed. A maximum pressure of 92 kbar was recorded just prior to the autoclave being immersed in the ice bath. The core was transferred from the autoclave to the shear transfer chamber, sheared, and then transferred into the logging chamber. This proved to be a difficult operation due to the tight tolerances of the ball valves. To help the core from increasing in temperature, ice bags were laid over the transfer chambers during this operation. The logging chamber

#### *In-Situ Sampling and Characterization of Naturally Occurring Marine Methane Hydrate Using the D/V JOIDES Resolution.*

was placed in the ice bath overnight (which reduced the pressure to ~60 kbar) before being transferred to the Geotek V-MSCL for analysis.

#### *Pressure Core Logging and Analysis*

After having been stored in an ice bath overnight, the HYACINTH logging chamber containing Core 204-1244E-8Y (FPC 9) was loaded into the Geotek Vertical Multi-Sensor Core Logger (V-MSCL). Initially, the pressure at this stage was 60 bar. Over the next 12 hr, 17 high-resolution GRA logs were recorded. Between the logging runs, the pressure was slowly and incrementally released, and 3.8 L of gas was collected and analyzed in a process similar to that performed on Core 204-1249F-2E (HRC 4). The initial gamma density profile indicated a single distinct zone of low density (at the logging interval of 31–37 cm), provisionally interpreted as a hydrate layer, which when depressurized formed a thin gas layer. The density anomaly interpreted to be a hydrate can be accounted for by 0.5 cm of hydrate (crystal density = 0.92 g/cm<sup>3</sup>) in the 5-cm-diameter core. After all the gas had been removed, the core was X-rayed, run through the MST, split, and digitally imaged. Three IW samples were taken from Core 204-1244E-8Y (FPC 9).

It is interesting to note that in the APC cores immediately above and below Core 204-1244E-8Y (FPC 9; Cores 7H and 9H), the thermal images from the IR camera show approximately six to eight low temperature anomalies percore. This frequency of one to two anomalies per meter is commensurate with the two anomalies in density provisionally interpreted from Core 204-1244E-8Y (FPC 9). It is possible that all the hydrate in these regions of low concentration exists in the hydrate veins, and none is disseminated in the pore space.

### **Site 1245**

#### *Pressure Core Sampler*

The ODP PCS was deployed five times at Site 1245. All deployments were successful (i.e., a core under pressure was recovered). The main objectives of the deployments were (1) to construct a detailed profile of concentration and composition of natural gases in the upper part of the section (0–300 mbsf) and (2) to identify the presence/absence and concentration of gas hydrate within the GHSZ. Specific depth intervals were targeted for deployment of the PCS. Three cores (Cores 204-1245C-3P [17–18 mbsf], 8P [57–58 mbsf], and 16P [120–121 mbsf]) were recovered from above the BSR. The other two cores (Cores 204-1245B-17P [147.1–148.1 mbsf] and 33P [291.2–292.2 mbsf]) were recovered from below the BSR.

The PCS chambers were degassed for 334–4685 min after recovery. Pressure was recorded during degassing experiments. Gas was collected in a series of sample increments (splits), and most were analyzed for molecular composition. In addition, gas

#### *In-Situ Sampling and Characterization of Naturally Occurring Marine Methane Hydrate Using the D/V JOIDES Resolution.*

splits were sub-sampled for shore-based analyses. After degassing, the PCS chambers were disassembled. The lengths of the cores were measured, and samples were taken for analysis of physical properties.

Gas was collected in 20- to 1070-mL increments. The cumulative volume of released gas varies from 315 (Core 204-1245C-3P) to 19,025 mL (Core 16P) (Table T21). The volume of the last gas splits varies from 10 (Core 204-1245C-8P) to 20 mL (Cores 17P and 16P). This observation suggests that almost all gas present in the cores was collected. Gases released from the PCS are mixtures of air (N<sub>2</sub> and O<sub>2</sub>), CH<sub>4</sub>, CO<sub>2</sub>, and C<sub>2</sub>+ hydrocarbon gases. The abundance of air components in the PCS gas samples (2.6%–29.3% of gas mixtures) suggests that air was not always properly displaced from the PCS by seawater during deployments. Methane is the dominant natural gas present in collected gas splits. The molecular composition of gases from the PCS is similar to the composition of gas voids at adjacent depths.

Sediments in cores recovered with the PCS have lithologies that are similar to sediments recovered by the APC and XCB at adjacent depths. However, the porosity of sediments from the PCS is often different from the porosity of sediments at adjacent depths for reasons that are not yet understood. Porosity values measured in samples from APC and XCB cores taken near the PCS were used to estimate the in situ methane concentrations.

The concentration of in situ methane was estimated based on data from the degassing experiments (i.e., total volume of methane) and core examination (i.e., length of recovered core and the porosity of sediments). The calculation yields equivalent concentrations varying from 10.2 to 1,116.6 mM of methane in pore water. These concentrations have been compared with the theoretical methane-solubility curve extrapolated from values calculated for higher pressures (greater depths) (Handa, 1990; Duan et al., 1992).

Preliminary analysis suggests that gas hydrates have been present in relatively high concentrations (12%–16% of pore volume) in Core 204-1245C-16P recovered from above the BSR. In addition to high gas concentrations, strong evidence of the presence of gas hydrate was found in the pressure record of core degassing. The estimate of gas hydrate saturation is consistent with those based on well logging data. However, other cores retrieved from above the BSR (Cores 204-1245C-3P and 8P) suggest that only dissolved methane is present in many intervals within the GHSZ. No free gas seems to be present in intervals ~15 and ~160 m below the BSR (Cores 204-1245B-17P and 33P, respectively). Additional comparisons of measured methane concentrations with theoretical methane solubility, both above and below the BSR, will be performed on shore to better estimate if methane was present in situ in solution, in free phase, or as gas hydrate.

### *HYACINTH Pressure Core Sampling*

Four deployments of the HYACINTH pressure coring tools were made at Site 1245, two each with the HRC and FPC. The HRC cores (Cores 204-1245B-46E [HRC 5] and 204-1245C-29E [HRC 6]) were at 407 and 201 mbsf, respectively. The FPC cores (Cores 204-1245C-18Y [FPC 7] and 27Y [FPC 8]) were at 129 and 195 mbsf, respectively.

All the cores were located below the BSR (located at ~134 mbsf), apart from Core 204-1245C-18Y (FPC 7), which was ~5 m above the BSR. Technical and operational difficulties prevented any cores from being recovered under full pressure for further analysis. The FPC recovered a good core (90 cm) from 129 mbsf but apparently had difficulty penetrating the stiffer lithology at 195 mbsf and only recovered a 15-cm-long section. We recovered a 38-cm core (Core 204-1245B-46E; HRC 5) in indurated claystone, but recovery of Core 204-1245C-29E (HRC 6) was hampered by operational difficulties when the active heave compensator (AHC) failed and only a 20-cm-long core was recovered.

### *HYACE Rotary Corer Operations*

Two HRC deployments, Cores 204-1245B-46E (HRC 5) and Core 204-1245C-29E (HRC 6) were made at depths of 407 and 201 mbsf, respectively. The first attempt to run Core 204-1245B-46E (HRC 5) was aborted after difficult hole conditions required high pump rates, which were incompatible with the HRC operation.

On the second attempt, the tool was lowered at 50–70 m/min and stopped at 1245 m with the drill string already at TD to minimize the risk of borehole instability. It was lowered on the wireline to the landing position, and 5 m of slack wire was paid out before closing the blowout preventer (BOP). Pumping began at 80 gallons per minute (gpm), and a pressure peak was observed at 620 psi (first shear pin sheared). Pumping continued at 110 gpm, but a second pressure peak (which would have indicated full stroke) was not observed after 24 min. Pumping was stopped, and the BOP was opened. The drill string was picked up to 1285.3 m before pumping was continued for 1 min at 90 gpm, in an attempt to ensure a full stroke. After pumping stopped, the tool was raised on the wireline, at first slowly and then at 60–70 m/min, to the surface. When broken out of the drill string, it was observed that the central rod was not fully retracted until several jerks on the tugger line had occurred. The DSA tool was removed and was returned to the trestles on the pipe racker for disassembly.

We observed that the liner had broken above the core catcher, the piston cap had unscrewed, high loads had damaged a bearing, and the valve had not closed. Despite this, 38 cm (recovery = 38%) of stiff, indurated claystone was recovered. We concluded that a variety of factors could have caused the problems encountered, including poor motor performance, but these problems were attributed to insufficient heave compensation and

### *In-Situ Sampling and Characterization of Naturally Occurring Marine Methane Hydrate Using the D/V JOIDES Resolution.*

poor hole conditions. The HRC was completely overhauled and the motor replaced before the next deployment (Core 204-1245C-29E [HRC 6]).

The HRC was deployed in Hole 1245C as Core 204-1245C-29E (HRC 6) at 201 mbsf. The tool was run into the hole at 40–70 m/min and stopped at 1030 m. Pumping was stopped, the tool was lowered onto the landing shoulder, and 5 m of slack wire was paid out. The drill string was then lowered to TD and held with 15 klb (weight on bit). The BOP was closed, and pumping began slowly with both passive and active heave compensation activated. A pressure peak was observed at 650 psi (first shear pin sheared) and pumping continued at 85 gpm. However, at this stage a sudden problem with the AHC occurred (the string was bouncing with weight on bit changing rapidly between 5 and 45 klb), and it was switched off while the passive compensator remained on. Coring could not continue, and the drill string was picked up ~5 m while pumping at 100 gpm. After pumping was stopped, the tool was lifted on the wireline slowly for the first 20 m (7 m/min) and then at 110 m/min while circulating. The tool was broken out of the string, the DSA tool was removed, the strongbacks replaced, and the DSA tool was returned to the trestles on the pipe-racker. We found that a full stroke had been achieved and the core liner had retracted into the autoclave with a 20-cm-long core (Core 204-1245C-29E) at the top, but the autoclave flapper valve had not closed. The inner sleeve had become stuck at the valve, which may have been caused by the sudden motions when the AHC failed.

#### *Fugro Pressure Corer Operations*

Two FPC deployments, Core 204-1245C-18Y (FPC 7) and Core 204-1245C-27Y (FPC 8), were made at depths of 129 and 195 mbsf, respectively. During the coring procedure for Core 204-1245C-18Y (FPC 7), the AHC was turned off because it appeared to increase the variability of the weight on bit. A full core (90 cm long) was recovered, but the lower autoclave valve had not fully closed. The fall path of the valve was modified before the next deployment. During recovery of Core 204-1245C-27Y (FPC 8), the AHC was used. However, the inner rod failed to stroke out completely, indicating that the formation was too stiff for the hammer mechanism. This resulted in the recovery of a short core (15 cm long) and an imploded liner with inverted catcher fingers. It should be noted that the APC cores taken on either side of Core 204-1245C-27Y (FPC 8), namely Cores 204-1245C-26H and 28H, only recovered 4.8 and 3.8 m, respectively. Consequently, the working hypothesis that the operational limit of the FPC hammer mechanism is similar to the working limit of the APC appears to have been confirmed in this type of silty clay formation.

#### **Site 1246**

##### *Pressure Core Sampler and HYACINTH Pressure Corers*

Neither the PCS nor the HYACINTH pressure corers were deployed at Site 1246.

##### *In-Situ Sampling and Characterization of Naturally Occurring Marine Methane Hydrate Using the D/V JOIDES Resolution.*

**Site 1247***Pressure Core Sampler*

The ODP PCS was deployed three times at Site 1247. Two of these deployments were successful (i.e., a core under pressure was recovered). The ball valve did not fully close during the other deployment. The main objectives of the deployments were (1) to construct a detailed profile of concentration and composition of natural gases in the upper part of the section (0–125 mbsf) and (2) to identify the presence/absence and concentration of gas hydrate within the GHSZ. Specific depth intervals were targeted for deployment of the PCS. One core (Core 204-1247B-4P [22.6–23.6 mbsf]) was recovered in shallow sediments, and one core (Core 16P [123.3–124.3 mbsf]) was recovered from above the BSR at ~129 mbsf.

The PCS chambers were degassed for times from 547 to 3454 min after recovery on board. Pressure was recorded during degassing experiments. Gas was collected in a series of sample increments (splits), and most were analyzed for molecular composition. In addition, gas splits were subsampled for onshore analyses. After degassing, the PCS chambers were disassembled. The lengths of the cores were measured, and samples were taken for analysis of physical properties.

Gas was collected in 15- to 550-mL increments. The measured incremental and cumulative volumes were plotted vs. time (Fig. F30). The cumulative volume of released gas varies from 195 (Core 204-1247-4P) to 6025 mL (Core 16P). No gas was released during the last openings in both degassing experiments, suggesting that all gas present in the cores was collected.

Gases released from the PCS are mixtures of air (N<sub>2</sub> and O<sub>2</sub>), CH<sub>4</sub>, CO<sub>2</sub>, and C<sub>2</sub>+ hydrocarbon gases. The abundance of air components in the PCS gas samples (5.6%–52.9% of gas mixtures) suggests that air was not properly displaced from the PCS by seawater during deployments. Methane is the dominant natural gas present in collected gas splits. The molecular composition of gases from the PCS is similar to the composition of gas voids at adjacent depths. Sediments in cores recovered with the PCS have lithologies that are similar to sediments recovered with the APC at adjacent depths. Porosity values measured on samples from APC cores taken near the PCS were used to estimate the methane concentration in situ.

The concentration of methane in situ was estimated based on data from the degassing experiment (i.e., total volume of methane) and core examination (i.e., length of recovered core and the porosity of sediments). The calculation yields equivalent concentrations varying from 4.3 to 292.4 mM of methane in pore water. These concentrations have been compared with the theoretical methane-solubility curve extrapolated from values calculated for higher pressures (depths) (Handa, 1990; Duan et al., 1992).

*In-Situ Sampling and Characterization of Naturally Occurring Marine Methane Hydrate Using the D/V JOIDES Resolution.*

Preliminary analysis of gas concentrations suggests that gas hydrate may have been present in small concentrations (perhaps <3% of pore volume) in Core 204-1247B-16P, although no evidence of the presence of gas hydrate was found in the pressure record of core degassing. Methane concentration measured in shallow Core 204-1247B-4P is consistent with the trend of concentrations that can be extrapolated based on the headspace measurements. This confirms that the PCS can be successfully used to study methane generation and flux in shallow sediments. Additional comparison of measured methane concentrations with theoretical methane solubility above and below the BSR will be performed on shore to better estimate if methane was present in situ in solution, in free phase, or as gas hydrate.

#### *HYACINTH Pressure Corers*

No HYACINTH pressure corers were deployed at Site 1247.

#### **Site 1248**

##### *Pressure Core Sampler and HYACINTH Pressure Corers*

Neither the PCS nor HYACINTH pressure corers were deployed at Site 1248.

#### **Site 1249**

##### *Pressure Core Sampler*

The ODP PCS was deployed seven times at Site 1249. Only three of these deployments were successful (i.e., a core under pressure was recovered). The ball valve failed to actuate during the other four deployments. The main objectives of the deployments were (1) to construct a detailed profile of concentration and composition of natural gases in the upper part of the section (0–80 mbsf) and (2) to identify the presence/absence and concentration of gas hydrate within the GHSZ. Specific depth intervals were targeted for deployment of the PCS. All three cores (Cores 204-1249C-6P [33.5–34.5 mbsf] and 14P [71.4–72.4 mbsf] and 204-1249F-4P [13.5–14.5 mbsf]) were recovered from above the BSR at ~115 mbsf.

The time to degass the three PCS chambers ranged from 967 to 11,268 min. Pressure was recorded during degassing experiments. Gas was collected in a series of sample increments (splits), and most were analyzed for molecular composition. In addition, gas splits were sub-sampled for onshore analyses. After degassing, the PCS chambers were disassembled. The lengths of the cores were measured, and samples were taken for analysis of physical properties. Gas was collected in 2- to 1300-mL increments. The measured incremental and cumulative volumes are plotted vs. time. The cumulative volume of released gas varies from 4,800 (Core 204-1249F-14P) to 95,110 mL (Core 4P). The volume of the last gas splits varies from 2 (Core 204-1249C-6P) to 20 mL (Core

*In-Situ Sampling and Characterization of Naturally Occurring Marine Methane Hydrate Using the D/V JOIDES Resolution.*

204-1249F-4P). This measurement suggests that almost all gas present in the cores was collected.

Gases released from the PCS are mixtures of air (N<sub>2</sub> and O<sub>2</sub>), CH<sub>4</sub>, CO<sub>2</sub>, and C<sub>2</sub>+ hydrocarbon gases. The abundance of air components in the PCS gas samples (0.6%–6.9% of gas mixtures) suggests that air was not always properly displaced from the PCS by seawater during deployments. Methane is the dominant natural gas present in collected gas splits. The molecular composition of gases from the PCS is similar to the composition of gas voids at adjacent depths. Sediments in cores recovered by the PCS have lithologies that are similar to sediments recovered by the APC and XCB at adjacent depths. Porosity values measured on samples from APC and XCB cores taken near the PCS were averaged and used to estimate the methane concentration in situ.

The concentration of in situ methane was estimated based on data from the degassing experiments (i.e., total volume of methane) and core examination (i.e., length of recovered core and the porosity of sediments). The calculation yields equivalent concentrations varying from 215.7 to perhaps >5000 mM of methane in pore water. These concentrations have been compared with the theoretical methane-solubility curve extrapolated from values calculated for higher pressures (depths) (Handa, 1990; Duan et al., 1992).

Preliminary analysis suggests that gas hydrates have been present in relatively high concentrations (perhaps >40% of pore volume) in the shallowest Core 204-1249F-4P recovered from ~14 mbsf. In addition to high gas concentrations, strong evidence of the presence of gas hydrate was found in the pressure record of core degassing. Gas hydrate concentration in Core 204-1249C-6P (~34 mbsf) is estimated to be >5% of pore volume. Unfortunately, the core was not maintained at 0°C during the degassing experiment, and no information about the presence of gas hydrate in the core can be obtained from the pressure record.

The wide range in the estimates of methane concentrations is related to the uncertainty about the lengths of the recovered core. Full 1-m-long cores were recovered during successful deployments at Site 1249; therefore, the lowest methane concentration values presented are the most reliable. Relatively low gas hydrate concentrations (~2% of pore volume) are estimated in Core 204-1249F-14P (~72 mbsf). Interestingly, the pressure record suggests that only dissolved gas was present in the core. The estimated decrease of gas hydrate saturation with increasing depth at Site 1249 is consistent with similar trends proposed based on well logging data and Cl<sup>-</sup> anomalies. Additional comparisons of measured methane concentrations with theoretical methane solubility both above and below the BSR will be performed on shore to better estimate if methane was present in situ in solution, in free phase, or as gas hydrate.

*HYACINTH Pressure Coring*

We deployed the HYACINTH pressure coring tools five times at Site 1249 near the summit of Hydrate Ridge. During the middle of Leg 204, the FPC and HRC tools were each used in an effort to capture massive hydrate samples under pressure from 8 mbsf. This experiment was repeated at the very end of Leg 204, again using both the FPC and HRC at 13.5 mbsf. In addition, a further HRC core was taken deeper in more disseminated hydrate at 37.5 mbsf.

Core 204-1249D-2Y (FPC 5) recovered a core from 8 mbsf that was initially thought to be under in situ pressure. However, it transpired that the pressure had been released during the ascent, only to build up once the core was at the surface. These difficulties culminated in an exploding core that still contained some remnants of hydrate. Core 204-1249F-13Y (FPC 6) recovered a nearly full core from a depth of 70.4 mbsf. However, difficulties with the lower autoclave valve again prevented the core from being recovered at in situ pressures.

Core 204-1249F-2E (HRC 4) was taken at the same depth (8 mbsf) as Core 204-1249D-2Y (FPC 5). Despite some difficulties at the surface, a 80- to 90-cm-long core (as determined by core logging) was recovered under full pressure. It was cooled in the ice bath to maintain stability and successfully sheared and transferred into the HYACINTH logging chamber. It was subsequently logged repeatedly in the Geotek V-MSCL while being degassed over the following 2 days.

Core 204-1249G-2E (HRC 7) was taken a little deeper (13.5 mbsf) than Core 204-1249F-2E (HRC 4). A successful 75-cm core containing massive hydrate layers was recovered at full pressure and transferred into a HYACINTH storage chamber. It was subsequently frozen in Helium under pressure and successfully transferred into liquid nitrogen for preservation. It is probably the most pristine sample of natural gas hydrate ever recovered and preserved.

Core 204-1249H-2Y (FPC 10) was taken at the same depth as Core 204-1249G-2E (HRC 7) (13.5 mbsf). A successful (75 cm) core was recovered at full pressure, and a good GRA log was obtained from the core in the storage chamber showing massive hydrate layers. This core was designated as a “reference core” and companion to the APC and XCB cores that were taken and re-pressurized under methane. It was kept in the refrigerator ready for transportation to TAMU for further study.

Core 204-1249L-5E (HRC 8) was taken from deeper at this site (37.5 mbsf) in an attempt to recover pristine material under pressure from a region where the hydrate is present in lower concentrations and may be more disseminated. Some pressure was lost during disassembly, but it was rapidly re-pressurized to in situ pressures before being transferred to the logging chamber.

*In-Situ Sampling and Characterization of Naturally Occurring Marine Methane Hydrate Using the D/V JOIDES Resolution.*

*HYACE Rotary Corer Operations*

Three HRC deployments were made at Site 1249. Core 204-1249F-2E (HRC 4) was taken at Site 1249, which was near the summit of Hydrate Ridge at 777 meters below sea level (mbsl). It is well known that massive hydrate exists near the surface and core recovery using regular APC and XCB coring through the upper 50 m was particularly poor in the previous holes. The purpose of this pressure coring attempt was to recover an undisturbed sample from massive hydrate just below the seafloor. Although the sediments in this near-surface environment would normally be extremely soft and highly unsuited to pressure coring with the HRC, it was thought possible that the massive hydrate ice structure would be hard enough to lend itself to rotary coring.

Core 204-1249F-2E (HRC 4) was deployed at 8 mbsf after an APC core was shot at the surface. Drilling procedures at these shallow depths mean that in practice these are separate holes. The tool was prepared on the piperacker and lifted into the vertical position and lowered into the drill string as in previous deployments. The DSA tool was attached and run in the hole at 40 m/min. After landing and lowering the HRC to TD, 5 m of slack wire was payed out to ensure that no tension was accidentally applied to the tool. The bottom of pipe (BOP) was closed and pumping started at 50 gallons per minute (gpm), causing the pressure to rise to 620 psi, which indicated that the tool had been activated (started rotating). With almost no load on bit we pumped for 12 min with 80 gpm before pumping for 8 min with 120 gpm. The drill string was lifted about 4 m, followed by a further 1-min pumping at 80 gpm. Slowly the wireline was pulled at 8 m/min for the first 16 m, after which it was increased to 74 m/min.

At the surface the tool was disassembled on the pipe racker, which took ~35 min before the tool could be moved to the transfer area outside the downhole tools shop. While breaking out the accumulator it was clear that there was high pressure inside the autoclave, which was measured with the pressure gauge. While mounting the pressure gauge, a very short high pressure burst was heard. Pressure was measured at ~220 kbar, and the autoclave chamber was then cooled down in the ice trough where the pressure soon dropped to ~120 kbar. Once the core was stable it was transferred through the shear transfer chamber and into the logging chamber, which was in turn placed in the ice trough for cooling and was left there and monitored overnight. The following morning the temperature and pressure was stable at around 0°C and 110 kbar. It was transferred to the Geotek V-MSCL, where it was degassed and logged over the next 2 days (see below). It transpired that the core (~90 cm long; 90% recovery) contained ~40% methane hydrate, which accounted for the rapid pressure rise at the surface (presumably caused by the partial dissociation of hydrate). During disassembly of the tool we discovered that the burst disk (230–270 kbar) had failed. This presumably occurred on deck, but rapid expulsion of sediment had immediately blocked the small orifice and, hence, no significant pressure had been lost.

*In-Situ Sampling and Characterization of Naturally Occurring Marine Methane Hydrate Using the D/V JOIDES Resolution.*

Following the success of the HRC at this site earlier in the leg (Core 204-1249F-2E [HRC 4]), a second HRC core (Core 204-1249G-2E [HRC 7]) was taken at 13.5 mbsf. This is the same depth as Core 204-1249H-2Y (FPC 7) but in a different hole. The tool was deployed as in previous deployments.

Once on the trestles it was clear that the valve had closed, and ice bags were placed along the length of the autoclave to keep the system cold during the breakdown of the tool. Once outside the downhole tools laboratory the autoclave was kept under ice bags while the pressure was measured at ~80 kbar (the same as in situ pressures). The core was successfully transferred from the autoclave into the shear transfer chamber and then into the storage chamber at full pressure before being placed in an ice bath prior to logging. The logging revealed that a core about 75 cm long was retrieved and contained significant amounts of hydrate (the lower 25 cm appeared to be water).

Having recovered good pressure cores at this site from near the top of the section where the hydrates were relatively massive (10 and 13.5 mbsf), there was interest in recovering a core from slightly lower in the section where the hydrates were thought to be more disseminated. Consequently, the final deployment of the HRC during this leg was at the bottom of Hole 1249L (Core 204-1249L-5E [HRC 9]). The only real issue was whether the nature of the sediment in this region would lend itself to being cored by the HRC and held by the core catcher. The deployment was run similarly to previous deployments with the DSA tool. It was run into the hole at 70 m/min while circulating and rotating. Pumping and rotation was stopped while the tool was landed, and 5 m of slack wire was payed out. The drill string was lowered to TD, followed by the wireline. Weight on bit was set at 7,000–10,000 klb. Again, the active heave was not working effectively (max heave = ~2 m), and, therefore, we relied only on the passive heave compensator. The BOP was closed and pumping began slowly.

Coring continued after the first pressure peak (450 psi) for 20 min at 90 gpm and ~360 psi. A second spike was observed (indicating full stroke) after the drill string had been lifted 3 m above TD. Pumping continued at 100 gpm for 1 min before the tool was lifted on the wireline slowly at 7 m/min for the first 20 m and then continued at 70 m/min while circulating. Once the tool was broken out of the drill string and laid on the trestle, the flapper valve was observed to have closed and care was taken to ensure that the autoclave was cooled with ice bags during the disassembly. However, during the later part of the disassembly some pressure leaked away when the connecting rod was removed. The leak was occurring in the piston extension rod. Only 30 kbar remained when measured, and the autoclave was immediately pumped up to 80 kbar to stabilize any hydrate. The core was then transferred under pressure into the logging chamber and kept in the ice bath until logged in the V-MSCL. We found a 30-cm-long core without any significant hydrate layers. It is thought that these sediments were too soft to be retained by the type of sleeve catcher used.

*Fugro Pressure Corer Operations*

Three FPC cores were taken at Site 1249. The first deployment of the FPC at Site 1249 was Core 204-1249D-2Y (FPC 5). The purpose of attempting a shallow core at this site was the same as for Core 204-1249F-2E (HRC 4), to recover massive hydrate from just below the seafloor at ~8 mbsf. This deployment proceeded smoothly with the same operational procedures being used as previously. Active heave compensation was used throughout. On recovery it was clear that a full stroke had been achieved and that the autoclave had sealed. However, when the onboard FPC data logger was analyzed, it was clear that it was not sealed and had depressurized coming to the surface. The autoclave had then sealed at the surface, allowing the pressure to rise to ~20 kbar.

The rapid rise in pressure to 20 kbar indicated that hydrate was present in Core 204-1249D-2Y (FPC 5). We connected the autoclave to the shear transfer chamber, pressurized the complete system to ~70 kbar (to stabilize the system and put any hydrate back into the stability field), and attempted to make the transfer. However, problems with the transfer (caused by expansion) meant that the core had to be depressurized and removed manually. Having done this, the liner then burst under internal pressure and some very soupy mud was collected from the floor in a plastic bag. It was clearly cold to the touch and even contained a few remnants of hydrate. Some optimism was gained from this deployment, as it was clear that the valve had seated properly during the handling of the tool at the surface allowing a build up of pressure to occur.

A second FPC deployment (Core 204-1249F-13Y [FPC 6]) was made at 70.4 mbsf. At this depth, the hydrate was less massive and a core with virtually full recovery was achieved. Everything worked perfectly other than the sealing valve that had not fully closed. It would appear from an analysis that the sleeve might be coming down too quickly on top of the valve, causing it to jam on the edge of the sleeve in the “nearly closed” position. It was thought that removing the spring above the sleeve and lifting the pipe string more slowly after coring might help prevent this jamming.

Following the success of the FPC at Site 1244 (Core 204-1244E-8Y [FPC 9]), a third FPC core (Core 204-1249H-2Y [FPC 10]) was taken at a depth of 13.5 mbsf in Hole 1249H. This is the same depth as Core 204-1249G-2E (HPC-7) but in a different hole. The tool was deployed as in previous deployments. With the tool at TD (801 mbsl), the pressure was increased to 700 psi, and, after shearing, the pressure was raised to 800 psi and the tool hammered smoothly for ~6 min. At the end of the run the pressure was increased briefly to 850 psi, but this caused the hammering to become irregular. The same lifting procedure was followed as with the successful Core 204-1244E-8Y (FPC 9). However, to assist in the closing of the lower valve the FPC was stopped as it came out off the landing shoulder. We then pumped and rotated to provide some string vibration, which may have helped the valve to seat and seal properly. Half a minute later we continued to lift the FPC out of the drill string in the normal manner. Once on the trestle, it was clear that the valve had closed. Analysis of the data logger showed we had full in

situ pressure (~80 kbar) so the autoclave was attached to the shear transfer chamber and manipulator. After considerable difficulty, caused by the tight tolerances in the ball valves, the core was transferred, cut, and moved into a HYACINTH storage chamber, where it was logged showing that a core ~75 cm long was retrieved containing significant amounts of hydrate (the lower 25 cm appeared to be water).

#### *Pressure Core Logging and Analysis*

Core 204-1249F-2E (HRC 4) was stored within the logging chamber in the refrigerator at 5°C overnight before being loaded into the VMSCL. The core was first logged at low resolution to get a quick impression of what type of core had been recovered. It was immediately clear that a nearly full core (85–90 cm) had been recovered with relatively low average densities. Interpretation of VP continued to prove difficult.

Over the next few hours, more detailed logs were run while the core warmed up slowly and increased in pressure. Temperature measurements were taken by inserting a probe in the ball-valve spindle. This provided only an approximation of the core temperature, even though the logging chamber was insulated by foam whenever possible and the chamber ends were insulated with “bubble wrap” as far as practically possible. When the temperature and pressure had increased to 16°C and 160 kbar, respectively, the complete chamber was again returned to the refrigerator to stabilize overnight. In the morning (at 5°C), the pressure had dropped to 85 kbar (close to in situ conditions again).

Over the next 2 days, the GRA density logs were obtained repeatedly during the process of degassing. Gas was collected using an inverted measuring cylinder in water as was used to degas the PCS. Temperature was allowed to rise slowly while the pressure was varied in an effort to control the rate at which gas was released during the process of depressurization and hydrate dissociation. At the end of day 2, the chamber was again left in the refrigerator to stabilize overnight. Throughout day 3, the core was completely degassed, warmed to room temperature, and completely depressurized.

Over the course of the measurement period, >101.5 L of gas was collected, and 24 GRA density logs were obtained along the length of the core. The gas was subsampled during the degassing process for compositional analysis in the onboard chemistry laboratory. The GRA density logs clearly showed how the physical structures within the core changed during the measurement period. Characteristic features interpreted as gas, hydrate, sediment, and water could be correlated and traced between logs. It was clear from these logs where gas was forming and where and when it was escaping from the core. Methane hydrate and water are difficult to distinguish via density alone, but when hydrate dissociates, the gas layers generated are easily apparent in the GRA density logs.

By the time all the gas had been removed at the end of the degassing process, the sediment had completely liquefied and most of it was removed from the chamber by bleeding it as a slurry through the pipework. It was collected, allowed to settle, and dried,

#### *In-Situ Sampling and Characterization of Naturally Occurring Marine Methane Hydrate Using the D/V JOIDES Resolution.*

and the total weight enabled a mass balance calculation to be performed. It was calculated that the core consisted of ~40% by volume of methane hydrate and 60% by volume of fine-grained sediment with an average bulk density of 1.3 g/cm<sup>3</sup> (67% porosity). If hydrate is expressed as a percentage of pore volume, as is done elsewhere in this volume, then this core contained ~50% hydrate by pore volume.

Core 204-1249G-2E (HRC 7) was logged inside the storage chamber after having been stabilized at ~6°C. The density log shows that ~25 cm of material may have fallen out of the end of the core, but the remainder shows detailed structure indicating several layers of massive hydrate above a water interval. It was decided to attempt to preserve this core as a “pristine example” in liquid nitrogen for study in the laboratory. This could then be used as a reference core to compare with samples taken without pressure preservation and as a complementary reference core to Core 204-1249H-2Y (FPC 10) (see below). The problem was, of course, how to remove the core from the pressure vessel without the gas in solution instantly coming out of solution and without the hydrate starting to dissociate. We decided to freeze the core. First, the core was cooled in the storage chamber to 0°C in an ice bath for several hours. Following this, the seawater pressurizing fluid was replaced by Helium using a high-pressure regulator after the pressure inside the chamber was first reduced to 63 kbar (maximum regulator pressure).

Despite some difficulties caused by small amounts of sediment in the pipes, the operation was successful and the storage chamber with core was then rapidly logged as a check, which showed that the sediment section had not moved and that the water section still remained in the core. The chamber was then placed in the freezer at –10°C for more than 24 hr before being rapidly logged again, which showed that some of the water had escaped and some had frozen. This caused some concern because it left a gas pocket inside the liner. To remove the core, the chamber was connected to manipulator and wrapped in ice bags. Hot water and rags were applied to the manipulator end of the chamber to unfreeze the contact between the core and the inside of the chamber. Hot water was also applied at the ball-valve end to free the bleed pipes and pressure gauge, which was frozen, and did not read the inside gas pressure correctly. Once clear, the pressure inside the chamber was measured at ~62 kbar. This pressure was then released slowly (~5 min) so as to allow time for the pressure inside the core liner to escape. When the pressure was zero, the ball valve was opened and the manipulator extended slowly to push the core from the chamber. Rapid gas expansion shot some frozen core containing massive hydrate from the chamber. However, this was easily collected and placed directly in liquid nitrogen. The core was further extruded with care (surrounded by steel tube), and further core sections were cut off and placed in liquid nitrogen. It was clear that a substantial part of this core contained massive hydrate, as could be clearly seen from the core ends and through the core liner during its brief exposure.

Core 204-1249H-2Y (FPC 10) was logged inside a HYACINTH storage chamber, after having been stabilized at ~6°C. The density log showed a 75-cm-long core above a water interval of ~25 cm, indicating that some material may have fallen out of the end of the

core. However, the sediment section shows detailed structure indicating several layers of massive hydrate. A thicker layer of hydrate (60- to 80-cm logging depth) shows a small interval where the average density is only  $\sim 0.75$  g/cm<sup>3</sup>, clearly demonstrating that free gas does exist in situ inside the massive hydrate structure.

Core 204-1249L-5E (HRC 8) was logged inside one of the HYACINTH logging chambers. The GRA density log revealed a short core at the top of the liner ( $\sim 30$  cm), with a column of water beneath. There were no apparent signs of low-density layers that would be interpreted as hydrate. Consequently, the core was depressurized and the gas collected (total volume = 2.325 L). Two samples were collected and analyzed in the onboard chemistry laboratory.

## Site 1250

### *Pressure Core Sampler*

The ODP PCS was deployed seven times at Site 1250. Five deployments were successful (i.e., a core under pressure was recovered). The ball valve did not fully close during the other deployments. The main objectives of the deployments were (1) to construct a detailed profile of concentration and composition of natural gases in the upper part of the section (0–140 mbsf) and (2) to identify the presence/absence and concentrations of gas hydrate within the GHSZ. Specific depth intervals were targeted for deployment of the PCS. Three cores (Cores 204-1250C-9P [71–72 mbsf] and 204-1250D-5P [35–36 mbsf] and 13P [103.5–104.5 mbsf]) were recovered from above the BSR at  $\sim 112$  mbsf. Two other cores (Cores 204-1250D-18P [135.2–136.2 mbsf] and 204-1250F-4P [119–120 mbsf]) were recovered from below the BSR.

The PCS cores were degassed for 579–1800 min after recovery on board. Pressure was recorded during degassing experiments of all cores, except for Core 204-1250F-4P. Gas was collected in a series of sample increments (splits), and most were analyzed for molecular composition. In addition, gas splits were sub-sampled for onshore analyses. After degassing, the PCS was disassembled. The lengths of the cores were measured, and samples were taken for analysis of physical properties. Gas was collected in 10- to 810-mL increments. The cumulative volume of released gas varies from 1385 (Core 204-1250D-18P) to 5390 mL (Core 204-1250F-4P). The volume of the last gas splits varies from 10 (Cores 204-1250C-9P and 204-1250D-13P) to 30 mL (Core 204-1250D-5P). This observation suggests that almost all gas present in the cores was collected.

Gases released from the PCS are mixtures of air (N<sub>2</sub> and O<sub>2</sub>), CH<sub>4</sub>, CO<sub>2</sub>, and C<sub>2</sub>+ hydrocarbon gases. The abundance of air components in the PCS gas samples (3.0%–8.3% of gas mixtures) suggests that air was not always properly displaced from the PCS by seawater during deployments. Methane is the dominant natural gas present in collected gas splits. The molecular composition of gases from the PCS is similar to the composition of gas voids at adjacent depths. Sediments in cores recovered by the PCS

*In-Situ Sampling and Characterization of Naturally Occurring Marine Methane Hydrate Using the D/V JOIDES Resolution.*

have lithologies similar to sediments recovered by the APC and XCB cores at adjacent depths. Porosity values measured in APC and XCB cores taken near the PCS were averaged and used to estimate the methane concentrations in situ.

The concentrations of methane in situ were estimated based on data from the degassing experiment (i.e., total volume of methane) and core examination (i.e., length of recovered core and the porosity of sediments). The calculation yields equivalent concentrations varying from 65.7 to 278.3 mM of methane in pore water. These concentrations have been compared with the theoretical methane-solubility curve extrapolated from values calculated for higher pressures (greater depths) (Handa, 1990; Duan et al., 1992). Preliminary analysis of gas concentrations suggests that gas hydrate may have been present in concentrations varying from 0.6% to 2.2% of pore volume in all three cores (Cores 204-1250C-9P and 204-1250D-5P and 13P) recovered from above the BSR. Interestingly, no evidence of gas hydrate presence was found in the pressure record of core degassing. Free gas appears to be present in relatively high concentrations (perhaps around 4% of pore space) at a depth of ~7.5 m below the BSR (Core 204-1250F-4P). Only dissolved methane seems to be present in the core (Core 204-1250D-18P) retrieved from ~24 m below the BSR. Additional comparison of measured methane concentrations with theoretical methane solubility above and below the BSR will be performed on shore to better estimate if methane was present in situ in solution, in free phase, or as gas hydrate.

#### *HYACINTH Pressure Coring and Logging*

The HYACINTH pressure coring tools were deployed twice at Site 1250: one with the FPC (Core 204-1250C-18Y [FPC 4]) and one with the HRC (Core 204-1250D-17E [HRC 3]). After the lessons learned from the procedures and the tool adjustments made at Site 1251, we hoped that a pressurized core might be recovered from this site. A good core was recovered with the FPC, but full retraction into the autoclave was prevented as a result of inadvertent line tension during the coring operation. The HRC, on the other hand, recovered a short core at full in situ pressure, which was considered a significant success. Core 204-1250D-17E (HRC 3) was then transferred under full pressure and logged in the V-MSCL before being depressurized. Unfortunately, the DSA tool was still dogged by technical difficulties and failed to provide any useful downhole data during the coring operations. However, the rig floor data proved valuable in analyzing some aspects of the behavior during each deployment, especially given the fact that there had been a brief tension load on the wireline during the FPC deployment.

After transferring Core 204-1250D-17E (HRC 3) to the logging chamber, the density profile was measured in the V-MSCL, where we discovered how short the core was (20 cm). This short core had sediment densities of ~1.65 g/cm<sup>3</sup> and produced some obvious gas layers when depressurized.

#### *In-Situ Sampling and Characterization of Naturally Occurring Marine Methane Hydrate Using the D/V JOIDES Resolution.*

### *HYACE Rotary Corer Operations*

The HRC was deployed at Site 1250 in a water depth of 796 m. Core 204-1250D-17E (HRC 3) was taken in the bottom of Hole 1250D at 134.2 mbsf. Lithologies at this depth were lightly indurated silty clays that were being cored with full recovery by the APC. These sediments were considered suitable for the FPC, and it was thought that they might be stiff enough to be cored using the HRC. A modified finger catcher was made and fitted for this deployment in the hope that it might help retain the core in this type of formation. The deployment went well, with the procedures being essentially the same as for previous runs. The HRC was lowered in the drill string at 72 m/min while circulating and rotating. Pumping was stopped at 890 m, the tool was lowered down slowly to the landing position, and a slack of 4 m was given on the wireline. The drill string was then lowered to TD with the wireline following. The blowout Preventer (BOP) on the wireline was closed, and pumping was started at 82 gallons per minute (gpm). A pressure spike was observed at 540 psi, indicating that coring had begun, and then pumping continued at 95 gpm for 20 min before stopping and opening the BOP. The drill string was lifted to 937 m before the BOP was closed again and pumping continued for 2 min (to ensure full stroke) at 80 gpm. The BOP was again opened, and the tool was lifted on the wireline very slowly for the first 16 m before being raised to the surface at 110 m/min. During the coring operation the weight on bit was set at ~15,000 klb, and both the active and passive heave compensators were activated. The tool was recovered and placed on the trestles in the usual way. It was disassembled and the autoclave moved to the transfer system where an internal pressure of 88 kbar was measured. The core was retracted into the shear transfer chamber under full pressure where it was sheared and successfully moved into the logging chamber. After the core had been logged in the V-MSCL, it was depressurized in stages before being removed and curated as a 28-cm-long core. Note that this short core was the first of its kind to have been recovered and logged in a liner under full in situ pressure.

### *Fugro Pressure Corer Operations*

A single FPC deployment was made at Site 1250 in a water depth of 796 m. Core 204-1250C-18Y (FPC 4) was recovered from the bottom of Hole 1250C at 137.5 mbsf. Lithologies at this depth were lightly indurated silty clays that were suited to the APC and considered suitable for the FPC hammer mechanism. Operationally, the deployment ran smoothly as per previous deployments with the downhole procedures being followed and the active heave compensator being used throughout. A good core was recovered (84 cm long) but the inner rod had not stroked out completely and the core had only partially retracted into the autoclave. The pressure was released by drilling small holes in the liner prior to removing the core. Once again during this deployment the FPC data logger worked well but the Lamont DSA tool only collected data from the very beginning part of the test. An analysis of the rig data concluded that at one time a significant tension had been applied on the wireline during the coring operation (which probably prevented a full

### *In-Situ Sampling and Characterization of Naturally Occurring Marine Methane Hydrate Using the D/V JOIDES Resolution.*

stroke occurring) and should be avoided by paying out more slack wire on subsequent deployments.

### **Site 1251**

#### *Pressure Core Sampler*

The PCS was deployed nine times at Site 1251. Eight of these deployments were successful (i.e., a core under pressure was recovered). Only water was recovered during the other deployment because the tool actuated prematurely. The main objectives of the deployments were: (1) to construct a detailed profile of concentration and composition of natural gases in the upper part of the section (0–300 mbsf) and (2) to identify the presence/absence and concentration of gas hydrate within the GHSZ. Specific depth intervals were targeted for deployment of the PCS. Six cores (Cores 204-1251B-12P [104.1–105.1 mbsf] and 18P [153.6–154.6 mbsf]; 204-1251D-6P [45.9–46.9 mbsf], 10P [76.4–77.4 mbsf], and 21P [173.4–174.4 mbsf]; and 204-1251G-2P [20–21 mbsf]) were recovered from above the BSR at ~193 mbsf. Successful retrieval and degassing of Core 204-1251G-2P suggests that the PCS can be deployed at shallow seafloor depths. The other two cores (Cores 204-1251B-35P [290.6–291.6 mbsf] and 204-1251D-29P [227.5–228.5 mbsf]) were recovered from below the BSR.

The time to degas the PCS chambers ranged from 672 to 1567 min. Pressure was recorded during degassing experiments and gas was collected in a series of sample increments (splits), and most were analyzed for molecular composition. In addition, gas splits were subsampled for onshore analyses. After degassing, the PCS chambers were disassembled. The lengths of the cores were measured, and samples were taken for analysis of physical properties. Gas was collected in 5- to 720-mL increments. The measured incremental and cumulative volumes are plotted vs. time (Fig. F36). The cumulative volume of released gas varies from 1320 (Core 204-1251G-2P) to 3365 mL (Core 204-1251B-12P) (Table T18). The volume of the last gas splits varies from 5 (Core 204-1251B-12P) to 20 mL (Core 204-1251D-6P). This observation suggests that almost all gas present in the cores was collected.

Gases released from the PCS are mixtures of air (N<sub>2</sub> and O<sub>2</sub>), CH<sub>4</sub>, CO<sub>2</sub>, and C<sub>2</sub>+ hydrocarbon gases. The abundance of air components in the PCS gas samples (2.7%–53.2% of gas mixtures) suggests that air was not properly displaced from the PCS by seawater during deployments. Methane is the dominant natural gas present in collected gas splits. The molecular composition of gases from the PCS is similar to the composition of gas voids at adjacent depths. Sediments in cores recovered with the PCS have lithologies that are similar to sediments recovered by the APC at adjacent depths. Porosity values measured on samples from APC cores taken near the PCS were used to estimate the methane concentration in situ.

*In-Situ Sampling and Characterization of Naturally Occurring Marine Methane Hydrate Using the D/V JOIDES Resolution.*

The concentration of methane in situ was estimated based on data from the degassing experiment (i.e., total volume of methane) and core examination (i.e., length of recovered core and the porosity of sediments). The calculation yields equivalent concentrations varying from 46.9 to 157.6 mM of methane in pore water. These concentrations have been compared with the theoretical methane-solubility curve extrapolated from values calculated for higher pressures (depths) (Handa, 1990; Duan et al., 1992).

Preliminary analysis of gas concentrations suggests that gas hydrate may have been present in small concentrations (<1% of pore volume) in Cores 204-1251B-12P and 204-1251D-6P. In addition to relatively high gas concentrations, evidence of the presence of gas hydrate was found in the pressure record of core degassing. However, other cores retrieved from the GHSZ, including Core 204-1251D-21P recovered from ~173.9 mbsf, just above the gas hydrate-bearing intervals inferred from IR thermal anomalies in Cores 22X and 24X at depths from 175 to 191 mbsf, suggest that only dissolved methane is present in some intervals within the GHSZ. A high concentration of methane in Core 204-1251B-35P may indicate the presence of free gas in the deep subsurface at ~291.1 mbsf (~100 m below the BSR), but only dissolved methane appears to be present in Core 204-1251D-29P, recovered from ~32 m below the BSR. Additional comparison of measured methane concentrations with theoretical methane solubility above and below the BSR will be performed on shore to better estimate if methane was present in situ in solution, in free phase, or as gas hydrate.

#### *HYACINTH Pressure Cores*

Five deployments of the HYACINTH pressure coring tools were made at Site 1251: three with the FPC and two with the HRC. These were the first deployments made during Leg 204 and were primarily considered to be engineering tests. One of the most important successes was the improvement in the handling of the tools and the downhole procedures compared with tests that had been conducted during previous legs (Legs 194 and 201). As a result, the total rig time used per deployment was limited to about 1.5 hr for each tool at this water depth (1224 m). A number of minor technical and operational issues arose with each tool during the tests, which were addressed at each stage during the testing program. The final outcome at the end of Site 1251 was that the HRC had recovered a short 22-cm-long core (22% recovery) under pressure (but lower than in situ pressures) and the FPC had recovered good cores, 70–80 cm in length (70%–80% recovery), but without retaining pressure. Unfortunately, the DSA tool failed to provide any downhole data during the coring operations, which limited the ability for downhole performance analysis. However, the rig floor data will prove valuable in analyzing some aspects of the behavior during each deployment. The transfer chamber system was tested, but expanding cores and coring-related problems prevented a satisfactory transfer.

*HYACE Rotary Corer Operations*

The first two HRC deployments, Cores 204-1251B-48E (HRC 1) and 204-1251D-30E (HRC 2), were made at Site 1251, where the BSR is at 196 mbsf and which coincided with the transition between the use of the APC and XCB (194.6 mbsf) in Hole 1251B. This is relevant because it has been generally proposed that the type of material that is best suited for the HRC is at the upper limit of shear strengths that can be cored using the APC.

Core 204-1251B-48E (HRC 1) was collected in Hole 1251B at 396.9 mbsf, where the clay sediments are well indurated and the mechanical properties were considered well suited for the “dry auger bit” used by the HRC. Shear strengths in recovered cores from this depth are well in excess of the maximum shear strength that can be measured with the hand-held Torvane (250 kPa). Although large amounts of gas expansion were occurring in shallower parts of the hole, by this depth these expansion effects had almost disappeared and recovery with the XCB had been generally very good.

The tool was assembled for the first time on the pipe racker in 3 hr and fitted with the new strongbacks (one of these had been slightly shortened for easier handling on the rig floor). It was raised into a vertical position, and the strongbacks were removed as it was lowered into the shuck where the DSA tool was attached. This handling procedure (using the strongbacks) only took about 20 min and was a significant improvement compared to the last engineering tests of the tool during Leg 194, when it was assembled in a vertical position. It was then lifted into the drill pipe and lowered on the wireline while circulating and rotating. The tool was lowered onto the landing shoulder when the drill string rotation and circulation had been stopped, and slack wire was payed out. Problems with cleaning the hole resulted in lifting the tool out of the landing position at one time during the procedure. Pumping began slowly to build up pressure to activate the tool and continued at 93 gallons per minute (gpm), which causes the core barrel to rotate and cut core. However, a final pressure spike was not observed (even after 18 min) that would have indicated that the full stroke had been reached. Pumping was stopped while the drill string was lifted and continued for 2 min afterward to ensure full stroke. The tool was then raised on the wireline (slowly for the first 16 m) to the surface. The DSA tool was removed, and the HRC was broken into three vertical sections vertically and then taken aft to the pipe racker and laid on the trestles. On examination of the autoclave chamber, it was found that the core liner had broken (no core recovered) and that the by-pass port, which gives the indication of end-stroke, had not opened. The evidence suggests that the tool may have been activated while it was still in the hanging position prior to landing at TD.

A second deployment of the HRC was planned at the bottom of Hole 1251B, but the hole was abandoned after poor hole conditions developed at around 445 mbsf. The HRC was again deployed at this site, Core 204-1251D-30E (HRC 2), at a depth of 229.5 mbsf. Although the lithology was softer at this depth compared with the material at ~400 mbsf,

*In-Situ Sampling and Characterization of Naturally Occurring Marine Methane Hydrate Using the D/V JOIDES Resolution.*

it was still considered useful (although not ideal) as a test for the HRC rotary cutter. The test proceeded smoothly with the handling on the rig floor being the same as for the previous deployment. This time there were no hole cleaning problems and pumping began after lowering to TD with the wireline slack. Active heave compensation was used throughout. Pumping was continued at 100 gpm for 15 min without observing any significant pressure spikes. The drill string was raised off bottom and a further 2 min of pumping (92 gpm) should have ensured full stroke of the coring barrel. The tool was then raised on the wireline slowly for the first 16 m and then continued at 110 m/min before being broken out of the drill string at the rig floor and placed in the adjacent shuck. The DSA tool was removed and the strongbacks attached before the tool was transferred to the trestles on the pipe-racker rather than being disassembled vertically. This procedure saves about 40 min compared with the vertical disassembly procedure.

This time the barrel had fully retracted, the flapper valve had closed, and the pressure was measured at ~20 kbar (much less than in situ pressure). However, the core got stuck during the transfer process, and therefore was manually removed. A 22-cm-long core (recovery = 22%) was recovered, but sediment smeared on the inside of the liner indicated that the majority of the cored material had not been retained in the barrel during retrieval, indicating that this type of catcher is not suitable for these soft formations. A leak was found later in the upper part of the autoclave section, which explained the loss of high pressure inside the chamber.

#### *Fugro Pressure Corer Operations*

The first three FPC deployments, Cores 204-1251B-21Y (FPC 1) and 40Y (FPC 2) and 204-1251D-28Y (FPC 3) were made at Site 1251 in a water depth of 1224 m. Core 204-1251B-21Y (FPC 1), at 171.7 mbsf, was in lithologies that were still suitable for the APC (XCB coring began at 194.6 mbsf) and where large amounts of gas expansion were occurring. Shear strengths measured with the hand-held Torvane in Core 204-1251B-22H were ~160 kPa, although it should be noted that in situ strengths are likely to be higher, perhaps by up to a factor of 1.5. Operationally, the deployment ran smoothly with the active heave compensator being used throughout (including pull-out). The total time taken for the complete operation was 1.5 hr.

On recovery, it was apparent that the coring mechanism had undergone a full stroke but had not fully retracted into the autoclave. However, a good-quality 0.71-m-long core had been cut (recovery = 71%). Under normal circumstances of autoclave recovery, the core would have been cut free from the piston under full pressure in the shear transfer chamber. We attempted to remove this core from the piston with a hacksaw; however, after one cut the core liner exploded violently, leaving a pile of shattered liner and sediment on the deck. Obviously the liner was under significant stress from the gas expansion, with the piston and the lower part of the core providing good seals. As the liner was first cut, a stress concentration probably occurred in the liner, allowing the catastrophic failure to propagate. An analysis indicated that a latching mechanism did not

#### *In-Situ Sampling and Characterization of Naturally Occurring Marine Methane Hydrate Using the D/V JOIDES Resolution.*

operate smoothly, which prevented the core from fully retracting into the autoclave. This was modified prior to the next deployment. Both the FPC and the DSA data loggers stopped prematurely and failed to capture data during the operations on the bottom.

A second deployment of the FPC was made in Hole 1251B at 329.6 mbsf, Core 204-1251B-40Y (FPC 2). At this depth, the sediments had not changed significantly in character apart from being more indurated. Shear strengths were outside the range of the hand-held Torvane device ( $>250$  kPa). The operational procedures were the same as for Core 204-1251B-21Y (FPC 1) and again went smoothly, taking only  $\sim 1.5$  hr. On recovery, it was apparent that this time the coring mechanism had fully retracted into the autoclave. However, a visual examination revealed that the lower flapper valve (which seals the lower end of the autoclave) had not fully closed, and hence, the autoclave was not pressurized. Subsequent investigations revealed that the flapper valve was unable to seal because of debris that fell out of the retracted liner onto the valve seating. We also discovered that the core liner had imploded. This was probably caused on pull out as a result of not fully stroking into the sediments. Unfortunately, both the FPC and the DSA data loggers again failed to capture the test interval and, hence, could not provide any diagnostic information about the tool's behavior.

The final FPC deployment at this site, Core 204-1251D-28Y (FPC 3), was made at the bottom of Hole 1251D at 226.5 mbsf. All operations were as for previous deployments except that the driller observed a 100-psi increase in pressure indicating an "end of stroke." After setting the tool on the trestles, we found that a good core had been taken (full stroke) but retraction into the autoclave had been prevented because one of the upper seals had been dislodged. The seal was caught by the holes inside the core barrel during retrieval and jammed the liner in the core barrel. This made it impossible to pull the core out of the autoclave. This was rectified prior to the next deployment. Care was taken when releasing the pressure inside the liner by drilling small holes and then cutting rather than simply using a hacksaw as with Core 204-1251B-21Y (FPC 1). The core was removed for logging and curation. During this deployment, the FPC pressure and temperature logger worked well but the DSA tool only collected data from the very beginning part of the test.

## **Site 1252**

### *Pressure Core Sampler and HYACINTH Pressure Corers*

No PCS or HYACINTH pressure corers were deployed at Site 1252.

## LEG 204 – SUMMARY OF RESULTS

### Site 1244

#### *Principal Scientific Results*

On the basis of visual observations, smear slides, and correlation with physical property data (especially magnetic susceptibility), the sedimentary sequence can be divided into three primary lithostratigraphic units, with 3 subdivisions in the second unit. Lithostratigraphic Unit I (from the seafloor to 69 mbsf) and Unit II (69-245 mbsf) are both characterized by hemipelagic clay interlayered with turbidites, with thicker, coarser turbidites common in Unit II. Individual turbidites are characterized by sand and silt layers that fine upwards to bioturbated, sulfide-rich silty clay and clay. The turbidites are particularly well developed in the interval from 160-230 mbsf. A 60-cm-thick layer at 216 mbsf that is especially rich in detrital ash shards corresponds to a strong, regional seismic reflection referred to here as reflection B'. The lithology changes to more indurated and fractured claystone interbedded with glauconite-bearing to glauconite-rich silts and sands below 245 mbsf, corresponding to the top of the seismically incoherent zone that we tentatively attribute to the accretionary complex.

Biogenic components vary downcore, with siliceous microfossils dominating. Biostratigraphic boundaries based on diatoms correlate well with lithostratigraphic unit boundaries and with seismic stratigraphic boundaries identified in the 3-D seismic data. Sediments overlying a regional unconformity at ~45 mbsf (approximately the boundary between lithostratigraphic Units I and II) yield diatoms that define a biostratigraphic age of 0.3 Ma. This unconformity is also sampled at Site 1255 at 130 mbsf. Lithostratigraphic Unit III has an age of 2.4-2.7 Ma.

Physical properties data are generally consistent with the lithostratigraphic, biostratigraphic and seismic stratigraphic boundaries. The boundary between lithostratigraphic Units I and II is marked by a localized decrease in wet bulk density. As mentioned in the previous paragraph, the turbidites of lithostratigraphic Unit II are particularly well developed in the interval from 160-230 mbsf. This interval is characterized by high values of whole-core magnetic susceptibility. The widest and strongest magnetic susceptibility peak, at 168 mbsf, correlates with seismic reflection Horizon B. This horizon is also coincident with an increase in wet bulk density. We also note excellent correlation between moisture and density (MAD) measurements on core samples with measurements of density and porosity obtained via LWD.

One novel aspect of Leg 204 is the regular use of both hand-held and track-mounted infrared (IR) cameras to image all cores. Cores from within the GHSZ were imaged several times by the physical properties scientists. The hand-held IR camera proved to be very effective for rapid identification of the location of hydrate specimens within the cores. Gas hydrate samples were recovered as whole rounds in Cores 1244C-8H and

*In-Situ Sampling and Characterization of Naturally Occurring Marine Methane Hydrate Using the D/V JOIDES Resolution.*

1244C-10H (samples from 63, 68 and 84 mbsf) and preserved detailed shore-based studies. A few pieces were dissociated for chemical analysis (discussed below). In all three cases, the hydrate occurred as layers or nodules several mm to 1.5 cm thick aligned at an angle of 45-60° to the core liner, suggesting formation along steeply dipping fractures.

The track-mounted IR camera imaged the cores systematically, and these records were used to confirm hydrate occurrences spotted by the hand-held cameras, to develop techniques for detecting more subtle signatures of disseminated hydrate, and to track the temporal evolution of the thermal signature of hydrate dissociation. The IR thermal imaging of the cores on the catwalk indicated the presence numerous occurrences of nodular and/or disseminated hydrates extending from ~45 mbsf to the BSR at 124 mbsf. Cl anomalies (discussed in the next paragraph) also indicate that gas hydrate occurs intermittently within this 79-m-thick zone. Moreover, the top and bottom of this zone of direct and indirect hydrate indicators corresponds very closely to a zone of strong and highly variable resistivity in the LWD data (discussed below), confirming that the LWD data are a valuable tool for predicting the occurrence of hydrate in the sediments.

Geochemical analysis of interstitial waters has revealed that depth variations in the concentration of several different chemical species correlate with the hydrate stability zone. The most direct correlation is seen in Cl concentrations. Above the first occurrence of hydrate (from the seafloor to ~45 mbsf), Cl concentration in the pore water is similar to that in seawater. Between 45 mbsf and the BSR at ~125 mbsf, there are numerous low Cl spikes that likely reflect the freshening effect of dissociated hydrate on the interstitial waters. Correlation of Cl data with the IR camera data indicates that the spatial sampling of Cl anomalies is biased, which smoothes estimates of hydrate concentration based on Cl anomalies. Additional work to better quantify this bias is planned for other sites. Never the less, these data can be used to obtain a rough estimate of hydrate concentration if a “no-hydrate” background concentration can be estimated. At Site 1244, Cl concentrations from the BSR to 300 mbsf decrease linearly at a rate of ~0.35 mM/m. This suggests a diffusive gradient between seawater and low Cl fluids in the accretionary complex. The reduced chlorinity at depth may reflect dehydration of clay minerals deeper in the accretionary complex. Considering uncertainties in the background concentration of Cl, we estimate that 2-8% of the pore space is occupied by hydrate, with locally higher and lower concentrations. The Cl concentration profile within the deepest, incoherent seismic facies is approximately constant, suggesting a zone of fluid advection and mixing, consistent with LWD, physical properties, and core observations, all of which suggest a pervasively fractured medium.

The ratio of methane to ethane (C1/C2 ratio) also shows a clear correlation with the presence of hydrate, with step-like decreases in this ratio both at 40 mbsf and at the BSR in gases obtained by the headspace technique and by extracting gas from void space in the cores. This observation will be discussed further in the Site Summary for Site 1255. Slightly lower C1/C2 ratios are observed in gas obtained by dissociating discrete hydrate

*In-Situ Sampling and Characterization of Naturally Occurring Marine Methane Hydrate Using the D/V JOIDES Resolution.*

samples, suggesting some fractionation of C2 into hydrate. The molecular composition of gases released from three successful Pressure Core Samplers (PCS) is similar to that of the headspace gases. It has not yet been determined whether in situ methane concentrations of 57 mM, 62 mM and 95 mM from depths of 120, 131 and 142 mbsf, respectively, are above or below solubility. There are the first in situ gas concentrations obtained from Hydrate Ridge.

Samples were taken to support a range of shore-based microbiological studies, but there are no results to report at this time. Measurements of sulfate concentration in the interstitial waters, which indicate that the boundary between microbial methane consumption and generation is located at 8 mbsf at this site, were used to guide high-resolution sampling for microbiological studies.

Downhole tools employed at this site included 4 APCT runs, 1 DVTP run, 1 DVTPP run and 3 PCS runs. Seven downhole temperature measurements (including the average of waterline temperatures) were used to define a linear temperature gradient of 0.0575 °C/m, similar to the temperature gradient determined at ODP Site 892 during Leg 146. This temperature gradient predicts that the BSR should be at a depth of 135 mbsf, based on the pure methane and seawater stability curve and seismic velocities obtained from a 3-D ocean bottom seismometer survey conducted in 2000 in tandem with the 3-D reflection survey. Resolution of the apparent mismatch of 10 m between the BSR depth determined from the seismic data and that calculated from the observed temperature gradient awaits a more detailed analysis of the uncertainties in the temperature measurements and better constraint on the velocity of the sediments between the BSR and the seafloor, which will be obtained from VSP experiments to be conducted during the second half of Leg 204. The pore pressure dissipation measurement made by the DVTPP follows the expected pattern, but detailed analyses to determine whether in situ pressure departs from hydrostatic pressure awaits post-cruise study. The three PCS deployments were successful, as was discussed in the previous paragraph.

The LWD data obtained at this site are of excellent quality and provide spectacular images of electrical resistivity within the borehole. As mentioned above, high-amplitude, variable resistivity from 40-130 mbsf suggests the presence of hydrate and correlates with other indirect and direct indicators of hydrate presence. Sinusoidal patterns in the resistivity images of the borehole wall suggest that gas hydrate is concentrated in steeply dipping fractures as well as along bedding planes. The data also show strong borehole breakouts, which are indicative of a northeast-southwest oriented axis of least compressive stress.

In summary, Site 1244, which is the first site that was logged and cored during Leg 204, has provided strong evidence that gas hydrates are common within the hydrate stability zone on the Oregon continental margin and that they are a major factor influencing the biogeochemical evolution of the margin. It is also clear that the integration of geophysical remote sensing data such as 3D seismic reflection surveying, Logging While

*In-Situ Sampling and Characterization of Naturally Occurring Marine Methane Hydrate Using the D/V JOIDES Resolution.*

Drilling, and IR thermal scanning provides a reliable “roadmap” to guide further sampling and analysis.

## **ODP Site 1245**

### *Principal Scientific Results*

Biostratigraphic observations from the 540 m of core recovered at Site 1245 indicate that the entire 540 m-thick sequence is younger than 1.65 Ma. Distinct changes in sedimentation rate occurred at 55 and 150 mbsf. Sediments deeper than 150 mbsf were deposited from 1.0 to 1.6 Ma at a rate of ~62 cm/kyr, whereas the overlying strata were deposited at a slower rate of 10-23 cm/kyr. Lithostratigraphic analysis indicates that the dominant lithologies are clay with carbonate concretions and foraminifer-rich interlayers in the upper 0-31 mbsf, underlain by diatom-bearing clay and silty clay with frequent sand-rich turbidites containing a few glass-rich layers from 31.5-212.7 mbsf. Included within this deeper sequence is seismic Horizon A, characterized by two thick, ash-rich, sandy layers between 174 and 181 mbsf. Between 212.7 and 419.3 mbsf, nannofossil-rich claystone and silty claystone with glauconite layers and turbidites are seen, underlain by claystone containing thick turbidites and heterogeneous mud clasts.

The precruise 3D seismic reflection site-survey and the LWD data obtained in Hole 1245A provided a “roadmap” that was used to guide the sampling and analysis strategy at this site. The LWD data, which were acquired in the first hole drilled at this site, were processed and available for interpretation for ~ 4 weeks prior to coring. Data are of excellent quality. The logs show a marked increase in the amplitude and variability of formation resistivity between 48 and 131 mbsf (Log Unit II), which was interpreted to indicate the extent of the zone within which gas hydrates would be found. High resistivity layers are both subhorizontal, indicating accumulation of gas hydrate parallel to bedding, and steeply dipping, indicating that hydrate fills fractures. Archie saturation calculations predict a hydrate concentration of ~10-30% of the pore volume in layers distributed throughout this interval.

The estimated depth distribution of hydrate obtained from the LWD data was confirmed by several other proxies used to infer hydrate distribution as well as by the actual samples of hydrate that were recovered (54 – 129 mbsf). Low chlorinity anomalies are detected in samples of interstitial waters from 55 – 125 mbsf and are interpreted to reflect in situ hydrate concentrations that are generally below 3%, with one anomaly suggesting a concentration of 15%. Low temperature anomalies were observed with the infrared (IR) cameras between 50 and 129 mbsf. Estimates of total in situ methane concentration obtained from a Pressure Core Sampler (PCS) at 57 mbsf indicated a concentration very close to in situ saturation, and a PCS located at 120 mbsf indicated that in situ methane concentration just above the BSR is an order of magnitude greater than saturation at in situ conditions. Two PCS runs below the BSR yielded concentrations slightly below saturation. The consistency between these multiple independent estimates of the depth

*In-Situ Sampling and Characterization of Naturally Occurring Marine Methane Hydrate Using the D/V JOIDES Resolution.*

range of the zone of hydrate occurrence gives us considerable confidence in the validity of these estimates. Models will be investigated post-cruise to relate the depth to the top of hydrate to the depth of the sulfate/methane interface (SMI), observed at ~ 7 mbsf at this site, and to more precisely predict the in situ methane concentration as a function of depth within the hydrate stability zone.

In addition to being used to rapidly identify the temperature range and potential location of hydrate samples in cores on the catwalk, the IR camera was used to estimate the distribution and texture of hydrate downhole. Approximately 80 IR anomalies were identified and classified. In Site 1245B, 75% of the anomalies suggested disseminated hydrate and 25% suggested nodular hydrate; in Site 1245C, 60% of the anomalies suggested disseminated hydrate and 17% suggested nodular hydrate. The IR data were also used to investigate the relationship between IR imaging, chlorinity anomalies in interstitial pore water and hydrate distribution in the core by conducting a controlled experiment on a section of core known to contain hydrate (Section 204-1245C-7H-5), as identified on the catwalk using the IR camera. When the core liner was split and removed, a 2 cm-thick, steeply-dipping layer of hydrate was found. After allowing the hydrate to dissociate for 90 minutes, closely spaced sediment samples were taken near the hydrate, including one sample from where the hydrate had been. The chlorinity anomaly is strongly attenuated 5 cm away from the hydrate sample and has disappeared 10 cm from the hydrate. Since normally only 2 interstitial water samples are taken in each 9.5 m-long core, the chlorinity measurements are spatially biased. Frequent low chlorinity anomalies downcore must indicate extensive distribution of hydrate. Additional comparison and calibration between data sets with different length scales and sensitivity to hydrate concentration should improve our ability to estimate in situ concentrations from such data.

The LWD data provided the first evidence obtained during Leg 204 for the hypothesis that seismic Horizon A is a significant regional feature. At all 4 sites where Horizon A was crossed during the LWD phase of Leg 204, it is characterized by a very distinctive, strong, double-peaked, low density anomaly (< 1.5 gm/cc compared to 1.85 gm/cc in adjacent sediments) that is ~ 4 m-wide. Coincidence of this LWD density anomaly with the estimated depth of Horizon A in the seismic data provided confirmation that the velocities used for converting the seismic data to depth were accurate enough to predict the depth of target horizons to within a few meters, pending processing of wireline acoustic data. The direct correlation between the low density layers and the thick ash layers mentioned above was confirmed by bulk density and magnetic susceptibility measurements made on the cores.

Another major result of Site 1245 was the discovery of significant concentrations of higher order hydrocarbons beneath the BSR. Methane/ethane ( $C_1/C_2$ ) ratios in headspace samples reach values < 100 between 130 and 180 mbsf. When combined with the measured in situ temperature gradient (~0.055 °C/m) and the observation that the  $C_1/C_2$  anomaly is due entirely to an increase in ethane concentration, the data suggest that

*In-Situ Sampling and Characterization of Naturally Occurring Marine Methane Hydrate Using the D/V JOIDES Resolution.*

thermogenic hydrocarbons are migrating from deeper in the accretionary complex. Lithium anomalies observed in association with Horizon A support this interpretation. In addition to  $C_2$ , enrichments in  $C_3$  and other higher order hydrocarbons were also observed. At Site 1245, the minimum in the  $C_1/C_2$  ratio occurs around 150 mbsf, ~30 m above Horizon A. At some of the other sites it is below Horizon A, suggesting a complex relationship between Horizon A, subsurface fluid transport, and the possible formation of hydrates of methane and other hydrate-forming gases.

In summary, Site 1245 provided confirmation that multiple proxies for in situ hydrate occurrence, including electrical resistivity measured downhole, core temperatures measured on the catwalk, and chloride anomalies measured in interstitial waters extracted from sediment samples, are consistent with direct measurements of gas concentration in predicting the distribution and concentration of gas hydrates in the subsurface, although additional analysis is needed to more precisely understand and calibrate these different proxies. It also demonstrated that a distinctive seismic event underlying the BSR and referred to as Horizon A results from the presence of a pair of low-density ash-bearing sand layers that are likely to be fluid conduits. It provided evidence for migration of higher hydrocarbons beneath the gas hydrate stability zone, although determining details of the role of seismic Horizon A in this migration will only be resolved through integration of data from several sites. Finally, it provided important lithostratigraphic and biostratigraphic data for reconstructing the geologic history of this hydrate-bearing system, including the rate at which the system formed and lithologic controls on fluid migration and hydrate distribution.

## **Site 1246**

### *Principal Scientific Results*

The precruise 3D seismic reflection site-survey and the LWD data obtained in Hole 1246A provided a “roadmap” that was used to guide the sampling and analysis strategy at this site. As mentioned above, the seismic data define the link between Sites 1244 and 1246 and suggest approximate depths to Horizons B and B’ and the BSR of ~60, 100 and 114 mbsf, respectively. The LWD data, which were acquired in the first hole drilled at this site, were processed and available for interpretation for 3 weeks prior to coring. These logs provided a first look at the probable distribution of hydrate within the GHSZ. Based on the Archie relationships between electrical resistivity and porosity, LWD data suggested that hydrate should occur intermittently between 53 and 109 mbsf. The LWD data also indicate that Horizon B is characterized by relatively high density and resistivity, as was found at Site 1244. Unlike Site 1244, no prominent low density anomaly is found associated with Horizon B’ at Site 1246.

Use of the infrared (IR) camera continued, both to rapidly identify gas hydrate through the core liner and to investigate the distribution and texture of hydrate in the cores and visualize the process of dissociation. Temperature anomalies in the IR thermal images

*In-Situ Sampling and Characterization of Naturally Occurring Marine Methane Hydrate Using the D/V JOIDES Resolution.*

suggest the intermittent presence of hydrate from ~15-117 mbsf, a somewhat more extensive depth range than is indicated by other hydrate proxies (see discussion of interstitial waters and LWD). In addition, several of the IR thermal anomalies are correlated with changes in the lithologic and physical properties of the sediments and with anomalies in chemistry of the pore waters. These changes are in turn correlated with seismic Horizon B. Whole rounds of core containing particularly strong IR temperature anomalies, and therefore suspected of containing gas hydrate veins or nodules, were recovered from 66.5, 96.6, and 105.0 mbsf and preserved in liquid nitrogen for detailed shore-based studies. A gas hydrate sample recovered from 109.5 mbsf was divided into two pieces; one piece was allowed to dissociate on board for chemical analysis (discussed below) and the other was preserved

On the basis of visual sediment descriptions, examination of smear slides, and correlation with physical property data (especially magnetic susceptibility), the sedimentary sequence can be divided into two primary lithostratigraphic units. Lithostratigraphic Unit I (from the seafloor to 21.7 mbsf) is a Late Pleistocene to Holocene unit characterized by dark greenish gray diatom and nannofossil-bearing hemipelagic clay. Lithostratigraphic Unit II, which extends to the base of the Hole 1246B, is defined by the onset of graded silt and sand layers, which represent a series of turbidites of varying thicknesses bounded by erosional contacts and separated by periods of bioturbated hemipelagic sedimentation. Layers comprised of >50% sand are found at 62, 71 and 136 mbsf, respectively. The sandy layer at 62 mbsf (found in Core 204-1246B-8H) can be correlated with the base of seismic Horizon B. (Note that the thickness and base of this layer is not defined because whole rounds were taken for microbiology and interstitial water analyses prior to core description). The overlying graded sequence is ~2 m-thick and is gray colored, in sharp contrast to most of the sediment cored during this Leg. The gray color results from a high percentage of quartz grains. This zone contains fewer biogenic components than adjacent strata, suggesting rapid deposition. A similar sequence is found at 56 mbsf in Core 204-1246B-7H, although the base of this upper turbidite sequence contains less sand.

Detailed analysis of physical properties data reveals that the two turbidite sequences that comprise Horizon B are each characterized by a high density and high magnetic susceptibility anomaly and that each layer is ~2.5 m thick. Preliminary synthetic seismograms calculated based on the density log confirm that the resulting double-peaked density anomaly that extends from 54 to 67 mbsf explains the complicated waveform of seismic Horizon B at this site. The relatively high density probably results from the grain size and packing of the sediments. The source of the high magnetic susceptibility has not yet been identified. A thin (<50 cm-thick), high resistivity anomaly also appears near the base of each of these turbidites, suggesting the presence of hydrate. Low temperatures measured on the catwalk with the IR camera are additional indirect indicators for the presence of gas hydrate in the lowermost coarse-grained portion of each turbidite sequence. A sample thought to contain hydrate was recovered from the base of the lower turbidite (Interval 204-1246B-8H-S04, 25-30cm) and was preserved in liquid nitrogen for

post-cruise analysis. Samples of this coarse-grained layer were also taken for interstitial water and microbiology studies.

The correlation between physical properties, lithology and seismic horizon B' at Site 1246, where it occurs a few meters above the BSR, is not clear. A thin (<1 cm-thick) volcanic ash-rich layer is observed at 96 cm depth in section 4 of Core 204-1246B-11H (~95 mbsf). Strong, narrow (<1 m) high resistivity and thermal anomalies indicative of the presence of gas hydrate are observed at 96-97 mbsf in the LWD and IR data, respectively. A sample thought to contain hydrate was recovered in section 5 of Core 204-1246B-11H at this depth. Recovery in Core 204-1246B-11H was 80%, and the primary lithological source of Horizon B' may not have been recovered. Shore-based studies are planned to determine the age and provenance of this ash and to compare it to the ash recovered from Site 1244. The ash data will complement the biostratigraphic ages, which suggest an age of ~0.3 Ma at Horizon B'. Seismic modeling will also provide constraints on the nature of fluids in this horizon. At Site 1244, where Horizon B' is found at 216 mbsf (well below the gas hydrate stability zone), it is associated with a 60 cm-thick layer that is rich in detrital shards of volcanic glass and corresponds to a distinctive low density anomaly in the LWD and shipboard physical properties data. We will test the model that Horizon B' contains free gas at Site 1244 and that the disappearance of the density anomaly at Site 1246 results from formation of gas hydrate.

Geochemical analyses of interstitial waters made during Leg 204 have revealed variations in the concentration of several different chemical species with depth that correlate with the GHSZ. At Site 1246, the most direct correlation is based on chloride concentrations, which show a pattern similar to that observed at most other sites, with the exception of those at the southern summit of Hydrate Ridge. From the seafloor to ~40 mbsf, chloride concentrations are similar to those of seawater suggesting that no hydrate is present. Between 40 mbsf and the BSR at ~114 mbsf, there are numerous low chloride spikes that likely reflect the dilution of porewater by water from dissociated hydrate. The lowest chloride value at this site (~430 mM) is from a sample that fortuitously coincided with the coarse-grained basal zone of the Horizon B turbidite discussed above. Assuming the "no-hydrate" background concentration of chloride that was estimated for Site 1244, the amplitude of this chloride anomaly suggests that 23% of the pore space in this layer is filled by hydrate. Ba, Li and Na are depleted in this interval, and Ca, Mg and Sr are depleted in the overlying sample, located ~3 m higher in the section. The correlation of interstitial water chemistry with specific horizons defined by lithologic and physical properties suggests that modeling of these chemical data will provide constraints on the origin, evolution and flow rate of fluids that transport methane into and through the GHSZ.

Analyses of the organic chemistry of gases at Site 1246 indicate that processes here are similar to those at Site 1244. The ratio of methane to ethane ( $C_1/C_2$  ratio) shows a step-like decrease at the BSR, which reflects an increase in  $C_2$  beneath the BSR rather than a change in methane concentration. The presence of propane ( $C_3$ ) below the BSR suggests

*In-Situ Sampling and Characterization of Naturally Occurring Marine Methane Hydrate Using the D/V JOIDES Resolution.*

the upward migration of higher hydrocarbons from below, and the absence of  $C_3$  within the GHSZ (with one exception at ~22 mbsf) indicates that gas above solubility in this zone should be in the form of Structure I rather than Structure II hydrate. The apparent fractionation of  $C_2$  into gas hydrate, which was reported at sites 1244 and 1251 from analyses made of gases obtained from dissociated hydrate samples, is not apparent here. However, this may be an artifact of sampling since only one hydrate sample was available for gas analysis at Site 1246. Because no Pressure Core Sampler (PCS) runs were made at this site, no in situ gas concentration estimates are possible.

The methane/sulfate boundary at Site 1246 falls between 4 and 7 mbsf but is poorly defined due to sparse sampling; it is slightly shallower than at Site 1244, where it is identified at 9 mbsf. Variations in the depth of the methane/sulfate boundary among Leg 204 sites will be compared to variations in depth to the first occurrence of hydrate as part of a postcruise study.

Five downhole temperature measurements were made at Site 1246. The APCT tool that was used showed a short offset  $-2^\circ\text{C}$  between the 1<sup>st</sup> and 2<sup>nd</sup> runs. Correcting for this offset, the data suggest a temperature gradient of  $0.049^\circ\text{C}/\text{m}$ , which is lower than the gradient of  $0.057^\circ\text{C}/\text{m}$  measured at Sites 1244 and 1251. This temperature gradient predicts that the BSR should occur at 150 mbsf, considerably deeper than the observed depth of ~114mbsf. This observation is consistent with results from other sites near the crest of Hydrate Ridge, whereas sites located away from the crest show much less of a difference between measured and predicted temperatures at the BSR.

In summary, the multidisciplinary approach that characterizes ODP has been used to document multiple correlations between geological and geophysical parameters and the presence of gas hydrate at Site 1246. The primary preliminary result is that seismic Horizon B is caused by a pair of high magnetic susceptibility, high density, and low porosity layers ~2.5 m thick and spaced 10 m apart. Sedimentological analysis indicates that each layer is formed by a turbidite sequence with a complicated internal structure indicating deposition, erosion and redeposition. Electrical resistivity, IR temperature and geochemical anomalies are associated with the basal, coarser-grained layers of each of the two turbidites that constitute Horizon B, indicating that hydrates preferentially form here. Indirect and direct indicators of hydrate were also found associated with Horizon B'. Postcruise work is planned to determine the source of the magnetic susceptibility anomaly, and to correlate lithological and physical properties of these horizons between Site 1244 and Site 1246. Additional efforts will be focused on modeling the seismic response of this horizon as it changes from a fluid-rich layer beneath the BSR to a hydrate-bearing layer above it, and to constrain the source and evolution of the fluids using the geochemical data.

## ODP Site 1247

### *Principal Scientific Results*

As at Site 1245, biostratigraphic observations from the 220 m of core recovered in Hole 1247B indicate that the entire 540 m-thick sequence is younger than 1.65 Ma. Sediments deeper than ~165 mbsf were deposited at a rapid, but poorly constrained, rate. These strata are correlative with strata yielding a linear sedimentation rate of 62 cm/k.y. at Site 1245. The interval from ~150-165 mbsf, which contains Horizon A, yields a relatively slow sedimentation rate of 4 cm/k.y. based on nannofossils. Overlying strata were deposited at a rate of 9-22 cm/k.y., similar to what is observed at Site 1245.

Lithostratigraphic analysis indicates that the dominant lithologies are clay with authigenic carbonates and foraminifer-rich interlayers in the upper 0-27 mbsf (Lithostratigraphic Unit I), underlain by diatom-bearing clay and silty clay with frequent sand-rich turbidites containing a few glass-rich layers from 27-212.7 mbsf. Lithostratigraphic Unit III (60-220 mbsf) is distinguished from Unit II by an increase in turbidites and biogenic components. Included in Lithostratigraphic Unit II is seismic Horizon A. Unlike at the other sites where Horizon A was sampled and found to correspond to two ash layers, at Site 1247B a soft sediment debris flow bounded by turbidites was found. Because the signature of Horizon A in the LWD data from Hole 1247A, located only 75 meters from Hole 1247B, is very similar to that observed at the Sites 1245, 1248 and 1250, we conclude that the change in amplitude of Horizon A between the two holes at Site 1247 results from a dramatic local change in lithology rather than from processes related to gas hydrates.

As at other sites, the apparent top of the zone of hydrate occurrence as indicated by a variety of different proxies is generally consistent. The onset of high and variable electrical resistivity and of thermal anomalies observed with the infrared (IR) camera on the catwalk are both at ~45 mbsf. High resistivity layers are subhorizontal, indicating accumulation of gas hydrate parallel to bedding, and steeply dipping, indicating that hydrate fills fractures. The onset of low chlorinity anomalies is at ~55 mbsf. The onset of in situ methane oversaturation as projected from headspace and Pressure Core Sampler measurements is ~38 mbsf.

The above proxies are also consistent with similar depths for the base of the gas hydrate stability zone (GHSZ). The deepest IR thermal anomaly is at 118 mbsf. The deepest chlorinity anomaly is at 114 mbsf. A PCS indicating a volume of methane greater than in situ concentration was taken at 123 mbsf. Seismic velocities from the sonic log and the VSP complement these interpretations by clearly resolving a velocity decrease indicative of the presence of free gas beneath 129-134 mbsf.

The significant concentrations of higher order hydrocarbons found beneath the BSR at Site 1245 were also observed at Site 1247. Here, low values of the methane/ethane ratio

*In-Situ Sampling and Characterization of Naturally Occurring Marine Methane Hydrate Using the D/V JOIDES Resolution.*

( $C_1/C_2 < 100$ ) persist to a slightly deeper depth than at Site 1245 (~220 mbsf, compared to ~180 mbsf at Site 1245). Hole 1247B did not extend deep enough to resolve the deeper increase in  $C_1/C_2$  and then a return to a “normal”  $C_1/C_2$  decrease with depth below 250 mbsf. The relationship between the anomalously low  $C_1/C_2$  ratios and fluid migration along Horizon A remain unclear.

One of the notable results from this site was identification of a new hydrate proxy that has the potential to provide valuable constraints on the dynamics of hydrate formation. It was found that many samples collected from the depth range in which other proxies indicate the presence of hydrate showed ethane enrichment and propane depletion. This was attributed to fractionation of ethane and exclusion of propane ( $C_3$ ) during the formation of Structure I hydrate. The observed pattern of anomalies, relative to baseline  $C_1/C_2$  and  $C_1/C_3$  concentrations defined by the majority of samples, can be explained by invoking the presence of gas hydrates within those samples that dissociated on recovery.

Another interesting result was that Horizon A shows a low amplitude chlorinity low and methane high in addition to the Li enrichment observed coincident with this horizon at other sites. Given the expectation that Horizon A should be more permeable where it is characterized by coarse-grained, ash-rich layers than where it consists of a clay-rich debris flow, these observations are surprising and have not yet been explained. The Li enrichment is similar in amplitude to that observed at other sites and is clearly associated with Horizon A, thus supporting the interpretation of a stratigraphic horizon that transports fluids from greater depth.

The depth of the sulfate/methane interface (SMI) at this site is well-constrained by high resolution samples and is determined to be at 11 mbsf. Assuming that this depth is entirely controlled by anaerobic methane oxidation, a methane flux of  $2.5 \times 10^{-3}$  mmol  $\text{cm}^{-2} \text{yr}^{-1}$  is inferred, which is about 1.4 times greater than at the Blake Ridge and about 30% less than at Site 1251. However, the assumptions on which this estimate is based do not seem to be valid for the entire interval above the SMI, leading to considerable uncertainty in this estimate.

The in situ temperature measurements in Hole 1247B yielded a very precisely defined slope of  $0.0524$  °C/m (correlation coefficient of 0.999) and did not reveal any sign of a positive temperature anomaly at Horizon A. This observation will be used to place an upper bound on the rate of fluid transport from depth along this horizon that can be compared to rates obtained from the chemical anomalies.

In summary, Site 1247 provided further confirmation that multiple proxies for in situ hydrate occurrence are consistent with direct measurements of gas concentration in predicting the distribution and concentration of gas hydrates in the subsurface. These include electrical resistivity and porosity measured downhole via LWD, core temperatures measured on the catwalk, and chloride anomalies measured in interstitial waters extracted from sediment samples. A new proxy – ethane enrichment and propane

*In-Situ Sampling and Characterization of Naturally Occurring Marine Methane Hydrate Using the D/V JOIDES Resolution.*

depletion – was discovered that holds promise for constraining hydrate dynamics. Results from this site also indicate that lateral changes in the amplitude of Horizon A in the interval between the BSR and a faint “second BSR” probably result from lithologic changes rather than from the presence of more stable hydrates of higher order hydrocarbons, as had been speculated, leaving open the question of the origin of this “second BSR.” Finally, the small chlorinity depletion and methane enhancement associated with Horizon A, which is not observed at Sites 1245, 1248 and 1250, leads to the apparently contradictory conclusion that Horizon A is a more active conduit for deeper fluids where it is composed of a clay-rich debris flow than where it is composed of a pair of coarse-grained, ash-rich sandy silt.

## **ODP Site 1248**

### *Principal Scientific Results*

Two lithostratigraphic units were recognized at Site 1248. Unit I, of Holocene to Late Pleistocene age, is characterized by dark-greenish gray diatom-bearing clay and silty clay and extends from the seafloor to 39 mbsf. These fine-grained lithologies are commonly structureless except for sulfide mottles. Lithostratigraphic Unit II (39-149 mbsf), of Middle to Early Pleistocene age, is dominated by homogenous silty clays with varying amounts of biogenic components. Sand silt-sized turbidites are intercalated as minor lithologies throughout this unit.

High concentrations of beige to white volcanic glass shards were observed in the tail of a few turbidites in Core 204-1248C-14H; these are concentrated around 130 mbsf. This depth interval is well correlated with the occurrence of the regional seismic reflector Horizon A, which appears as a high amplitude reflection within the seismic stratigraphic framework of southern Hydrate Ridge. Its regional extent was mapped in the precruise 3-D seismic survey, where it is observed as a reflector dipping away from the southern summit of Hydrate Ridge. A detailed examination of the sediments at Site 1245 revealed that the volcanic ash is a major sedimentary constituent that was also found at the Horizon A level of other sites (Sites 1250 and 1247).

Site 1248 Logging-While-Drilling data clearly show Horizon A as a two-m-thick anomalous interval, characterized by high resistivity and low density values within the depth interval from ~126 mbsf to ~128 mbsf. These results are indicative of a sand layer containing free gas. Physical property measurements on discrete samples of the cores from Site 1248 confirm the low-density character of Horizon A sediments, which is interpreted to be due to the reduced grain density of the ash. The presence of volcanic ash in Horizon A reduces the grain density because amorphous silica particles in the ash have distinctly lower grain densities than other sedimentary components like quartz, feldspar and clay minerals. Sediments from the interval of Horizon A do not show higher porosity values than the surrounding sediments. The distinctly larger grain size of the ash-rich sediments, however, implies a different packing structure and possibly higher

*In-Situ Sampling and Characterization of Naturally Occurring Marine Methane Hydrate Using the D/V JOIDES Resolution.*

permeability in these intervals, which suggests that Horizon A is a potential fluid migration conduit.

Organic geochemistry measurements on gases remaining in cores from Site 1248 reveal high methane contents throughout. In addition to the high methane levels, there is a surprising variation in ethane content with depth.  $C_1/C_2$  is  $<1,000$  near the seafloor, increasing to 10,000 near the base of the gas hydrate stability zone (GHSZ), then decreasing sharply below the BSR. In addition to ethane, propane ( $C_3$ ) is present in relatively high concentrations in the upper 120 mbsf, and is even more abundant in headspace gas below that depth. The gas analyses at Site 1248 reflect the complex mixing of gases from two hydrocarbon sources. Mixed microbial and thermogenic gases occur in the uppermost 40 mbsf followed downhole by an intermediate interval ( $\sim 40$  to  $\sim 100$  mbsf) dominated by microbial gas. Mixed microbial and thermogenic gas also occurs in the deepest sediments at Site 1248 (below 100 mbsf), with thermogenic gas possibly being injected at Horizon A at  $\sim 130$  mbsf. The data thus suggest rapid advection of deeper gas to the seafloor, bypassing the lower part of the GHSZ.

Analyses of gases from a few dissociated hydrate samples from the shallow zone above 40 mbsf showed that while methane occupies most of the water cages of the hydrate structure, higher hydrocarbons are also present. Gas hydrates at Site 1248 are probably primarily Structure I hydrate that incorporate ethane molecules within their cage structure. However, in Sample 204-1248C-2H, 0-10 cm, from 7.37 mbsf, a higher concentration of propane than ethane suggests that Hydrate Structure II is present. Although thermogenic Structure II gas hydrates are common in petroleum provinces such as the Gulf of Mexico and the Caspian Sea, this hydrate type was not known from Hydrate Ridge prior to ODP Leg 204.

Interstitial water geochemistry results clearly show the influence of gas hydrate formation at Site 1248. Based on the chloride distribution in the pore water, the presence of hydrate is suggested from the seafloor to the BSR at 115 mbsf. The data indicate 25% gas hydrate content in the pore space of the uppermost 20 mbsf, whereas LDW resistivity data indicate up to 50% occupancy due to gas hydrates. Below 20 mbsf, gas hydrate content calculated from chloride anomalies ranges from 2-5% pore volume saturation. This pattern of chloride distribution is well documented by direct gas hydrate sampling and by the hydrate-related fabrics observed by the sedimentologists at this site. Soupy and mousse-like textures occur predominantly in silty clay and diatom-bearing silty clay after dissociation of hydrates. These were particularly common in the uppermost 20 mbsf. At these depths more massive gas hydrate samples were recovered, whereas further downcore small nuggets and thin veins of hydrate were sampled. The samples were identified by thermal IR data imaging of cores on the catwalk using a hand-held IR camera. Post-acquisition processing of the IR data shows a principal correlation to the pore-volume saturation derived by LDW resistivity logs, the chloride pore water data, and the sedimentological observations of the occurrence of dissociated hydrate layers.

*In-Situ Sampling and Characterization of Naturally Occurring Marine Methane Hydrate Using the D/V JOIDES Resolution.*

High advective flow rates in the uppermost 20 mbsf of the sediments drilled at Site 1248 are indicated by several findings. Sulfate concentrations were near zero even in the shallowest pore water sample implying a high methane flux from below that feeds microbial anaerobic methane oxidation (AMO). By consuming the near-seafloor sulfate, a consortium of bacteria and Archaea is responsible for AMO close to the seafloor during which millimolar quantities of dissolved sulfide are created. High sulfide concentrations were found within the the uppermost core. In addition, authigenic carbonates that were described in the cores are probably caused by higher dissolved carbon dioxide production, which is another result of higher AMO rates. High interstitial alkalinity throughout the cores provides further evidence for carbonate precipitation.

Temperature measurements from downhole tools (3 APCT, 1 DVTP and 2 DVTP-P runs) were used to calculate a temperature gradient of  $0.038^{\circ}\text{C}/\text{m}$ , considerably lower than expected. However, if 2 outlier measurements are excluded the gradient is  $0.055^{\circ}\text{C}/\text{m}$ , identical to the gradient determined from 9 measurements at Site 1245. This temperature gradient predicts the base of the GHSZ at 130 mbsf, assuming methane and standard mean seawater for the calculation. This is 15 m deeper than indicated by the seismic and LWD data and is consistent with a general pattern of greater mismatch between measured *in situ* temperature and BSR depth near the summit of Hydrate Ridge, the cause of which has not yet been determined.

In summary, gas hydrate is present throughout the sediment column from the seafloor to the BSR at Site 1248 as documented by IR imaging, LWD data, chloride anomalies in the pore water, analyses of sedimentary fabric and direct sampling of gas hydrates in a couple of intervals. The Holocene to Pleistocene sediments drilled here indicate strong advective fluid flow near the summit of southern Hydrate Ridge. There is abundant hydrate in near-surface sediments and no sulfate in the shallowest interstitial water samples collected at Site 1248, clearly indicating active flow of methane-bearing fluids. Authigenic carbonate formation occurs close to the seafloor, probably induced by anaerobic methane oxidation. The occurrence of authigenic carbonate as well as gas hydrate probably causes the high reflectivity that was mapped during deep-tow sidescan sonar survey of the seafloor. Advective flow is also indicated by the shallow occurrence of thermogenic hydrocarbons mixed with microbial gases. Gases obtained from dissociation of a shallow gas hydrate sample revealed a higher concentration of propane than ethane ( $\text{C}_3 > \text{C}_2$ ) in addition to methane. Such a gas composition should form Structure II hydrate, although we were not able to confirm this on board. Structure II gas hydrate is well known from petroleum basins like the Gulf of Mexico, although this is the first indication of Structure II hydrate along an accretionary margin.

## ODP Site 1249

### Principal Scientific Results

Based on visual observations, smear-slide analyses, physical property measurements, seismic stratigraphy and logging data, the sediments at Site 1249 were divided into 3 lithostratigraphic Units. Each of the three units is known from other sites on the western flank of Hydrate Ridge (Sites 1250, 1248, 1247 and 1245), and a good correlation exists between the sites. Due to poor core recovery resulting at least in part from the presence of massive hydrate at Site 1249, lithostratigraphic Units I and II at this site were combined into a single unit, referred to as Unit I-II. This unit, of Holocene to Early Pleistocene age, is composed of clay and silty clay with varying biogenic components and lithology that changes from nannofossil-bearing to diatom-bearing and diatom-rich. Lithostratigraphic Unit III, of Early Pleistocene age, has similar lithologies to Unit I-II. The upper boundary of Unit III with Unit I-II is defined by the occurrence of visible turbidites in the cores, an increase in grain size, a slight increase in calcareous components, and a slight decrease in biogenic opal. The boundary between these lithostratigraphic units, which varies in depth among the holes from 51 to 59 mbsf, is coincident with seismic Horizon Y, which is interpreted to be a regional angular unconformity.

Site 1249 was the site where the highest concentration of gas hydrates was observed, and a large amount of whole-round sampling was conducted. Massive hydrates pieces were recovered in the uppermost two cores. Due to interbedding of layer up to several cm thick of pure gas hydrate layer with soft sediment, cores disturbance was great and most of the original gas hydrate fabrics were probably not preserved. Soupy and mousse-like textures, probably related to gas hydrate presence were observed by the sedimentologists. Soupy textures can result from the dissociation of massive gas hydrate, a process that releases a considerable amount of water into the sediment. Mousse-like textures result from the dissociation of disseminated gas hydrates in fine-grained sediments. Temperature anomaly profiles from the catwalk-track IR camera support this generalized model for gas hydrate distribution. Downhole gas hydrate presence can also be inferred from LWD resistivity data, and the Archie relationship between resistivity and porosity implies gas hydrate saturations in the pore space at Site 1249 that range from 10% to 92%.

Shipboard analysis of downhole temperatures using conventional techniques results in considerable scatter in the data. The data indicate a relatively low temperature gradient of 0.047-0.051 and predict a depth to the base of the gas hydrate stability zone that is 20 m deeper than the BSR. The explanation for this discrepancy has not yet been explained. One possible factor is that thermal conductivities measured on core samples are not representative of in situ thermal conductivity when large concentrations of hydrate are present in situ. Preliminary examination of the data suggests that the raw data recorded by the temperature probes can be inverted to determine in situ thermal conductivity and

that the in situ thermal conductivities are indicative of variable, and in some cases large, concentrations of gas hydrate.

Investigations of the interstitial water composition at Site 1249 show the signature of gas hydrate formation in several ways, and these data will be used post-cruise to determine rates of hydrate formation. Pore fluids recovered from the upper 20 mbsf show pronounced enrichment in dissolved chloride concentration. The highest chloride concentration was 1368 mM in a dry-looking sediment. Formation of such a brine is only possible in a system in which the rate of gas hydrate formation exceeds the rate at which excess salts can be removed by diffusion and/or advection. Small negative anomalies below 10 mbsf were also found due to the freshening effect on pore water of hydrate dissociation during recovery. The presence of brines in the upper 20 mbsf is also reflected by the concentration of other dissolved species such as  $\text{Na}^+$ ,  $\text{K}^+$ ,  $\text{Ba}^{2+}$ ,  $\text{Sr}^{2+}$ , and  $\text{Mg}^{2+}$  because these ions are excluded from the hydrate structure and enriched in the residual pore water. Superimposed on the enrichment due to brine formation is the effect of rapid advection of fluids that have been formed at deeper depth and modified by chemical processes occurring in near-surface sediments.

In comparison to other sites, headspace samples at Site 1249 showed extremely high methane contents. These large quantities of gas can only be caused by the presence of gas hydrate in the headspace samples. Ethane and propane are also present in high concentrations, and enrichment of these gases at shallow depth reflect the presence of migrated thermogenic hydrocarbons. This is consistent with the observations of active gas venting at this location. Gases from several decomposed hydrate specimens were analyzed and showed that some of the hydrates contained propane and butane, suggesting the presence of Structure II hydrate.

In order to determine in situ methane concentrations, PCS cores were successfully obtained at 14, 34 and 72 mbsf. The degassing experiments revealed concentrations from 215.7 to 5,033.9 mM, which are above methane saturation at in situ temperature and pressure conditions, providing additional evidence for the presence of gas hydrates. For the deepest core, at 72 mbsf, a gas hydrate concentration is estimated to be 2.2 % of the pore volume. Shallow samples show higher concentrations of 7-34% and 60-76 % gas hydrate in the pore space at 34 and 14 mbsf, respectively.

One of the highlights of Site 1249 was the success of the new HYACINTH pressure sampling tools at recovering hydrate-bearing cores at in situ pressures. HRC and FPC cores from 14 mbsf (Core 204-1249G-2E and Core 204-1249H-2Y) both recovered high concentrations of gas hydrate. Cores were retrieved and successfully transferred under in situ pressure to a storage chamber and then logged. In multiple gamma density logs, both cores showed a spectacular interlayering of sediments with low-density layers revealing densities slightly lower than 1 g/cm<sup>3</sup>. Since pure methane hydrate has a density of ~0.92 g/cm<sup>3</sup> we interpret these low density layers to be relatively pure hydrate layers. In addition, a low density spike (0.75 g/cm<sup>3</sup>) in a 8 cm-thick gas hydrate layer indicates the

*In-Situ Sampling and Characterization of Naturally Occurring Marine Methane Hydrate Using the D/V JOIDES Resolution.*

presence of free gas. The presence of free gas within gas hydrate samples had been postulated from the porous structure of seafloor samples from Hydrate Ridge and from gas release observations during TV-grab sampling. A second indicator of free gas came from the HRC core. A small explosion pushed gas hydrate and sediment interlayers out of the liner from two intervals while the core was being transferred from the pressure vessel to liquid nitrogen. This sudden gas release can only be explained by the expansion of small volumes of free gas that existed in situ within the gas hydrate layer.

In summary, Holocene to Early Pleistocene sediments of Lithostratigraphic Units I-II and II at Site 1249 are well correlated with other sites along the western flank of southern Hydrate Ridge. Site 1249 was cored to a depth of 90 mbsf; thus this entire sequence lies within the gas hydrate stability zone and large quantities of gas hydrates were sampled. Unfortunately core recovery at this site was limited because of the presence of massive hydrate close to the seafloor. Rapid growing of massive hydrates in the uppermost 20 mbsf induces a brine formation, which leads to chloride values in the interstitial water of up to 1368 mM. This is the greatest chloride enrichment due to hydrate ever found to date. Degassing of the PCS from Core 204-1249F-4P revealed 95 L gas, which is the greatest volume of gas ever measured with the PCS. Based on the methane in situ concentration of 5,034 M from this PCS, the gas hydrate concentration was estimated to be 60-70% of the pore volume. Further highlights were the first density measurements from gas hydrates under in situ conditions using the HYACINTH pressure coring and laboratory transfer systems. These cores showed direct evidence for free gas within gas hydrate layers 13 mbsf on southern Hydrate Ridge. The coexistence of free gas and gas hydrates well within the hydrate stability zone is only possible when no water is available for further hydrate formation.

### **ODP Site 1250**

#### *Principal Scientific Results*

On the basis of visual sediment descriptions, physical property measurements, Logging-While-Drilling data and seismic correlation, the sedimentary sequence at Site 1250 was divided into three lithostratigraphic units. Lithostratigraphic Unit I, of Holocene to Late Pleistocene age, extends from the seafloor to 9.5 mbsf and is mainly composed of dark-greenish gray clay or silty clay, which is generally diatom-bearing or diatom-rich. Lithostratigraphic Unit II (9.5-14 mbsf), of Late Pleistocene age, is principally composed of similar lithologies as Unit I, but these are intercalated with thin silt and fine sand layers which are not found in Unit I. Based on their appearance, these multiple layers of coarser grain-size are clearly single events that have been rapidly deposited from turbidity currents. Lithostratigraphic Unit III, from 14 to 181 mbsf, consists of silty clay that is nanofossil-rich or diatom-rich, with an age range of Late Pleistocene to Early Pliocene.

*In-Situ Sampling and Characterization of Naturally Occurring Marine Methane Hydrate Using the D/V JOIDES Resolution.*

The boundary between Lithostratigraphic Units II and III is correlated with Horizon Y, a seismic reflector that corresponds to a regional stratigraphic unconformity identified in the 3-D seismic data. This boundary is well defined by a 6-m-thick sequence of coarse-grained, high-frequency thin turbidite layers that includes individual sand layers up to 20 cm-thick. Logging-While-Drilling data recorded a high density peak around seismic Horizon Y, which was confirmed by shipboard physical property measurements. Shipboard MST-data reveal, in addition, a large positive excursion of magnetic susceptibility caused by a higher content of magnetic minerals within the sand layers at the boundary between Lithostratigraphic Units II and III.

Lithostratigraphic Unit III at Site 1250 is divided in two Subunits. Subunit IIIA includes several mass wasting deposits, of which a debris-flow layer between 86.5 and 100 mbsf was the most pronounced example. This deposit was characterized by the occurrence of mud clasts up to 5 cm in diameter and several soft sediment deformation features. Subunit IIIB has a distinctly higher abundance of calcareous nannofossils and foraminifers than Subunit IIIA. The boundary between the stratigraphic Subunits IIIA and IIIB is marked by several light-colored ash-rich layers, which are composed of volcanic glass-rich silt to silty volcanic ash, typically a few cm-thick. This ash-rich interval is well defined in the LWD data by a low-density anomaly and corresponds to the regional seismic reflector known as Horizon A. Physical property measurements on discrete samples at Site 1250 revealed low grain densities in this depth interval, which are explained by the low grain density of the amorphous silicate components of the ash. However, this provides only a partial explanation for the low density values and high resistivity values found in the LDW data, and free gas is probably present at Horizon A. The vertical VSP indicates a drop in P-wave velocity associated with this horizon, which also suggests free gas.

Infrared (IR) imaging of the cores at Site 1250 enabled the on-catwalk identification of gas hydrates, and 20 samples were taken which are thought to contain hydrate based on their temperature anomaly. IR-track imaging revealed 40 temperature anomalies between 14 and 109 mbsf in Hole 1250C and 57 anomalies between 6 and 113 mbsf in Hole 1250D. The depth range of the cold temperature anomalies correlates well with the depth distribution of mousse-like and soupy textures observed by the sedimentologists during core description. The lowermost gas hydrate piece was sampled in Hole 1250F at 100.23 mbsf, which is slightly above the base of the GHSZ at 114 mbsf as defined in the P-wave sonic log.

Chloride concentrations in the pore water at Site 1250 document the different geochemical processes linked to the presence of gas hydrates. In the upper 50 mbsf, an enrichment in dissolved chloride shows the in situ effect of rapid and recent gas hydrate formation. Due to hydrate formation, dissolved ions are excluded from the hydrate structure and become enriched in the residual pore fluids. The fact that we observe this enrichment means that the rate of hydrate formation exceeds the rate at which excess salts can be removed by diffusion and/or advection. Below 50 mbsf, the chloride shows a

*In-Situ Sampling and Characterization of Naturally Occurring Marine Methane Hydrate Using the D/V JOIDES Resolution.*

gently-sloping baseline toward fresher chloride values. Using this baseline curve, the negative chloride anomalies were used to calculate the amount of gas hydrate responsible for the dilution of each sample. The peak amounts are up to 15% gas hydrate filling of the available pore space with average values ranging from 0 to 6%.

The presence of a high concentration of gas hydrate in the uppermost 10 mbsf had been predicted prior to sampling based on a large LWD resistivity peak. To substantiate both these results and the chloride data, a variety of specimens of gas hydrate were collected from the uppermost 35 mbsf. The hydrate samples show a wide range of morphologies, ranging from massive to nodular, and are often embedded in soupy sediments, which are interpreted to result from decomposition of disseminated hydrate and fluidization of the sediment by hydrate water.

Analyses of other elements in the interstitial waters document that Site 1250 is in a seafloor environment that is strongly influenced by seepage. Sulfate concentrations are zero in the shallowest sample because of the upward flux of methane and anaerobic methane oxidation. In addition, alkalinity is anomalously high in the upper tens of meters reflecting fluid advection. Authigenic carbonate formation is documented by discrete carbonate samples close to the seafloor.

Analyses of gas sampled in cores at Site 1250 show high methane content throughout with no decrease close to the seafloor. This is in agreement with the lack of sulfate in the pore water and the high advection rates. Void gas samples show that the ethane content is also relatively high, and there is a hydrocarbon enrichment ( $C_3$ - $C_5$ ) close to the seafloor that indicates lateral migration of wet gas hydrocarbons coming from a deeper source. A distinct increase in ethane at 102-107 mbsf, beneath the gas hydrate stability zone, could be due to release of ethane from decomposed gas hydrate. An increase in propane and n-butane is probably due to migration of hydrocarbons from deeper depths.

Migration of fluids from deeper is also indicated by interstitial water geochemistry, which shows increasing lithium concentrations with depth. This is believed to reflect the diagenetic remobilization of lithium deeper in the accretionary wedge. Superimposed on the downhole linear increase in lithium is a peak in the sediments around seismic reflector Horizon A, indicating focused fluid transport along this zone associated with seismic Horizon A.

In order to obtain in situ gas concentrations and to determine whether methane is saturated under in situ conditions, the Pressure Core Sampler (PCS) was deployed successfully five times. Three PCS deployments above the BSR show concentrations clearly above methane saturation, which predicts gas hydrate concentrations of 0.6-2.2% within the pore volume of the cores. Gas concentrations in the PCS from the deployments below the BSR show that, based on the solubility curve, one sample (Core 204-1250F-4P) taken 7.5 m below the BSR had free gas which should approximately occupy 50% of the available pore space. The second sample (Core 204-1250D-18P) from ~24 m below

*In-Situ Sampling and Characterization of Naturally Occurring Marine Methane Hydrate Using the D/V JOIDES Resolution.*

the BSR had a gas concentration below saturation, which would exist as dissolved gas under in situ conditions.

At Site 1250, there were nine APC temperature measurements made. These data were used to calculate a temperature gradient of  $0.049^{\circ}\text{C}/\text{m}$ , which is lower than expected and predicts the base of the GHSZ at 138 mbsf, assuming methane and standard mean seawater for the calculation. This is 26 m deeper than the level of the GHSZ indicated by the seismic and LWD data and is consistent with a general pattern of greater mismatch between measured in situ temperature and BSR depth near the summit of Hydrate Ridge. The cause of this discrepancy is yet not known.

In summary, hemipelagic fine-grained sediments interbedded with turbidites at Site 1250 are Quaternary in age (younger than 1.6 Ma) and contain gas hydrates in varying amounts. Based on chloride anomalies in interstitial water samples and on PCS in situ gas concentration measurements and calculations, the concentrations of hydrate are estimated to be between <1% to a few % of the pore space. Much higher concentrations of hydrates near the seafloor are indicated by LWD resistivity data and direct sampling. Positive chloride anomalies in the pore water in the upper 40 mbsf reveal rapid and active formation of gas hydrates during recent times. High methane concentration, no sulfate, high alkalinity and carbonate diagenesis in the uppermost sediments also document high advection rates of fluid migration, similar to what was observed at the other seep-related sites (Site 1248 and Site 1249). The presence of free gas just below the BSR is documented by the concentrations of methane well above in situ solubility found in a PCS core from below the BSR and by sonic log P-wave data.

### **ODP Site 1251**

#### *Principal scientific results*

Based on the major and minor lithologies and additional criteria like fabric, physical properties, microscopic, chemical and XRD analysis, the hemipelagic strata and turbidite sequences recovered at Site 1251 were divided in three lithostratigraphic units. Lithostratigraphic Unit I, subdivided into three subunits, extends from the seafloor to 130 mbsf and is characterized dominantly by dark greenish gray clay to silty clay ranging from Holocene to Pleistocene age (0 to ~0.3 Ma). Clay and silty clay, some of which is diatom-bearing, is interlayered with several coarse-grained high-frequency turbidites (Subunit IA; 0-23 mbsf). Subunit IB (23-34 mbsf) is characterized by unsorted pebble-sized mudclasts in a clay matrix and a series of soft-sediment deformation fabrics representing a debris flow unit. This unit can be traced regionally based on its chaotic character in seismic reflection records and reaches a maximum thickness of ~70 m in the center of the slope basin. Stratified diatom-bearing silty clays comprise Subunit IC (34-130 mbsf), which shows clear seismic stratification. The base of Subunit IC is defined to correspond to a prominent angular unconformity imaged in the seismic data, although there is no apparent lithologic discontinuity at that boundary.

*In-Situ Sampling and Characterization of Naturally Occurring Marine Methane Hydrate Using the D/V JOIDES Resolution.*

Hemipelagic clays of Middle Pleistocene age, partly enriched in siliceous and calcareous biogenic components, form Lithostratigraphic Unit II (130-300 mbsf). Unit III (300-443 mbsf) consists of partly lithified clays that show a downcore transition to claystones. A distinct enrichment of green glauconite grains in a 120-cm-thick interval on top of Lithostratigraphic Unit III is probably associated with a major unconformity or period of very low sedimentation rate that is defined by biostratigraphic data to have lasted from 1.6 to 1.0 Ma. Between 320-370 mbsf, the sediments contain a greater amount of biogenic opal, which is well documented by smear slide estimates and XRD-analyses. Authigenic carbonates of various morphologies and mineralogical compositions as well as glauconite grains are scattered throughout this unit. Biostratigraphic investigations using diatoms and calcareous nannofossils assign these sediments to an Early Pleistocene and Late Pliocene age including the Pleistocene/Pliocene boundary around 375 mbsf.

Major downcore changes in physical property data are generally in agreement with seismic stratigraphy and lithostratigraphic boundaries. The uppermost sediments of Lithostratigraphic Units I and II are characterized by uniformly increasing bulk density values and follow a standard compaction curve. The generally increasing trend in both bulk densities from MST and in routine density measurements on discrete samples (MAD) is interrupted by a 50-m-thick sediment sequence between 320 and 370 mbsf in which the bulk densities drop significantly to lower values and porosity values increase. This change in physical properties is caused by higher amounts of biogenic opal-A, which is an amorphous silica component of low grain density and high skeleton porosity. Magnetic susceptibility values at Site 1251 are characterized by generally uniformly low values. Various high-amplitude MS peaks are correlated with either turbidites, enrichments of magnetic minerals resulting from low sedimentation rates or with diagenetic iron formation in certain horizons.

Thermal imaging of cores using the infrared (IR) cameras provided the best method of detecting intervals of hydrate occurrence in the cores at Site 1251, especially when the hydrate occurred in disseminated form. Discrete samples of hydrate were not seen in Hole 1251B, although several zones with cold anomalies have been identified. The IR temperature anomalies observed in Hole 1251B were relatively small ( $\Delta T = \sim 1-1.5^\circ\text{C}$ ) compared to an IR temperature anomaly ( $\Delta T = \sim 6^\circ\text{C}$ ) encountered at Hole 1251D between 190-197 mbsf, which coincides with an interval, from which samples thought to contain hydrate (on the basis of IR anomalies) were obtained and preserved in liquid nitrogen. The data thus indicate higher gas hydrate concentration just above the BSR, which agrees with the chloride data obtained from interstitial water measurements (see below). Due to low recovery of this interval, the BSR was not sampled in Hole 1251B. Small thermal anomalies between 40 and 200 mbsf are interpreted to be indicative of disseminated gas hydrate.

Interstitial water geochemistry at Site 1251 focused on hydrate-related changes in chlorinity pattern, changes in fluid composition in relation to dewatering of the sediments

*In-Situ Sampling and Characterization of Naturally Occurring Marine Methane Hydrate Using the D/V JOIDES Resolution.*

and biogeochemical processes within the sediments. Like in other accretionary wedges, the profile of dissolved chloride at Site 1251 decreases downcore from present seawater values close to the seafloor. At Site 1251 the chloride decrease in the interstitial water corresponds to an increase in dissolved lithium, revealing a fluid source from deeper sediments of the accretionary complex. The dissolved chloride distribution at Site 1251 shows only one distinct negative anomaly, seen in several samples taken just above the BSR from around 190-200 mbsf. This is consistent with the IR temperature and visual observations, indicating that hydrate occurs in this interval at Site 1251. Based on the lowest chloride value measured below an estimated background concentration, gas hydrate occupies up to 20% of the pore space in this zone just above the BSR. This finding is in contrast to all other sites drilled during the leg, where repeated excursions to low-chlorinity values record the presence of gas hydrate over much larger depth intervals above the BSR.

A number of different processes control whether methane reaches levels above saturation within the GHSZ. An important process controlling the methane distribution in the sediments at Site 1251 is methane consumption due to anaerobic methane oxidation using sulfate as an oxidant. Methane consumption or methane flux at the sulfate-methane interface (SMI) can be estimated from the sulfate and methane concentration gradients. At Site 1251 over half the sulfate being reduced is due to anaerobic methane oxidation. Sulfate depletion at the SMI at 4.5 mbsf also leads to higher concentrations of dissolved barium below the SMI.

High residual methane concentrations were measured in cores at Site 1251 using the headspace technique. These methane values increased rapidly below the level of sulfate depletion to minimum methane concentrations of 10 mM at a depth of 6 mbsf. In order to obtain more reliable *in-situ* gas concentrations, the Pressure Core Sampler (PCS) was deployed nine times. The PCS deployments revealed methane concentrations between 46.4 to 158.4 mM at depths between 20 and 290 mbsf. The methane concentration at 20 mbsf is compatible with the shallower headspace methane estimates, and provides the gradient from which the methane flux is calculated. Based on measured methane concentrations slightly above solubility, two PCS deployments within the GHSZ (at 45 and 104 mbsf) show evidence for gas above saturation, implying gas hydrate occurrence. Observations below the BSR are ambiguous. A PCS sample from 32 m below the BSR did not show gas concentration above solubility whereas one from 100 m below the BSR did.

Beside methane ( $C_1$ ), higher hydrocarbons like ethane ( $C_2$ ) ethylene ( $C_2^-$ ) and propane ( $C_3$ ) traces were also detected throughout the sequence cored at Site 1251. The composition of gas samples recovered from both expansion voids in the core liner and headspace measurements show a systematic change from high  $C_1/C_2$  ratios above the BSR at a depth of 196 mbsf at Site 1251, to lower ratios below that depth. This order-of-magnitude decrease in the  $C_1/C_2$  ratio is caused by an abrupt increase of ethane rather than by a change in methane concentration. This could be caused by ethane storage in gas

hydrates and a recycling process whereby ethane-enriched gas hydrates at the base of the GHSZ dissociate in response to subsidence of the slope basin and the resulting upward migration of the GHSZ through the sediment column. An alternative mechanism to explain these observations is that the GHSZ is a barrier to  $C_2$  migration. Additional analysis of the gas composition in hydrate samples from Leg 204 should permit us to distinguish between these two mechanisms.

Temperatures measurements obtained with 5 APCT runs and 3 DVTP-P deployments were used to calculate a linear temperature gradient of  $0.0575^\circ\text{C}/\text{m}$  at Site 1251, which is very similar to temperature profiles from other sites on Hydrate Ridge. Extrapolating laboratory measurements of gas hydrate stability for pure methane in water of 3.5% salinity, this temperature gradient predicts that the base of the GHSZ is  $\sim 196$  mbsf, in excellent agreement with the calculated BSR depth of  $\sim 196$  mbsf determined from 3D-seismic reflection and OBS-derived seismic velocity data.

The recorded LWD data in the basin sediments east of Hydrate Ridge in Hole 1251A are of high quality. There is minimal reduction in vertical resolution due to the faster penetration rate during the collection of the data. Resistivity and density log variations indicate thin-bedded changes in lithologies throughout the hole below 130 mbsf, which most likely reflects the downhole occurrence of interbedded turbidites that were observed during core description. There is a little direct evidence for the presence of gas hydrate in the LWD-data, except for a suggestion in the resistivity data of hydrate at 90-110 mbsf and again immediately above the BSR. The Archie relation for estimating gas hydrate saturation from the resistivity log data implies gas hydrate saturation up to 18%. The resistivity data also indicate the presence of free gas extending for  $\sim 100$  m below the BSR. Borehole breakouts are well developed below 300 mbsf and indicate an east-west axis of compressive stress.

In summary, drilling at Site 1251 recovered a sequence of well-stratified hemipelagic sediments of the slope basin adjacent to Hydrate Ridge. Major lithostratigraphic units were characterized and are, in most cases, separated by clearly-defined unconformities in the seismic record. Thermal, sedimentological, geophysical and geochemical proxies for hydrate occurrence, as well as direct sampling, were used to document the presence and dynamics of gas hydrates in host sediments younger than 500,000 years old. At this site, significant hydrate accumulations seem to be limited to two intervals, 90-110 mbsf and just above the BSR at 190-200 mbsf. This contrasts with the hydrate distribution at the other sites cored during Leg 204, where hydrate is found throughout most of the hydrate stability zone.

## ODP Site 1252

### *Principal scientific results*

Although this site showed evidence for only very limited occurrences of gas hydrate, it was very interesting in that it showed very clear correlations between lithostratigraphic observations, physical properties measurement and wireline logging results throughout. It was the first site to show significant postdepositional carbonate formation beneath the upper 10s of meters.

Based on the major and minor lithologies and additional criteria like fabric, physical properties and microscopic analysis, the sediments recovered at Site 1252 were divided in three lithostratigraphic units. Lithostratigraphic Unit I, subdivided into three subunits, extends from the seafloor to 96.5 mbsf and is dominated by dark greenish gray clay to silty clay ranging in age from 0 to ~0.3 Ma. Unit IA is characterized by strong negative density gradient in the MST data which probably results from the onset of gas exsolution at ~7 mbsf. The lower boundary of Unit I is defined by the same unconformity that was sampled at a depth of 130 mbsf at Site 1251. At both sites, this unconformity is clearly seen in seismic data and is compatible with biostratigraphic data, but does not have a striking lithological signature. At Site 1252, it is overlain by an apparent debris flow called Unit ID, the top of which corresponds to a strong anomaly in magnetic susceptibility. Unit ID pinches out just west of Site 1251. In contrast, a debris flow that comprises Unit IB at Site 1251 is not present at Site 1252. Unit IC at both sites is strikingly similar both in its lithologic description and in its seismic reflection character.

Unit II at Site 1252 is a dark green foraminifer-rich silty clay that is intercalated with lighter-colored layers of fine sand and coarse silt turbidite layers. These thin turbidites result in a nearly continuous zone of high magnetic susceptibility. In contrast to Site 1251, where Unit II is approximately 180 m-thick, Unit II at Site 1252 is only about 20 m thick. This is due primarily to the location of this site where Unit II laps onto the west flank of uplifted "accretionary complex" sediments. Units IB/C through Unit II are characterized by a normal increase in density and decrease in porosity with depth that is probably caused by sediment compaction.

The boundary between Unit II and Unit III is marked by a 5 m-thick series of glauconite-rich sands, including a 2 cm-thick layer of almost pure glauconite sand. This is underlain by a layer of authigenic carbonate that required a transition from APC to XCB coring at 125 mbsf. Wireline density, resistivity and chemical (uranium and potassium contents) logs all show very high values over ~6 meters at this depth, consistent with extensive carbonate precipitation that forms concretions and cement. This boundary corresponds closely with the top of the uplifted "accretionary complex" sediments in the core of the anticline/diapir and is referred to as Unit IIIA. It is underlain, from 210 mbsf to the base of the hole at 260 mbsf, by Unit IIIB, distinguished from Unit IIIA by an increase in biogenic opal and a decrease in silt. Biostratigraphic age of Unit III is 1.6 to > 2 Ma.

*In-Situ Sampling and Characterization of Naturally Occurring Marine Methane Hydrate Using the D/V JOIDES Resolution.*

The density profile of Unit III is unusual. Physical properties measurements (MST gamma logs and MAD bulk density) indicate that the density decreases by 0.2 g/cm<sup>3</sup> (from 1.8 g/cm<sup>3</sup> to 1.6 g/cm<sup>3</sup>) over a distance of ~25 m below the carbonate-rich zone and then is variable but with an average value of about 1.7 g/cm<sup>3</sup> and no systematic increase until the base of the hole at 260 mbsf. The wireline density logs show similar behavior, with a local increase to nearly 2.0 g/cm<sup>3</sup> in the carbonate layers underlain by a nearly constant density of 1.7 g/cm<sup>3</sup> with occasional thin (~2 m-thick) low density (~1.5 g/cm<sup>3</sup>) excursions. This anomalous density profile, similar to but better defined than what was observed in lower part of the section at Sites 1244 and 1251 suggests that diapirism driven by this density difference should be considered as a possible mechanism contributing to the tectonic evolution of the accretionary prism.

Thermal imaging of cores using the infrared (IR) cameras indicated only very limited hydrate occurrence at Site 1252. Two possible hydrate samples were preserved from depths of 83 (in Unit ID) and 99 mbsf (in Unit II). The chloride concentration in the interstitial pore water and the C1/C2 ratios in void-space gas samples also did not show anomalies indicative of dissociated hydrate, unlike what was observed at other sites (see, for example, discussion of Site 1247). In contrast, Unit IIIA showed several examples of "classic" moussy and soupy texture in cores recovered from above the base of the gas hydrate stability zone. A sample of the soupy sediment was taken for post-cruise chloride analysis.

The chloride profile shows a general decrease with depth similar to that observed at Sites 1244 and 1251 and attributed to diffusion or slow advection of fresher pore waters generated by dewatering of sediments deeper in the accretionary complex. A closer look at the chloride profile suggests segments of different slope that can be roughly correlated with lithologic boundaries, suggesting lithologic control on permeability.

The thermal gradient of 0.059 measured at Site 1252 is similar to the gradients of 0.057 oC/m measured at Site 1251 and 0.058 oC/m measured at Site 1244 and predicts the base of gas hydrate stability at 170 mbsf, consistent with the estimate of 170 mbsf obtained by projecting the BSR observed in the core of the anticline laterally by 200 m.

In summary, Site 1252 provided the best sampling of the older (> 1.65 Ma) sediments that comprise the uppermost part of the seismically incoherent facies referred to as the "accretionary complex." This zone is characterized by a density inversion relative to the base of the overlying slope basins and an anomalous density versus depth profile. This observation suggests that gravitational instability should be considered and modeled as a possible driving force contributing to the evolution of forearc structure here. The data from this site also reinforce previous observations that the accretionary complex is characterized by low chlorinity interstitial waters and is relatively permeable. Although this site yielded little direct evidence of gas hydrate, sediment textures and limited IR

thermal anomalies indicate that some hydrate was present, even though no BSR is observed at this site.

## CONCLUSION

The primary accomplishment of the JOI Cooperative Agreement with DOE/NETL in this quarter was the deployment of tools and measurement systems on ODP Leg 204, to characterize and investigate gas hydrate deposits on Hydrate Ridge, offshore Oregon from July to September 2002.

Leg 204 was originally scheduled to begin in San Francisco, California and end in San Diego. Due to an impending West Coast dock strike both port calls were ultimately moved to Victoria, B. C. Leg 204 officially began with the first line ashore Westcan Terminal B at 0655 hrs 7 July 2002.

In many ways the leg turned out to be extraordinary. All science objectives were successfully achieved during the course of drilling/coring the 7 primary sites. In addition, 2 alternate sites were also successfully cored. Finally, a series of additional holes were cored at the crest of Hydrate Ridge (Site 1249) specifically geared toward the rapid recovery and preservation of hydrate samples as part of a hydrate geriatric study funded by the Department of Energy (DOE). This was yet another example of ODP/TAMU flexibility and responsiveness as well as a demonstrated ability to orchestrate and/or respond to interagency cooperative efforts. Bulleted highlights of the leg are shown below followed by a more descriptive discussion.

### Summary of Leg 204 Gas Hydrate Coring

- The leg was planned as a 59.4 day leg – ended up as 57.1 day leg
- 50.4 days (88.3%) of time was spent on-site operating; 6.7 days (11.7%) in port/transit
- A record 23 moves were made using dynamic positioning totaling 29 NMI (43.8 hours)
- 3 positioning beacons were used – successfully deployed and recovered 21 times
- Plan included 23 holes at 7 sites – ultimately 45 holes were drilled/cored at 9 sites
- Water depths ranged from 788.5 mbrf to 1228.0 mbrf
- Penetration depths varied from 9.5 to 540.3 mbsf
- 8 of 9 sites drilled using LWD (resistivity at bit, NMR, density/neutron) technology
- 11 holes were drilled using a tricone bit for LWD/RAB-8 or wire line logging
- 33 holes were cored with the APC and/or XCB coring systems; 1 hole was RCB cored
- Over all 3674.5 meters were cored and 3068.3 meters or 83.5% were recovered
- 9 rendezvous took place during the leg using 7 helicopters and 2 supply boats
- 42 personnel were exchanged on/off the ship - these included an engineer from DOE National Technology Laboratory and a drilling engineer from ChevronTexaco
- Series of holes at end of leg were dedicated to the rapid recovery and preservation of hydrate samples as part of a hydrate geriatric study co-funded by the NSF and DOE
- 50 meters of hydrate core recovered/stored under pressure in a methane environment
- 35 meters of additional samples recovered/stored in 6 liquid nitrogen dewars
- Cores scanned for hydrate “cold spots” with track mounted infrared camera

*In-Situ Sampling and Characterization of Naturally Occurring Marine Methane Hydrate Using the D/V JOIDES Resolution.*

- Some cores also processed through linear x-ray machine from Lawrence-Berkley NEL

#### Summary of Leg 204 Special Tools Deployments

- 30 out of 39 successful runs with the TAMU Pressure Core Sampler (PCS)
- 16 out of 16 successful runs with Davis-Villinger Temperature Tool w/Pressure
- 8 out of 8 successful runs with Davis-Villinger Temperature Tool (DVTP)
- 61 out of 61 successful runs with the TAMU Advanced Piston Corer Temperature Tool
- 107 of 110 successful runs with Temp/Pressure/Conductivity (TPC) “Methane” Tool
- 1 out of 2 successful deployments of the Fugro-McClelland Piezoprobe
- 2 of 10 cores recovered w/pressure using Hyacinth Fugro Pressure Corer (FPC)
- 4 of 8 cores recovered under pressure using the Hyace Rotary Corer (HRC)
- 28 runs with LDEO Drill String Accelerometer (DSA) tool; 17+ all/partially successful
- 8 of 8 cores successfully recovered using the RAB-8 logging-while-coring technology
- Whirlpak glass micro-beads and Perfluorocarbon tracers (PFT’s) used on 85 cores

Leg 204 operations were not only complicated with all of the special tool deployments and rendezvous scheduled. Operations on the Southern Hydrate Ridge also required continual coordination with several other oceanographic research vessels. The R/V *Sonne*, a German research vessel, operated in the same area deploying and recovering instrumented sea floor landers. The R/V *Ewing*, from LDEO, worked in conjunction with the *Resolution* conducting 2-ship seismic operations and also conducted independent research including the setting of OBS packages on the sea floor. The R/V *Atlantis*, from Woods Hole Oceanographic Institution (WHOI), was on-site for 4-days of Alvin diving at the ridge crest. And finally, the *New Horizon*, a Scripps Institution of Oceanography (SIO) vessel, was on-location briefly doing independent oceanographic research work.

The first part of Leg 204 was dedicated to logging-while-drilling (LWD) to identify regions of rapid change in physical properties prior to coring. This permitted the optimization of special tools to measure in situ temperature and pressure and to retrieve cores at in situ pressure.

The leg also included a two-ship seismic program conducted in conjunction with the R/V *Ewing* to acquire vertical, constant offset, and walkaway vertical seismic profiles (VSP). A new Schlumberger tool called the Vertical Seismic Imager (VSI) was used for most of the VSP work whereas the older Well Seismic Tool (WST) was used for the remaining holes. Deployment of the VSI tool was problematic because of its more fragile construction and because the tool is not designed to have the electric line slacked off during the data acquisition period. None-the-less the tool worked well enough to fully achieve the seismic objectives.

Eight of the sites were drilled using LWD technology. A developmental logging-while-coring (LWC) system jointly developed by Lamont-Dougherty Earth Observatory

*In-Situ Sampling and Characterization of Naturally Occurring Marine Methane Hydrate Using the D/V JOIDES Resolution.*

(LDEO), Anadrill, and Texas A & M University (TAMU) was also successfully tested using a Resistance-At-Bit (RAB-8) LWD tool. This marked the first time ever that core samples have been recovered simultaneously with LWD data.

Several other specialized tools developed all or in part by TAMU were successfully deployed during the leg. These include the Pressure Core Sampler (PCS), Methane Tool (MT), Advanced Piston Corer Temperature (APCT) shoe, Davis-Villinger Temperature Probe (DVTP), and the Davis-Villinger Temperature Probe with pressure (DVTPP).

Two other developmental pressure-coring systems developed by the European consortium referred to as Hyacinth were deployed. These tools were designed to allow transfer of a pressurized core sample from the down hole tools autoclave chamber to a pressurized logging chamber. The Fugro Pressure Corer (FPC) and Hyace Rotary Corer (HRC) were deployed 10 times and 8 times respectively. Two runs with the FPC and 4 runs with the HRC successfully recovered core at or near in situ pressure. Functionally the pressurized core transfer and logging chambers worked well although some tolerance variations with the FPC made the transferring the FPC cores more problematic.

Prior to the leg TAMU worked with Fugro-McClelland on the adaptation of their Piezoprobe tool to the ODP/TAMU bottom hole assembly (BHA). This tool was deployed twice on the first site with the second attempt fully successful. Data from this electric line deployed tool will be compared to DVTPP data. The DVTPP tool is deployed in a much faster and simpler fashion by being free fall deployed and then recovered using the standard ODP coring line.

LDEO deployed their Drill String Accelerometer (DSA) tool to gather down hole data in support of the Hyacinth tool deployments and also as part of an experimental study using the Advanced Piston Corer (APC) as an energy source. The APC impact energy was recorded using Ocean Bottom Seismic (OBS) stations placed on the sea floor earlier by the R/V Ewing. Initial results indicated that this experiment was successful and that useful data was obtained.

While the scientific and operational achievements were impressive the leg was extremely demanding because of the confined operating area. All 9 drill sites were located within 3.6 nmi of each other. Due to the close proximity of the sites all moves between sites were done using the ship's dynamic positioning system. Because of the commonality of the coring BHA's to be used, most of these moves were made with the pipe suspended below the ship. When a BHA change or bit replacement was required the move was made simultaneously with the pipe trip to/from the surface. With no transit time other than traveling to and from port, and limited pipe trips between sites, the operating time available for drilling and coring was considerable. For the 57.1 day leg 50.4 days or 88.3 % of the available time was spent on-site. The remaining 6.7 days were spent in port (4.14 days) and underway (2.54 days).

*In-Situ Sampling and Characterization of Naturally Occurring Marine Methane Hydrate Using the D/V JOIDES Resolution.*

Leg 204 operations were confined to an area located ~50 nmi off the coast of Oregon. The close proximity of land meant that this leg was a candidate for numerous changes of personnel and equipment. An initial supply boat rendezvous was planned to allow removal of specialized, and expensive, VSP equipment along with an Anadrill VSP engineer. This soon grew to include numerous other personnel changes via helicopter and another supply boat bringing out special pressure vessels, dewars, and liquid nitrogen to support the add-on effort to recover and preserve the additional hydrate samples. Ultimately there were a total of 9 rendezvous completed with the *JOIDES Resolution* including 7 helicopters and 2 supply vessels. Leg 204 officially ended at 0900 hours 2 September 2002 with the first line ashore Westcan Terminal B in Victoria, B. C.

The primary objectives of the JOI proposal to DOE/NETL, which resulted in Cooperative Agreement #DE-FC26-01NT41329, were to sample and characterize methane hydrates using the systems and capabilities of the D/V *JOIDES Resolution* during ODP Leg 204, to enable scientists the opportunity to establish the mass and distribution of naturally occurring gas and gas hydrate at all relevant spatial and temporal scales, and to contribute to the DOE methane hydrate research and development effort. The goal of the work was to provide expanded measurement capabilities on the *JOIDES Resolution* for a dedicated hydrate cruise to Hydrate Ridge off Oregon (ODP Leg 204) so that hydrate deposits in this region are well characterized. This goal was accomplished along with many other aspects of this project, which have contributed to ongoing hydrate studies and joint industry project preparation to characterize hydrate deposits in the Gulf of Mexico.

The projects identified in the JOI proposal were all focused on providing enhanced capabilities for existing tools and developing new approaches to the study of naturally-occurring marine methane hydrate. This was accomplished by the development and testing of tools and measurement systems on ODP Leg 201 (Peru Margin) and their extensive use on ODP Leg 204 (Hydrate Ridge, offshore Oregon) to characterize, sample, and preserve large quantities of naturally-occurring methane hydrate for onshore studies.

This project involved very complex operational planning and the enhancement or development of complicated downhole sampling and measurement tools, as well as well-thought out approaches to laboratory procedures and measurements, some requiring the deployment of specialized equipment never before used in scientific ocean drilling. Further detailed information, including methods and procedures used throughout each of these two expeditions, and data provided by these deployments, can be obtained online, for Leg 201 at <[http://www-odp.tamu.edu/publications/201\\_IR/201TOC.HTM](http://www-odp.tamu.edu/publications/201_IR/201TOC.HTM)> and for Leg 204 at <[http://www-odp.tamu.edu/publications/204\\_IR/204TOC.HTM](http://www-odp.tamu.edu/publications/204_IR/204TOC.HTM)>.

*In-Situ Sampling and Characterization of Naturally Occurring Marine Methane Hydrate Using the D/V JOIDES Resolution.*

## REFERENCES

- Arsenault, M.A., Tréhu, A.M., Bangs, N., and Nakamura, Y., 2001. P-wave tomography of Hydrate Ridge, Oregon continental margin. *Eos, Trans.*, 82:604. (Abstract)
- Austin, J.A., Jr., Christie-Blick, N., Malone, M.J., et al., 1998. Proc. ODP, Init. Repts., 174A: College Station, TX (Ocean Drilling Program).
- Berner, R.A., 1970. Sedimentary pyrite formation: an update. *Geochim. Cosmochim. Acta*, 48:605-615.
- Binns, R.A., Barriga, F.J.A.S., Miller, D.J., et al., 2002. Proc. ODP, Init. Repts., 193 [CDROM]. Available from: Ocean Drilling Program, Texas A&M University, College Station TX 77845-9547, USA.
- Blum, P., 1997. Physical properties handbook: a guide to the shipboard measurement of physical properties of deep-sea cores. ODP Tech. Note, 26 [Online]. Available from World Wide Web: <<http://www.odp.tamu.edu/publications/tnotes/tn26/INDEX.HTM>>. [Cited 2001-09-02].
- Boetius, A., Ravensschlag, K., Schubert, C.J., Rickert, D., Widdel, F., Gieseke, A., Amann, R., Jorgensen, B.B., Witte, U., and Pfannkuche, O., 2000. Microscopic identification of a microbial consortium apparently mediating anaerobic methane oxidation above marine gas hydrate. *Nature*, 407:623-626.
- Bohrmann, G., Greinert, J., Suess, E., and Torres, M., 1998. Authigenic carbonates from Cascadia Subduction Zone and their relation to gas hydrate stability. *Geology*, 26/7:647-650.
- Bohrmann, G., Linke, P., Suess, E., Pfannkuche, O., and Scientific Party, 2000. R/ V *SONNE* cruise report, SO143 TECFLUX-I-1999. *GEOMAR Rpt.*, 93.
- Bohrmann, G., Suess, E., Rickert, D., Kuhs, W.F., Torres, M., Trehu, A., and Link, P., 2002. Properties of seafloor methane hydrates at Hydrate Ridge, Cascadia margin. *Fourth Int. Conf. Gas Hydrates*, Yokohama, Japan. (Abstract).
- Booth, J.S., Winters, W.J., and Dillon, W.P., 1994. Circumstantial evidence of gas hydrate and slope failure associations on the United States Atlantic continental margin. In Sloan, E.D., Happel, J., and Hantow, M.A. (Eds.), *Int. Conf. Nat. Gas Hydrates*, 7:487-489.
- Borowski, W.S., Paull, C.K., and Ussler, W., III, 1996. Marine pore-water sulfate profiles indicate in situ methane flux from underlying gas hydrate. *Geology*, 24:655-658.
- In-Situ Sampling and Characterization of Naturally Occurring Marine Methane Hydrate Using the D/V JOIDES Resolution.*

- Boudreau, B.P., and Canfield, D.E., 1993. A comparison of closed and open system models for porewater and calcite saturation state. *Geochim. Cosmochim. Acta*, 57:317-334.
- Buffet, B.A., and Zatsepina, O.Y., 1999. Metastability of gas hydrate. *Geophys. Res. Lett.*, 26:2981-2984.
- Carson, B., Seke, E., Paskevich, V., and Holmes, M.L., 1994. Fluid expulsion sites on the Cascadia accretionary prism: mapping diagenetic deposits with processed GLORIA imagery. *J. Geophys. Res.*, 99:11959-11969.
- Clague, D., Maher, N. and Paull, C.K., 2001. High-resolution multibeam survey of Hydrate Ridge, offshore Oregon. In Paull, C.K., and Dillon, W.P. (Eds), *Natural Gas Hydrates: Occurrence, Distribution, and Detection*. Am. Geophys. Union, Geophys. Monogr. Ser., 124:297-306.
- Davis, E.E., Villinger, H., MacDonald, R.D., Meldrum, R.D., and Grigel, J., 1997. A robust rapid-response probe for measuring bottom-hole temperatures in deepocean boreholes. *Mar. Geophys. Res.*, 19:267-281.
- Dickens, G.R., 2001. Modeling the global carbon cycle with a gas hydrate capacitor: significance for the latest Paleocene thermal maximum. In Paull, C.K., and Dillon, W.P. (Eds), *Natural Gas Hydrates: Occurrence, Distribution, and Detection*. Am. Geophys. Union, Geophys. Monogr. Ser., 124:19-40.
- Dickens, G.R., Borowski, W.S., Wehner, H., Paull, C.K., and the ODP Leg 164 Scientific Party, 2000a. Data report: Additional shipboard information for the pressure core sampler (PCS). In Paull, C.K., Matsumoto, R., Wallace, P.J., and Dillon, W.P. (Eds.), *Proc. ODP, Sci. Results, 164*: College Station, TX (Ocean Drilling Program), 439-443.
- Dickens, G.R., Castillo, M.M., and Walker, J.G.C., 1997. A blast of gas in the latest Paleocene: simulating first-order effects of massive dissociation of oceanic methane hydrate. *Geology*, 25:259-262.
- Dickens, G.R., O'Neil, J.R., Rea, D.K., and Owen, R.M., 1995. Dissociation of oceanic methane hydrate as a cause of the carbon isotope excursion at the end of the Paleocene. *Paleoceanography*, 10:965-971.
- Dickens, G.R., Paull, C.K., Wallace, P., and the ODP Leg 164 Scientific Party, 1997. Direct measurement of in situ methane quantities in a large gas hydrate reservoir. *Nature*, 385: 427-428.
- Dickens, G.R., Wallace, P.J., Paull, C.K., and Borowski, W.S., 2000b. Detection of methane gas hydrate in the pressure core sampler (PCS): volume-pressure-time relations
- In-Situ Sampling and Characterization of Naturally Occurring Marine Methane Hydrate Using the D/V JOIDES Resolution.*

during controlled degassing experiments. In Paull, C.K., Matsumoto, R., Wallace, P.J., and Dillon, W.P. (Eds.), Proc. ODP, Sci. Results, 164: College Station, TX (Ocean Drilling Program), 113–126.

Dickens, G.R., Schroeder, D., Hinrichs, K.-U., and the Leg 201 Scientific Party, 2003. The pressure core sampler (PCS) on Ocean Drilling Program Leg 201: general operations and gas release. In D'Hondt, S.L., Jørgensen, B.B., Miller, D.J., et al., Proc. ODP, Init. Repts., 201, 1–22 [CD-ROM]. Available from: Ocean Drilling Program, Texas A&M University, College Station TX 77845-9547, USA.

Duan, Z., Møller, N., Greenberg, J., and Weare, J.H., 1992. The prediction of methane solubility in natural waters to high ionic strengths from 0° to 250°C and from 0 to 1600 bar. *Geochim. Cosmochim. Acta*, 56:1451–1460.

Garrels, R.M., and Perry, E.A., 1974. Cycling of carbon, sulfur, and oxygen through geologic time. In Goldberg, E.D. (Ed.), *The Sea* (Vol. 5): *Marine Chemistry: The Sedimentary Cycle*: New York (Wiley), 569-655.

Graber, K.K., Pollard, E., Jonasson, B., and Schulte, E. (Eds.), 2002. Overview of Ocean Drilling Program Engineering Tools and Hardware. ODP Tech. Note, 31 [Online]. Available from World Wide Web: <<http://www-odp.tamu.edu/publications/tnotes/t31/INDEX.HTM>>. [Cited 2002-07-03]

Greinert, J., Bohrmann, G., and Suess, E., 2001. Gas hydrate-associated carbonates and methane-venting at Hydrate Ridge: classification, distribution and origin of authigenic lithologies. In Paull, C.K., and Dillon, W.P. (Eds.), *Natural Gas Hydrates: Occurrence, Distribution, and Detection*. Am. Geophys. Union, Geophys. Monogr. Ser., 124:99-114.

Guerin, G., Goldberg, D., and Meltser, A., 1999. Characterization of in situ elastic properties of gas-hydrate bearing sediments on the Blake Ridge. *J. Geophys. Res.*, 104:17781-17795.

Handa, Y.P., 1990. Effect of hydrostatic pressure and salinity on the stability of gas hydrates. *J. Phys. Chem.*, 94:2652–2657.

Heeseman, M., 2002. Modeling and analysis of transient pressure measurements in ODP boreholes for undisturbed formation pressure estimation [Diplomarbeit im Fach Geophysik]. University of Bremen.

Holbrook, W.S., Hoskins, H., Wood, W.T., Stephen, R.A., Lizzarralde, D., and the Leg 164 Science Party, 1996. Methane gas-hydrate and free gas on the Blake Ridge from vertical seismic profiling. *Science*, 273:1840-1843.

Holland, H.D., 1978. *The Chemistry of the Atmosphere and Oceans*: New York (Wiley).

*In-Situ Sampling and Characterization of Naturally Occurring Marine Methane Hydrate Using the D/V JOIDES Resolution.*

- Housen, B.A., and Musgrave, R.J., 1996. Rock-magnetic signature of gas hydrates in accretionary prism sediments. *Earth Planet. Sci. Lett.*, 139:509-519.
- Housen, B.A., and Musgrave, R.J., 1996. Rock-magnetic signature of gas hydrates in accretionary prism sediments. *Earth Planet. Sci. Lett.*, 139:509–519.
- Hovland, M., Lysne, D. and Whiticar, M., 1995. Gas hydrate and sediment gas composition, Hole 892A. In Carson, B., Westbrook, G.K., Musgrave, R.J., and Suess, E. (Eds.), *Proc. ODP, Sci. Results*, 146 (Pt 1): College Station, TX (Ocean Drilling Program), 151-161.
- Hyndman, R.D., and Davis, E.E., 1992. A mechanism for the formation of methane hydrate and seafloor bottom-simulating reflectors by vertical fluid expulsion. *J. Geophys. Res.*, 97:7025-7041.
- Karlin, R., 1983. Paleomagnetism and diagenesis of hemipelagic sediments in the northeast Pacific Ocean and the Gulf of California [Ph.D. dissert.]. Oregon State Univ., Corvallis.
- Kastner, M., Kvenvolden, K.A., Whiticar, M.J., Camerlenghi, A., and Lorenson, T.D., 1995. Relation between pore fluid chemistry and gas hydrates associated with bottom-simulating reflectors at the Cascadia margin, Sites 889 and 892. In Carson, B., Westbrook, G.K., Musgrave, R.J., and Suess, E. (Eds.), *Proc. ODP, Sci. Results*, 146 (Pt 1): College Station, TX (Ocean Drilling Program), 175–187.
- Kastner, M., Sample, J.C., Whiticar, M.J., Hovland, M., Cragg, B.A., and Parkes, J.R., 1995. Geochemical evidence for fluid flow and diagenesis at the Cascadia convergent margin. In Carson, B., Westbrook, G.K., Musgrave, R.J., and Suess, E. (Eds.), *Proc. ODP, Sci. Results*, 146 (Pt 1): College Station, TX (Ocean Drilling Program), 375-384.
- Katz, M.E., Pak, D.K., Dickens, G.R., and Miller, K.G., 1999. The source and fate of massive carbon input during the latest Paleocene thermal maximum. *Science*, 286:1531-1533.
- Kennett, J., Hendy, I.L., Behl, 1996. First MASTER Workshop on Gas Hydrates, Ghent, Belgium.
- Kimura, G., Silver, E.A., Blum, P., et al., 1997. *Proc. ODP, Init. Repts.*, 170: College Station, TX (Ocean Drilling Program).
- Kulm, L.D., Suess, E., Moore, J.C., Carson, B., Lewis, B.T., Ritger, S.D., Kadko, D.C., Thornburg, T.M., Embley, R.W., Rugh, W.D., Massoth, G.J., Langseth, M.G., Cochrane, G.R., and Scamman, R.L., 1986. Oregon subduction zone: venting, fauna, and carbonates. *Science*, 231:561-566.

*In-Situ Sampling and Characterization of Naturally Occurring Marine Methane Hydrate Using the D/V JOIDES Resolution.*

- Kvenvolden, K.A., 1995. A review of the geochemistry of methane in natural gas hydrate. *Org. Geochem.*, 23:997-1008.
- Kvenvolden, K.A., and Lorenson, T.D., 2001. The global occurrence of natural gas hydrate. In Paull, C.K., and Dillon, W.P. (Eds.), *Natural Gas Hydrates: Occurrence, Distribution, and Detection*. Am. Geophys. Union, Geophys. Monogr. Ser., 124:3-18.
- Linke, P., Suess, E., and Scientific Party, 2001. R/V *SONNE* cruise report, SO148 TECFLUX-II-2000. *GEOMAR Rpt.*, 98.
- MacDonald, I.R., Boland, G.S., Baker, J.S., Brooks, J.M., Kennicutt, M.C., II, and Bidigare, R.R., 1989. Gulf of Mexico hydrocarbon seep communities II. Spatial distribution of seep organisms and hydrocarbons at Bush Hill. *Mar. Biol.*, 101:235-247.
- MacKay, M.E., 1995. Structural variation and landward vergence at the toe of the Oregon accretionary prism. *Tectonics*, 14:1309-1320.
- MacKay, M.E., Moore, G.F., Cochrane, G.R., Moore, J.C., and Kulm, L.D., 1992. Landward vergence and oblique structural trends in the Oregon margin accretionary prism: implications and effect on fluid flow. *Earth Planet. Sci. Lett.*, 109:477-491.
- MacKay, M.E., Jarrad, R.D., Westbrook, G.K., Hyndman, R.D., and Shipboard Scientific Party, 1994. ODP Leg 146, Origin of BSRs: geophysical evidence from the Cascadia accretionary prism. *Geology*, 22:459-462.
- Mikada, H., Becker, K., Moore, J.C., Klaus, A., et al., 2002. Proc. ODP, Init. Repts., 196 [CD-ROM]. Available from: Ocean Drilling Program, Texas A&M University, College Station TX 77845-9547, USA.
- Moore, J.C., Klaus, A., et al., 1998. Proc. ODP, Init. Repts., 171A [CD-ROM]. Available from: Ocean Drilling Program, Texas A&M University, College Station, TX 77845-9547, U.S.A.
- Nisbet, E.G., 1990. The end of the ice age. *Can. J. Earth Sci.*, 27:148-157.
- Nisbet, E.G., and Piper, D.J., 1998. Giant submarine landslides. *Nature*, 392:329-330.
- O'Brien, P.E., Cooper, A.K., Richter, C., et al., 2001. Proc. ODP, Init. Repts., 188 [CDROM]. Available from: Ocean Drilling Program, Texas A&M University, College Station, TX 77845-9547, USA.
- ODP Leg 146 Scientific Party, 1993. ODP Leg 146 examines fluid flow in Cascadia margin. *Eos*, 74:345-347.

Ostermeier, R.M., Pelletier, J.H., Winker, C.D., Nicholson, J.W., Rambow, F.H., and Cowan, K.M., 2000. Dealing with shallow-water flow in the deepwater Gulf of Mexico. *Proc. Offshore Tech. Conf.: Dallas (Offshore Tech. Conf.)*, 32:75–86.

Parkes, R.J., Cragg, B.A., and Wellsbury, P., 2000. Recent studies on bacterial populations and processes in marine sediments: a review. *Hydrogeol. Rev.*, 8:11–28.  
Paull, C.K., Matsumoto, R., Wallace, P.J., et al., 1996. *Proc. ODP, Init. Repts.*, 164: College Station, TX (Ocean Drilling Program).

Paull, C.K., Matsumoto, R., Wallace, P.J., et al., 1996. *Proc. ODP, Init. Repts.*, 164: College Station, TX (Ocean Drilling Program).

Paull, C.K., and Ussler W., III, 2001. History and significance of gas sampling during the DSDP and ODP. In Paull, C.K., and Dillon, W.P. (Eds.), *Natural Gas Hydrates: Occurrence, Distribution, and Detection*. Am. Geophys. Union, Geophys. Monogr. Ser., 124:53-66.

Paull, C.K., Ussler, W., III, and Borowski, W.A., 1994. Sources of biogenic methane to form marine gas-hydrates: in situ production or upward migration? *Ann. N.Y. Acad. Sci.*, 715:392-409.

Paull, C.K., Ussler, W., III, and Dillon, W.P., 1991. Is the extent of glaciation limited by marine gas-hydrates? *Geophys. Res. Lett.*, 18:432-434.

Pettigrew, T.L., 1992. Design and operation of a wireline pressure core sampler. ODP Tech Note, 17 (Ocean Drilling Program), College Station, TX.

Pribnow, D.F.C., Kinoshita, M., and Stein, C.A., 2000. Thermal data collection and heat flow recalculations for ODP Legs 101–180. Institute for Joint Geoscientific Research, GGA, Hanover, Germany, 0120432. Available from World Wide Web: <<http://www-odp.tamu.edu/publications/heatflow/ODPReprt.pdf>>. [Cited 2002-07-03]

Rack, F.R., 2001. Preliminary Evaluation of Existing Pressure/Temperature Coring System: Washington, D.C. (Joint Oceanographic Institutions). Available from World Wide Web: <<http://NETL.CERTREC.COM>> Login = NETL; Password = ARCHIVE; File Name = HYD\_00037\_2001.PDF [Cited 2004-02-15].

Rempel, A.W., and Buffett, B.A., 1998. Mathematical models of gas hydrate accumulation. In Henriot, J.P., and Mienert, J. (Eds.), *Gas Hydrates; Relevance to World Margin Stability and Climate Change*, Spec. Publ. Geol. Soc. London, 137:63-74.

Revelle, R., 1983. Methane hydrates in continental slope sediments and increasing atmospheric carbon dioxide. In *Changing Climate: Washington* (National Academy Press), 252-261.

*In-Situ Sampling and Characterization of Naturally Occurring Marine Methane Hydrate Using the D/V JOIDES Resolution.*

Ruppel, C., 1997. Anomalously cold temperatures observed at the base of the gas hydrate stability zone on the U.S. Atlantic passive margin. *Geology*, 25:699-702.

Sample, J.C., and Kopf, A., 1995. Isotope geochemistry of syntectonic carbonate cements and veins from the Oregon Margin: implications for the hydrogeologic evolution of the accretionary wedge. In Carson, B., Westbrook, G.K., Musgrave, R.J., and Suess, E. (Eds.), *Proc. ODP, Sci. Results*, 146 (Pt 1): College Station, TX (Ocean Drilling Program), 137-148.

Sassen, R., Sweet, S.T., Milkov, A.V., Defreitas, D.A., Kennicutt, M.C., and Roberts, H.H., 2001. Stability of thermogenic gas hydrate in the Gulf of Mexico: constraints on models of climate change. In Paull, C.K., and Dillon, W.P. (Eds.), *Natural Gas Hydrates: Occurrence, Distribution, and Detection*. Am. Geophys. Union, Geophys. Monogr. Ser., 124:131-144.

Schluter, M., Linke, P., and Suess, E., 1998. Geochemistry of a sealed deep-sea borehole on the Cascadia margin. *Mar. Geol.*, 148:9-20.

Shipley, T.H., Ogawa, Y., Blum, P., and Bahr, J.M. (Eds.), 1995. *Proc. ODP, Sci. Results*, 156: College Station, TX (Ocean Drilling Program).

Suess, E., and Bohrmann, G., 1997. FS *SONNE* cruise report, SO110:SO-RO (*SONNE-ROPOS*), Victoria-Kodiak-Victoria, July 9-Aug. 19, 1996. *GEOMAR Rpt.*, 59:181.

Suess, E., Torres, M.E., Bohrmann, G., Collier, R.W., Rickert, D., Goldfinger, C., Linke, P., Heuser, A., Sahling, H., Heeschen, K., Jung, C., Nakamura, K., Greinert, J., Pfannkuche, O., Trehu, A., Klinkhammer, G., Whiticar, M.J., Eisenhauer, A., Teichert, B., and Elvert, M., 2001. Sea floor methane hydrates at Hydrate Ridge, Cascadia margin. In Paull, C.K., and Dillon, W.P. (Eds.), *Natural Gas Hydrates: Occurrence, Distribution, and Detection*. Am. Geophysical Union, Geophys. Monogr. Ser., 124:87-98.

Suess, E.M., Torres, M.E., Bohrmann, G., Collier, R.W., Greinert, J., Linke, P., Rehter, G., Trehu, A.M., Wallmann, K., Winckler, G., and Zulegger, E., 1999. Gas hydrate destabilization: enhanced dewatering, benthic material turnover, and large methane plumes at the Cascadia convergent margin. *Earth Planet. Sci. Lett.*, 170:1-15.

Suess, E., von Huene, R., et al., 1988. *Proc. ODP, Init. Repts.*, 112: College Station, TX (Ocean Drilling Program).

Techmer, K.S., Kuhs, W.F., Heinrichs, T., Bohrmann, G., 2001. Scanning electron microscopic investigations on natural and synthetic gas hydrates: new insights into the formation process. *Eos, Trans.*, 82:173. (Abstract).

*In-Situ Sampling and Characterization of Naturally Occurring Marine Methane Hydrate Using the D/V JOIDES Resolution.*

Teichert, B.M.A., Eisenhauer, A., and Bohrmann, G., 2001. Chemoherm buildups at the Cascadia Margin (Hydrate Ridge) - evidence for long-term fluid flow. *2001 MARGINS Meet.*, Kiel, 208.

Torres, M.E., Bohrmann, G., Brown, K., deAngelis, M., Hammond, D., Klinkhammer, G., McManus, J., Suess, E., and Trehu, A.M., 1999. Geochemical observations on Hydrate Ridge, Cascadia margin, July, 1999. *Oregon State Univ. Data Rpt.* 174, ref. 99-3.

Torres, M.E., Colbert, S., Collier, R.W., deAngelis, M., Hammond, D., Heeschen, K., Hubbard, D., McManus, J., Moyer, C., Rehder, G., Tréhu, A.M., Tyron, M., and Whaling, P., 1998. Active gas discharge resulting from decomposition of gas hydrates on Hydrate Ridge, Cascadia margin. *Eos, Trans.*, 79:461.

Trehu, A.M., and Bangs, N., 2001. 3-D seismic imaging of an active margin hydrate system, Oregon continental margin, report of cruise TTN112. *Oregon State Univ. Data Rpt.* 182.

Tréhu, A.M., Bangs, N.L., Arsenault, M.A., Bohrmann, G., Goldfinger, C., Johnson, J.E., Nakamura, Y., and Torres, M.E., 2002. Complex subsurface plumbing beneath southern Hydrate Ridge, Oregon continental margin, from high-resolution 3-D seismic reflection and OBS data. Fourth Int. Conf. Gas Hydrates: Yokohama, Japan, 19023:90–96.

Trehu, A.M., and Flueh, E., 2001. Estimating the thickness of the free gas zone beneath Hydrate Ridge, Oregon continental margin, from seismic velocities and attenuation. *J. Geophys. Res.*, 106:2035-2045.

Trehu, A.M., Lin, G., Maxwell, E., and Goldfinger, C., 1995. A seismic reflection profile across the Cascadia subduction zone offshore central Oregon: new constraints on methane distribution and crustal structure. *J. Geophys. Res.*, 100:15101-15116.

Trehu, A.M., Torres, M.E., Moore, G.F., Suess, E., and Bohrmann, G., 1999. Temporal and spatial evolution of a gas-hydrate-bearing accretionary ridge on the Oregon continental margin. *Geology*, 27:939-942.

Wallace, P.J., Dickens, G.R., Paull, C.K., and Ussler, W., III, 2000. Effects of core retrieval and degassing on the carbon isotope composition of methane in gas hydrate- and free gas-bearing sediments from the Blake Ridge. In Paull, C.K., Matsumoto, R., et al., Proc. ODP, Sci. Results, 164: College Station, TX (Ocean Drilling Program), 101–112.

Wefer, G.P., Heinze, M., and Berger, W.H., 1994. Clues to ancient methane release. *Nature*. 369:282.

*In-Situ Sampling and Characterization of Naturally Occurring Marine Methane Hydrate Using the D/V JOIDES Resolution.*

Whittle, A.J., Sutabutr, T., Germaine, J.T., and Varney, A., 2001. Prediction and measurement of pore pressure dissipation for a tapered piezocone. *Geotechnique*, 51:601–617.

Xu, W., and Ruppel, C., 1999. Predicting the occurrence, distribution, and evolution of methane gas hydrate in porous marine sediments. *J. Geophys. Res.*, 104:5081-5096.

**LIST OF ACRONYMS AND ABBREVIATIONS**

AND	Azimuthal Density Neutron
AMO	Anaerobic Methane Oxydation
APC	Advanced Piston Corer
APCM	Advanced Piston Corer-methane tool
APCT	Advanced Piston Corer-temperature tool
APS	Accelerator Porosity Sonde
BHA	Bottom Hole Assembly
BSR	Bottom Simulating Reflector
CH4	Methane
CM	Centimeter
CO2	Carbon Dioxide
DIT	Dual Induction Tool
DOE	Department of Energy
DSA	Drill-String Accelleration Tool
DSI	Dipole Sonic Imager
DVTP	Davis Villinger Temperature Probe
DVTPP	Davis Villinger Temperature Probe with Pressure
EU	European Union
FMS	Formation Micro-Scanner
FPC	Fugro Pressure Corer
GHSZ	Gas Hydrate Stability Zone
GPS	Global Positioning System
GRA	Gamma Ray Attenuation
GRP	Glass Reinforced Plastic
GVR	GeoVision Resistivity
HE	Helium
HLDT	Hostile Environment Litho-Density Tool
HNGS	Hostile Environment Gamma Ray Sonde
H2S	Hydrogen Sulfide
HR	Hydrate Ridge
HRC	HYACE Rotary Corer
HYACE	Hydrate Autoclave Coring Equipment
HYACINTH	Deployment of HYACE tools In New Tests on Hydrates
IR-TIS	Infrared Thermal Imaging System
IW	Interstitial Water
JOI	Joint Oceanographic Institutions
JOIDES	Joint Oceanographic Institutions for Deep Earth Sampling
KG	Kilogram
KM	Kilometer
LDEO	Lamont Doherty Earth Observatory (Columbia University)
L/L	Liters per Liter
LXS	Linear X-ray Scanner

LTC	Laboratory Transfer Chamber
LWD	Logging While Drilling
MBRF	Meters Below Rig Floor
MBSF	Meters Below Sea Floor
MCDB	Motor Driven Core Barrel
MH	Methane Hydrate
mL	Milliliter
MSCL-V	Multi-Sensor Core Logger – Vertical
MST	Multi-Sensor Track
MWD	Measurement While Drilling
N <sub>2</sub>	Nitrogen
NETL	National Energy Technology Laboratory
NMR	Nuclear Magnetic Resonance
NSF	National Science Foundation
NW	Northwest
O <sub>2</sub>	Oxygen
ODP	Ocean Drilling Program
ODP-LC	Ocean Drilling Program – Logging Chamber
PCS	Pressure Core Sampler
PFT	Perfluorocarbon Tracer
PSI	Pounds per Square Inch
QSST	Inline Checkshot Tool
RAB	Resistivity at the Bit
RAB-c	Resistivity at the Bit with Coring
RCB	Rotary Core Barrel
ROP	Rate of Penetration
R/V	Research Vessel
Sw	Pore Water Saturation
TAMU	Texas A&M University
TAP	Temperature Acceleration Pressure Tool
TD	Total Depth
U-Th	Uranium-Thorium
VCD	Visual Core Descriptions
VP	Compressional Wave Velocity (P-Wave)
VND	Vision Neutron Density
VSP	Vertical Seismic Profiling
XCB	Extended Core Barrel
YR	Year

**List of ODP Leg 204 Shipboard Scientific Party Members**

Co-Chief Scientist - Gerhard Bohrmann (GEOMAR, Christian-Albrechts Universitat zu Kiel, Wischhofstrasse 1-3, Gebaude 4, Kiel 24148, Germany)

Co-Chief Scientist - Anne M. Trehu (College of Oceanic and Atmospheric Sciences, Oregon State University, 104 Oceanography Administration Building, Corvallis OR 97331-5503, USA)

ODP Staff Scientist - Frank R. Rack (Joint Oceanographic Institutions, Inc., 1755 Massachusetts Avenue, Northwest, Suite 700, Washington D.C. 20036, USA)

Inorganic Geochemist - Walter S. Borowski (Earth Sciences Department, Eastern Kentucky University, 512 Lancaster Avenue, Roark 103, Richmond KY 40475-3102, USA)

Inorganic Geochemist – Hitoshi Tomaru (Graduate School of Science, University of Tokyo, Science Building 5, 7-3-1 Hong, Bunkyo-ku, Tokyo 113-0033, Japan)

Inorganic Geochemist - Marta E. Torres (College of Oceanic and Atmospheric Sciences, Oregon State University, 104 Oceanography Administration Building, Corvallis OR 97331-5503, USA)

Organic Geochemist - George E. Claypool (8910 West 2nd Avenue, Lakewood CO 80226, USA)

Organic Geochemist – Young-Joo Lee (Petroleum and Marine Resources Research Division, Korea Institute of Geoscience and Mineral Resources (KIGAM), 30 Kajung-Dong, Yusong-Gu, Daejon 305-350, Korea)

Organic Geochemist – Alexei Milkov (Geochemistry and Environmental Research Group, Texas A&M University, 833 Graham Road, College Station, TX 77845, USA)

PCS Scientist - Gerald R. Dickens (Department of Geology and Geophysics, Rice University, 6100 Main Street, Houston, TX 77005-1892, USA)

Logging Scientist - Timothy S. Collett (Branch of Petroleum Geology, U.S. Geological Survey, Denver Federal Center, Box 25046, MS 939, Denver CO 80225, USA)

Logging Scientist – Nathan Bangs (Institute for Geophysics, University of Texas at Austin, 4412 Spicewood Springs Road, Bldg. 600, Austin, TX 78759-8500, USA)

Geophysicist – Martin Vanneste (Department of Geology, Universitetet i Tromso, Dramsveinen 201, 9037 Tromso, Norway)

*In-Situ Sampling and Characterization of Naturally Occurring Marine Methane Hydrate Using the D/V JOIDES Resolution.*

Microbiologist - Melanie Holland (Department of Geologic Sciences, Box 871404, Arizona State University, Tempe, AZ 85287, USA)

Microbiologist – Mark E. Delwiche (Biotechnologies, Idaho National Engineering and Environmental Laboratory, 2525 N. Freemont St., Idaho Falls, ID 83415, USA)

Micropaleontologist (diatoms) – Mahito Watanabe (Geoscience Institute, Geological Survey of Japan, AIST, 1-1-1 Central 7 Higashi, Tsukuba 305-8567, Japan)

Physical Properties Specialist – Char-Shine Liu (Institute of Oceanography, National Taiwan University, P.O. Box 23-13, Taipei 106, Taiwan)

Physical Properties Specialist - Philip E. Long (Environmental Technology Division, Pacific Northwest National Laboratory, PO Box 999, Mail Stop K9-33, Richland WA 99352, USA)

Physical Properties Specialist - Michael Riedel (Geological Survey of Canada, Pacific Geoscience Centre, 9860 West Saanich Road, Sidney, BC V8L 4B2, Canada)

Physical Properties Specialist - Peter Schultheiss (GEOTEK Ltd., 3 Faraday Close, Drayton Fields, Daventry, Northants NN11 5RD, United Kingdom)

Sedimentologist - Eulalia Gracia (Institute of Earth Sciences (Jaume Almera), CSIC, Lluís Sole i Sabaris, 08028 Barcelona, Spain)

Sedimentologist - Joel E. Johnson (College of Oceanic and Atmospheric Sciences, Oregon State University, 104 Oceanography Admin. Bldg, Corvallis OR 97331, USA)

Sedimentologist – Xin Su (Center of Marine Geology, China University of Geosciences, Xueyuan Road 29, Beijing 100083, People's Republic of China)

Sedimentologist - Barbara Teichert (GEOMAR, Christian-Albrechts Universität zu Kiel, Wischhofstrasse 1-3, Kiel 24148, Germany)

Sedimentologist/Structural Geologist - Jill L. Weinberger (Scripps Institution of Oceanography, University of California, San Diego, 9500 Gilman Drive, Mail Code 0208, San Diego CA 92093-0244, USA)

Logging Staff Scientist - David S. Goldberg (Lamont-Doherty Earth Observatory, Borehole Research Group, Columbia University, Route 9W, Palisades NY 10964, USA)

Logging Staff Scientist - Samantha R. Barr (Department of Geology, University of Leicester, University Road, Leicester LE1 7RH, United Kingdom)

*In-Situ Sampling and Characterization of Naturally Occurring Marine Methane Hydrate Using the D/V JOIDES Resolution.*

Logging Staff Scientist - Gilles Guèrin (Lamont-Doherty Earth Observatory, Columbia University, Borehole Research Group, Palisades, NY 10964, USA)

Operations Manager - Michael A. Storms (Ocean Drilling Program, Texas A&M University, 1000 Discovery Drive, College Station TX 77845, USA)

Development Engineer - Derryl Schroeder (Ocean Drilling Program, Texas A&M University, 1000 Discovery Drive, College Station TX 77845, USA)

Development Engineer – Kevin Grigar (Ocean Drilling Program, Texas A&M University, 1000 Discovery Drive, College Station TX 77845, USA)

HYACINTH Engineer- Roeland Baas (Fugro Engineers, 2260 AG Leidschendam, The Netherlands)

HYACINTH Engineer - Floris Tuynder (Fugro Engineers, 2260 AG Leidschendam, The Netherlands)

HYACINTH Engineer - Felix Weise (Institute of Petroleum Engineering, Technical University of Clausthal, Clausthal, Germany)

HYACINTH Engineer - Thjunjoto (Maritime Technik, Technical University of Berlin, Berlin, Germany)

Piezoprobe Engineer – Terry Langsdorf (Fugro-McClelland Engineers, Houston, TX)

Peizoprobe Engineer – Ko-Min Tjok (Fugro-McClelland Engineers, Houston, TX)

Schlumberger Engineer - Kerry Swain (Schlumberger Offshore Services, 369 Tristar Drive, Webster, TX 77598, USA)

Schlumberger Engineer – Herbert Leyton (Schlumberger Offshore Services, USA)

Schlumberger Engineer – Stefan Mrozewski (Schlumberger Offshore Services, USA)

Schlumberger Engineer – Khaled Moudjeber (Schlumberger Offshore Services, USA)

Laboratory Officer - Brad Julson (Ocean Drilling Program, Texas A&M University, 1000 Discovery Drive, College Station, TX 77845-9547, USA)

Assistant Laboratory Officer – Tim Bronk (Ocean Drilling Program, Texas A&M University, 1000 Discovery Drive, College Station, TX 77845-9547, USA)

*In-Situ Sampling and Characterization of Naturally Occurring Marine Methane Hydrate Using the D/V JOIDES Resolution.*

Marine Lab Specialist: Yeoperson - Angie Miller (Ocean Drilling Program, Texas A&M University, 1000 Discovery Drive, College Station, TX 77845-9547, USA)

Marine Lab Specialist Photography - John Beck (Ocean Drilling Program, Texas A&M University, 1000 Discovery Drive, College Station, TX 77845-9547, USA)

Marine Lab Specialist Photography - Roy Davis (Ocean Drilling Program, Texas A&M University, 1000 Discovery Drive, College Station, TX 77845-9547, USA)

Marine Lab Specialist (Temporary) – Jason Deardorf (Ocean Drilling Program, Texas A&M University, 1000 Discovery Drive, College Station, TX 77845-9547, USA)

Marine Lab Specialist: Downhole Tools – Sandy Dillard (Ocean Drilling Program, Texas A&M University, 1000 Discovery Drive, College Station, TX 77845-9547, USA)

Marine Lab Specialist: Chemistry - Dennis Graham (Ocean Drilling Program, Texas A&M University, 1000 Discovery Drive, College Station, TX 77845-9547, USA)

Marine Laboratory Specialist: Curator - Jessica Huckemeyer (Ocean Drilling Program, Texas A&M University, 1000 Discovery Drive, College Station TX 77845, USA)

Marine Computer Specialist - Margaret Hastedt (Ocean Drilling Program, Texas A&M University, 1000 Discovery Drive, College Station TX 77845, USA)

Marine Lab Specialist: Chemistry – Brian Jones (Ocean Drilling Program, Texas A&M University, 1000 Discovery Drive, College Station, TX 77845-9547, USA)

Marine Lab Specialist (Temporary) – Peter Kannberg (Ocean Drilling Program, Texas A&M University, 1000 Discovery Drive, College Station, TX 77845-9547, USA)

Marine Electronics Specialist – Jan Jurie Kotze (Ocean Drilling Program, Texas A&M University, 1000 Discovery Drive, College Station, TX 77845-9547, USA)

Marine Computer Specialist - Erik Moortgat (Ocean Drilling Program, Texas A&M University, 1000 Discovery Drive, College Station TX 77845, USA)

Marine Electronics Specialist – Peter Pretorius (Ocean Drilling Program, Texas A&M University, 1000 Discovery Drive, College Station, TX 77845-9547, USA)

Marine Lab Specialist: Physical Properties – John W.P. Riley (Ocean Drilling Program, Texas A&M University, 1000 Discovery Drive, College Station, TX 77845-9547, USA)

*In-Situ Sampling and Characterization of Naturally Occurring Marine Methane Hydrate Using the D/V JOIDES Resolution.*

Marine Lab Specialist: Underway Geophysics – Johanna Suhonen (Ocean Drilling Program, Texas A&M University, 1000 Discovery Drive, College Station, TX 77845-9547, USA)

Marine Lab Specialist (Temporary) – Paul Teniere (Ocean Drilling Program, Texas A&M University, 1000 Discovery Drive, College Station, TX 77845-9547, USA)

Marine Lab Specialist: X-ray – Robert Wheatley (Ocean Drilling Program, Texas A&M University, 1000 Discovery Drive, College Station, TX 77845-9547, USA)

**APPENDIX A**

**PIEZOPROBE DISSIPATION TESTING FOR SITE 1244**

**ODP LEG 204, OFFSHORE OREGON**

**Ko Min Tjok**

**Jean M.E. Audibert**

**Fugro-McClelland Marine Geosciences, Inc.**

**Report No. 0201-4655**

**(5 pg. Report, plus 5 Plates)**

*In-Situ Sampling and Characterization of Naturally Occurring Marine Methane Hydrate  
Using the D/V JOIDES Resolution.*

Report No. 0201-4655  
August 28, 2002

6100 Hillcroft (77081)  
P.O. Box 40010  
Houston, Texas 77274  
Phone: 713-369-5600  
Fax: 713-369-5570

Joint Oceanographic Institutions (JOI)  
1755 Massachusetts Ave, NW, Suite 700  
Washington, D.C. 20036

Attention: Mr. Frank R. Rack, Ph.D.

**Ocean Drilling Program (ODP)  
Piezoprobe Dissipation Testing for Site 1244  
ODP Leg 204, Offshore Oregon**

This report presents the results of our piezoprobe dissipation test conducted at the above location. This study was authorized by your Purchase Order No. J020045, dated March 7, 2002.

## **1. Introduction**

During ODP Leg 204, Fugro-McClelland Marine Geosciences (FMMG) Inc. was contracted by Joint Ocean Institutions (JOI) to perform piezoprobe testing from the R/V *Joides Resolution* at ODP Site 1244, Offshore Oregon.

The objectives of this study were: (a) to adapt (modify) FMMG's piezoprobe tool for use with the ODP's Bottom Hole Assembly (BHA), and (b) to deploy and perform piezoprobe testing on ODP Leg 204. To accomplish these objectives, the following tasks were performed:

- (1) Modifications to Fugro's piezoprobe tool included design and fabrication of a protective sleeve, weight collars, hang off unions, connector, adaptors, lifting heads and communication module upgrade;
- (2) The piezoprobe tool was assembled and tested with the ODP's BHA at College Station, Texas; and
- (3) One piezoprobe test was successfully performed at Site 1244 (HR1A Location) to measure the in situ temperature and in situ pore water pressure and dissipation characteristics in the soil formation.

## **2. Modifications to Piezoprobe for ODP Leg 204**

The following modification were made to Fugro's piezoprobe:

- (1) Designed and fabricated a new shaft for the piezoprobe tool, with a protective sleeve to protect the piezoprobe tip as it is passed through the ODP BHA float valve.



- (2) Designed and fabricated two (2) sets of four (4) weight collars (10 feet long). The weight collars served to accommodate the long distance between the reaction point in the ODP BHA, and added weight required to lower the tool through the long drill string.



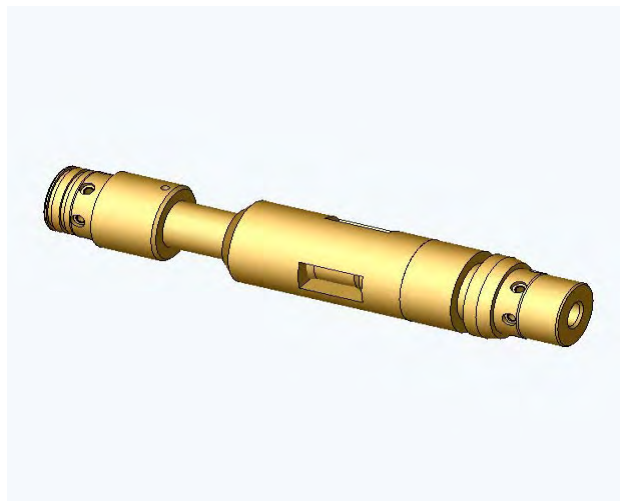
- (3) Designed and fabricated hang off unions. The hang off unions enabled the long tool to be assembled in the drill string



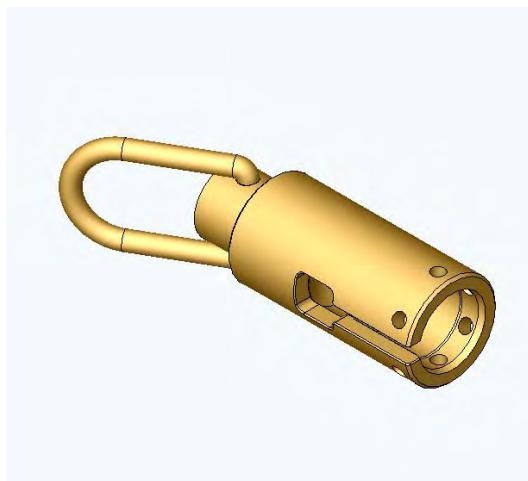
- (4) Designed and fabricated the interface connector between the connection on the end of the logging cable on the R/V Joides Resolution and Fugro's piezoprobe.



- (5) Designed and fabricated adaptors to connect the mechanical pawls to thick wall tube.



- (6) Designed and fabricated lifting heads with bail to accommodate longer and heavier system.



- (7) Upgraded communication module to accommodate long logging cable on R/V *Joides Resolution*.
- (8) Tested assembled system at College Station, Texas.

### 3. Piezoprobe Testing

Piezoprobe testing was performed using FMMG's wireline-operated, small-diameter tapered piezoprobe device to measure excess pore water pressure and dissipation characteristics and in situ temperature in the soil formation. The piezoprobe testing was conducted during ODP Leg 204 from July 9, 2002 to July 19, 2002, from the R/V *Joides Resolution*. The field activities are summarized chronologically in the Summary of Field Operations presented on Plate 1.

During ODP Leg 204, three piezoprobe tests were planned for the original testing program. The first attempt to deploy the piezoprobe tool at about 54m below seafloor in Hole 1244B was unsuccessful, because the connection between the end of the pig tail cable and the piezoprobe tool was disconnected downhole. The second attempt to repeat the piezoprobe test at about 53.5m below seafloor was successfully performed in Hole 1244C. The second piezoprobe test was cancelled due to the tight schedule of the ODP drilling program. The last test schedule to be deployed at the termination depth of the borehole (about 380m BML) was also cancelled due to squeezing of the hole formation and the borehole had to be abandoned at about 330m BML.

Prior to the deployment of the tool, the piezoprobe tool was pre-assembled on deck in three sections of approximately 20 feet long each. This was done to make it easier to handle the tool. The top section was made up of a top knob, a sinker bar, a pawl assembly and one thick wall extension complete with signal cable. The middle section consisted of two thick-walled extensions with signal cable. The bottom section consisted of one thick-walled extension, stinger rod, shroud assembly, Spartek gauge, needle tip probe assembly, and a curly cord signal cable.

After the borehole was drilled to the desired test depth, the top, middle and bottom sections of the piezoprobe tool were assembled together as they entered the drill pipe. The entire tool assembly was lowered on wireline through the drill pipe to the bottom of the borehole. While lowering the piezoprobe tool down the pipe the mud pump was pumping at a slow rate to maintain circulation in the hole. When the tool was about 30-40 meters from the bottom of the hole, the wireline winch lowering the piezoprobe tool was stopped and the drill bit was raised about 7meters above the bottom of the borehole. At this time the mud pump was turned off. The piezoprobe tool was then lowered until the top knob rested on the landing ring in



the BHA. The piezoprobe was allowed to sit for about thirty seconds to measure the hydrostatic pressure. The wireline winch operator was then instructed to pick up the slack by applying tension to the wireline until it supported the weight of the piezoprobe tool. The drill string was then lowered until the bit was about 3.5 meters from the bottom of the borehole. The heave compensation system was then activated.

To insert the piezoprobe tip into the virgin soil below the bottom of the borehole, the piezoprobe tool was lowered until the weight of the tool was supported by the soil. At this stage, with the tool resting on the bottom, the mechanical pawls were fully extended and located just below the landing ring. Subsequently the drill string was lowered to engage the pawls. The piezoprobe tip was then pushed with the drill string into the soil. The length of the push was about 0.6 to 1.0m beyond the bottom of the borehole, depending on the stiffness of the soils. After the tool was pushed, the drill string was raised about 1.5m to prevent contact with the pawls and the landing ring while the piezoprobe acquired data. The pressure transducer transmitted electronic signals through an armored cable to a computer on deck, where the data were continuously displayed in real time and stored digitally. The pore pressures were sampled at a rate of one reading per second during the test. When sufficient data had been obtained, the tool was retrieved. A schematic drawing showing the small diameter piezoprobe device is presented on Plate 2. A pore pressure transducer was used to measure the pore pressures in the soil formation, which was in contact with the sediment through a porous stone. Silicon oil was used as the pressure transducing fluid. A temperature transducer was also incorporated in the tool and the data were used to correct the measured pressures.

The absolute pressures recorded after measuring hydrostatic pressure are presented as plots of pore pressure versus elapsed time in Plates 3 and 4. The plots show peak pressure after insertion followed by pore pressure dissipation stabilizing at ambient condition. The excess pore-water pressure in the soil formation is the difference between the equilibrium piezometric pressure (ambient pressure) and the calculated hydrostatic pressure at the test depth. Calculated hydrostatic pressures are annotated on the plots. The temperature data recorded during the test and normalized excess pore-water pressure dissipation curve are presented in Plate 5.

We appreciate the opportunity to be of service to you on this project. Please call us if you have any questions or when we can be of further assistance.

Sincerely,

FUGRO-McCLELLAND  
Marine Geosciences, Inc.

A handwritten signature in blue ink, appearing to read "Ko Min Tjok".

Ko Min Tjok  
Senior Project Supervisor

A handwritten signature in black ink, appearing to read "Jean M. E. Audibert".

Jean M. E. Audibert, Ph.D., P.E.  
Engineering Department Manager

(KMT\JMEA\4655\1rpt.doc)  
Copies Submitted: (1)

<u>Date</u>	<u>Time</u>		<u>Description of Activities</u>
	<u>From</u>	<u>To</u>	
July 9, 2002	0900	1900	FMMG Engineer and EM technician travel from Houston to Ogden Point Dock, Victoria, BC, Canada and board R/V <i>Joides Resolution</i> .
	1900	2400	Standby onboard R/V <i>Joides Resolution</i> .
July 10, 2002	0000	0900	Standby onboard R/V <i>Joides Resolution</i> .
	0900	1100	Safety meeting.
	1100	1300	Standby onboard R/V <i>Joides Resolution</i> .
	1300	1400	Scientist meeting.
	1400	2400	Standby onboard R/V <i>Joides Resolution</i> .
July 11, 2002	0000	0830	Standby onboard R/V <i>Joides Resolution</i> .
	0830	0930	Pre-sail meeting.
	****	0930	R/V <i>Joides Resolution</i> departs Ogden Point Dock.
	0930	2400	Travel to Site 1244, Offshore Oregon.
July 12, 2002	0000	1030	Standby onboard R/V <i>Joides Resolution</i> .
	1030	1530	Pre-assemble the piezoprobe tool in three sections. Arrive on location and start rigging up BHA at about 1200 hrs.
	1530	1700	Perform trial run of the entire piezoprobe assembly with the BHA.
	1700	2400	Commence running drill pipe.
July 13, 2002	0000	0600	Standby onboard R/V <i>Joides Resolution</i> .
	0600	0800	Assembled the piezoprobe as they entered drill pipe.
	0800	0850	Rig up wireline.
	0850	1015	Lowering the piezoprobe to bottom of borehole.
	1015	1100	Attempt to set the tool downhole (loss communication with the tool).
	****	1100	Loss the tool downhole, because the connection between the end of the pig tail cable and the piezoprobe tool was disconnected downhole.
	1100	1200	Recover wireline and pig tail cable on deck.
	1200	1600	Pull pipe to recover piezoprobe tool.
1600	1935	Trip pipe downhole.	

## SUMMARY OF FIELD OPERATIONS

Ocean Drilling Program (ODP)  
Site 1244 (HR1A), Offshore Oregon

<u>Date</u>	<u>Time</u>		<u>Description of Activities</u>
	<u>From</u>	<u>To</u>	
July 13, 2002	1935	2400	Continue drilling and obtained APC cores.
July 14, 2002	0000	0030	Assembled the piezoprobe tool.
	0030	0230	Deploy and perform piezoprobe dissipation test at 53.5m below mudline (BML).
	0230	0315	Recover piezoprobe tool on deck.
	0315	2400	Standby for piezoprobe testing.
July 15, 2002	0000	2400	Standby for piezoprobe testing.
July 16, 2002	0000	0015	Advise by ODP that the schedule piezoprobe test at the termination of the borehole is cancelled due to squeezing of the hole formation and instructed to rig down the piezoprobe tool.
	0015	1000	Standby.
	1000	1700	Continue to rig down the piezoprobe equipment and prepare the piezoprobe equipment to be ship onshore.
	1700	2400	Standby onboard R/V <i>Joides Resolution</i> .
July 17, 2002	0000	2400	Standby onboard R/V <i>Joides Resolution</i> .
July 18, 2002	0000	2400	Standby onboard R/V <i>Joides Resolution</i> .
July 19, 2002	0000	1200	Standby for Helicopter.
	****	1200	FMMG personal depart R/V <i>Joides Resolution</i> by Helicopter.

## SUMMARY OF FIELD OPERATIONS

Ocean Drilling Program (ODP)  
Site 1244 (HR1A), Offshore Oregon

# Small Diameter Piezoprobe



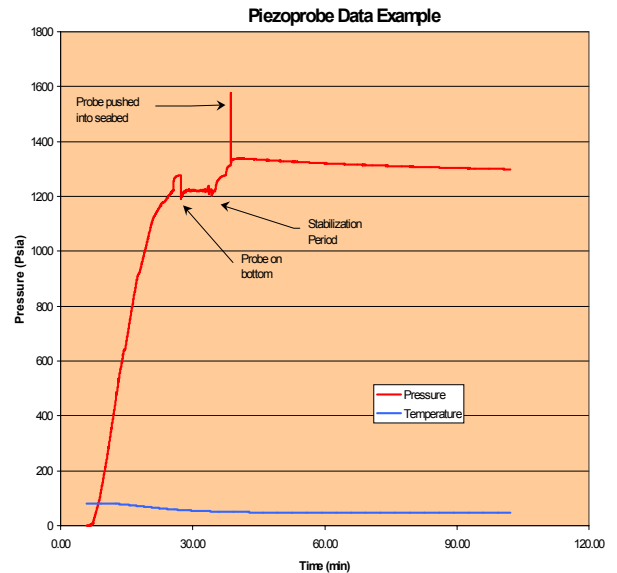
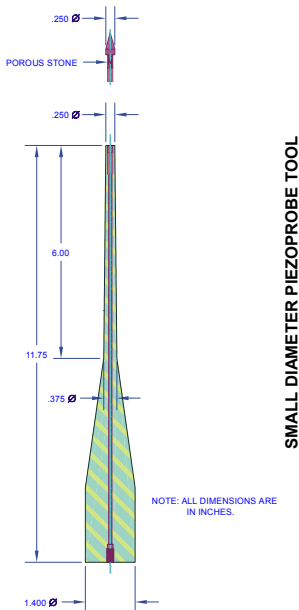
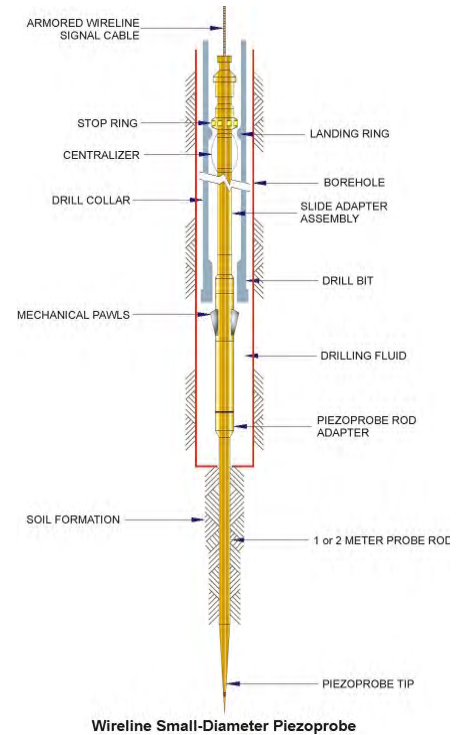
During testing, the pressure transducer transmits signals through the armored cable to a computer on deck of the vessel, where the data are continuously displayed in real time on the computer screen. Data are collected every second over the first hour and then once every 5 to 10 seconds. The frequency of reading accommodates the 90 to 95 percent dissipation in the first few hours of testing.

The data from the tests are synthesized to determine the excess pore pressure and the rate of pore pressure dissipation. Additionally, the data can be used to estimate the permeability and consolidation characteristics. The data has been utilized to better calculate the pile-soil set-up phenomenon for driven piles.

## General Tool Specifications

SPARTEK SS2700 Sapphire Pressure/Temperature

Temperature range:	150	°C (Max)
Pressure range:	5000	psia
Pressure resolution:	0.0004%	FS
Total system accuracy:	+/-0.022%	FS
Min. Sample rate:	1	HZ





## Small Diameter Piezoprobe



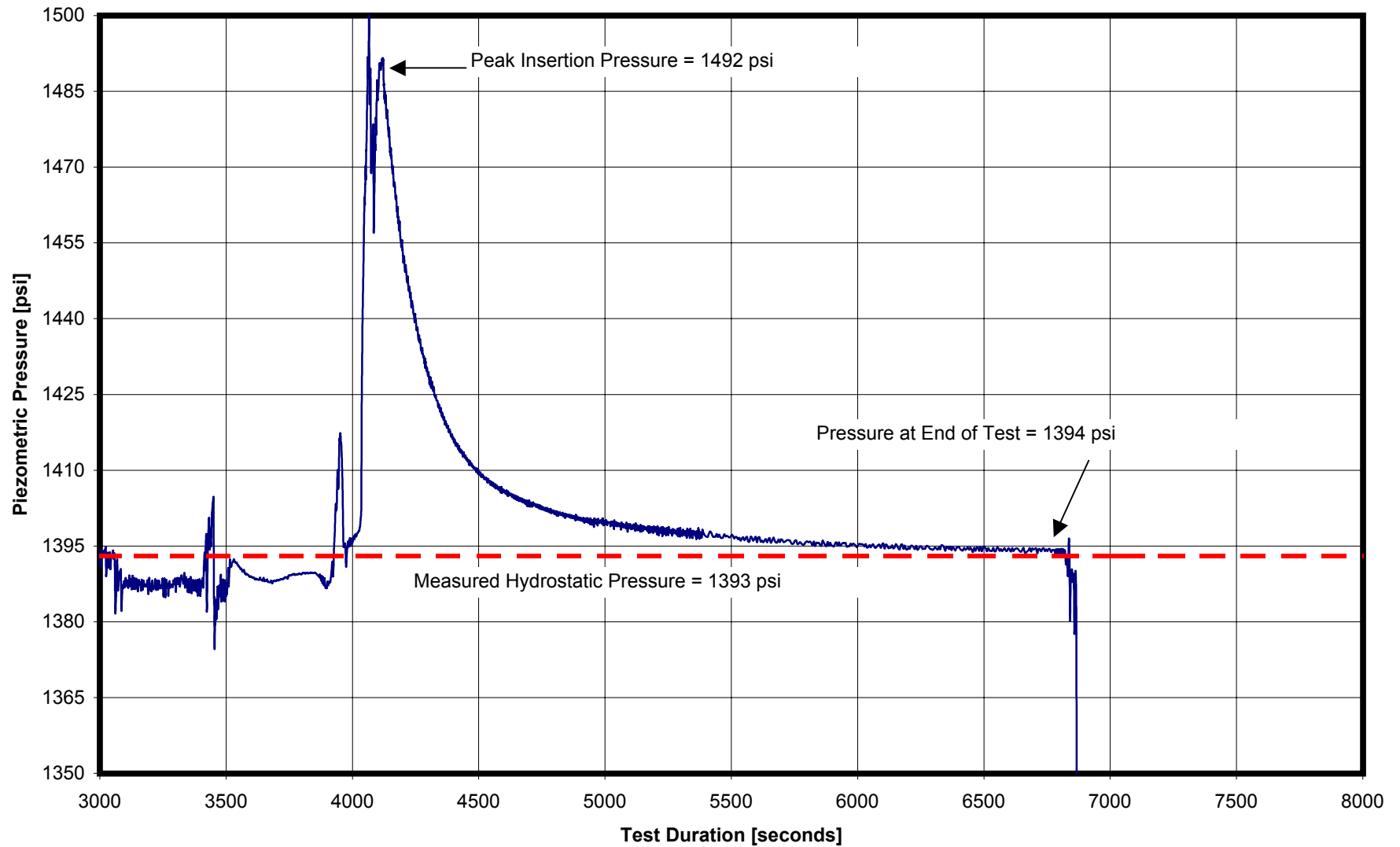
The small diameter Piezoprobe was designed to measure excess pore pressure and determine the dissipation characteristics of the sub-soils. In addition, results from the tests could be used to estimate the insitu permeability and consolidation characteristics of the soil, as well as provide insight into pile-soil set-up. The tool was made compatible with the Dolphin suite of in-situ tools to facilitate deployment.

The probe has a sleeve diameter of 1.4-inches reduced down to 1/4-inch at the tip of the tool. The pore pressure-measuring device is located at the tip of the tool. The pressure at the porous stone is measured using a Panex pressure transducer. The tool is capable of recording the pressure and temperature data on a remote memory unit attached to the tool, as well as in "real time" via a small umbilical to the vessels deck.

The tool is deployed using wireline techniques to enable testing to be performed at any designed depth. Once the test depth is achieved, the probe is lowered through the annulus of the drill string using an armored wireline signal cable and constant tension winch. The tool latches into the drillstring and is pushed into the soil using the weight of the drill pipe. The tool is typically pushed from 2 to 3 feet into the soil in front of the drill bit. After the tool is pushed into the virgin soil, the drillstring is raised to prevent contact with the drill pipe during data acquisition.

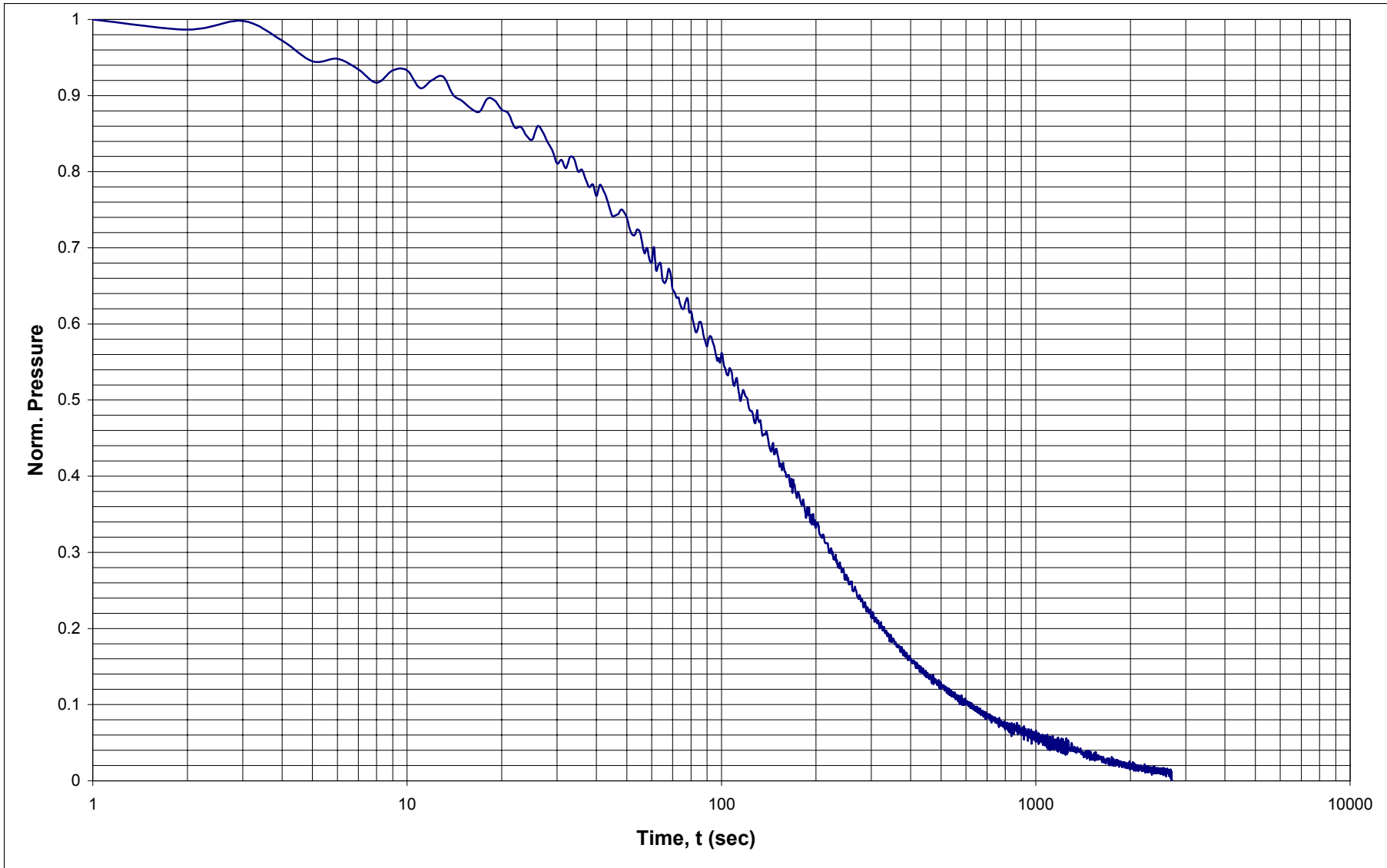
### Applications

- Measure excess pore pressure
- Measure pore pressure dissipation
- Estimate insitu permeability
- Estimate consolidation characteristics
- Estimate pile set-up characteristics

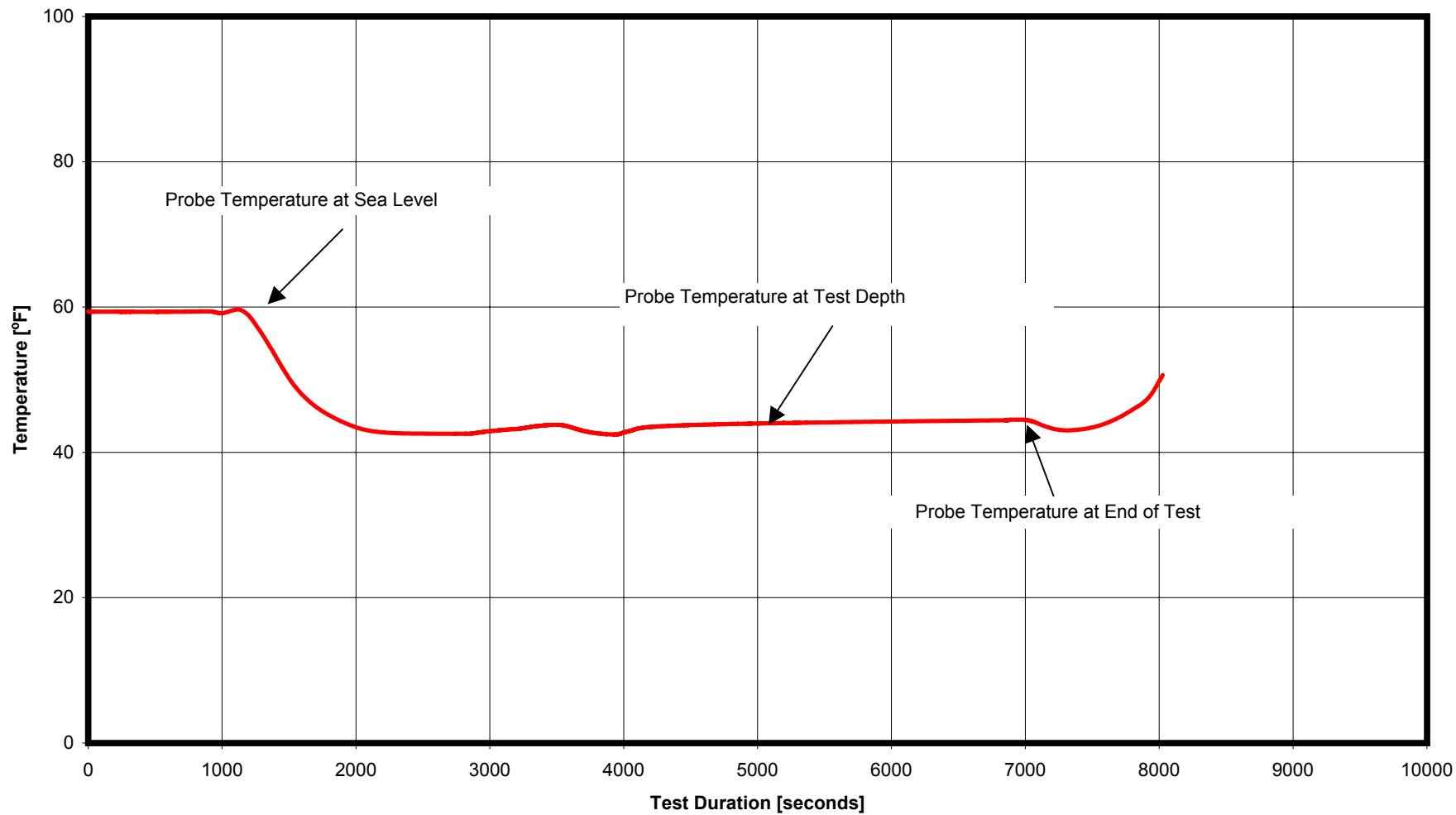


**Pore Pressure Dissipation versus Time**

Piezoprobe Test at 53.5m BML  
Site 1244 (Location HR1A)



**Normalized Pore Pressure versus Log Time Curve**  
Piezoprobe Test Depth: 53.5m (176-ft)  
Site 1244 (Location HR1A)



**Piezoprobe Temperature versus Time**  
Piezoprobe Test at 53.5m BML  
Site 1244 (Location HR1A)

**APPENDIX B**

**MEASURING PORE PRESSURE IN MARINE SEDIMENTS WITH  
PENETROMETERS: COMPARISON OF THE PIEZOPROBE AND DVTP-P  
TOOLS IN ODP LEG 204.**

**Brandon Dugan  
Pennsylvania State University**

**(19 pg. Report, plus 8 Figures)**

**Measuring Pore Pressure in Marine Sediments with Penetrometers: Comparison of the  
Piezoprobe and DVTP-P Tools in ODP Leg 204**

Brandon Dugan

Department of Geosciences

Penn State University, University Park PA 16801

Research Advisor: Peter B. Flemings

Report Authors: Brandon Dugan, Peter B. Flemings (Penn State University), Frank R. Rack  
(Joint Oceanographic Institutions, Inc.), Gerhard Bohrmann (GEOMAR), Anne M. Trehu  
(Oregon State University), Derryl Schroeder (Ocean Drilling Program), and the Shipboard  
Scientists of ODP Leg 204

## ABSTRACT

Fugro-McClelland Marine Geosciences Inc.'s piezoprobe, a penetration-based tool used to determine pore pressure and hydrologic properties within a borehole, was deployed for the first time in the Ocean Drilling Program (ODP) on ODP Leg 204 in July 2002. Analysis of the piezoprobe data suggests that *in situ* pore pressure is 9.5 MPa, which is approximately the hydrostatic pressure (9.53 MPa). The piezoprobe deployment and modeling of the results provides one of the first measurements of *in situ* permeability made within the borehole. From the piezoprobe dissipation data, we estimate of *in situ* permeability of approximately  $1.5 \times 10^{-17} \text{ m}^2$  for the hemipelagic clay. This is consistent with laboratory-measured permeability ( $\sim 1 \times 10^{-17} \text{ m}^2$ ) on hemipelagic clay samples from nearby ODP Site 892. The piezoprobe results were compared to a Davis-Villinger Temperature/Pressure Probe (DVTP-P) measurement made at the same depth, and in the same lithology, but in an adjacent borehole. The DVTP- P is also a penetration-based tool, however it has a much wider probe diameter. The DVTP-P generated a higher peak pressure that did not dissipate as much as the piezoprobe pressure, which resulted in a DVTP-P estimate of *in situ* pressure that nearly equals the overburden stress. The results suggest that a narrow diameter probe like the piezoprobe can be used to rapidly determine *in situ* pressure and hydrologic properties in sites investigated by the Ocean Drilling Program.

## INTRODUCTION

Rock deformation, sediment strength, and regional fluid fluxes are directly related to pore pressure and hydrologic properties of the sub-seafloor sediments. Three geologic systems that can be more completely defined through direct measurements of pressure are (1) fluid flow and stability of continental margins, (2) fault activation, decollement location and propagation, and geometry in accretionary prisms, and (3) free gas and water migration, hydrate formation, and rock strength in gas hydrate provinces.

The role that pore fluids have in sculpting continental slope geomorphology has intrigued scientists since the diverse structure of slopes was identified [1, 2] (Figure 1A). Excess fluid pressure has been attributed to landslides and failures on low angle slopes that would not fail without excess pressure [3, 4]. More recently focused fluid migration along permeable layers has been invoked as a major contributor to the timing and distribution of sediment deformation and failure [5, 6, 7, 8]. Models predict the magnitude of pressure required to generate slope instability and provide insights into the origins of the required excess pressure. Relatively few direct measurements exist to test the models, so the models are typically compared to pressure estimates from proxy data such as porosity [9] or seismic velocity [10].

Fluid migration within accretionary complexes has been described for its importance to heat and chemical transport [11] (Figure 1B). Fluids have also been cited as a driving force in the geometry and structure of accretionary complexes [12, 13, 14]. Porosity and seismic data have been used with models to estimate pressure, flow paths, and fluid fluxes [15, 16, 17]. These models also constrain the contribution of fluids to deformation, chemical transport, and heat flow. Validation of these models and their interpretations has not been extensive because of the lack of direct pressure measurements. The Ocean Drilling Program (ODP) has started to collect direct measurements of pressure, temperature, and pore fluid chemistry with long-term observatories (CORKs, ACORKs) [18, 19, 20].

The pressure and stress in gas hydrate provinces is not well defined, is lacking robust multiphase models, and has very few direct observations. These pressures and stresses, however, are critical to the dynamics of this multiphase system. Fluid pressure impacts the solubility of gas in water, governs the stability of gas hydrate [21, 22], defines the permeability of the system, and

pressure gradients dictate the flow field (Figure 1C). A detailed analysis of the complex hydrate system is required: (1) to define the volume of gas stored as hydrate and as free gas beneath hydrate [21]; (2) to understand the mechanics by which gas migrates and is released [23, 24, 25]; (3) to characterize the role of hydrate dissociation in slope failure [26, 27]; and (4) to estimate the potential role of catastrophic methane release on climate [28].

In this report, we describe the results of the Fugro-McClelland Marine Geosciences Inc.'s piezoprobe and the Davis-Villinger Temperature/Pressure Probe (DVTP-P) pressure measurements made on ODP Leg 204 at ODP Site 1244, Hydrate Ridge, offshore Oregon, USA. The tools are designed to make rapid measurements of pressure and hydrologic properties in low permeability sediments. We analyze the results from both tools, compare their results, and comment on the *in situ* conditions by analyzing the data that most accurately represent the natural system.

## **PRESSURE MEASUREMENT**

Direct pressure measurements are rare and expensive, but are required to advance research of submarine hydrodynamic systems. The ODP has historically relied on CORKs and ACORKs to monitor pressure, temperature, and fluid chemistry over many years. This characterizes the *in situ* conditions but the time and cost of acquiring data make the studies unrealistic for making robust and routine measurements beneath the seafloor.

An alternative approach to measuring *in situ* pressure is to use a penetration device. These measurements only take hours. Penetration devices that have been deployed in deep marine settings include free-fall penetration devices that sample pressure within a few meters of the seafloor. These include the Puppi [29, 30] and an early probe by Davis *et al.* [31]. A second class of instruments has been developed for use in boreholes. Two examples of these include the DVTP-P tool deployed on ODP Leg 190 [32] and the piezoprobe device [33, 34, 35].

The DVTP-P tool and the piezoprobe are similar devices. The tools have certain operational differences, with the key difference being the geometry of the tools (Figure 2). The tools induce a pressure pulse as they are inserted into sediments. The initial pressure response and its decay are defined by the insertion rate of the probe, the modulus of the sediment, and the bulk permeability

of the sediment. The tool geometry coupled with the penetration rate dictate the spatial distribution of induced pressure; for a similar insertion rate, these tools produce different excess pore pressure distributions because of their different geometries. The pressure dissipation is used to infer *in situ* pressure and rock properties [34, 35].

The piezoprobe has a narrow probe that is 170 mm long including the short, tapered tip. The probe has diameter of 6.4 mm. A larger diameter shoulder assembly connects the probe to the drillstring [34] (Figure 2). At the tip of the probe, a porous element allows communication of pore fluid with the pressure transducer.

The DVTP-P has a different geometry and thus a different pressure response. The DVTP-P has a longer and wider taper than the piezoprobe (Figure 2); its length is over twice that of the piezoprobe and the maximum diameter is almost twice that of the shoulder of the piezoprobe [36]. The pressure transducer is located farther from the probe tip than it is on the piezoprobe (Figure 2); this impacts the time required to interpret the *in situ* pressure and rock properties.

The tools have been designed to allow estimation of pressure and rock properties from the pressure data. The initial excess pressure during steady penetration can be related to the peak excess pressure and used to estimate the shear modulus of the sediments if conditions are undrained [37] or local permeability if partial drainage occurs [38]. After the tool insertion has ceased, the pressure dissipation allows estimation of the coefficient of consolidation [37, 39, 40], which can be used to infer permeability.

Penetration devices and long term monitoring stations will provide a full suite of pressure and rock property data beneath the seafloor that will increase our understanding of the sub-seafloor hydrologic system. The cooperative use of the devices will provide real-time and human-time scale data sets for understanding the dynamics of complex hydrodynamic systems. The data will also provide tests and calibrations of laboratory techniques used to interpret pressure, stress, and deformation. Many approaches have been used in the laboratory to estimate basin-scale pressures and rock properties from core samples [16, 41, 42, 43].

## **TEST SITE**

ODP Site 1244 is located on Hydrate Ridge in 895.43 m of water (Figure 3). The presence of

gas hydrate and free gas are interpreted based on a prominent bottom simulating reflector in seismic data [44]. One piezoprobe measurement was made at 53.66 meters below seafloor (mbsf) in Hole 1244C. This measurement was made in an interval of hemipelagic clay. A DVTP-P measurement was made in Hole 1244E at 52.6 mbsf in hemipelagic clay. Holes 1244C and E are located approximately 40 m apart. Site 1244 was dominated by hemipelagic clay with some turbiditic interlayers of silt and sand that find upward; the turbidite layers were most common and thickest between 69 and 245 mbsf. Below 245 mbsf, the lithology changes to indurated and fractured claystone with glauconite rich silt and sand interbeds.

At the depth of the piezoprobe and DVTP-P measurements, *in situ* porosity is between 61 and 64% (void ratio between 1.56 and 1.78), based on shipboard measurements of porosity from samples collected near the tool deployments (Figure 4). Porosity decreases downhole from 70% at the seafloor to just below 50% at 160 mbsf. The piezoprobe and DVTP-P deployments coincide to a depth where an increase in porosity is present (Figure 4).

Shipboard bulk density measurements were integrated to calculate the vertical hydrostatic effective stress ( $\sigma_{vh}'$ ) at Site 1244 (Figure 4);  $\sigma_{vh}'$  is the total overburden stress less hydrostatic fluid pressure ( $\sigma_{vh}' = \sigma_v - u_h$ ). The vertical hydrostatic stress at the piezoprobe deployment depth is 0.331 MPa. At the DVTP-P deployment depth,  $\sigma_{vh}'$  is 0.327 MPa. Measurements on samples from ODP Site 892 (located near Site 1244 in Figure 3) establish the permeability for the hemipelagic clay to be  $\sim 1 \times 10^{-17} \text{ m}^2$  (range =  $3.4 \times 10^{-17} - 8.5 \times 10^{-18} \text{ m}^2$ ) at *in situ* stress [16].

## **PIEZOPROBE AND DVTP-P DEPLOYMENT**

The piezoprobe was deployed on ODP Leg 204, Site 1244, Hole C on 14 July 2002. The deployment events for the test are described in Table 1 and the pressure history recorded by the piezoprobe is shown in Figure 5. We calculated the hydrostatic pressure ( $u_h$ ) by assuming a fluid density of  $1.024 \text{ g/cm}^3$  (Table 2). We calculated the overburden stress ( $\sigma_v$ ) by integrating core porosity and density measurements (Figure 4; Table 2). Thirty minutes into the deployment (#2, Figure 5A) the tool reached the seafloor. Thereafter it was lowered 53 meters to the bottom of the borehole (#4, Figures 5A, 5B). The tool pressure when the probe is at or near the base of the hole is slightly greater than the estimated hydrostatic stress (Figure 5B). This could be due to

poor tool calibration, a borehole fluid density greater than  $1.024 \text{ g/cm}^3$  (due to sediment in the borehole or greater salinity), or additional borehole pressure resulting from pumping. The piezoprobe test lasted 45 minutes (Table 1, Figure 5A). An initial peak pressure of 10.29 MPa declined ultimately to 9.615 MPa (Table 3). This final pressure is 0.08 MPa greater than  $u_h$  (Figure 6).

The DVTP-P test lasted 33.5 minutes with a peak pressure of 10.55 MPa and a final pressure of 9.79 MPa (Table 3; Figure 6). Abrupt jumps in the pressure data approximately five minutes after insertion may have resulted from tension on the probe. The DVTP-P measurement was made in Hole 1244E, approximately 40 m from the piezoprobe test at Hole 1244C. It is reasonable to assume that these probes are sampling approximately the same material. Differences between the two measurements are: (1) the initial penetration pressure of the DVTP-P is significantly greater than the piezoprobe, (2) the DVTP-P pressure does not decline to as low a pressure as the piezoprobe pressure does, and (3) the DVTP-P pressure is dropping more rapidly than the piezoprobe pressure at the end of the test (Figure 6).

The excess pore pressure ratio (Figure 7A) is the pore pressure ( $u$ ) normalized by the peak pore pressure ( $u_i$ ) (Table 3). It is a useful way to measure the relative dissipation that has occurred. In this case, we have normalized the pressure relative to the hydrostatic pressure ( $u_h$ ). From this plot is clear that the piezoprobe has dissipated significantly more relative to its peak pressure than the DVTP-P has dissipated. The normalized excess pore pressure (Figure 7B) is a measure of the magnitude of the pore pressure ( $u$ ) relative to the hydrostatic effective stress ( $\sigma_{vh}'$ ). The DVTP-P generates pore pressure three times greater than  $\sigma_{vh}'$ , while the piezoprobe generates pressure only two times  $\sigma_{vh}'$  (Figure 7B).

## PIEZOPROBE AND DVTP-P INTERPRETATION

We desire to interpret both the *in situ* pressure and hydraulic properties (e.g. permeability) from the piezoprobe test. Whittle *et al.* [34] propose that there is a characteristic dissipation curve associated with the piezoprobe and that given a soil model, permeability can be derived based on the following equation for normally consolidated clays,

$$T = \frac{s' kt}{g_w R_2^2} \quad (1)$$

$T$  is the time factor and  $s'$  is the mean effective stress. We have assumed  $s' = 0.67s_{vh}'$ .  $g_w$  is the unit weight of water,  $k$  is the hydraulic conductivity,  $t$  is time, and  $R_2$  is the radius of the piezoprobe at the shaft (35.6 mm).  $T_{50}$  is the time factor at 50% dissipation, while  $t_{50}$  is the absolute time at 50% dissipation. Whittle *et al.* [34] model  $T_{50}$  to be  $1.72 \times 10^{-3}$  for Boston Blue Clay with an overconsolidation ratio of 1.2.

To determine permeability we substitute  $T_{50}$  and  $t_{50}$  into Equation 1. However, to determine  $t_{50}$ , we must determine the final pressure,  $u^*$ . We assumed two values for  $u^*$ : 9.5 and 9.6 MPa. With these assumptions, two pore pressure ratio curves generated and  $t_{50}$  is determined to be 120 and 165 seconds (gray and black solid curves, Figures 8A, 8B). The two  $u^*$  values yield hydraulic conductivities of  $1.9 \times 10^{-8}$  cm/sec and  $1.4 \times 10^{-8}$  cm/sec. These hydraulic conductivities equate to permeabilities of  $1.96 \times 10^{-17}$  m<sup>2</sup> and  $1.43 \times 10^{-17}$  m<sup>2</sup>. The small variation in permeability suggests that the permeability is not very sensitive to the estimate of *in situ* pressure. These values are in the same range as those measured by [16].

To determine which of the proposed  $u^*$  values is appropriate, the curves are fitted to Whittle's normalized dissipation curve for Boston Blue Clay (dotted and dashed lines, Figures 8A, 8B) [34]. In linear time (Figure 8A) and log time (Figure 8B), it is clear that with  $u^* = 9.5$  MPa there is a much better fit of the modeled curve than with  $u^* = 9.6$  MPa.  $u^* = 9.5$  MPa is very close to the hydrostatic pressure ( $u_h = 9.53$  MPa).

This prediction is compared to an inverse time extrapolation (Figure 8C). In this approach, measured pressures are plotted as a function of inverse time and the y-intercept is an estimate of the *in situ* pressure ( $u_{it}$ ) [31, 33, 34]. We find  $u_{it}$  is 9.71 MPa for the DVTP-P and 9.59 MPa for the piezoprobe (Figure 8C).  $u_{it}$  is an overestimate of the *in situ* pressure [45] and thus the  $u^*$  of 9.5 MPa derived from the piezoprobe is a reasonable estimate.

In summary, analysis of the piezoprobe data suggests that *in situ* pore pressure (9.5 MPa) is nearly hydrostatic (9.53 MPa) and *in situ* permeability is approximately  $1.5 \times 10^{-17}$  m<sup>2</sup>. Over the time span of the piezoprobe test (45 minutes), 90% of the penetration-induced pore pressure was dissipated. It is important to recognize that the prediction of  $u^*$ , the *in situ* pressure, relies heavily

on the model-based normalized pressure dissipation curve derived specifically for the piezoprobe geometry and specific soil parameters. Whittle *et al.* [34] describe in detail the fact that because of the geometry of the piezoprobe where a large diameter shaft overlies a narrow diameter probe, there is a shelf in the pressure data (Figure 8B, between 100 and 1000 min). The pressure induced by the large diameter shaft that reaches the pressure transducer causes this shelf.

A second primary result is that the DVTP-P pressures have not dissipated as much as the piezoprobe pressures either relative to their peak pressures (Figure 7) or in absolute pressure (Figure 6). This is not surprising because the radius of the DVTP-P is three times that of the piezoprobe at the pressure port and the DVTP-P continues to widen above the pressure port (Figure 2). The dissipation time is proportional to the square of the radius (Equation 1). Thus, based on a cylindrical probe geometry,  $t_{50}$  for the DVTP-P should be nine times that of the piezoprobe, but experimentally it is only five times as great (Figure 8B).

## CONCLUSIONS

Deployment of the piezoprobe and the DVTP-P at Site 1244 of ODP Leg 1244 provided tests of both tools and estimates of *in situ* fluid pressures and rock properties. The piezoprobe data provide an estimate of *in situ* pressure equal to 9.5 MPa, which is nearly equal to the hydrostatic pressure at the depth of the experiment. The piezoprobe deployment and modeling of the results provides one of the first measurements of *in situ* permeability within the borehole. The dissipation data from the piezoprobe yield a permeability estimate of  $1.5 \times 10^{-17} \text{ m}^2$  for the hemipelagic clay; this is consistent with laboratory measurements ( $\sim 1 \times 10^{-17} \text{ m}^2$ ) on hemipelagic clay samples from nearby Site 892. The piezoprobe experiment only took approximately two hours from initial deployment until the tool was returned to the deck of the ship; 45 minutes of this time was the piezoprobe dissipation. The DVTP-P tool experiment, conducted in similar sediments, produced a significantly different pressure estimate. With 33 minutes of pressure dissipation, the DVTP-P pressure had dissipated to approximately the overburden stress and yields a pressure estimate of 9.71 MPa. Comparison of the DVTP-P and piezoprobe results suggest that a narrow diameter probe like the piezoprobe can be used to quickly and accurately determine *in situ* pressure and hydrologic properties of marine sediments.

The tests conducted on ODP Leg 204 are promising and suggest that future studies in marine geoscience and engineering can be strengthened with piezoprobe pressure and permeability observations. Continued use of the piezoprobe in sub-seafloor studies will expand research in a variety of geologic settings and will also provide real-time data that can be used to efficiently isolate regions of interest during emplacement of long term monitoring observatories.

## ACKNOWLEDGEMENTS

This work could not have been accomplished without the extraordinary efforts of the participants of ODP Leg 204. Assistance by J. Germaine (MIT) and A. Whittle (MIT) is deeply appreciated. Deployment of the piezoprobe was supported by the Ocean Drilling Program and the Department of Energy. This research used samples and/or data provided by the Ocean Drilling Program (ODP). ODP is sponsored by the US National Science Foundation and participating countries under management of Joint Oceanographic Institutions (JOI), Inc.

## REFERENCES

- [1] D.W. Johnson, *The Origin of Submarine Canyons : A Critical Review of Hypotheses*, 126 pp., Hafner, New York (1939).
- [2] P.A. Rona, "Middle Atlantic continental slope of United States; deposition and erosion", *AAPG Bulletin* 53(7), 1453-1465 (1969).
- [3] K. Terzaghi, "Mechanism of landslides", in: *Application of geology to engineering practice: Berkey volume*, 83-123, Geological Society of America, New York (1950).
- [4] E.G. Bombolakis, "Analysis of a Horizontal Catastrophic Landslide", in: *Mechanical Behavior of Crustal Rocks; The Handin Volume*, N.L. Carter, M. Friedman, J.M. Logan and D.W. Stearns, eds., 251-258, American Geophysical Union, Washington (1981).
- [5] B. Dugan and P.B. Flemings, "Overpressure and Fluid Flow in the New Jersey Continental Slope: Implications for Slope Failure and Cold Seeps", *Science* 289, 288-291 (2000).
- [6] B. Dugan and P.B. Flemings, "Fluid flow and stability of the US continental slope offshore New Jersey from the Pleistocene to the present", *Geofluids* 2(2), 137-146 (2002).

- [7] A. Boehm and J.C. Moore, "Fluidized sandstone intrusions as an indicator of paleostress orientation, Santa Cruz, California", *Geofluids* 2(2), 147-161 (2002).
- [8] W.C. Haneberg, "Groundwater Flow and the Stability of Heterogeneous Infinite Slopes Underlain by Impervious Substrata", in: *Clay and Shale Slope Instability*, W.C. Haneberg and S.A. Anderson, eds., 63-78, Geological Society of America, Boulder (1995).
- [9] B.S. Hart, P.B. Flemings and A. Deshpande, "Porosity and pressure; role of compaction disequilibrium in the development of geopressures in a Gulf Coast Pleistocene basin", *Geology* 23(1), 45-48 (1995).
- [10] N.L.B. Bangs, G.K. Westbrook, J.W. Ladd and P. Buhl, "Seismic Velocities from the Barbados Ridge Complex: Indicators of High Pore Fluid Pressures in an Accretionary Complex", *Journal of Geophysical Research* 95(B6), 8767-8782 (1990).
- [11] D.E. Karig and G.F. Sharman, "Subduction and Accretion in Trenches", *Geological Society of America Bulletin* 86(3), 377-389 (1975).
- [12] F.A. Dahlen, J. Suppe and D. Davis, "Mechanics of fold-and-thrust belts and accretionary wedges; cohesive Coulomb theory", *Journal of Geophysical Research* 89(12), 10087-10101 (1984).
- [13] D. Davis, J. Suppe and F.A. Dahlen, "Mechanics of fold-and-thrust belts and accretionary wedges", *Journal of Geophysical Research* 88(2), 1153-1172 (1983).
- [14] D.M. Saffer and B.A. Bekins, "Hydrologic Controls on the Morphology and Mechanics of Accretionary Wedges", *Geology* 30(3), 271-274 (2002).
- [15] B.A. Bekins and S. Dreiss, "A Simplified Analysis of Parameters Controlling Dewatering in Accretionary Prisms", *Earth and Planetary Science Letters* 109, 275-287 (1992).
- [16] K.M. Brown, "17. The Variation of the Hydraulic Conductivity Structure of an Overpressured Thrust Zone with Effective Stress", in: *Proceedings of the Ocean Drilling Program*, B. Carson, G.K. Westbrook, R.J. Musgrave and E. Suess, eds. 146, 281-289, Ocean Drilling Program, College Station (1995).
- [17] E. Screaton, D. Saffer, P. Henry, S. Hunze and Leg 190 Shipboard Scientific Party, "Porosity loss within the underthrust sediments of the Nankai accretionary complex: Implications for overpressures", *Geology* 30(1), 19-22 (2001).
- [18] E.E. Davis, K. Becker, T. Pettigrew, B. Caron and R. Macdonald, "CORK: A hydrologic

- seal and downhole observatory for deep-sea boreholes", in: *Proceedings of the Ocean Drilling Program, Initial Reports*, M.J. Mottl, E.E. Davis, A.T. Fisher and J.F. Slack, eds. 139, 42-53, Ocean Drilling Program, College Station (1992).
- [19] E.E. Davis and K. Becker, "Formation temperatures and pressures in a sedimented rift hydrothermal system; 10 months of CORK observations, holes 857D and 858G", *Proceedings of the Ocean Drilling Program, Scientific Results* 139, 649-666 (1994).
- [20] K. Becker, A.T. Fisher and E.E. Davis, "The Cork Experiment in Hole 949C: Long-Term Observations of Pressure and Temperature in the Barbados Accretionary Prism", *Proceedings of the Ocean Drilling Program Scientific Results* 156, 247-251 (1997).
- [21] K.A. Kvenvolden, "Gas hydrates-geological perspective and global change", *Reviews of Geophysics* 31(173-187.) (1993).
- [22] C. Ruppel, "Anomalously cold temperatures observed at the base of the gas hydrate stability zone on the U.S. Atlantic passive margin", *Geology* 25(8), 699-702 (1997).
- [23] W.S. Holbrook, D. Lizarralde, I.A. Pecher, A.R. Gorman, K.L. Hackwith, M. Hornbach and D. Saffer, "Escape of methane gas through sediment waves in a large methane hydrate province", *Geology* 30(5), 467-470 (2002).
- [24] R.D. Hyndman and E.E. Davis, "A mechanism for the formation of methane hydrate and Seafloor Bottom-Simulating reflectors by vertical fluid expulsion", *Journal of Geophysical Research* 97(B5), 7025-7041 (1992).
- [25] X. Liu and P.B. Flemings, "Stress-limited gas column height in the gas hydrate system of Blake Ridge", in: *Proceedings of the 4th Annual International Conference on Gas Hydrates*, Yokohama, Japan, (2002).
- [26] W.P. Dillon, W.W. Danforth, D.R. Hutchinson, R.M. Drury, M.H. Taylor and J.S. Booth, "Evidence for faulting related to dissociation of gas hydrate and release of methane off the Southeastern United States", in: *Gas Hydrates: Relevance to World Margin Stability and Climate Change*, J.-P. Henriot and J. Mienert, eds., Special Publications 137, 293-302, Geological Society, London (1998).
- [27] W.P. Dillon, J.W. Nealon, M.H. Taylor, M.W. Lee, R.M. Drury and C.H. Anton, "Seafloor collapse and methane venting associated with gas hydrate on the Blake Ridge; causes and implications to seafloor stability and methane release", in: *Geophysical Monograph*, C.K.

- Paull and W.P. Dillon, eds. 124, 211-233 (2000).
- [28] G.R. Dickens, M.M. Castillo and J.C.G. Walker, "A blast of gas in the latest Paleocene: Simulating first-order effects of massive dissociation of oceanic methane hydrate", *Geology* 25(3), 259-262 (1997).
- [29] P.J. Schultheiss and S.D. McPhail, "Direct indication of pore-water advection from pore pressure measurements in Madeira abyssal plain sediments", *Nature* 320(6060), 348-350 (1986).
- [30] R. Urgeles, M. Canals, J. Roberts and SNV "Las Palmas" Shipboard Party, "Fluid flow from pore pressure measurements off La Palma, Canary Islands", *Journal of Volcanology and Geothermal Research* 101, 253-271 (2000).
- [31] E.E. Davis, G.C. Horel, R.D. MacDonald, H. Villinger, R.H. Bennett and H. Li, "Pore pressures and permeabilities measured in marine sediments with a tethered probe", *Journal of Geophysical Research* 96(4), 5975-5984 (1991).
- [32] G.F. Moore, A. Taira, N.L. Bangs, S. Kuramoto, T.H. Shipley, C.M. Alex, S.S. Gulick, D.J. Hills, T. Ike, S. Ito, S.C. Leslie, A.J. McCutcheon, K. Mochizuki, S. Morita, Y. Nakamura, J.O. Park, B.L. Taylor, G. Toyama, H. Yagi and Z. Zhao, *Structural setting of the Leg 190 Muroto Transect*, 14 pp., Texas A & M University, Ocean Drilling Program, College Station, TX (2001).
- [33] R.M. Ostermeier, J.H. Pelletier, C.D. Winker and J.W. Nicholson, "Trends in Shallow Sediment Pore Pressures - Deepwater Gulf of Mexico", *Society of Petroleum Engineers SPE/IADC 67772* (2001).
- [34] A.J. Whittle, T. Sutabutr, J.T. Germaine and A. Varney, "Prediction and interpretation of pore pressure dissipation for a tapered piezoprobe", *Geotechnique* 51(7), 601-617 (2001).
- [35] A.J. Whittle, T. Sutabutr, J.T. Germaine and A. Varney, "Prediction and interpretation of pore pressure dissipation for a tapered piezoprobe", in: *Offshore Technology Conference*, Houston, (2001).
- [36] D. Schroeder, personal communication (2002).
- [37] M.F. Randolph and C.P. Wroth, "An Analytical Solution for the Consolidation Around a Driven Pile", *International Journal for Numerical and Analytical Methods in Geomechanics* 3, 217-229 (1979).

- [38] D. Elsworth, "Dislocation Analysis of Penetration in Saturated Porous Media", *Journal of Geotechnical Engineering* 117(2), 391-408 (1991).
- [39] R.C. Gupta and J.L. Davidson, "Piezoprobe Determined Coefficient of Consolidation", *Soil and Foundations* 26(3), 12-22 (1986).
- [40] D. Elsworth, "Analysis of Piezocone Dissipation Data Using Dislocation Methods", *Journal of Geotechnical Engineering* 119(10), 1601-1623 (1993).
- [41] D.E. Karig and G. Hou, "High-stress consolidation experiments and their geologic implications", *Journal of Geophysical Research* 97(1), 289-300 (1992).
- [42] D.M. Saffer, E.A. Silver, A.T. Fisher, H. Tobin and K. Moran, "Inferred Pore Pressures at the Costa Rica Subduction Zone: Implications for Dewatering Processes", *Earth and Planetary Science Letters* 177, 193-207 (2000).
- [43] W.J. Winters, "Stress History and Geotechnical Properties of sediment from the Cape Fear Diapir, Blake Ridge Diapir, and Blake Ridge", in: *Proceedings of the Ocean Drilling Program, Scientific Results*, C.K. Paull, R. Matsumoto, P.J. Wallace and W.P. Dillon, eds. 164, 421-429, Texas A & M University, Ocean Drilling Program, College Station, TX (2000).
- [44] G. Bohrmann, A.M. Trehu, J. Baldauf and C. Richter, "Drilling Gas Hydrates on Hydrate Ridge, Cascadia Continental Margin: Leg 204 Scientific Prospectus", <http://www-odp.tamu.edu/publications/>, (2002).
- [45] A.J. Whittle, personal communication (2002).

## TABLES

**Table 1: Piezoprobe Deployment Log**

Event #	Time GMT	Time (minutes since deployment)	Event Description
1	7:32:34	0.565	Sitting in pipe--tip in water
2	8:09:22	37.365	Setting bit 7 meters from bottom
3	8:16:27	44.449	Lowering
4	8:22:11	50.182	Taking hydrostatic pressure
5	8:26:23	54.365	Pulled up 1.3 meters off of landing ring, now ~8 feet off bottom
6	8:27:13	55.215	Lowering bit down to 3.5 meters off bottom
7	8:36:35	64.582	Stopped pumping
8	8:38:22	66.365	Tagging bottom
9	8:39:31	67.515	Pushing
10	9:26:30	114.498	End of test - pulling
11	9:28:20	116.332	Coming to surface
12	9:45:42	133.699	At top of pipe

**Table 2: Site Parameters**

	Site, hole	mbsf (meters)	Depth Below Sea Level (meters)	Overburden Stress, $\sigma_v$ (MPa)	Hydrostatic Pressure, $u_h$ (MPa)	Hydrostatic Effective Stress, $\sigma_{vh}'$ (MPa)
Seafloor	1244C	0.0	895.43	8.995	8.995	0.0
Piezoprobe (7/14/02)	1244C	53.66	949.09	9.867	9.534	0.331
Seafloor	1244E	0	893.3	8.974	8.974	0
DVTP-P#2, Run 19 (8/19/02)	1244E	52.6	945.9	9.829	9.502	0.327

\* calculations assume seawater density of 1.024 g/cm<sup>3</sup>

**Table 3: Key Pressure Readings and Calculations**

Test	Duration of Dissipation (min)	Peak Pressure, $u_i$ (MPa)	Pressure at End of Test (MPa)	Hydrostatic Pressure, $u_h$ (MPa)	Inverse Time Prediction, $u_{lt}$ (MPa)	Final Pressure, $u^*$ (MPa)
Piezoprobe	45	10.29	9.614	9.53	9.59	9.5
DVTP-P	33.5	10.55	9.79	9.598	9.71	-

**Table 4: Nomenclature**

Symbol	Definition	Dimensions
$k$	hydraulic conductivity	L/T
$R_2$	radius at transducer	L
$T$	time factor	dimensionless
$T_{50}$	time factor at 50% dissipation	dimensionless
$t$	Time	T
$t_{50}$	time at 50% dissipation	T
$u$	pore pressure	M/LT <sup>2</sup>
$u_h$	hydrostatic pressure	M/LT <sup>2</sup>
$u_i$	peak pressure	M/LT <sup>2</sup>
$u_{lt}$	inverse time pressure estimate	M/LT <sup>2</sup>
$u^*$	final pressure	M/LT <sup>2</sup>
$g_w$	unit weight of water	M/L <sup>2</sup> T <sup>2</sup>
$s'$	mean effective stress	M/LT <sup>2</sup>
$s_v$	overburden stress	M/LT <sup>2</sup>
$s_{vh}'$	vertical hydrostatic effective stress	M/LT <sup>2</sup>

## FIGURE CAPTIONS

Figure 1. Direct pressure observations are necessary to describe a variety of sub-seafloor processes and seafloor geomorphology. Arrows illustrate flow paths that have been postulated for the systems, but require direct measurements to verify. (A) Continental slopes are environments where slope failure and seeps are common. High fluid pressures are often attributed to failure along low angle slopes but few direct measurements of *in situ* pressure have been collected to test the models. (B) Pore fluid pressure affects the flow of fluids along the decollement and within faults in accretionary complexes. Pressures also control the geometry of the accretionary complex, e.g. the angle between the decollement and seafloor is small when excess pressures are high and is large when pressures are hydrostatic. The transition from the proto-decollement (minimal to no deformation) to the decollement (failure and faulting) is believed to be a function of flow and fluid pressure. (C) Gas hydrate provinces are dynamic hydrologic systems where gas and water pressures affect the formation and dissociation of gas hydrate. Permeability and gas storage are interpreted to be self-controlling based on the pressure state. The release of hydrates and gas is important for its role in global climate and for its contribution to seafloor geomorphology. GHZ = gas hydrate zone. FGZ = free gas zone.

Figure 2. Geometry of the DVTP-P and the piezoprobe. Both tools have pressure transducers near their tip, but the tools have different geometries. The DVTP-P has a long, tapered cone that extends beyond the drillbit. DVTP-P geometry modified from [36]. The piezoprobe has a short, wide shoulder that is attached to a narrow lance where the pressure transducer is located. Geometry of piezoprobe based on [34]. The geometry of the probe and location of the pressure transducer affects the time required to accurately estimate *in situ* conditions.

Figure 3. Hydrate Ridge is located offshore Oregon, USA (inset map). Bathymetry contour interval is 100 m. Site 1244 is located near the southern crest of Hydrate Ridge. Core samples from Site 892 on the northern crest of Hydrate Ridge were used to estimate *in situ* stress and pressures [16]. DVTP-P and piezoprobe measurements at Site 1244 will help to test these inferences based on consolidation behavior of the sediments from Site 892. Consolidation experi-

ments from Site 1244 will also be completed to estimate pressure and stress for comparison to piezoprobe and DVTP-P measurements.

Figure 4. Summary of ODP Site 1244. PP = piezoprobe. Lithology is based on shipboard observations. Hydrostatic effective stress ( $\sigma_{vh}'$ ) is determined from density measured in Hole 1244C. Porosity from Hole 1244C is based on shipboard measurements and plotted on a linear scale; minimum and maximum void ratio are identified for reference.

Figure 5. Pressure versus time for the piezoprobe deployment to 53.66 mbsf in Site 1244C on 14 July 2002. (A) Long term pressure record during the time the piezoprobe was near the seafloor. Hydrostatic pressure ( $u_h$ ) and overburden stress ( $s_v$ ) for the depth of the piezoprobe penetration are shown. The piezoprobe deployment events are identified by number and are explained in Table 1. (B) Expanded view of the pressure prior to penetration. These data are generally used to estimate hydrostatic pressure. (C) Expanded view of the end of the dissipation profile. Piezoprobe pressure equilibrates to approximately the hydrostatic pressure.

Figure 6. Comparison of piezoprobe pressure dissipation and DVTP-P pressure dissipation. The DVTP-P has a higher pressure than the piezoprobe during and after insertion; maximum pressure is 10.55 MPa for the DVTP-P versus 10.29 MPa for the piezoprobe. Hydrostatic pressure ( $u_h$ ) and overburden stress ( $s_v$ ) at the piezoprobe deployment depth are shown for reference.

Figure 7. (A) Excess pore pressure ratio. Assuming that the *in situ* pressure is hydrostatic ( $u_h$ ), the piezoprobe has dissipated 90% of its induced pressure while the DVTP-P has dissipated approximately 80% of its induced pressure. (B) Normalized pore pressure for the piezoprobe and DVTP-P. The piezoprobe has an initial pressure that is approximately two times the inferred *in situ* effective stress ( $\sigma_{vh}'$ ). The DVTP-P pressure has a higher insertion pressure that only declines to approximately the *in situ* hydrostatic effective stress (normalized pressure = 1).

Figure 8. (A) Pore pressure ratio dissipation plots in linear time for the piezoprobe data assuming  $u^*$  equals 9.5 MPa (solid grey line) or 9.6 MPa (solid black line). Modeled pore pressure ratio

dissipation plots in linear time are also shown assuming hydraulic conductivity is  $1.4 \times 10^{-8}$  cm/sec (dotted line) or  $1.9 \times 10^{-8}$  cm/sec (dashed line). Model results with either hydraulic conductivity are most similar to piezoprobe data assuming  $u^*$  equals 9.5 MPa (B) Pore pressure ratio dissipation plots in log time for the piezoprobe data assuming  $u^*$  equals 9.5 MPa (solid grey line) or 9.6 MPa (solid black line). Modeled pore pressure ratio dissipation plots in log time are also shown assuming hydraulic conductivity is  $1.4 \times 10^{-8}$  cm/sec (dotted line) or  $1.9 \times 10^{-8}$  cm/sec (dashed line). An *in situ* pressure of 9.5 MPa is consistent with model results. (C) Inverse time-pressure extrapolation to estimate *in situ* pore pressure for piezoprobe and DVTP-P data. DVTP-P data yield an estimate of 9.71 MPa whereas the piezoprobe data yield an estimate of 9.59 MPa.  $u^*$  values of 9.5 and 9.6 MPa used in (8A) and (8B) are shown for reference.  $u_h$  is also shown for reference.

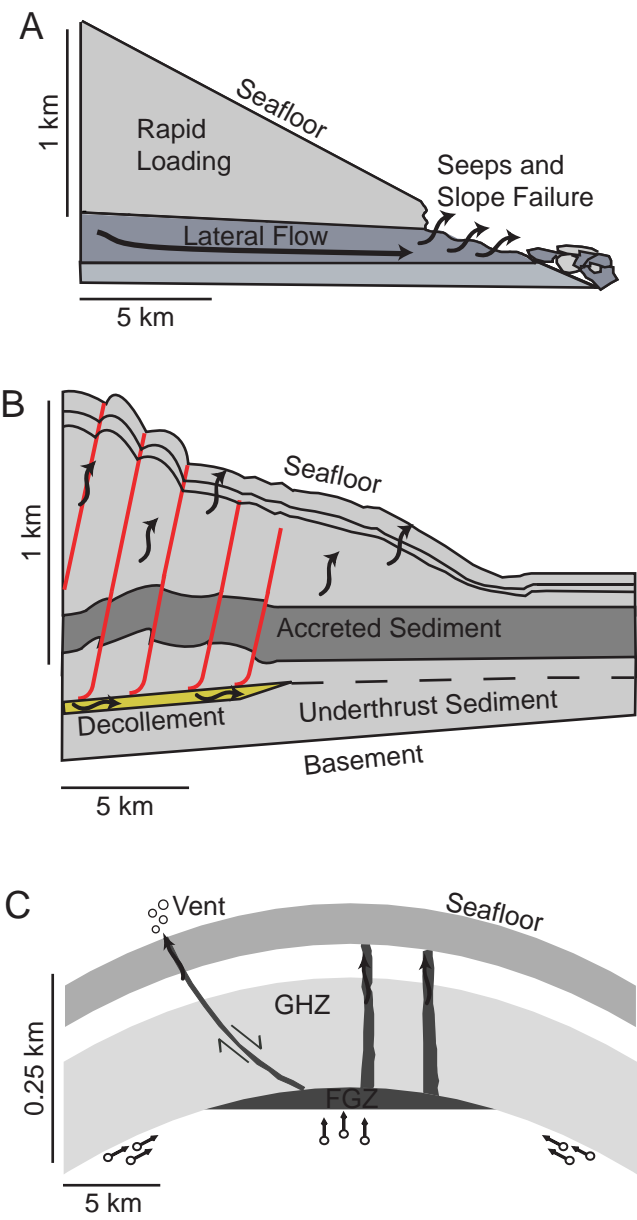


Figure 1  
Dugan

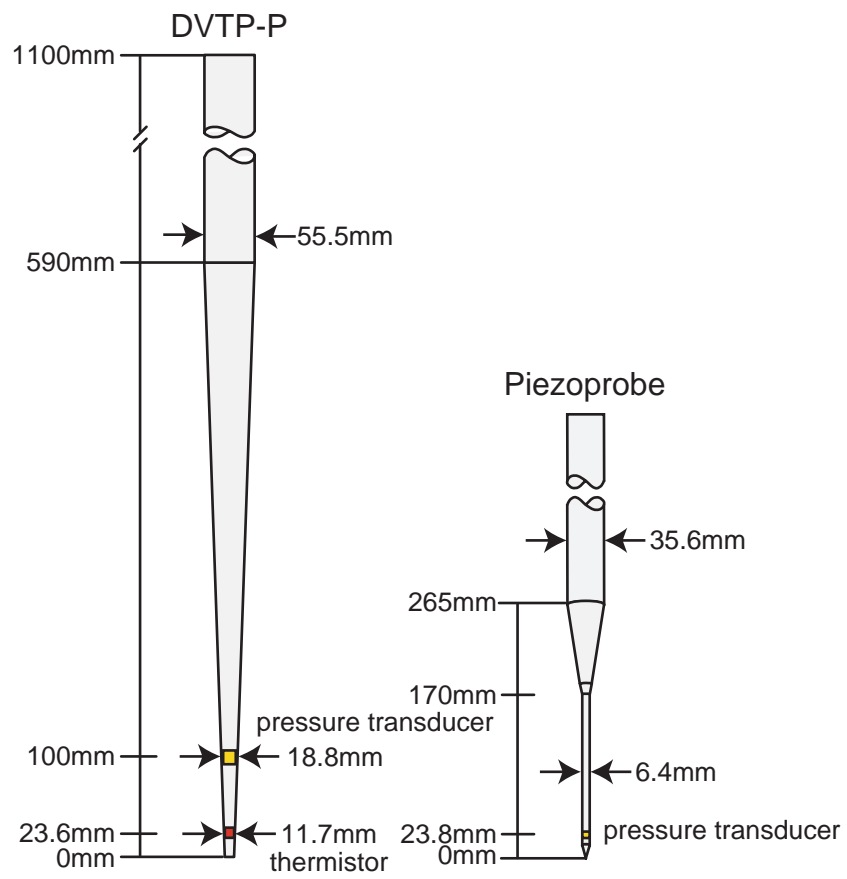


Figure 2  
Dugan

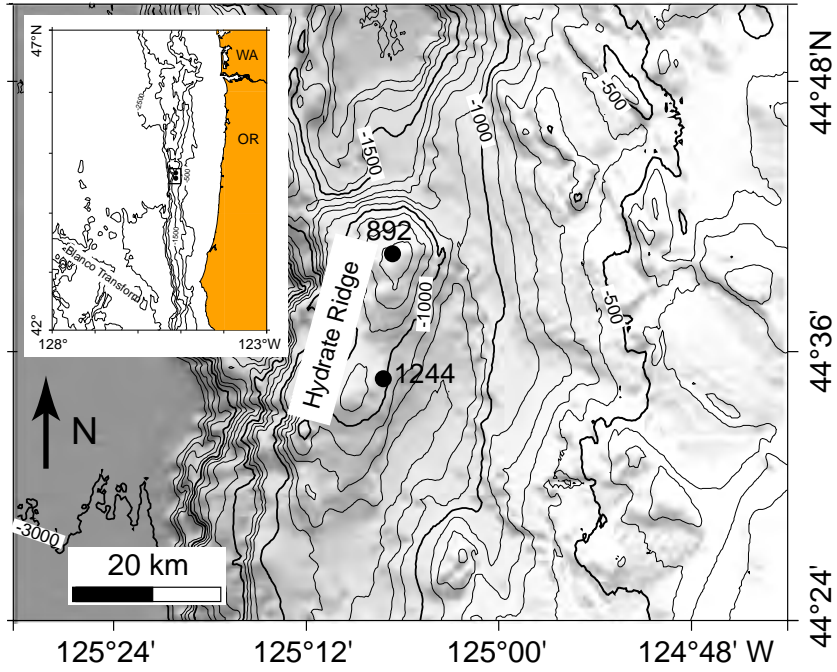


Figure 3  
Dugan

Site 1244

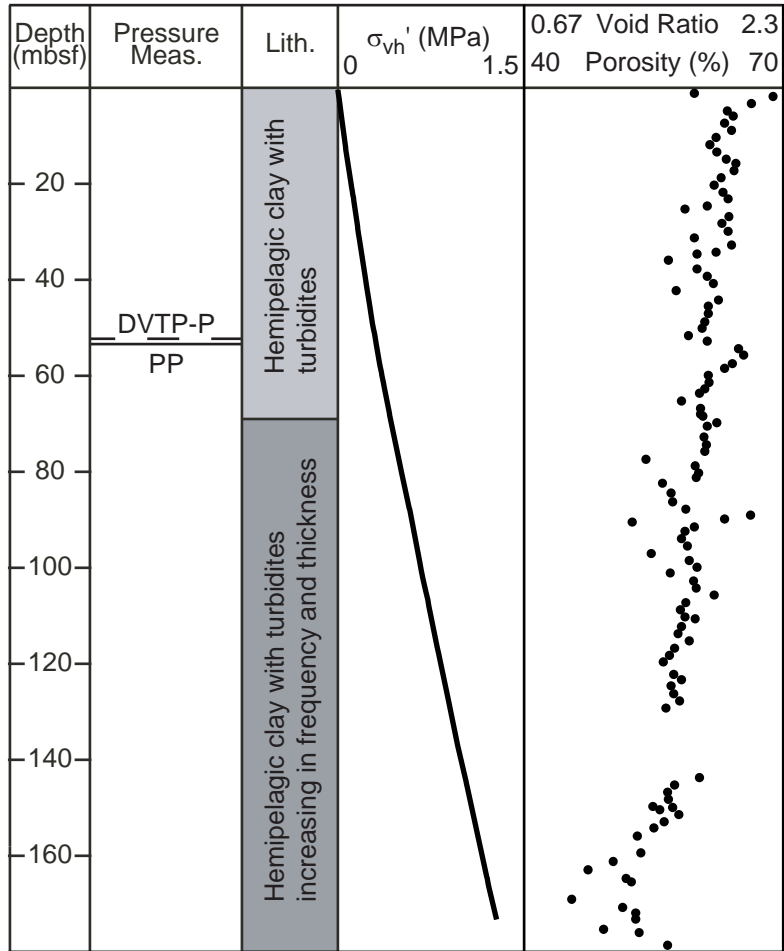


Figure 4  
Dugan

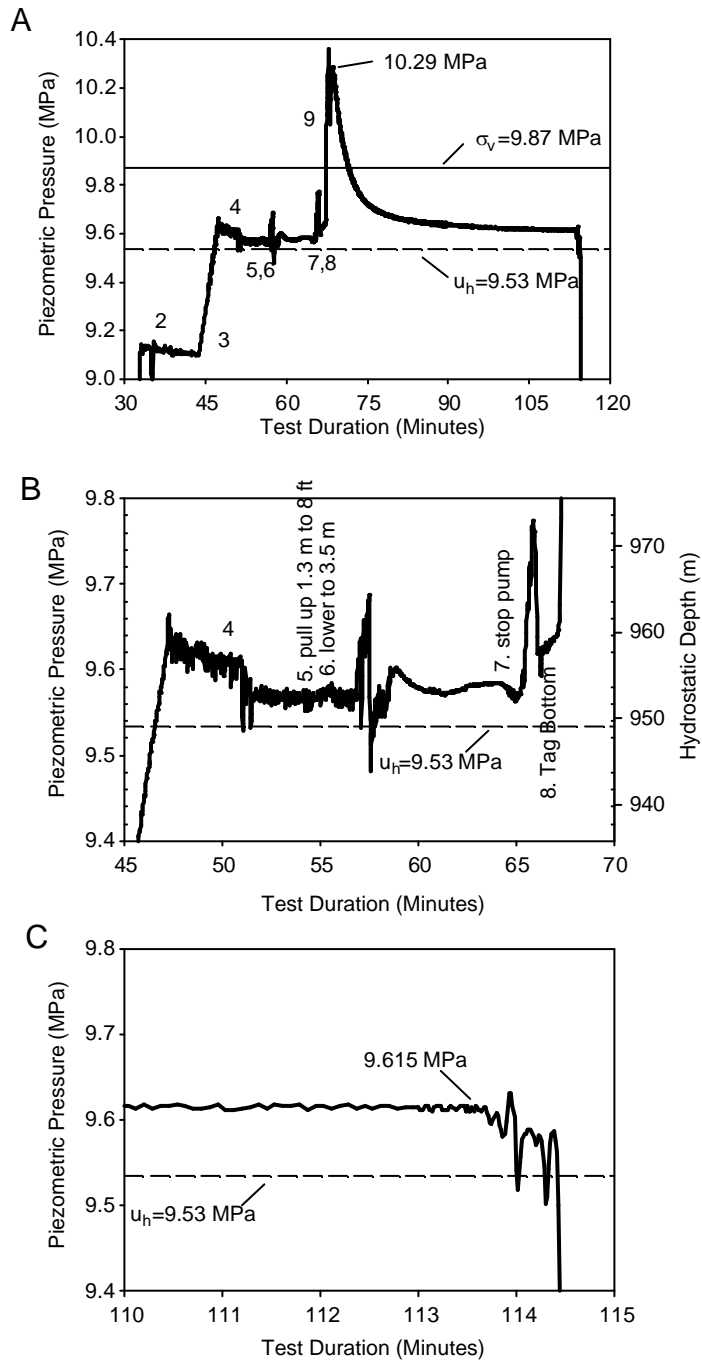


Figure 5  
Dugan

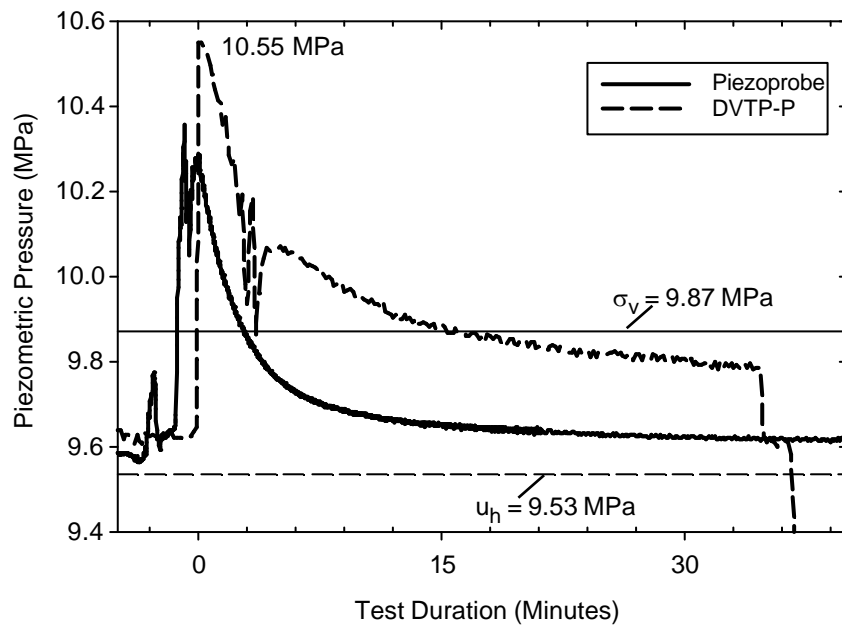


Figure 6  
Dugan

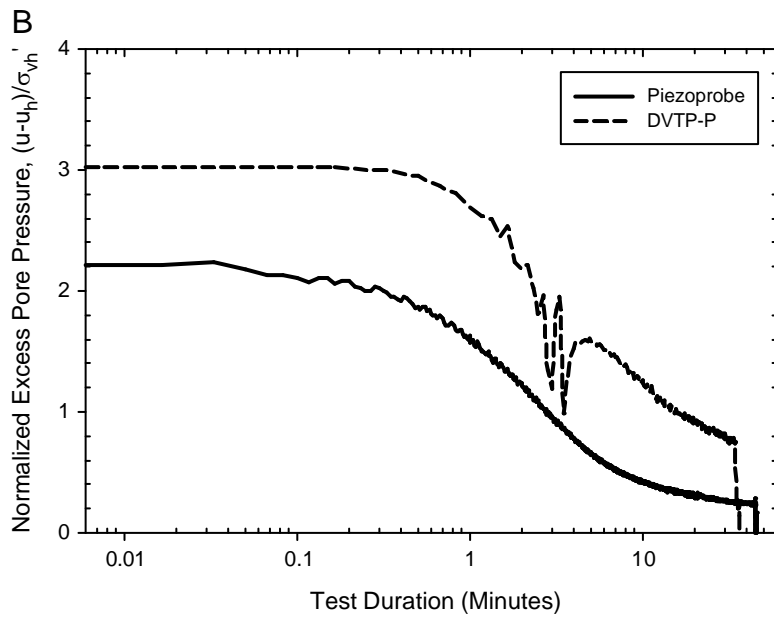
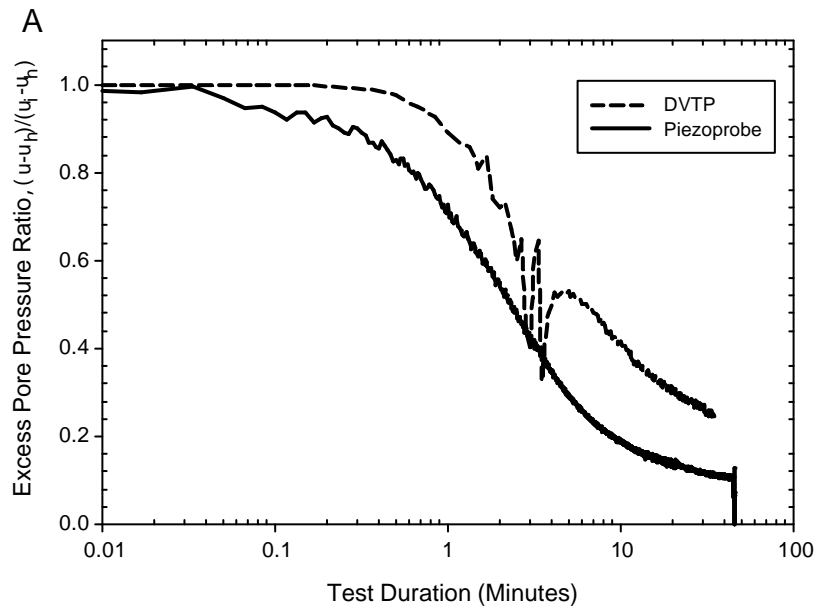


Figure 7  
Dugan

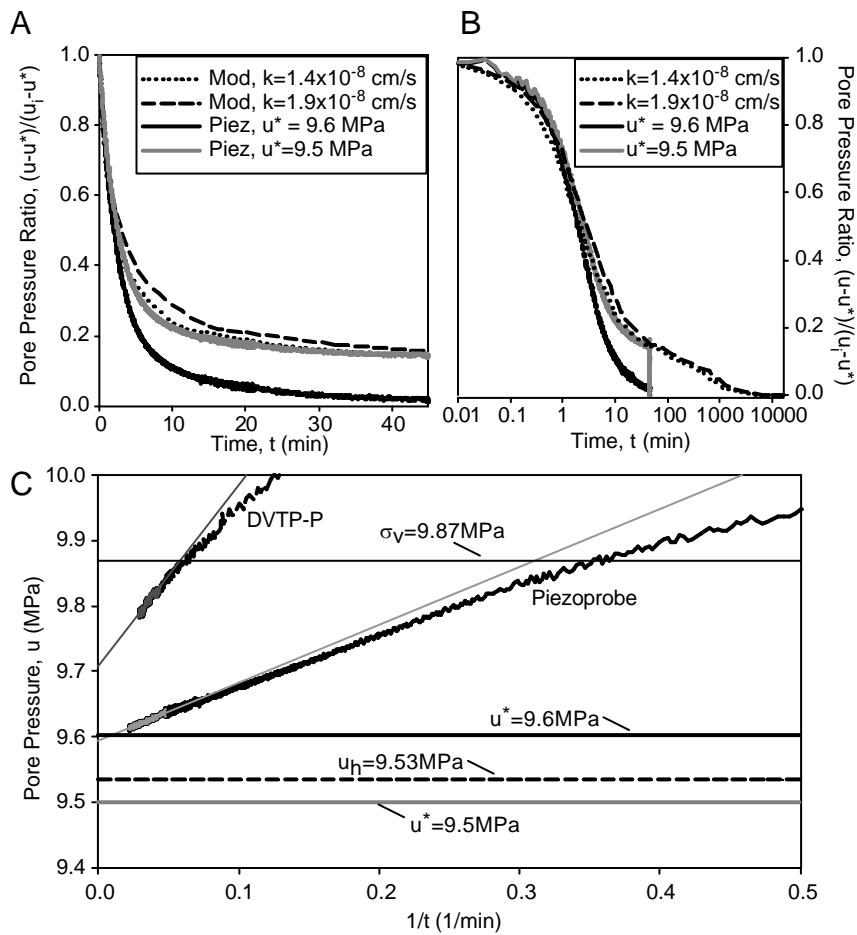


Figure 8  
Dugan

**APPENDIX C**

**GAMMA DENSITY LOGGING OF COLD, PRESSURIZED HYDRATE CORES  
FROM ODP LEG 204.**

**Peter Schultheiss  
Geotek Ltd., U.K.**

**(4 page Report, plus 35 Figures)**

**Gamma Density Logging  
of Cold, Pressurized Hydrate Cores  
from  
ODP Leg 204**

October 2002



GEOTEK Ltd  
3, Faraday Close  
Drayton Fields  
Daventry  
UK, NN11 5RD

## Gamma Density Logging of Cold, Pressurized Hydrate Cores from ODP Leg 204

Cores recovered at the end of ODP Leg 204 from the summit of Hydrate ridge (Site 1249) were rapidly stored to preserve the methane hydrate for further analysis. It is inevitable that some dissociation of hydrate will have occurred during the coring process as a result of a decrease in pressure and the increase in temperature during the core retrieval process. However, we knew from previous coring during the Leg that massive hydrate still existed in cores from Site 1249 when examined on the catwalk. For the cores that were preserved under pressure, significant efforts were made to ensure that the time between coring at the seabed and cutting the core into sections was minimized. In this way the minimum amount of dissociation will have occurred and the maximum amount of hydrate will be preserved. Some of the core sections were then rapidly frozen and stored in liquid nitrogen while others were rapidly repressurized in steel storage chambers (to about 500-600 psi) under methane gas and stored at around 4-5 °C. At these pressures and temperatures methane hydrates are stable and hence can be stored without any further dissociation occurring. All the samples were stored carefully under these conditions and shipped to ODP at College Station, Texas.



As a 'quick look' to determine the nature of the samples stored under pressure in the steel pressure vessels, the pressure vessels were subjected to gamma logging to determine the density structure. Logging took place at ODP using the GEOTEK vertical logging system during the period 7<sup>th</sup> to 14<sup>th</sup> October 2002. This was about 6 weeks after the samples had originally been recovered.

The cores were logged in the main core store at around 4-5 °C. A standard calibration section was run using aluminum and distilled water in a standard ODP liner placed inside one of the empty steel pressure vessels. This produced the calibration equation used to calculate density from the raw data:

$$D = -2.5066 * \ln(\text{CPS}) + 23.81$$

Where: D = density (g/cc) and CPS = gamma Counts Per Second

Each core section was logged from the top down at 0.5cm intervals. Count times were longer than normally used on ODP cores because of the steel pressure cylinder used (OD approx 90 mm, wall thickness approx. 7.5 mm.) Typical count rates in sediments were 7000 cps; therefore, a minimum total count time of 25 s was used. These count times produced total counts in excess of 150,000 counts, resulting in gamma density values that will have a precision of about 1-2%.

The data are plotted as density profiles. The bottom of the pressure vessel was used as a section depth reference; the last data point before the steel end cap was assigned a depth of 150 cm. Short core sections will appear to start at 80-90 cm.

Three different gamma density zones are identified:

- 1) greater than 1.4 g/cc – mainly sediment
- 2) 0.95 g/cc to 1.4 g/cc – sediment plus gas, may include some hydrate
- 3) less than 0.95 g/cc – contains some gas

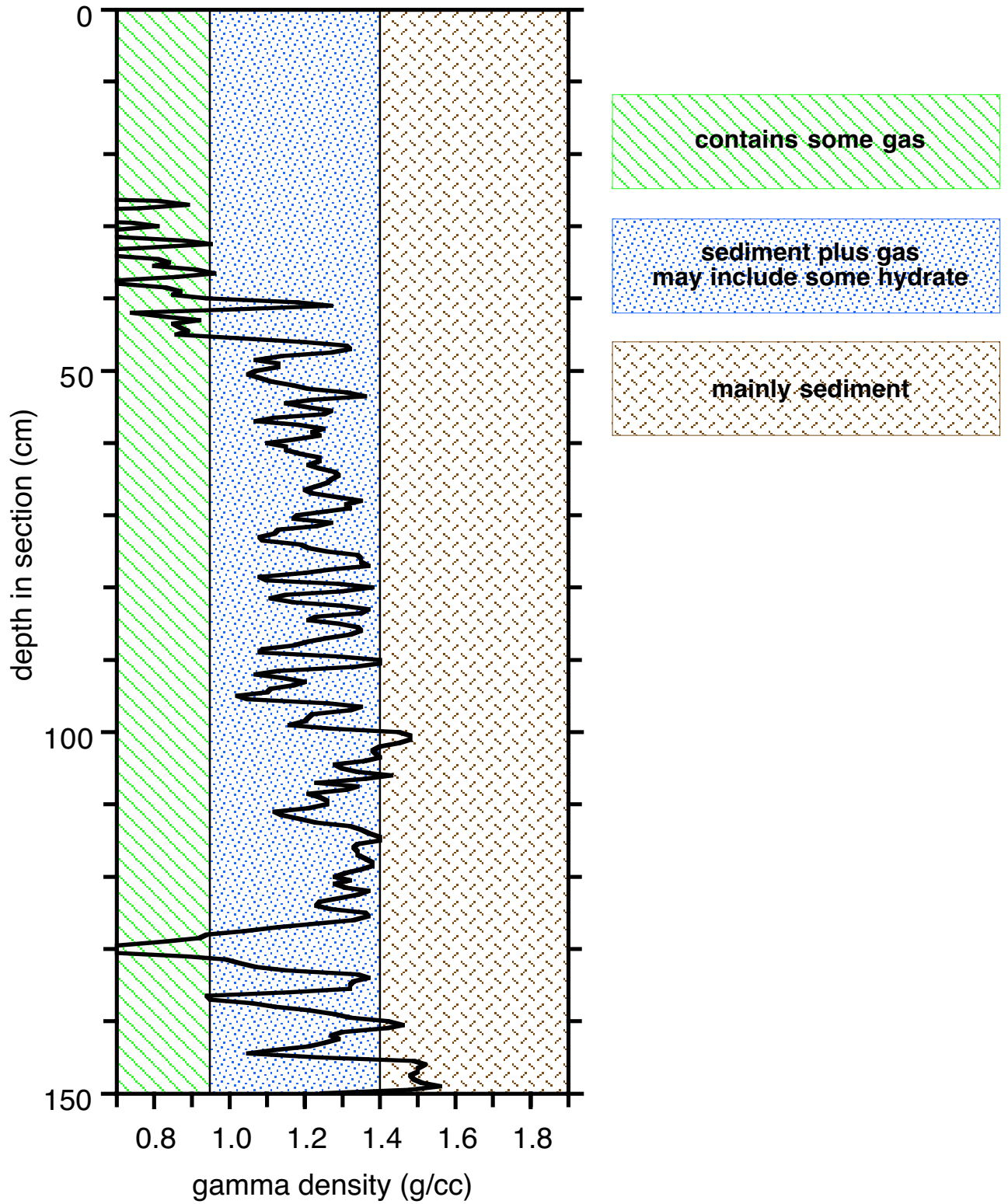
It should be remembered that the gamma density values represent the average density of a 5 mm diameter horizontal cylinder through the center of the core. Any values lower than 0.95 definitely contain some gas. Many (or possibly most) of the abundant low-density zones (0.95 to 1.4 g/cc) are sediment with sub-horizontal gas cracks. Densities above 1.4 g/cc are mainly sediment. There is no definitive method of ascertaining the existence of methane hydrate at any location in each core. However, the general nature of the density profiles in each core may act as a good guide to the occurrence of hydrates, especially as more information is gathered. For example, X-ray CT scanning may be able to determine more accurately the nature of the gas cracking, and hence allow an accurate assessment of the amounts of hydrate remaining in the core.

A summary table of the pressure vessels and cores is shown below. The pressures were recorded on 13<sup>th</sup> October 2002.

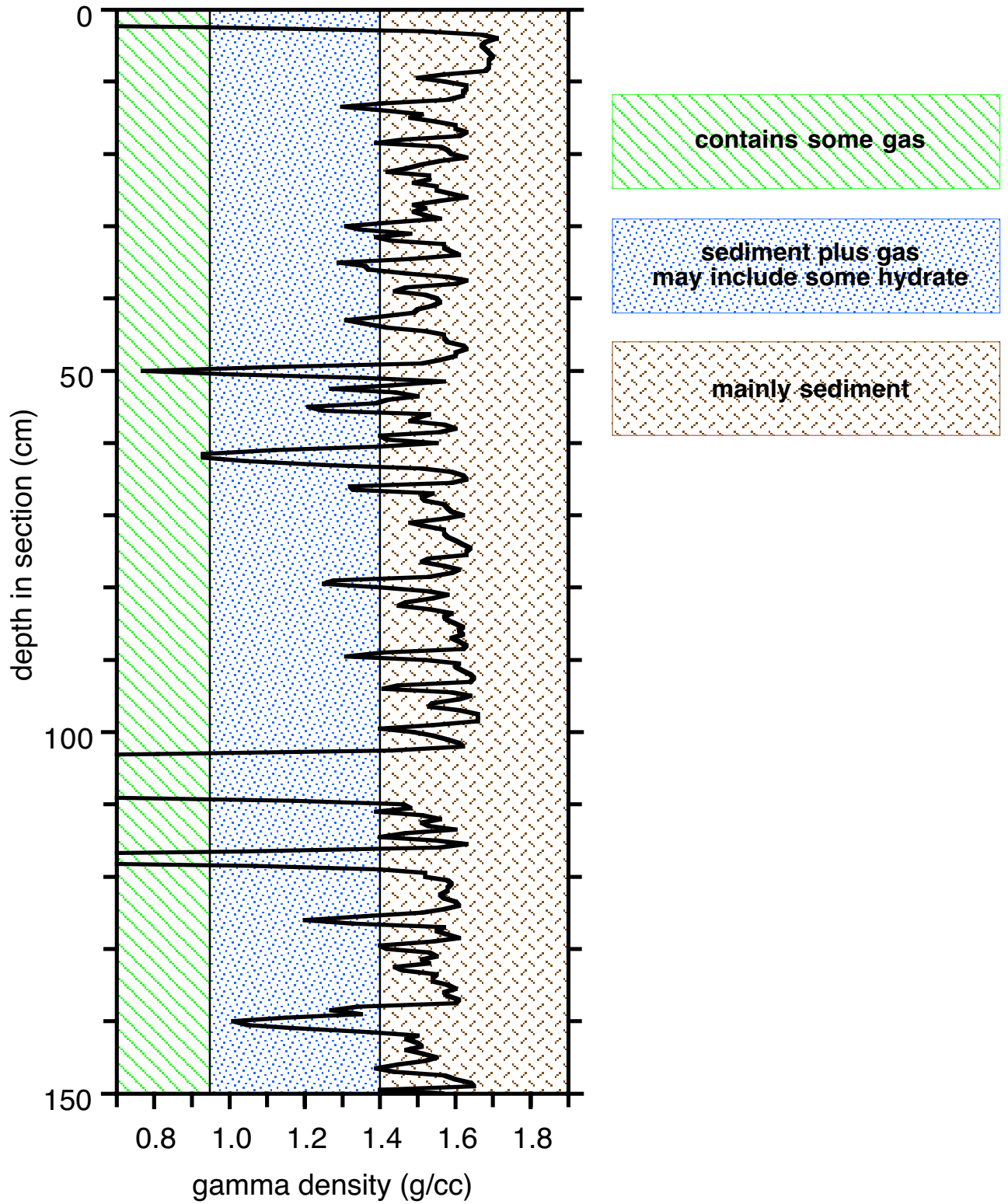
PV No	Core 204-1249-	Gamma Count Time s	Pressure psi		PV No	Core 204-1249-	Gamma Count Time s	Pressure psi
01	Empty	-	0		21	Empty	-	0
02	Empty	-	0		22	K-3H-2	25	540
03	G-3H-1	25	560		23	K-3H-1	30	540
04	H-3H-4	60	630		24	K-3H-5	30	560
05	H-6H-3	60	510		25	K-4H-1	60	550
06	H-3H-1	25	590		26	K-5H-4	25	530
07	H-5H-3	25	570		27	K-4H-2	25	650
08	H-6H-6	25	600		28	K-5H-1	25	500
09	H-4H-3	25	550		29	I-4H-6	25	700
10	H-4H-4	25	610		30	I-4H-2	25	570
11	H-6H-1	25	600		31	K-5H-2	30	490
12	H-5H-1	25	570		32	L-2H-2	25	600
13	H-5H-2	25	590		33	L-2H-3	60	590
14	H-6H-4	60	500		34	L-2H-1	25	520
15	H-6H-2	25	0		35	Empty	-	0
16	H-6H-5	25	560		36	L-4H-1	25	560
17	J-2H-1	25	650		37	L-4H-2	25	570
18	J-3H-4	25	660		38	L-3H-1	40	500
19	J-3H-1	30	640		39	Empty	-	0
20	I-4H-3	120	640		40	L-3H-3	40	540

Table 1. Pressure vessel (PV) numbers, core section identification, total gamma count time at each interval and the pressure reading for each vessel.

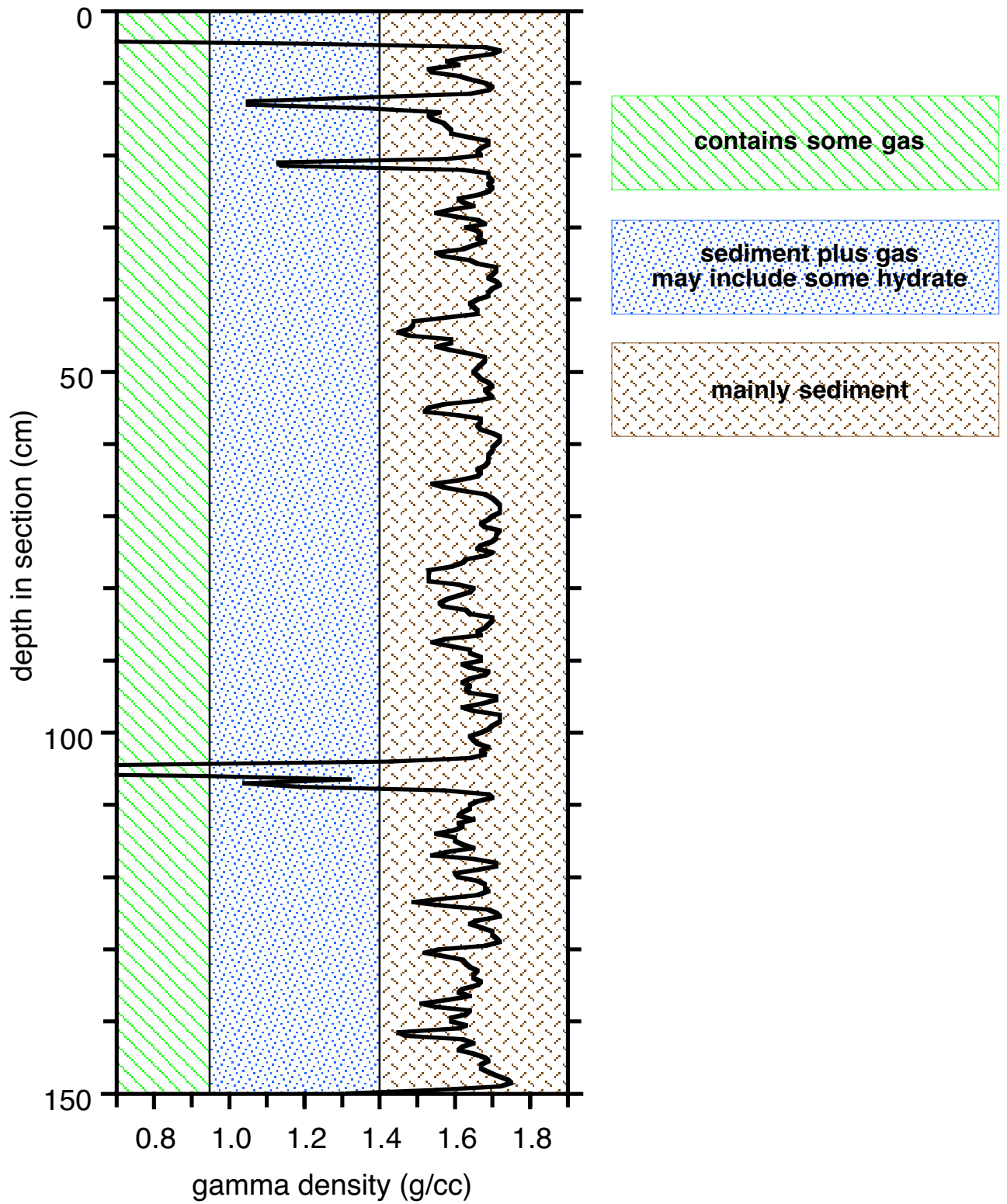
Section 204-1249G-3H-1  
Pressure Vessel 3



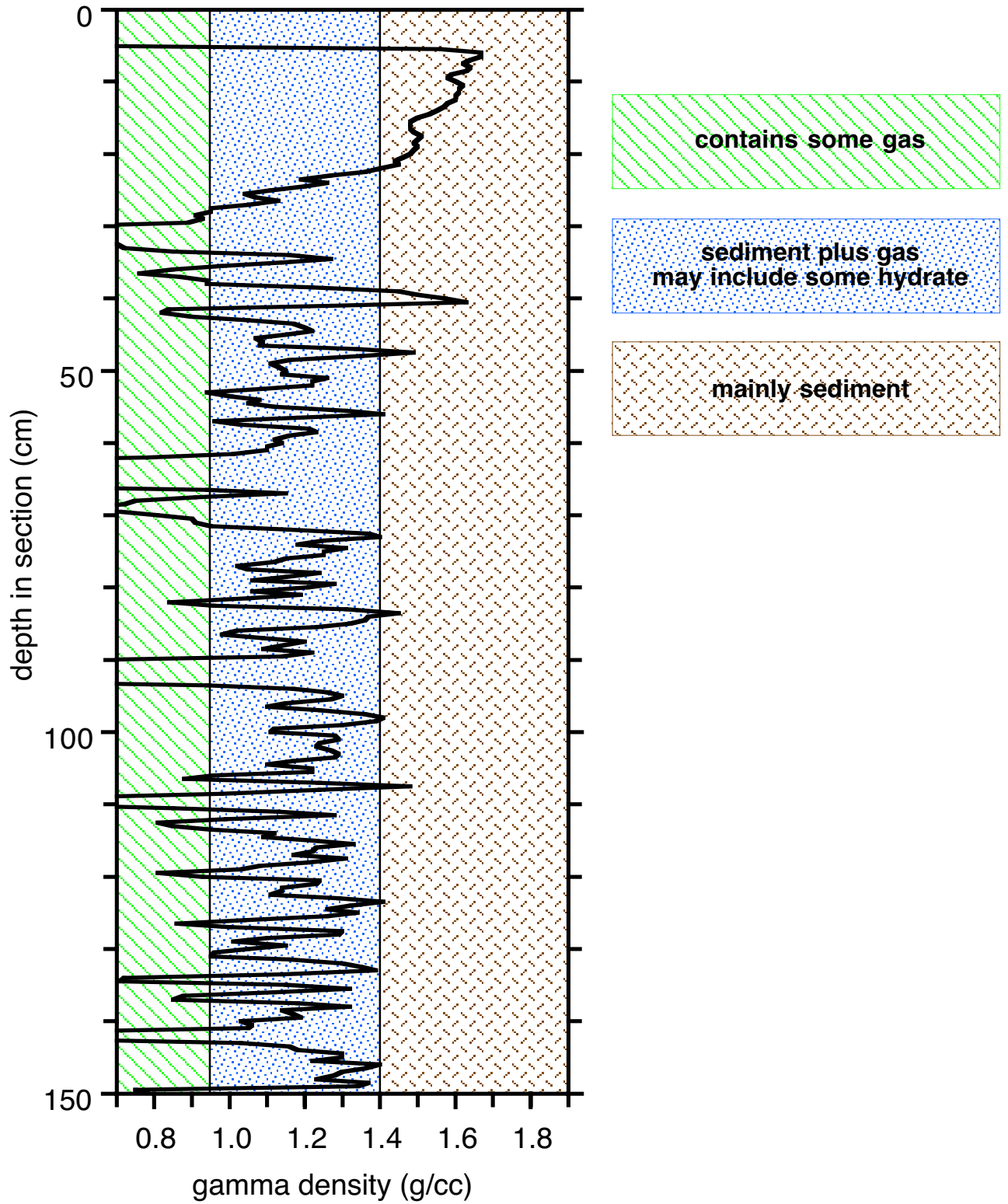
Section 204-1249H-3H-4  
Pressure Vessel 4



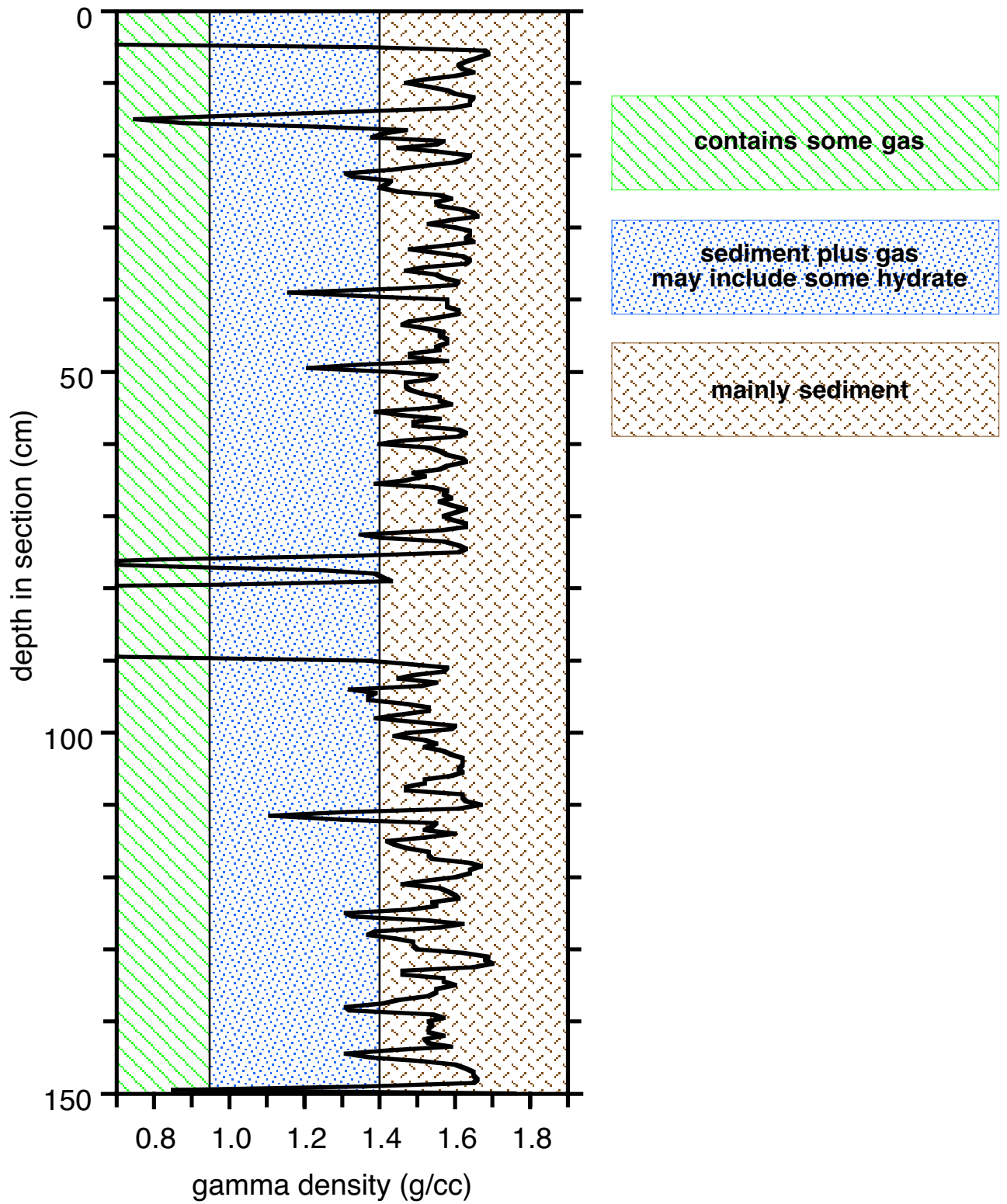
Section 204-1249H-6H-3  
Pressure Vessel 5



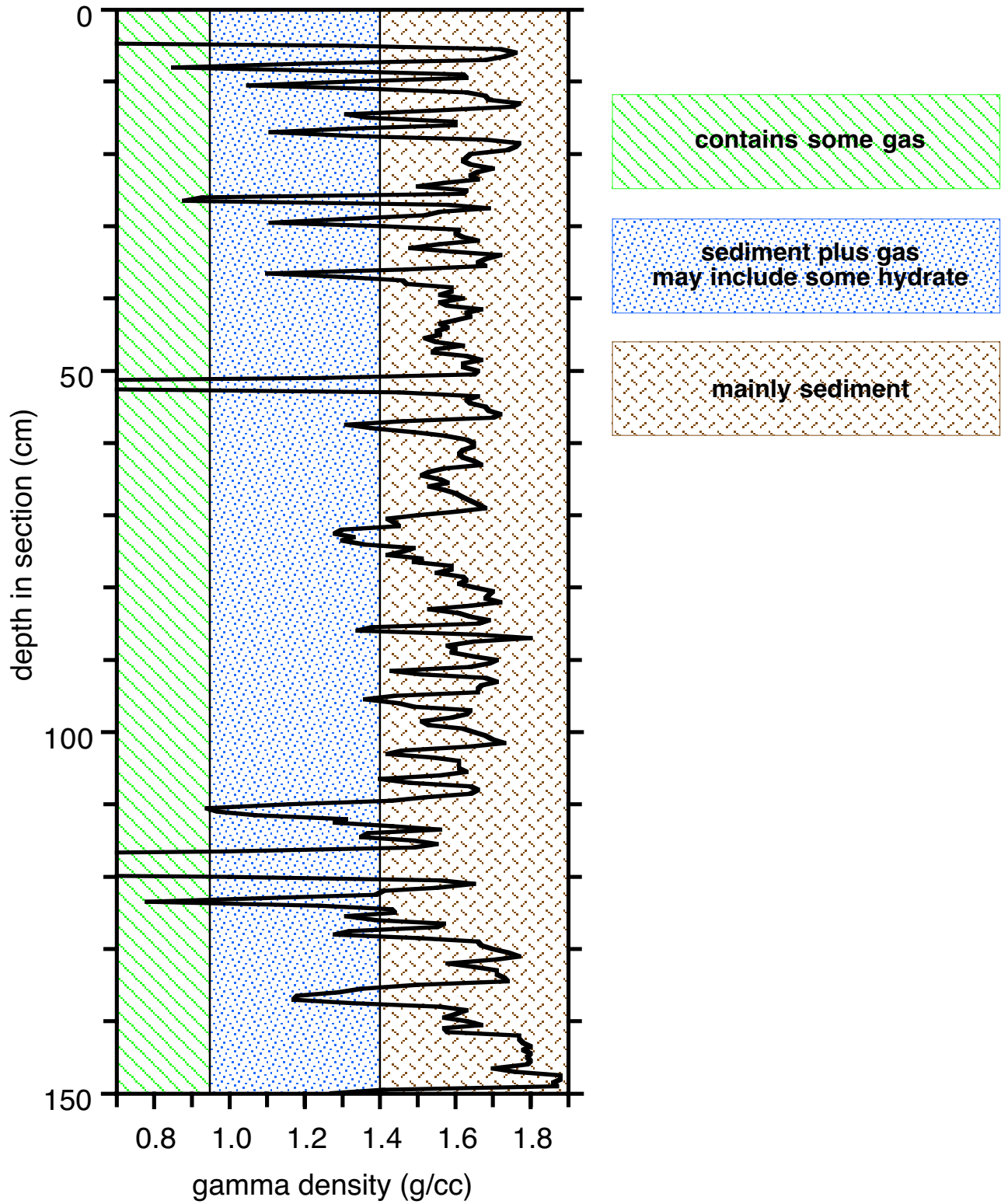
Section 204-1249H-3H-1  
Pressure Vessel 6



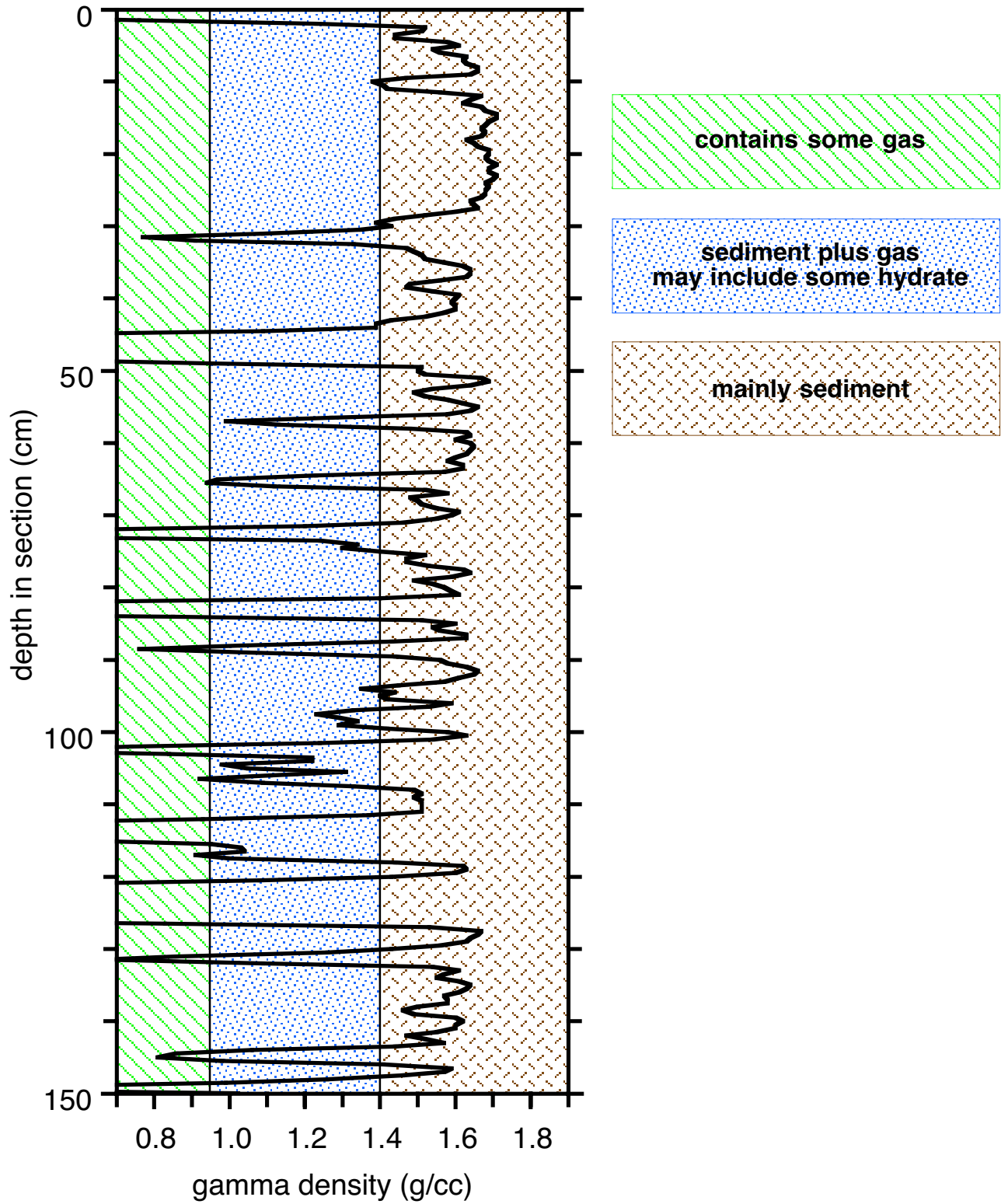
Section 204-1249H-5H-3  
Pressure Vessel 7



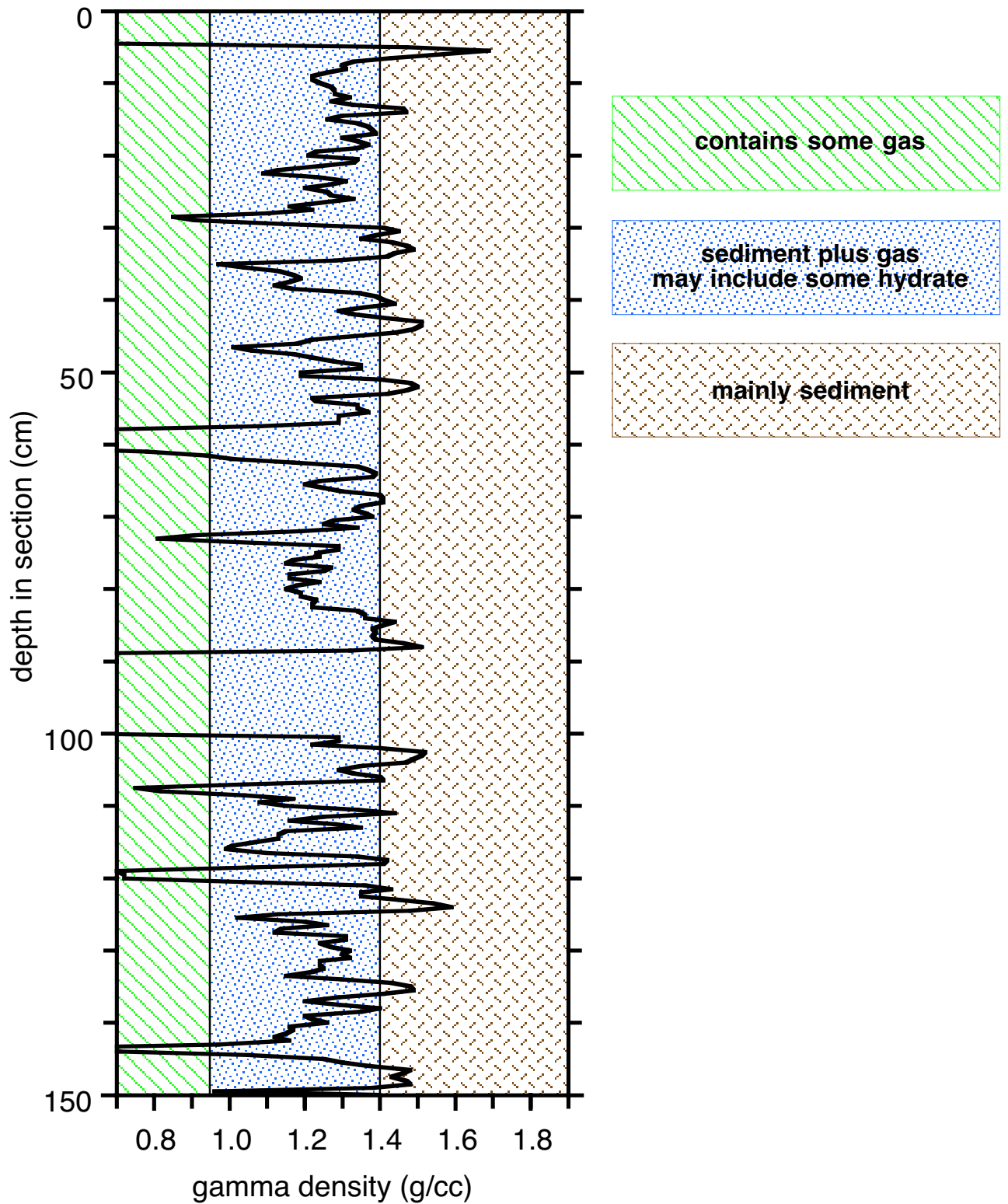
Section 204-1249H-6H-6  
Pressure Vessel 8



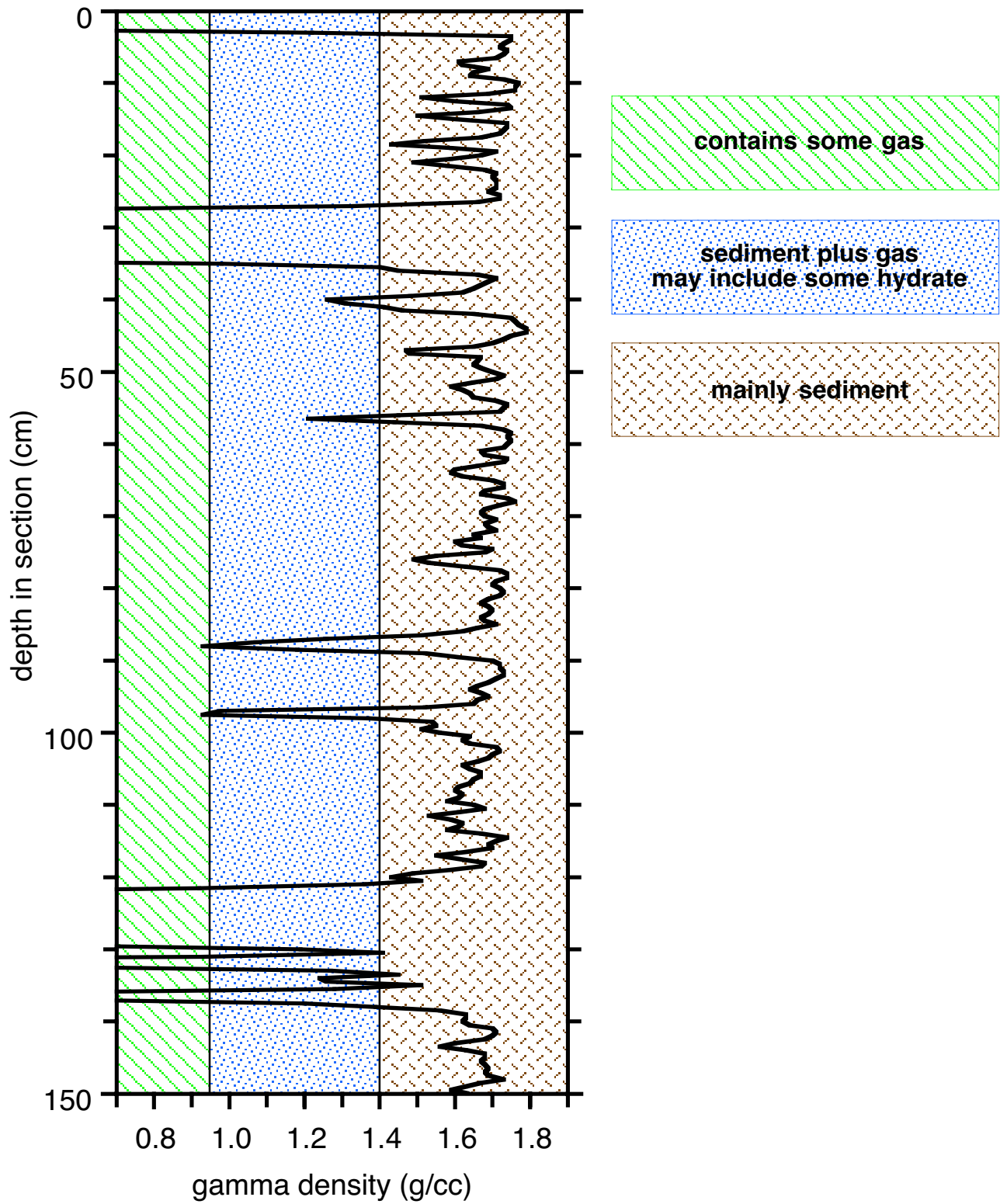
Section 204-1249H-4H-3  
Pressure Vessel 9



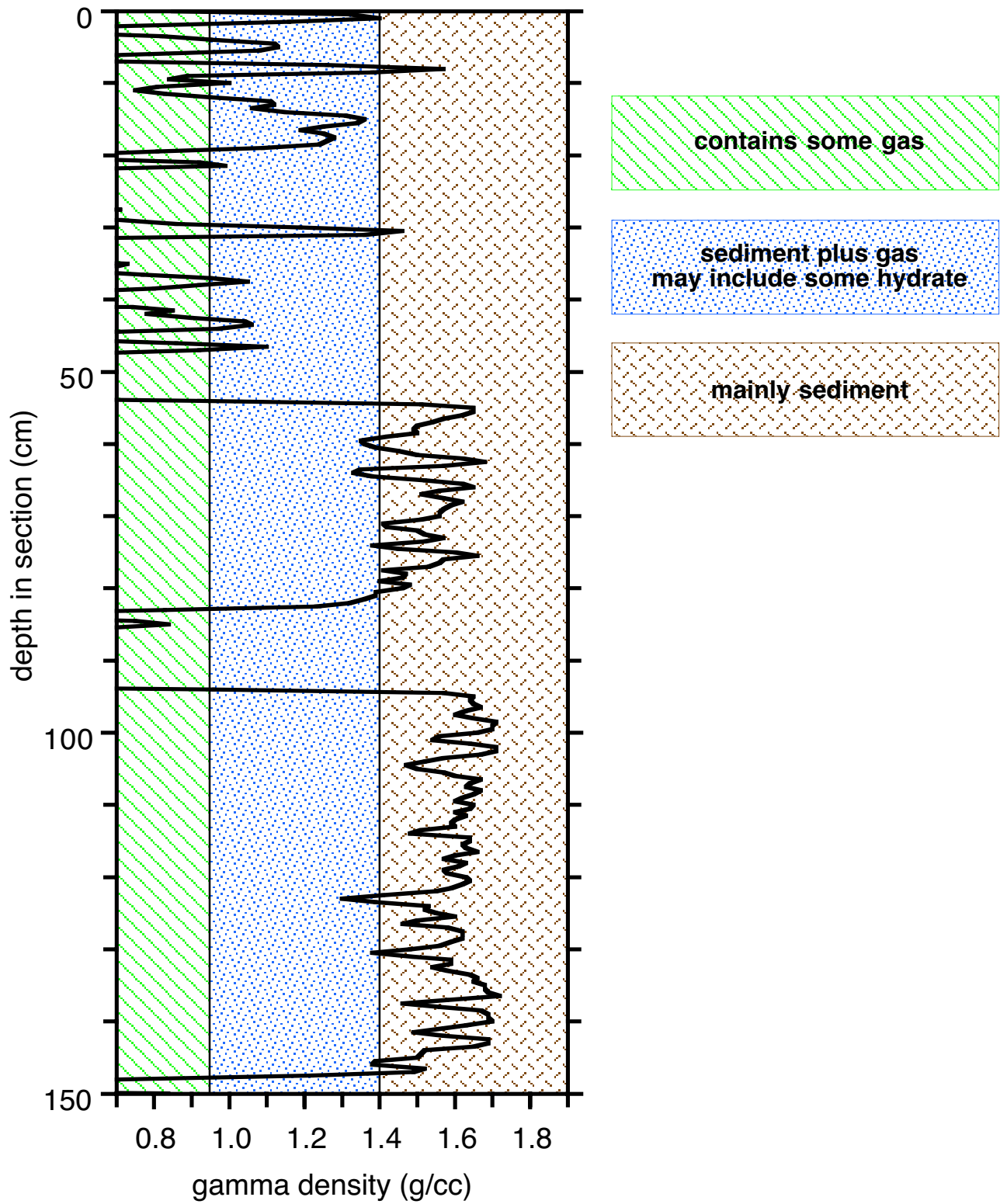
Section 204-1249H-4H-4  
Pressure Vessel 10



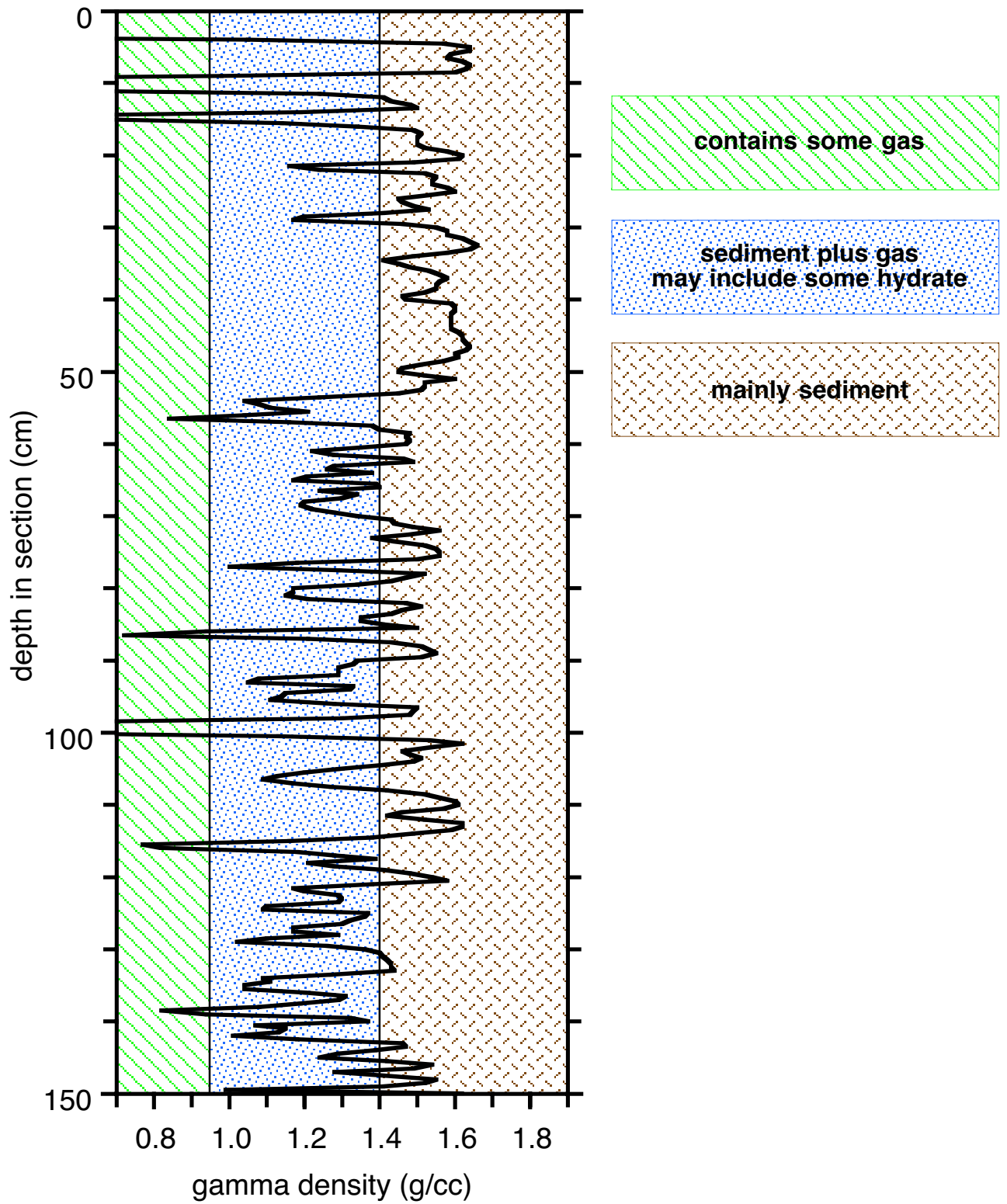
Section 204-1249H-6H-1  
Pressure Vessel 11



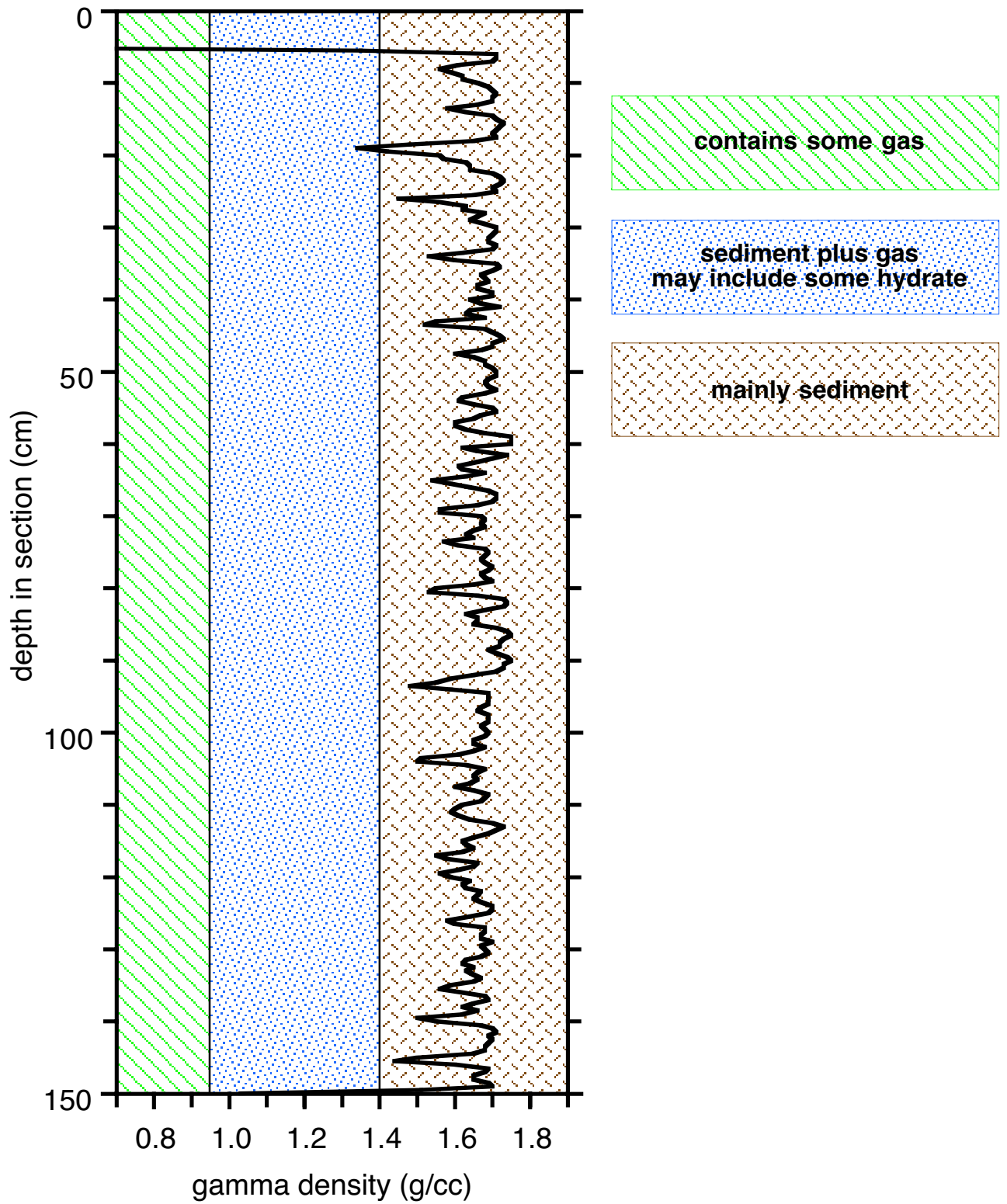
Section 204-1249H-5H-1  
Pressure Vessel 12



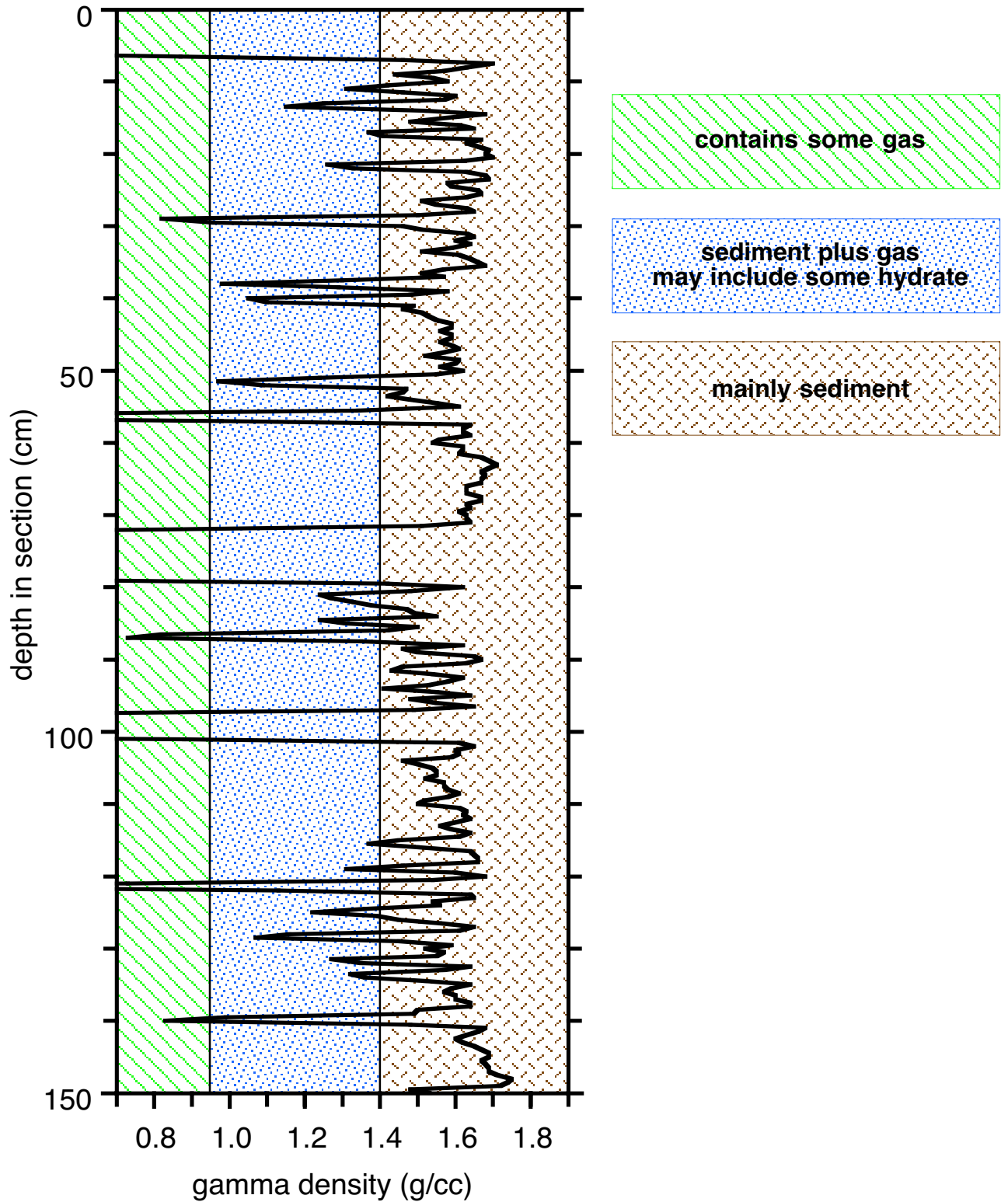
Section 204-1249H-5H-2  
Pressure Vessel 13



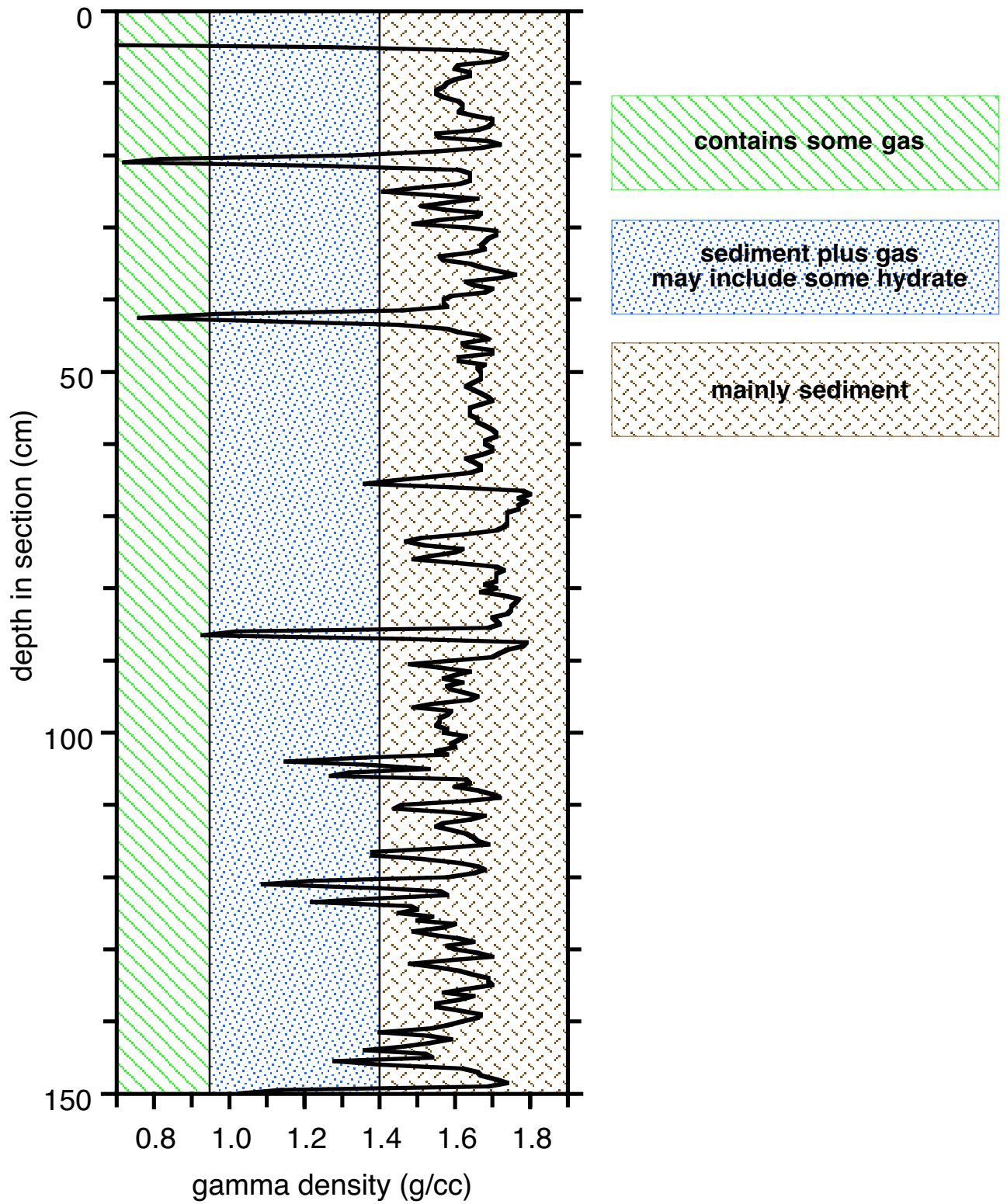
Section 204-1249H-6H-4  
Pressure Vessel 14



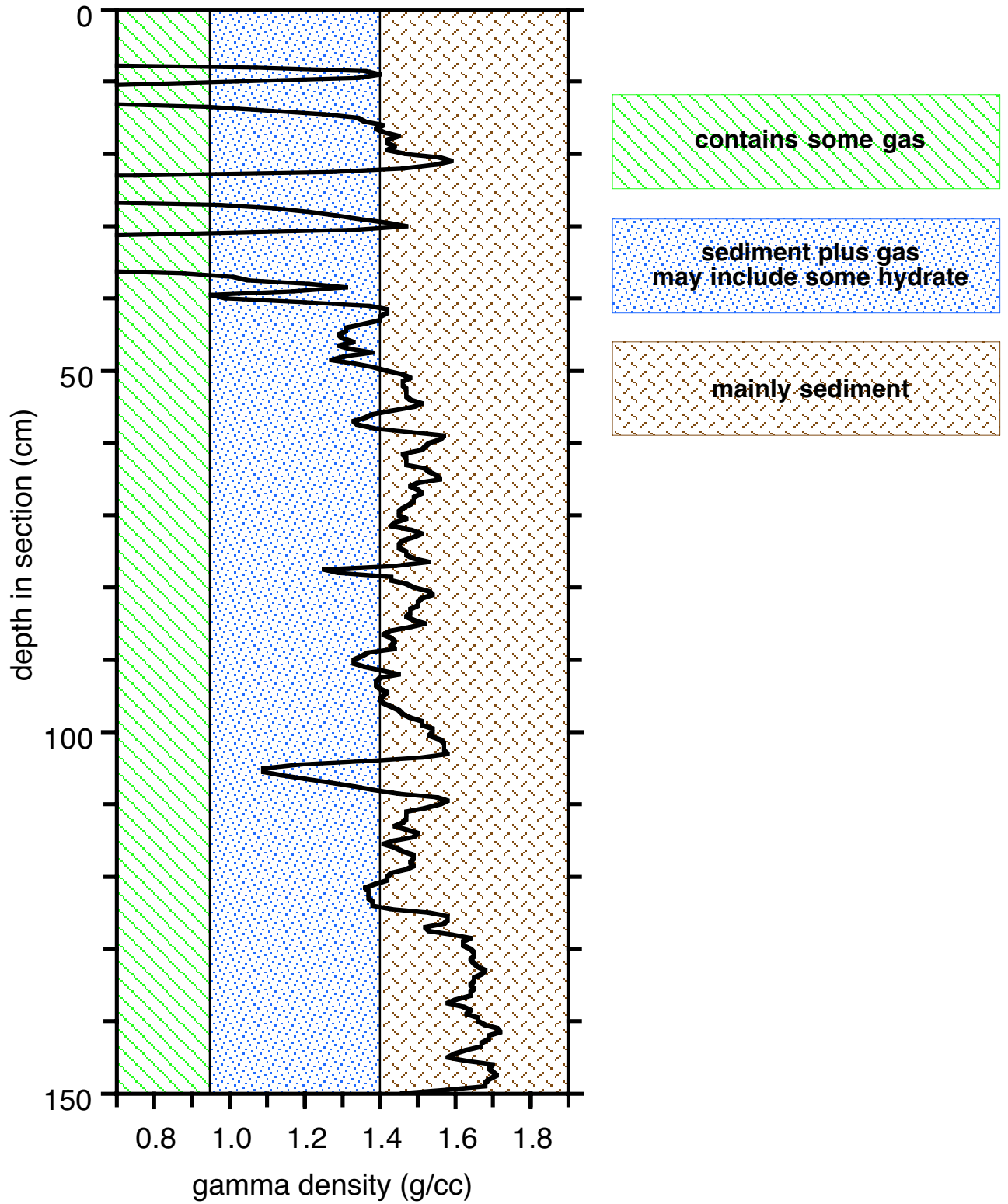
Section 204-1249H-6H-2  
Pressure Vessel 15



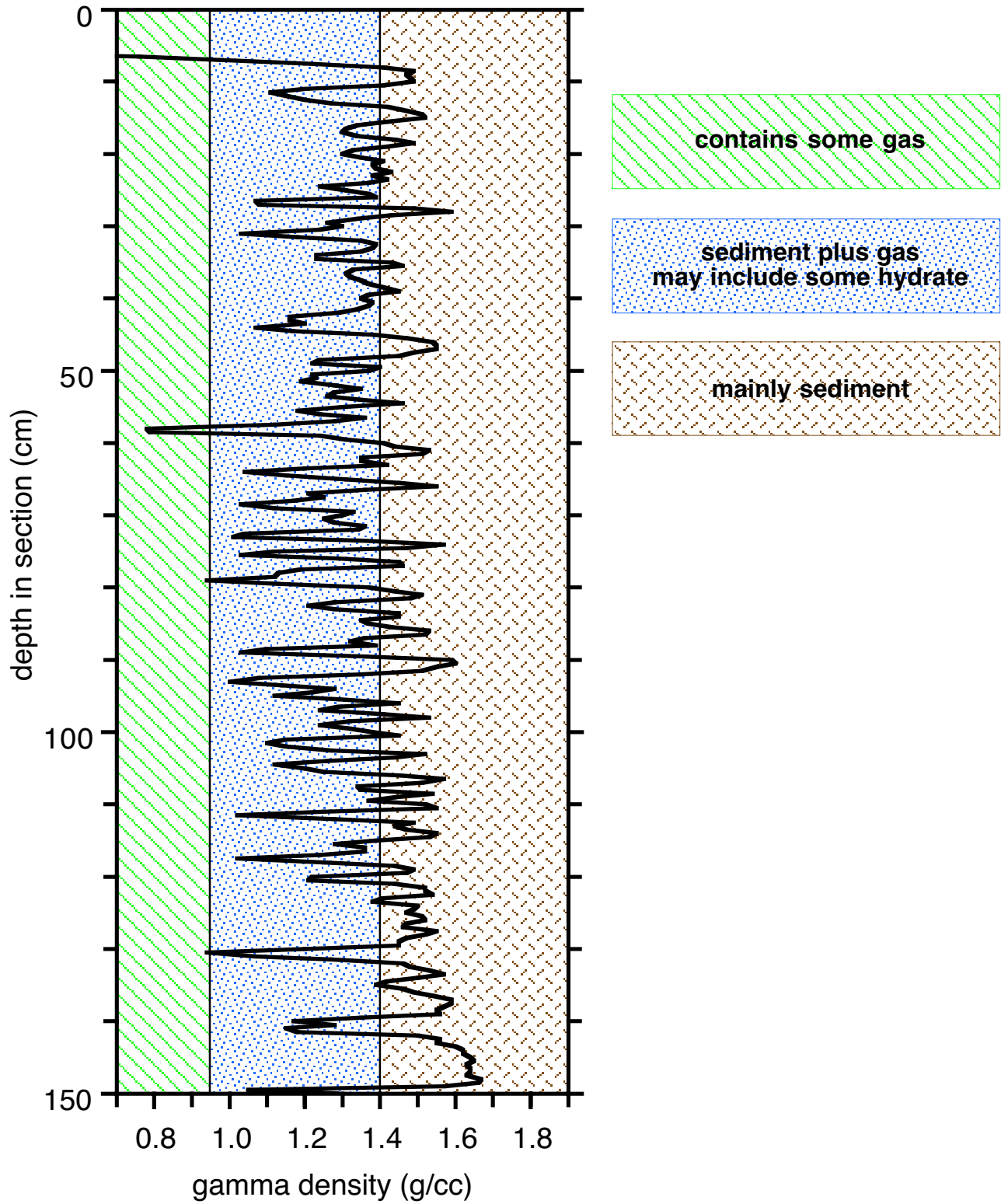
Section 204-1249H-6H-5  
Pressure Vessel 16



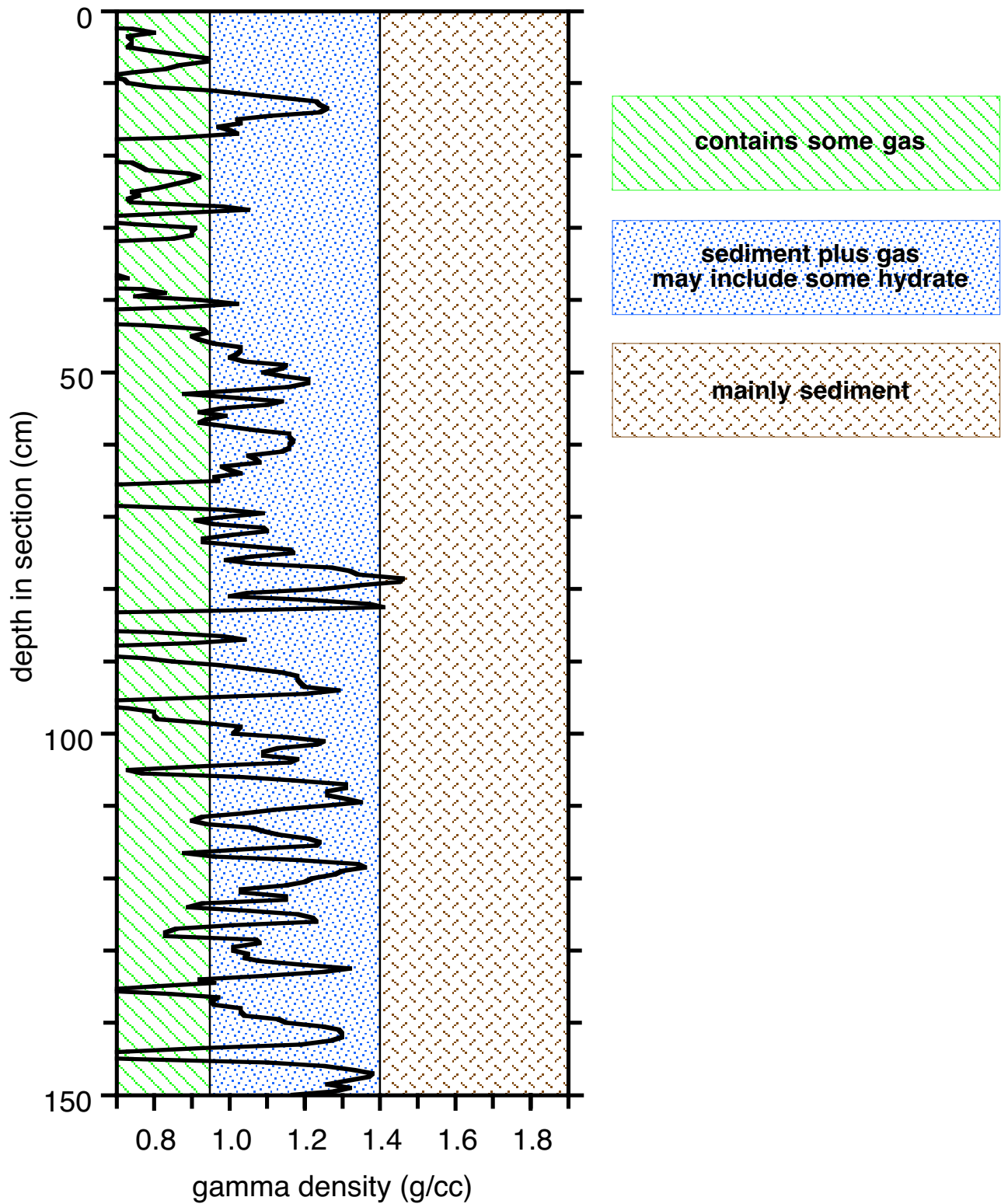
Section 204-1249J-2H-1  
Pressure Vessel 17



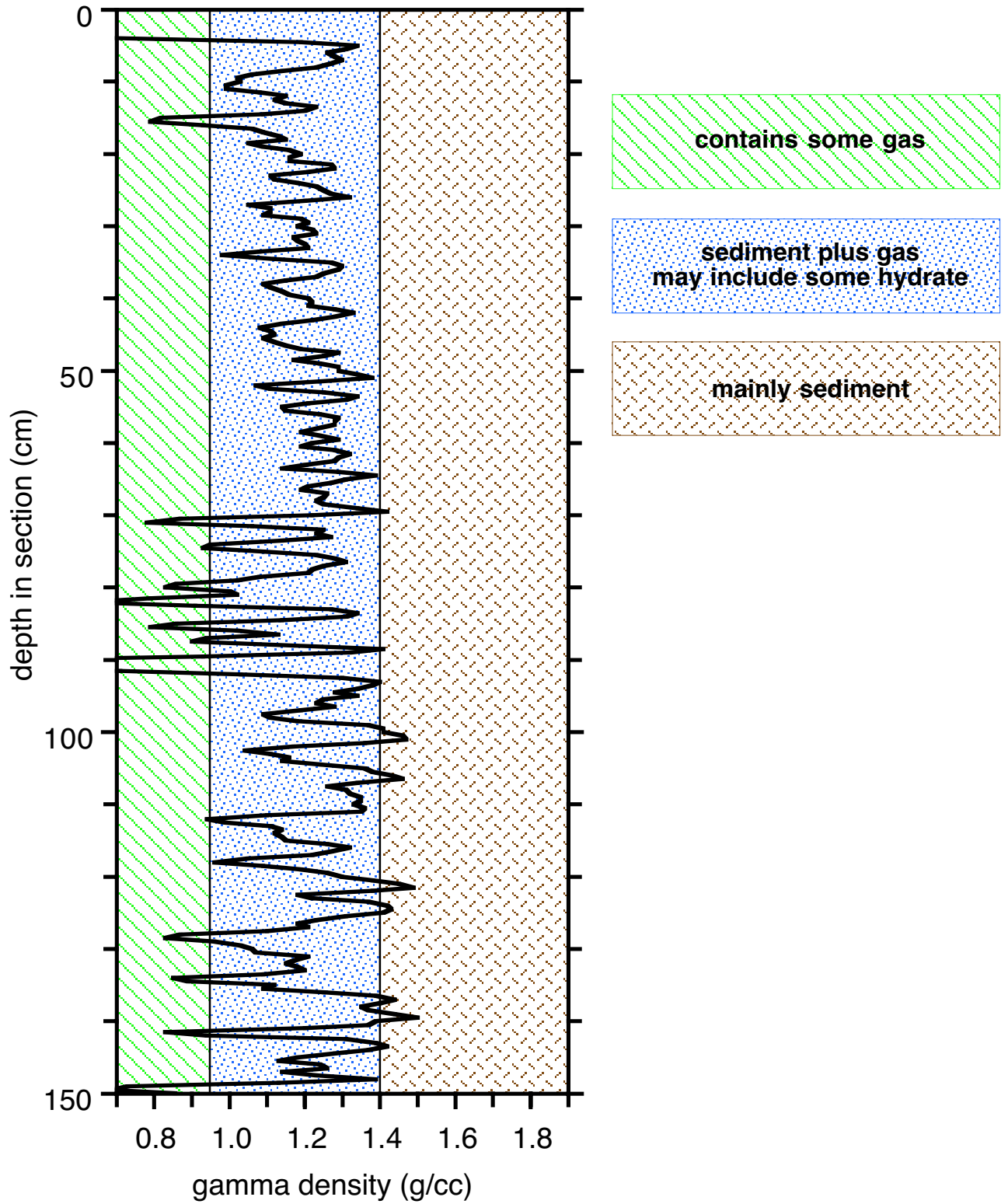
Section 204-1249J-3H-4  
Pressure Vessel 18



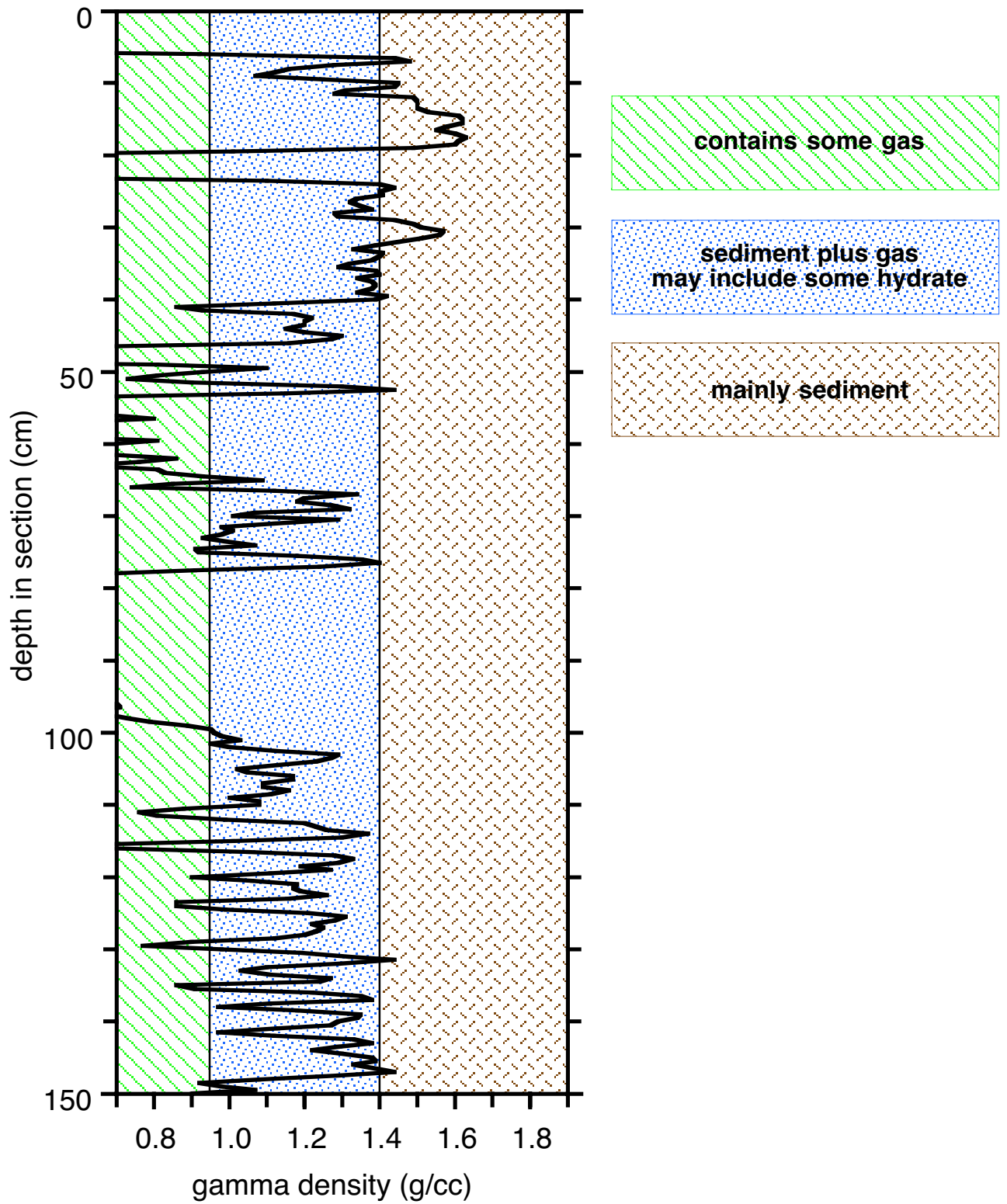
Section 204-1249J-3H-1  
Pressure Vessel 19



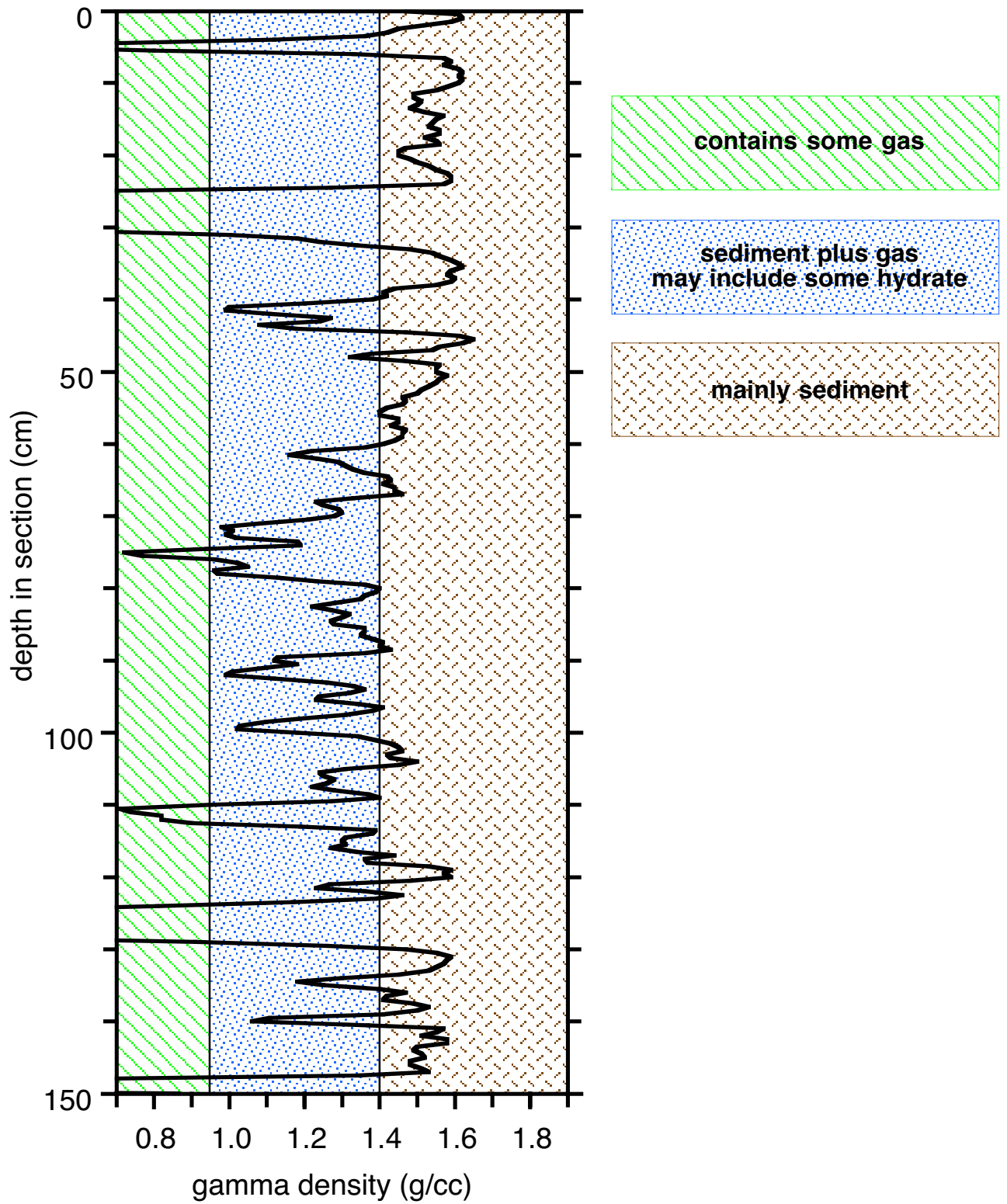
Section 204-1249I-4H-3  
Pressure Vessel 20



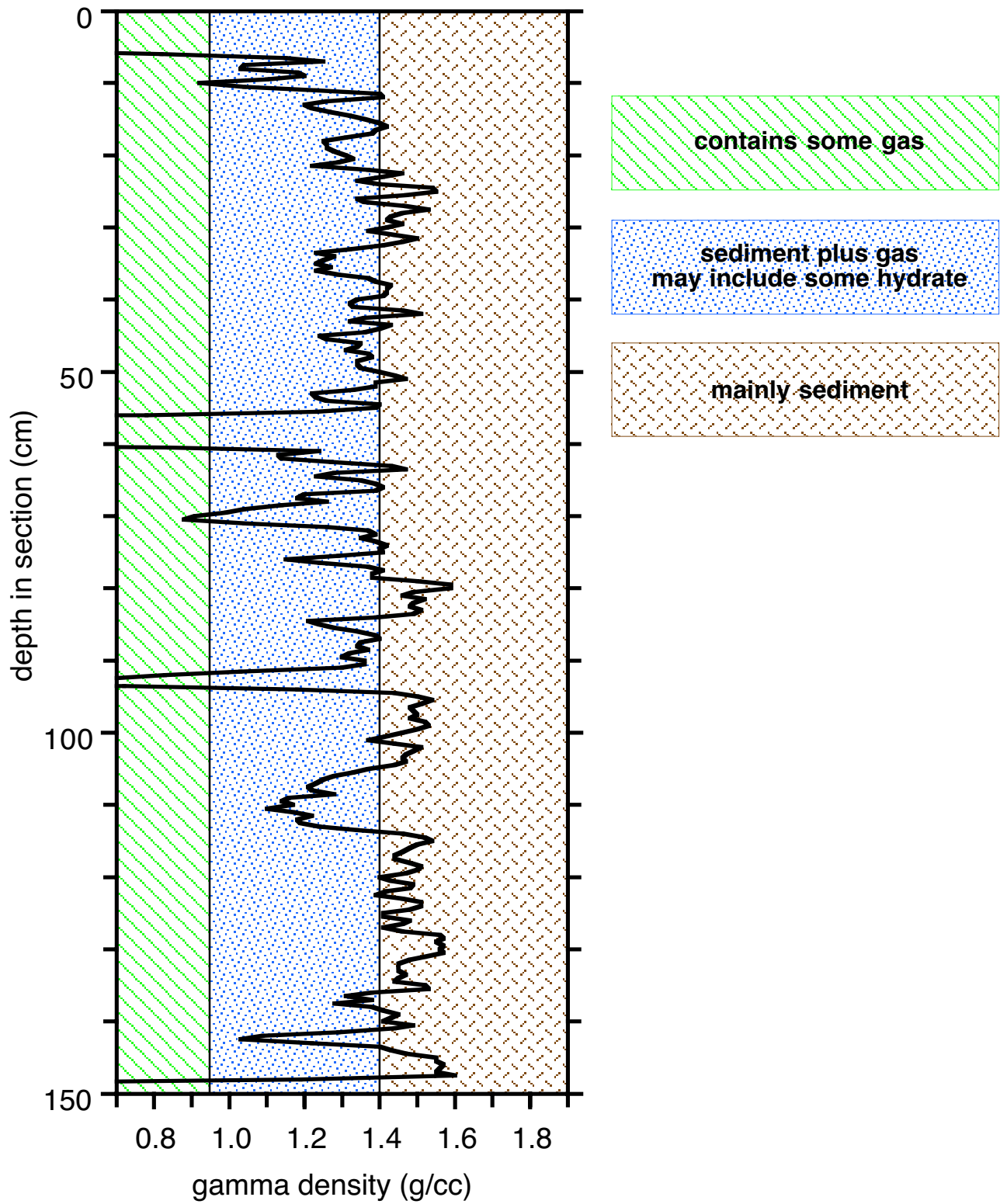
Section 204-1249K-3H-2  
Pressure Vessel 22



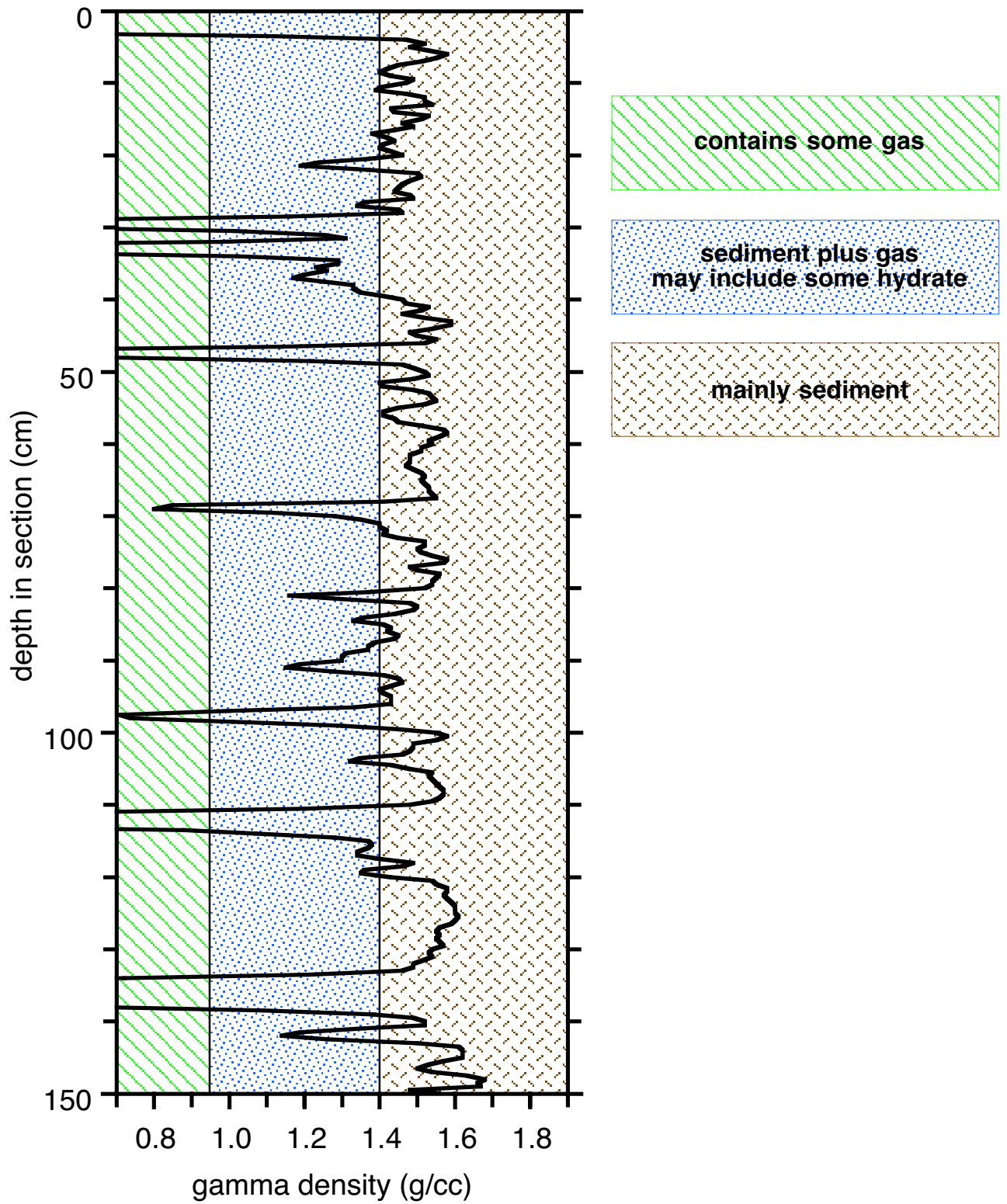
Section 204-1249K-3H-1  
Pressure Vessel 23



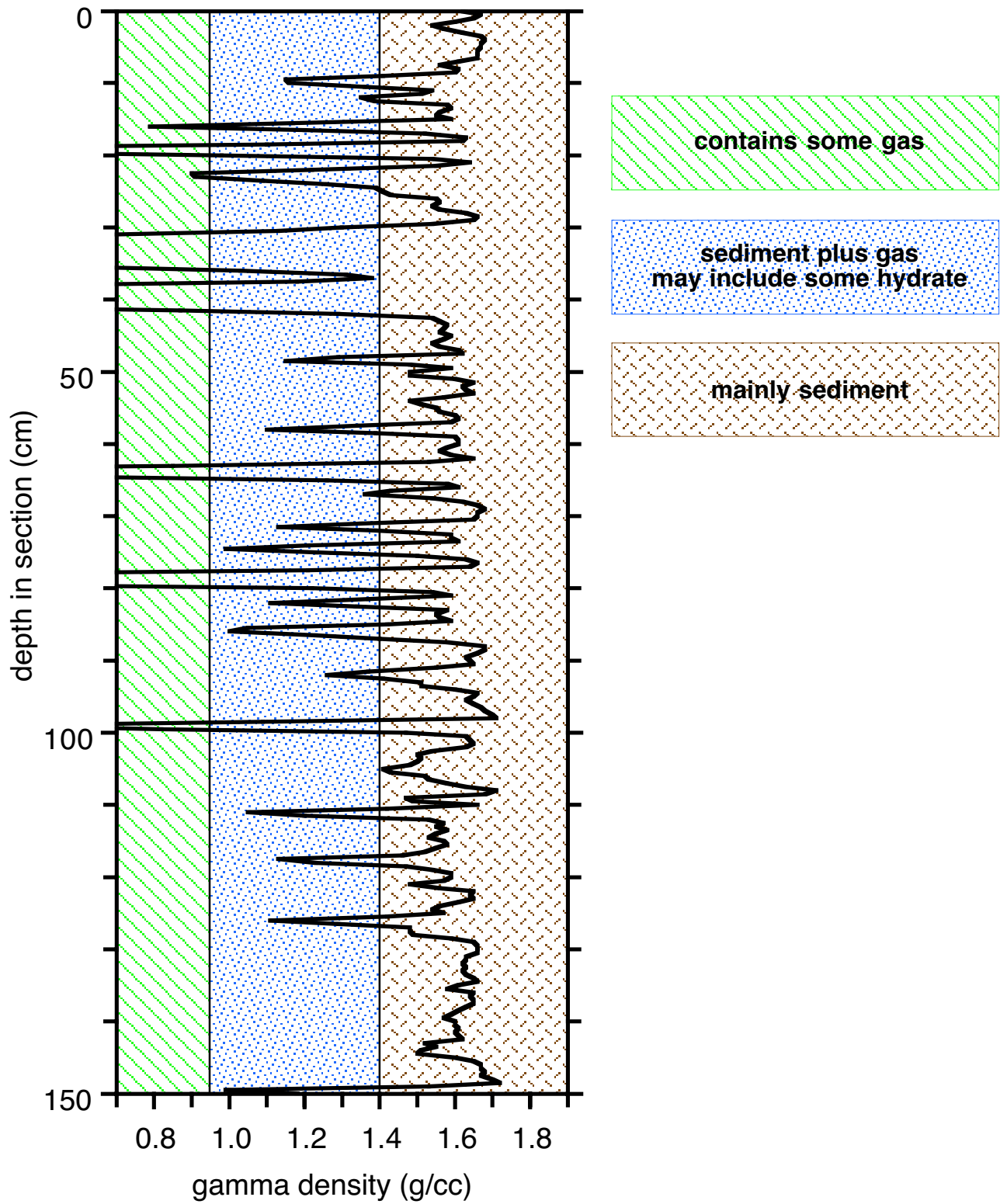
Section 204-1249K-3H-5  
Pressure Vessel 24



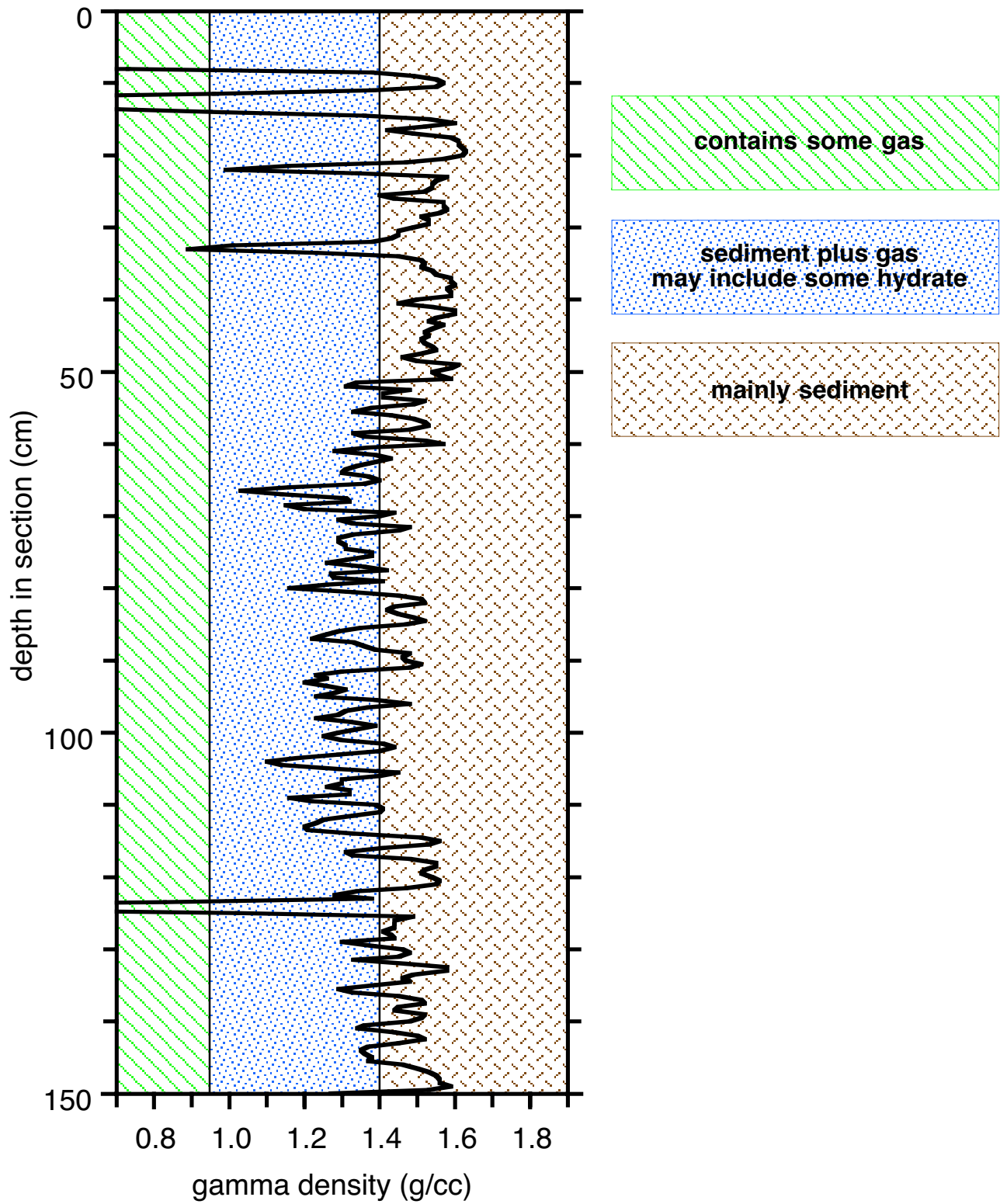
Section 204-1249K-4H-1  
Pressure Vessel 25



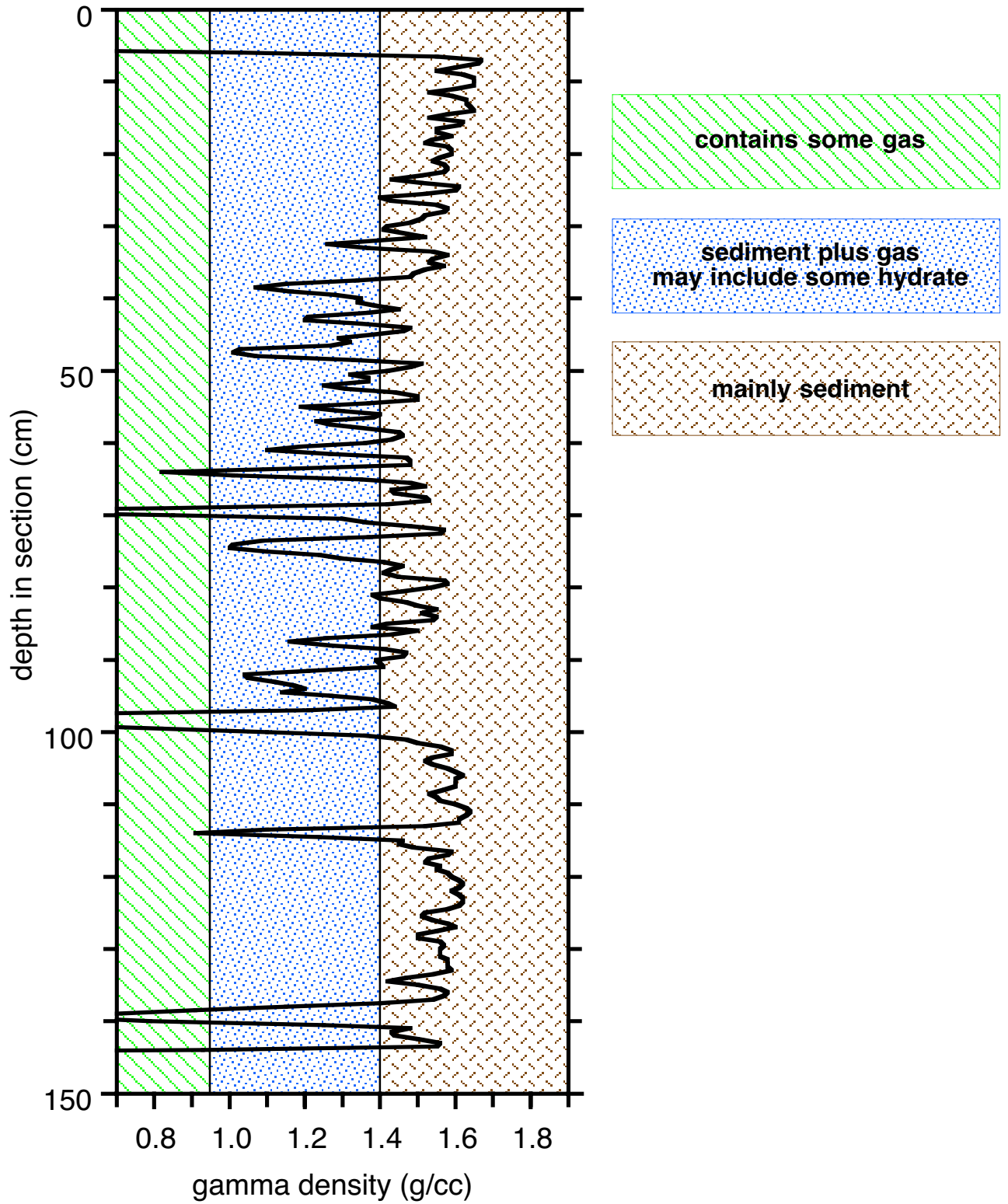
Section 204-1249K-5H-4  
Pressure Vessel 26



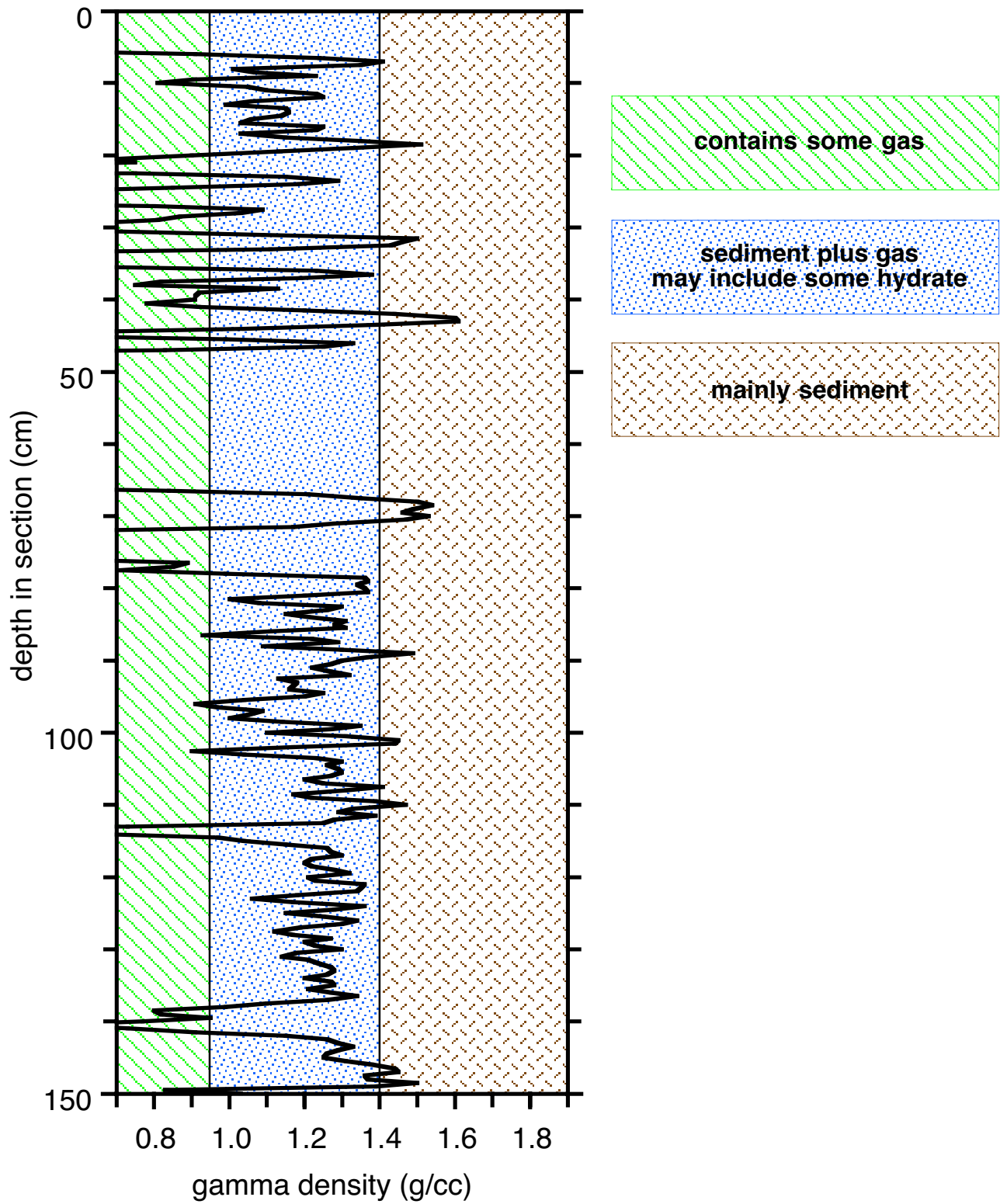
Section 204-1249K-4H-2  
Pressure Vessel 27



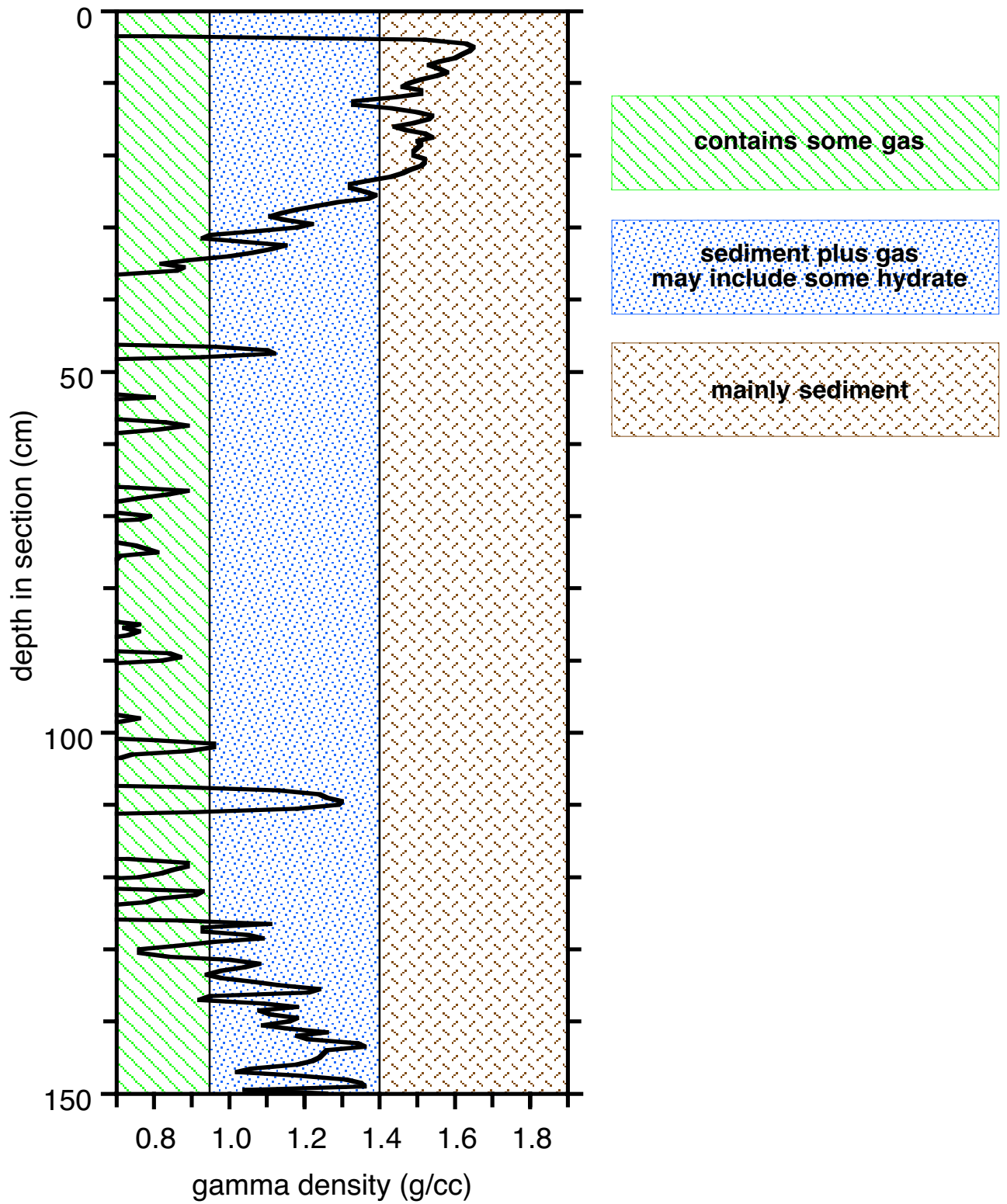
Section 204-1249K-5H-1  
Pressure Vessel 28



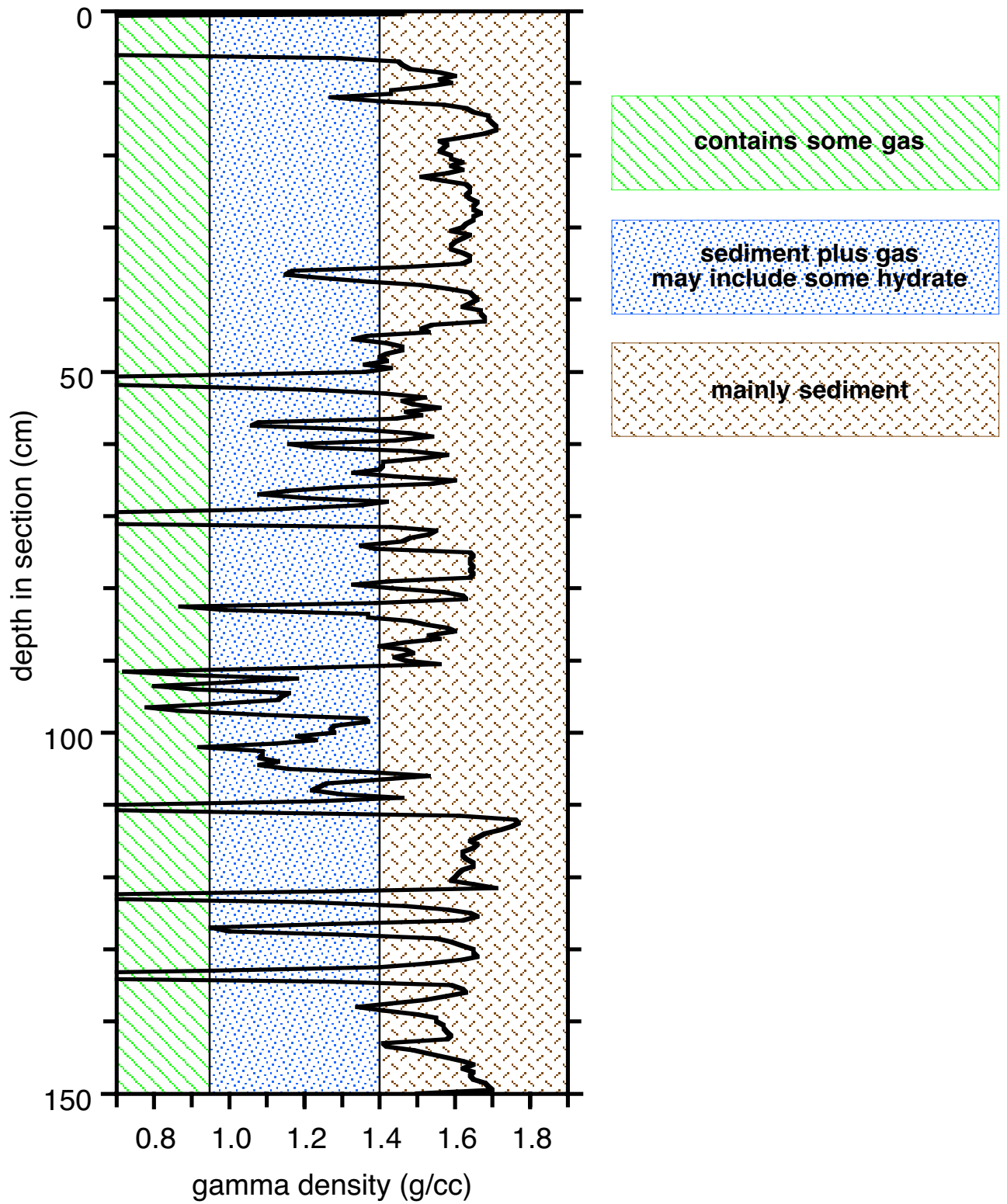
Section 204-1249I-4H-6  
Pressure Vessel 29



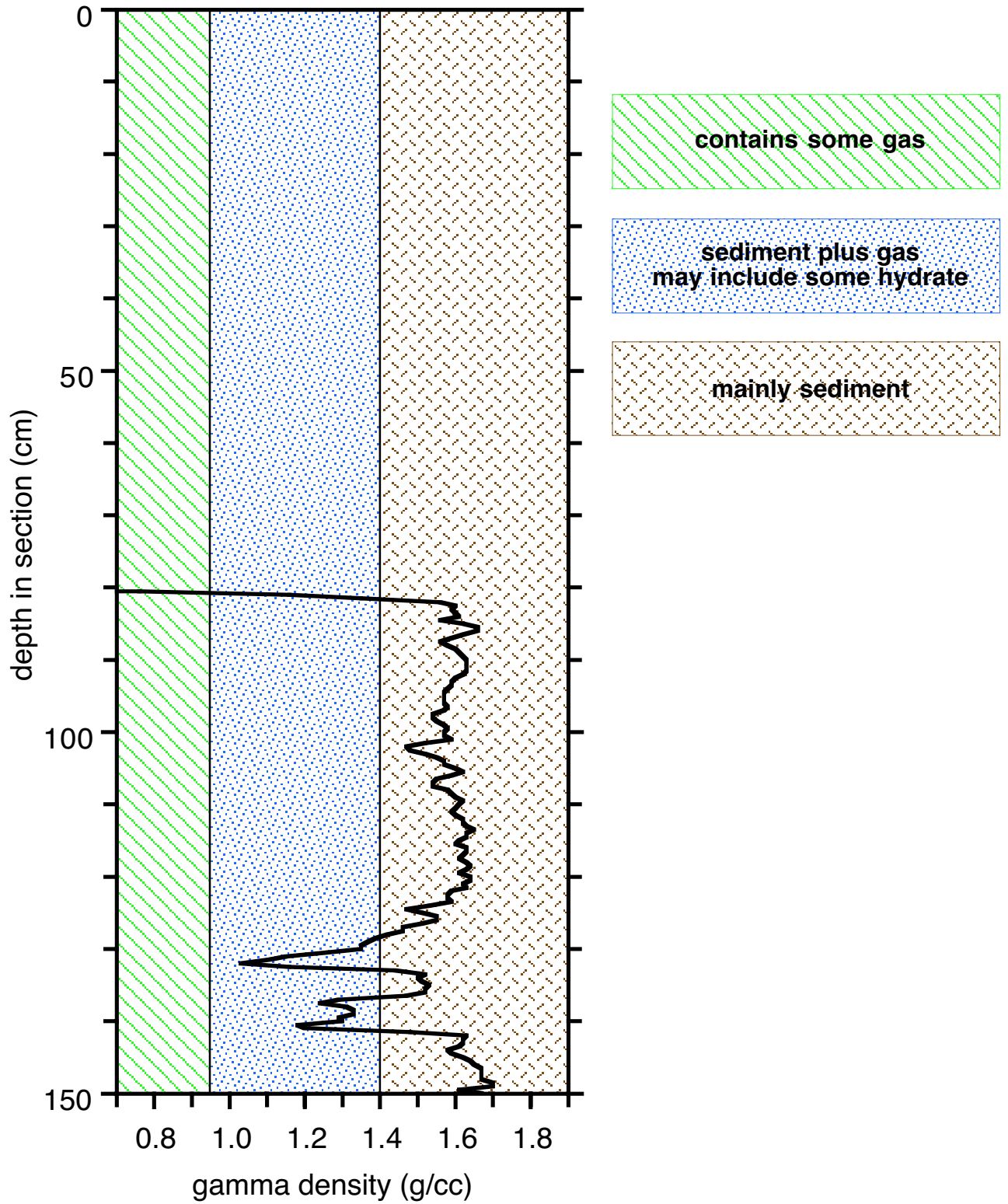
Section 204-1249I-4H-2  
Pressure Vessel 30



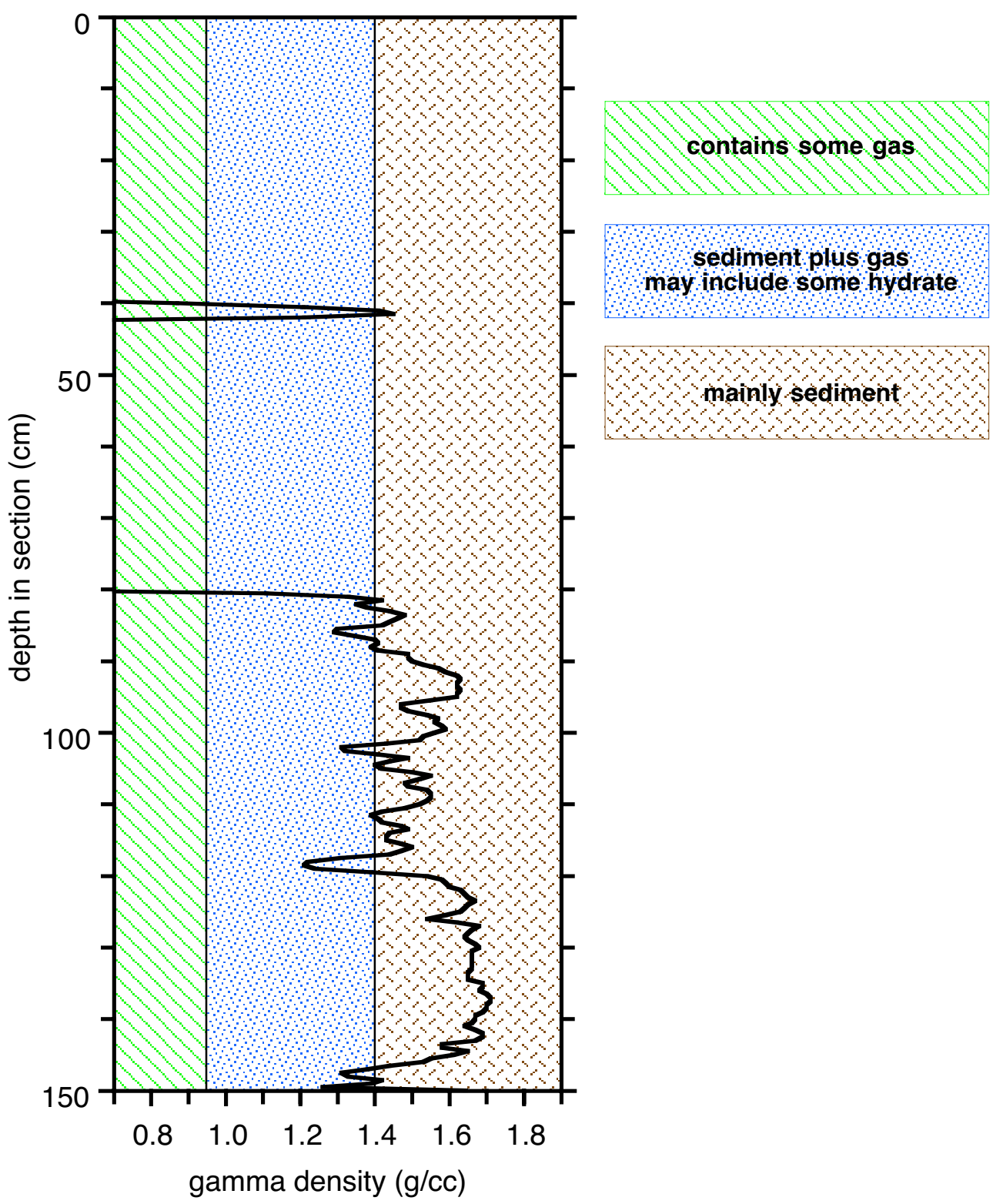
Section 204-1249K-5H-2  
Pressure Vessel 31



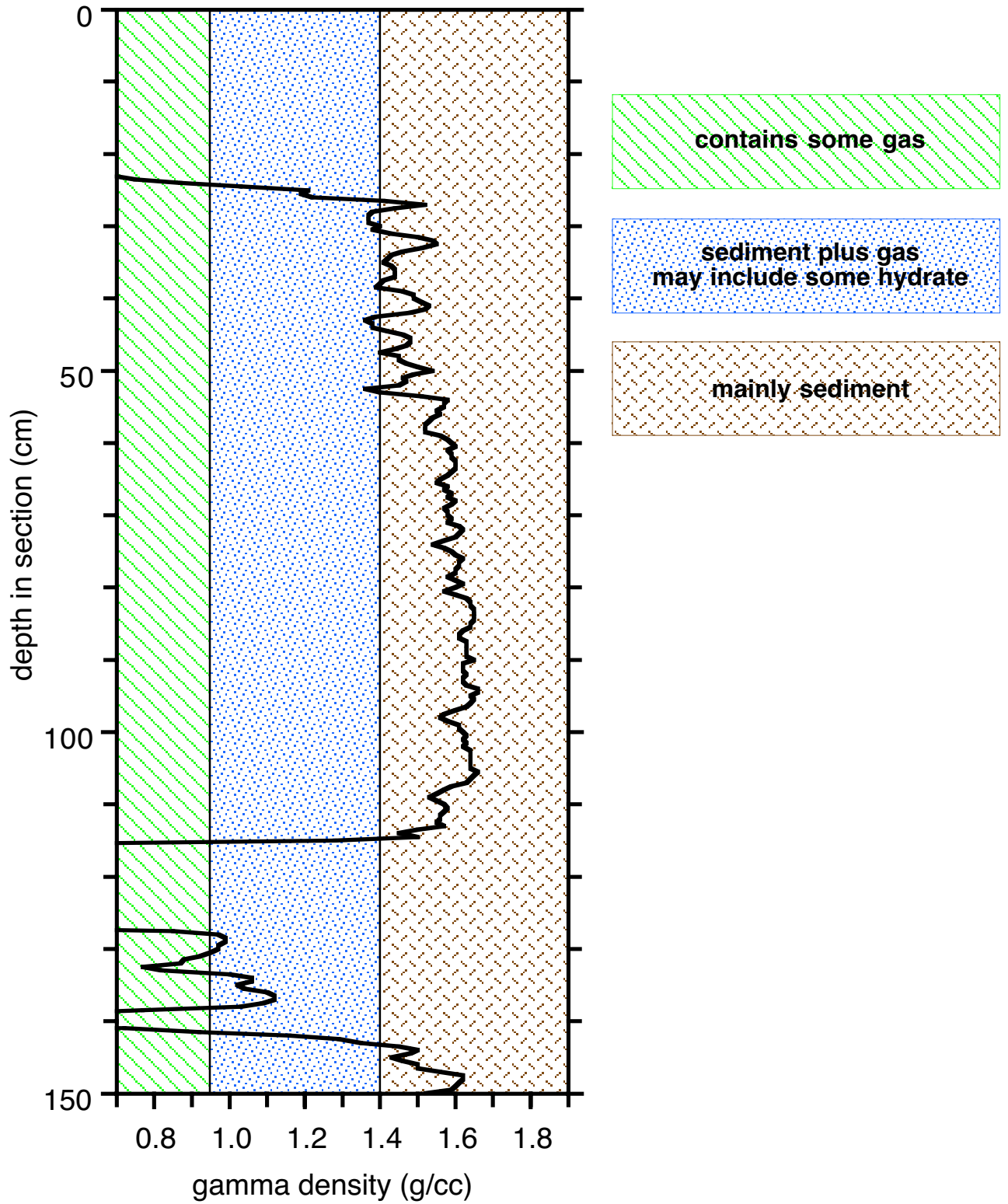
Section 204-1249L-2H-2  
Pressure Vessel 32



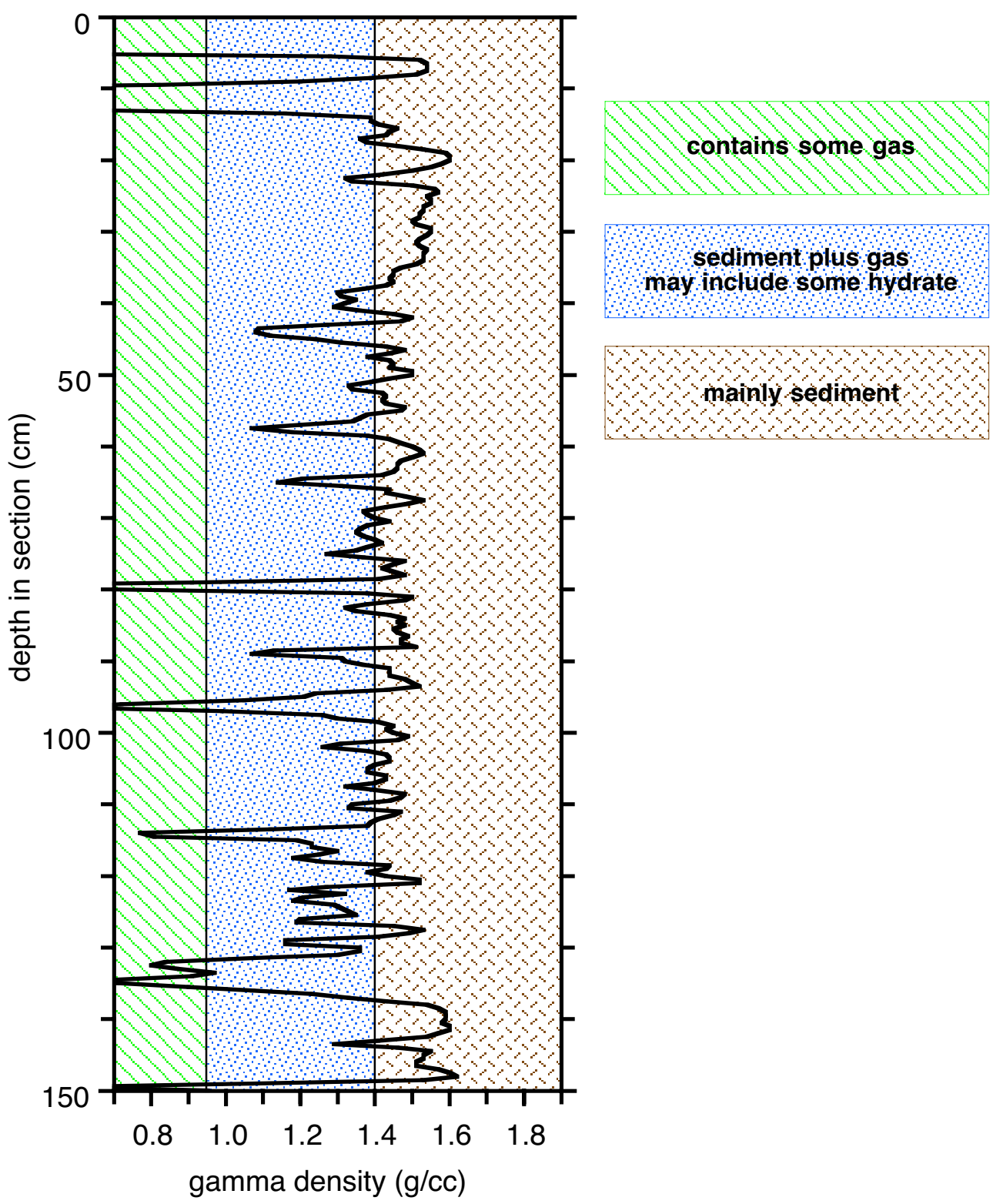
Section 204-1249L-2H-3  
Pressure Vessel 33



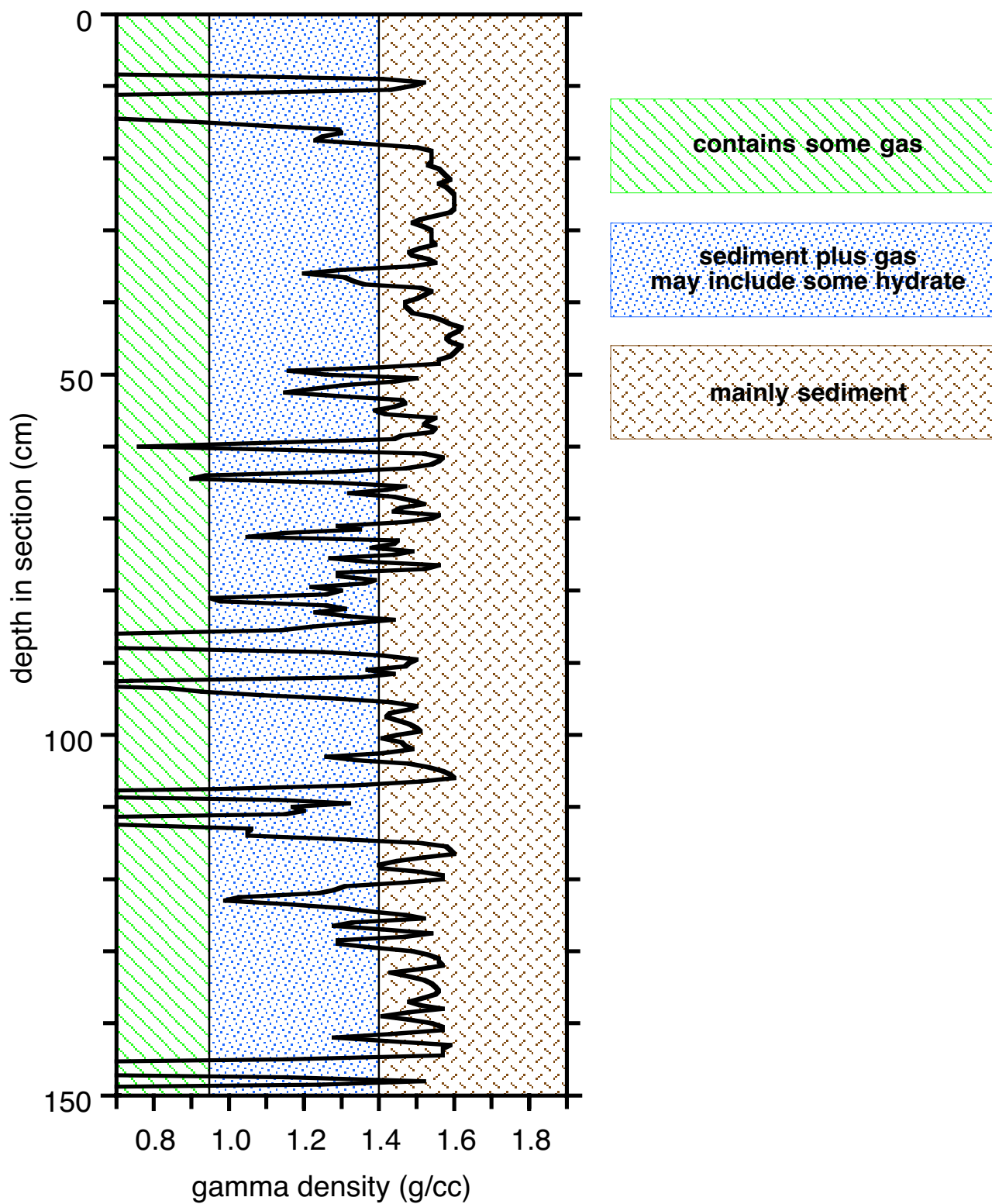
Section 204-1249L-2H-1  
Pressure Vessel 34



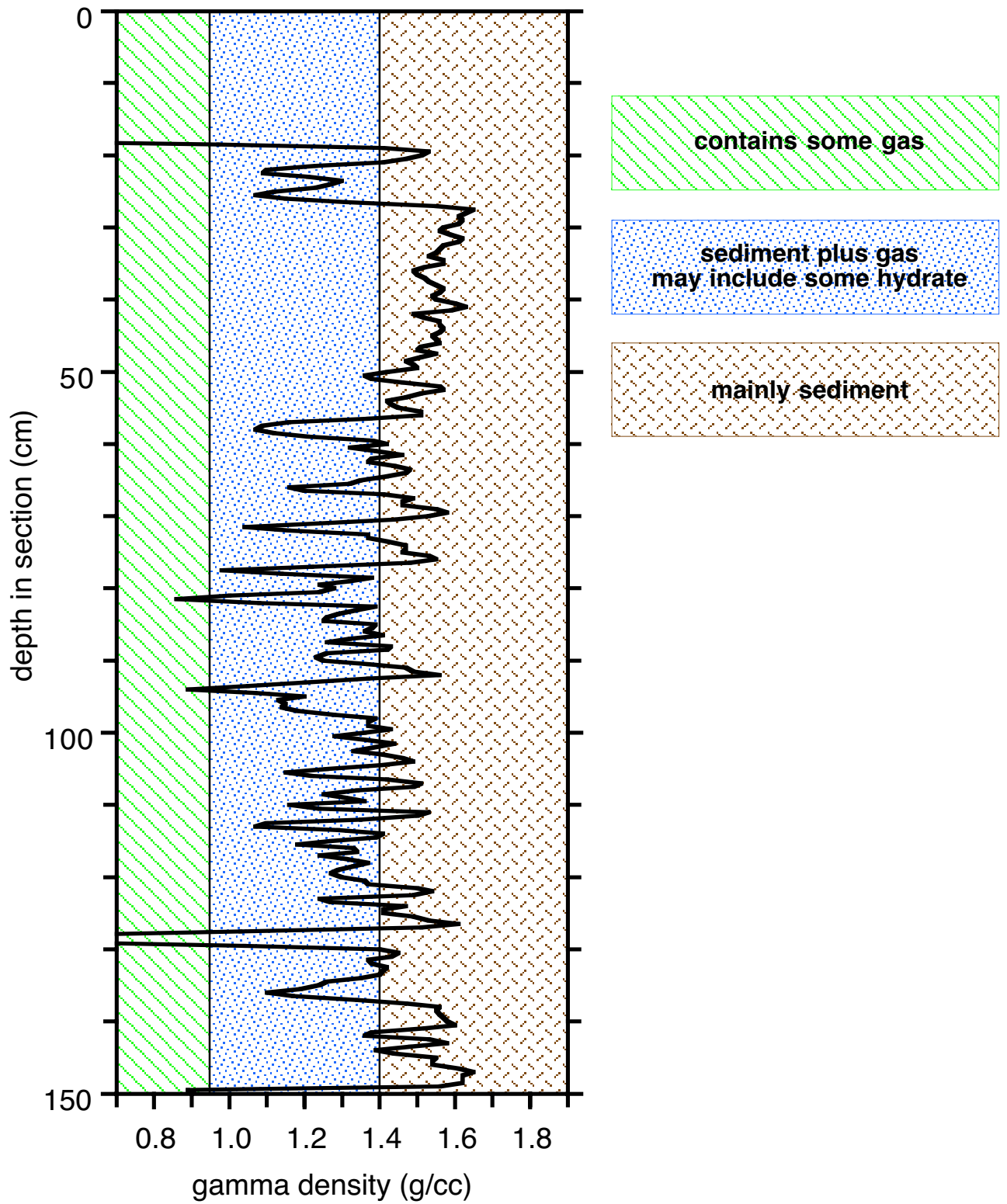
Section 204-1249L-4H-1  
Pressure Vessel 36



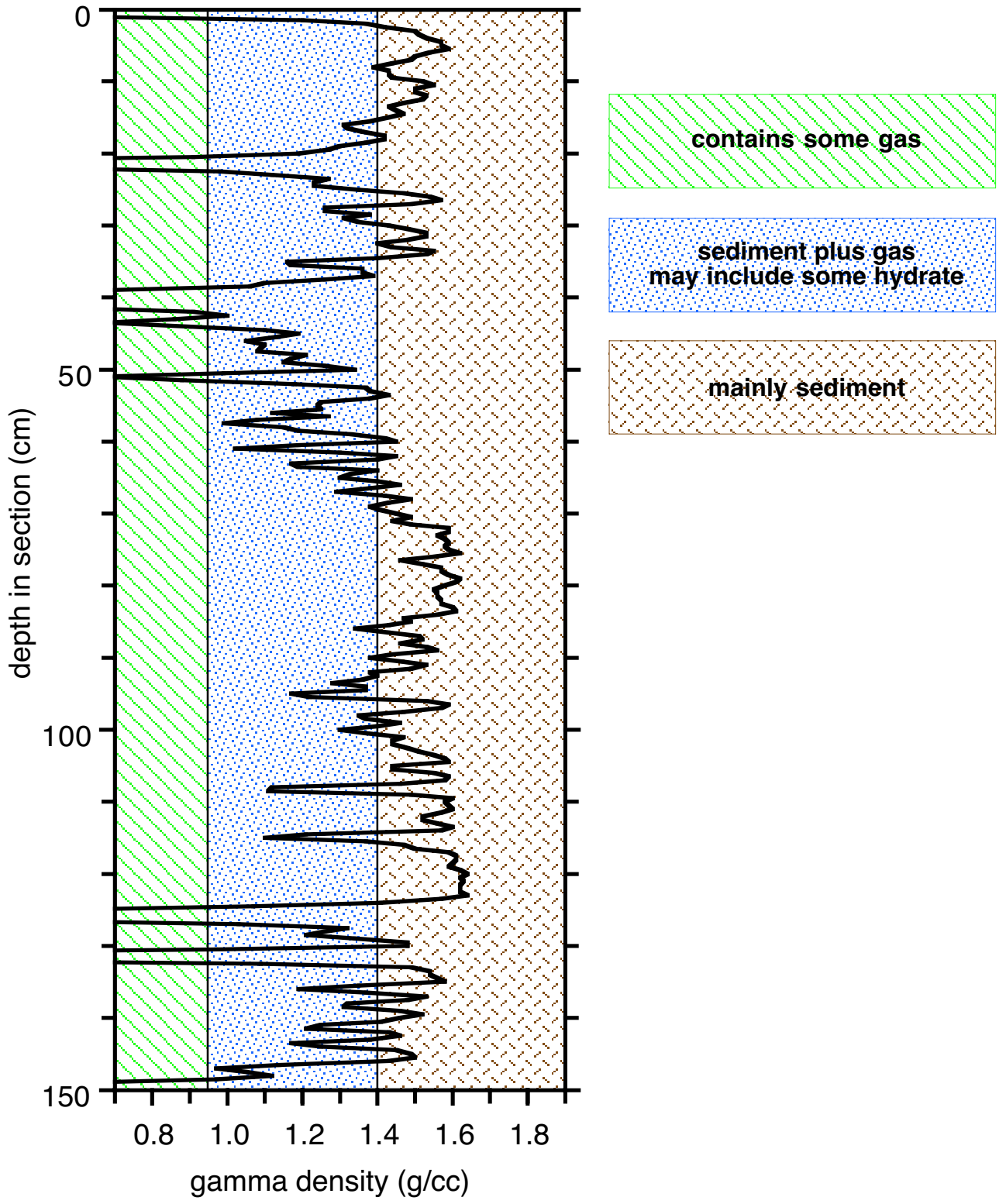
Section 204-1249L-4H-2  
Pressure Vessel 37



Section 204-1249L-3H-1  
Pressure Vessel 38



Section 204-1249L-3H-3  
Pressure Vessel 40



**APPENDIX D**

**STATUS OF ODP LEG 204 GERIATRIC STUDY SAMPLES STORED IN  
LIQUID NITROGEN CRYOFREEZERS IN THE ODP GULF COAST  
REPOSITORY.**

**Frank R. Rack  
Joint Oceanographic Institutions**

**(2 pg. Table)**

Table 1.

Status of ODP Leg 204 Geriatric Study Samples Stored in Liquid Nitrogen Cryofreezers in the ODP Gulf Coast Repository.

Cryofreezer	Hole	Core/Type/Section	Length (cm)	Comments
08	1249G	4H-3	43 cm-long	several pieces
08	1249K	4H-4	44 cm-long	solid piece, visible hydrate at end of section
08	1249I	4H-1	16-19 cm-long	tapered from 16 to 19 cm at lower end
08	1249L	1X-4	38 cm-long	slight taper at upper end, knob at lower end
08	1249J	2H-4	47 cm-long	2 main pieces, upper one longer than lower one
08	1249L	1X-1	48 cm-long	one solid piece
08	1249J	3H-5	45 cm-long	2 pieces; break at 10-11 cm
08	1249L	1X-3	33 cm-long	vuggy at upper end; squared off at lower end
Cryofreezer	Hole	Core/Type/Section	Length (cm)	Comments
04	1249I	4H-Rig Floor	large bag	sediment collected from rig floor after blow-off
04	1249I	1X-CC	18 cm-long	small bag
04	1249J	3H-CC	unknown	string on small bag broke; fell to bottom of cryofreezer
04	1249J	3H-2	48.5 cm-long	2 pieces; break at 18 cm; visible massive hydrate at break
04	1249J	3H-3	45 cm-long	2 pieces; break at 21 cm
04	1249J	2H-2	32 cm-long	2-3 main pieces; break at 17-18 cm; hydrate nodules/lenses
04	1249G	3H-2B	large bag	sediment collected from rig floor after blow-off
04	1249J	2H-3	31.5 cm-long	2 pieces; angular break at 16-18 cm; massive hydrate at break
04	1249K	3H-3	53 cm-long	3 pieces; breaks at 13-15 cm and 30-32 cm; visible hydrate
Cryofreezer	Hole	Core/Type/Section	Length (cm)	Comments
06	1249L	3H-2	28 cm-long	visible hydrate
06	1249L	3H-4	47 cm-long	
06	1249L	3H-CC	~17 cm-long	small bag
Cryofreezer	Hole	Core/Type/Section	Length (cm)	Comments
05	1249L	1X-2	45.5 cm-long	1 piece; vuggy at top
05	1249K	3H-CC and 3H-Rig Floor	large bag	sediment collected from rig floor after blow-off and CC sample
05	1249K	3H-4	50 cm-long	2 long pieces with visible disseminated hydrate at break
05	1249K	5H-3	45 cm long	5 pieces; visible hydrate in piece #3
05	1249K	5H-CC	unknown	string on small bag broke; fell to bottom of cryofreezer
05	1249K	1X-1	47 cm-long	
05	1249K	5H-Rig Floor	small bag	
05	1249K	4H-CC	small bag	
05	1249K	2H-CC	small bag	
05	1249L	1X-CC	small bag	
05	1249K	2H-1	46 cm-long	2 pieces; break at 10-12 cm
05	1249K	2H-2	50 cm-long	3 pieces; massive hydrate visible at break
05	1249K	4H-3	50 cm-long	2 pieces; no visible hydrate
05	1249K	1X-2	~30 cm-long	
Cryofreezer	Hole	Core/Type/Section	Length (cm)	Comments
07	1249I	2H-3	50 cm-long	2 pieces; break at 24-25 cm; visible hydrate at break
07	1249I	2H-2	12-14.5 cm-long	tapered end to 14.5 cm-long; no visible hydrate
07	1249I	2H-1	49-50 cm-long	angular break at 19-21 cm; lg. Void/vug at 25-30 cm; visible massive hydrate at break
07	1249I	4H-5	49-51 cm-long	breaks at 40 cm and 44-46 cm; visible nodular and massive hydrate
07	1249I	3H-3	24 cm-long	break at 3-4 cm; distinctive vugs and voids at lower end
07	1249I	4H-4	50 cm-long	breaks at 23 cm, 27 cm, and 31 cm; angular break at 38-41 cm; no visible hydrate
Cryofreezer	Hole	Core/Type/Section	Length (cm)	Comments
01	1249G	4H-3A	38 cm-long	2 pieces; break at 10-11 cm; no visible hydrate
01	1249G	3H-3	47.5 cm-long	3 pieces; visible massive hydrate at break
01	1249G	3H-4A	50 cm-long	no visible hydrate
01	1249G	3H-2B	43 cm-long	2 pieces; break at 33 cm; visible hydrate
01	1249G	3H-4C	34 cm-long	
01	1249G	3H-CC	small bag	
01	1249G	4H-CC	small bag	
01	1249G	3H-4B	51 cm-long	2 pieces; break at 11-12 cm; visible massive hydrate
01	1249G	4H-2	41 cm-long	visible massive hydrate
01	1249G	3H-2A	39.5 cm-long	no visible hydrate
01	1249G	1X-3	10-12 cm-long	
01	1249G	4H-4A	46 cm-long	visible hydrate lens at 8-10 cm; break at 34 cm (fractured section)
01	1249G	1X-CC	small bag	
01	1249G	4H-4B	32 cm-long	2 pieces; break at 13-14 cm; no visible hydrate
01	1249G	4H-1	38.5 cm-long	cloth-like textured interval near top; break at 26 cm; no visible hydrate

Cryofreezer	Hole	Core/Type/Section	Length (cm)	Comments
03	1249H	4H-6	31.5 cm-long	3 pieces; no visible hydrate
03	1249I	3H-1	48.5 cm-long	3 pieces; several lenses of hydrate in piece #2
03	1249I	1X-1	~19 cm-long	tapered upper end with possible hydrate visible, mud nodules
03	1249H	5H-Rig Floor	small bag	string broke; sample in bottom of cryofreezer
03	1249I	3H-2	28 cm-long	2 pieces; break at 19-20 cm; visible hydrate at break
03	1249I	1X-CC	small bag	samples consolidated in single larger bag
03	1249I	2H-CC	small bag	samples consolidated in single larger bag
03	1249I	3H-CC	small bag	samples consolidated in single larger bag
03	1249I	3H-Rig Floor	small bag	samples consolidated in single larger bag
03	1249I	4H-CC	small bag	samples consolidated in single larger bag
03	1249H	5H-CC	small bag	samples consolidated in single larger bag
03	1249H	6H-CC	larger bag	
03	1249H	5H-4	51 cm-long	3 pieces; breaks at 14-15 cm and 40-41 cm; visible hydrate at top
03	1249H	6H-7	42 cm-long	3 pieces; breaks at 31 cm and 36 cm; no visible hydrate
03	1249H	5H-6	~65 cm-long	3 pieces; breaks at 9-10 cm and 25 cm; wrapped as 2 pieces (#1 = ~24 cm-long, #2 = ~41 cm-long)
Cryofreezer	Hole	Core/Type/Section	Length (cm)	Comments
02	1249H	1H-1	49 cm-long	3 pieces; maybe some hydrate visible; H2S smell
02	1249H	4H-2	40 cm-long	2 pieces; break at 23-24 cm; very vuggy; no visible hydrate
02	1249H	1H-3	44 cm-long	2 pieces; angular break at 26-28 cm; very vuggy with visible hydrate; H2S smell
02	1249H	1H(X?)-CC	small bag	
02	1249H	1H-2	53 cm-long	2 pieces; break at 17-19 cm; massive hydrate visible throughout upper piece (both ends) and continuing into lower piece
02	1249H	4H-CC	small bag	
02	1249H	3H-CC (A) and 3H-Rig Floor	2 small bags	each sample is about 10 cm-long; consolidated in larger bag
02	1249H	3H-CC (B)	small bag	sample is about 10 cm-long
02	1249H	4H-5	33-34 cm-long	2 main pieces with 3-4 broken pieces in between; maybe some disseminated hydrate
02	1249H	4H-1	26-28 cm-long	vuggy at lower end
02	1249H	3H-3	55 cm-long	solid piece; perhaps some hydrate visible at lower end
02	1249H	4H-Rig Floor	large bag	sediment collected from rig floor after blow-off
02	1249H	3H-4 (3H-2?)	49 cm-long	2 pieces; break at 30-32 cm; maybe hydrate veins at lower end

**APPENDIX E**

**SUMMARY AND ANALYSIS OF  
VERTICAL SEISMIC PROFILING (VSP) EXPERIMENTS  
ON ODP LEG 204**

**GILLES GUERIN AND DAVID S. GOLDBERG  
LAMONT-DOHERTY EARTH OBSERVATORY OF COLUMBIA UNIVERSITY**

*In-Situ Sampling and Characterization of Naturally Occurring Marine Methane Hydrate  
Using the D/V JOIDES Resolution.*

## **General Overview**

Intermediate in scale and resolution between the borehole data and the 3-D seismic surveys, the Vertical Seismic Profiles (VSP) carried during Leg 204 were aimed at defining the gas hydrate distribution on hydrate ridge, and refining the signature of gas hydrate in the seismic data.

VSP surveys were attempted at five sites, following completion of the conventional logging operations. Bad hole conditions and operational difficulties did not allow to record any data in hole 1245E, but vertical and constant offset VSP were successful in holes 1244E, 1247B and 1250F, and walkaway VSP were successfully completed in holes 1244E, 1250F and 1251H. Three different tools were used for these surveys, which are summarized in table 1 and figure 1.

The vertical VSP allowed to calculate interval velocity that could be compared and validated with the sonic logs in the same wells. Figure 2 shows that, after a 5-sample smoothing, the interval velocity profiles in Holes 1244E and 1247B are in very good agreement with the sonic logs. Synthetic seismograms using the vertical VSP and a complete analysis of the walkaway data will be completed by Bangs, Trehu and collaborators.

## **Operations and data overview**

### **Hole 1245E**

After completion of the standard wireline logs, rig up of the VSI for the VSP survey started on 08/15/02 at 0830 local time. The plan was to conduct three types of survey during this run: vertical, constant offset and walkaway. The *R/V Maurice Ewing* was navigating nearby to provide support for the constant offset and the walkaway surveys. Despite the generally good hole conditions that were observed during the standard log runs, it became clear after a few attempts that it would prove difficult to get a proper clamping for any of the shuttles, even less three. The average hole size (ranging from 12 to 16 in) exceeded the maximum operational hole size for the VSI (12 in). Multiple shots were fired from the *Resolution* and from the *Ewing* without ever recording a consistent signal, at any of the attempted depth. It was then decided to abort this run and to try to use the one-component WST to conduct at least a vertical VSP. When the VSI reached the rigfloor it appeared that the arms of the three shuttles had been damaged during our numerous clamping attempts. The WST was then lowered in the hole, but the geophone stopped soon to work properly and the tool was brought back to replace the geophone. During the following lowering, and despite the proper behavior of the WST, it became obvious that the hole was too large and the formation too soft to get a good clamping. The survey was aborted, and the final rig down was complete at 0200 on August 16, 2002.

### **Hole 1251H**

After completion of conventional logs in Hole 1251H, rig up for the VSP survey started at 0345 on August 18, 2002. The triple combo and FMS/Sonic calipers had shown that the hole was irregular, which suggested that the three component WST-3 would be the most likely to provide data. This tool had been flown in since the previous failure of the VSI in Site 1245. It proved again difficult to get a consistently good clamping. However the signal appeared of good enough quality to proceed with a systematic vertical and

constant offset VSP. Stations were made over the entire hole every 7.5 meters, starting at 1405 mbrf. Satisfactory data were recorded for about 25% of the stations, the most consistently between 1350 and 1313 mbrf. After completion of the vertical/constant offset VSP, it was decided to attempt a walkaway VSP. It proved impossible to get good clamping at the initial target depths near the BSR, but a good station was found at 1320 mbrf and the Ewing shot two perpendicular lines, each taking ~2 hours. Final rig down was completed at 2030 on August 18, 2002. Figure 3 shows the data recorded by the three geophone components of the WST-3 on the first line (South to North)

#### **Hole 1244E**

All the conventional logging runs indicated very good hole conditions in Hole 1244E. The WST-3 rig-up started at 0130 local time, 08/21/02, and the vertical/constant offset VSP started without difficulty from the bottom of the hole (~1155 mbrf). Stations were made every 5 meters and the survey was completed without any problem, in excellent hole and sea conditions. Two walkaway stations, including two orthogonal lines each, were made at 1045 mbrf and 1020 mbrf, respectively. The final rig down ended at 0100 local time, 08/22/2002. Figure 4 shows a general overview of the two lines recorded with the vertical component geophone of the WST-3 at 1020 mbrf (=115 mbsf).

#### **Hole 1247B**

After completion of standard logs in Hole 1247B, rig-up of the WST-3 started at 0415, local time, 08/24/2002. Considering the good hole conditions, the plan was to conduct a complete survey including two walkaway stations. Initial tests before lowering the assembled tool string indicated serious problems, including the impossibility to properly close and open the arm, and it was decided to use the one component WST to perform only a vertical VSP. After lowering the tool, several unsuccessful attempts to record a decent signal indicated that the geophone was damaged. Because no spare geophone was available, and considering the extremely good hole and sea conditions, we decided to try using one of the shuttles of the VSI, which had been restored to its original configuration. The tool reached the bottom of the hole (1066 mbrf), and a vertical / constant offset survey was acquired without difficulties between 1060 mbrf and 930 mbrf, with stations every 5 meters. After completion of this survey, it proved impossible to get a satisfactory station that would allow to perform a walkaway. Considering the poor quality of the signal, it was suspected that the tool had been damaged and it was brought back to the rig floor for inspection. This confirmed that the arm had been damaged, possibly while the tool was on station too close to the bottom of the pipe. It was decided to abort any further attempt in order to preserve the remaining shuttles for the final VSP survey in Site 1250. Final rig-down was complete at 1730, 08/24/2002.

#### **Hole 1250F**

After completion of the standard logs in Hole 1250F, rig-up of a the single-shuttle VSI started at 0610, August 26, 2002. The tool was lowered to the bottom of the hole (980 mbrf) and the vertical/constant offset survey was recorded every 5 meters up to 890 mbrf. Coupling between the arm and the formation was poor in the upper part of the hole, and no reliable shots were recorded above 930 mbrf. Because of the generally poor signal, it

was suspected that the tool had been damaged and it was brought back to the surface. Inspection showed that it was in working order, and it was lowered again to try to find possible walkaway stations. After systematic attempts along most of the hole, three walkaway surveys were recorded at 945 mbrf, 898 mbrf and 979 mbrf. Final rig down was completed at 0630 on August 27, 2002, a few hours before the Schlumberger VSP engineer was to leave the ship. Figure 5 shows the data recorded by the three geophone components of the VSI on the first line (South to North)

**Table 1:** Summary of VSP operations during Leg 204

Hole	VSP spacing (m)	VSP interval (mbsf)	Tool used	Walkaway depth (mbsf)	Walkaway shots (S-N, W-E)
1251H	7.5	85-185	WST-3	100	591, 344
1244E	5	85-250	WST-3	140 115	563,560 474,543
1247B	5	85-215	VSI	N/A	N/A
1250F	5	85-175	VSI	90 140 170	445, 412 461, 458 424,337